SCIENTIA BRUNEIANA

OFFICIAL JOURNAL OF

THE FACULTY OF SCIENCE

UNIVERSITI BRUNEI DARUSSALAM

ISSN : 1819 - 9550 Volume : 15, 2016, **Special Issue**

First Published 2016 by
Faculty of Science,
Universiti Brunei Darussalam
Jalan Tungku Link
Bandar Seri Begawan BE1410
Brunei Darussalam

This journal consists of papers prepared by staff of Universiti Brunei Darussalam and peer reviewed by local and international referees.

Cataloguing in Publication Data

Scientia Bruneiana / Chief Editor Abby Tan Chee Hong

171 p.; 30 cm

ISSN : 1819-9550

1. Research – Brunei Darussalam. 2. Science – Brunei Darussalam

Q180.B7 B788 2016

Cover photo: Mudskippers of Brunei of the genera *Periophthalmus* and *Periophthalmodon*. a. *Periophthalmus malaccensis*. (Courtesy: Gianluca Polgar).

Printed in Brunei Darussalam by
Educational Technology Centre,
Universiti Brunei Darussalam

mk

SCIENTIA BRUNEIANA
Special Issue

Greetings from the Dean of UBD's Faculty of Science.

I am pleased to announce the publication of this special 2016 issue of *Scientia Bruneiana*, which celebrates the 30th anniversary of Universiti Brunei Darussalam by highlighting some of the more important and significant findings made by our researchers in various fields of the natural and applied sciences.

In the last 10 years, UBD has undergone a major transformation from a teaching-oriented university to one that is focused on both teaching and cutting-edge research. Central to this transformation has been a substantial increase in research funding, which has enabled the Faculty of Science to implement a number of high-profile flagship research projects. Notable outcomes have included a rapid increase in peer-reviewed publications and citations, and the satisfaction of seeing our own researchers extend the frontiers of knowledge in many new directions. This special issue showcases some of the innovative, high-impact research work being done here.

I would also like to extend an invitation to all researchers throughout the scientific world to submit your findings to Scientia Bruneiana. Your contribution could ignite a paradigm shift in science and technology. We especially welcome multi-disciplinary research, as we strongly believe great inventions arise from the intersection of different mindsets and disciplines of thought.

Finally, I would like to thank my colleagues in the Faculty of Science - particularly the authors, associate editors and subject editors whose efforts have made this special issue possible - for their continuous support.

Yours Sincerely
Abby Tan Chee Hong
Chief Editor
Scientia Bruneiana

SCIENTIA BRUNEIANA

A journal of science and science-related matters published twice a year by the Faculty of Science, Universiti Brunei Darussalam. Contributions are welcome in any area of science, mathematics, medicine or technology. Authors are invited to submit manuscripts to the editor or any other member of the Editorial Board. Further information including instructions for authors can be found in the notes to contributors section (final four pages at the end).

EDITORIAL BOARD

SCIENTIA BRUNEIANA is published by the Faculty of Science,
Universiti Brunei Darussalam, Brunei Darussalam BE 1410

ISSN : 1819-9550

1. Research – Brunei Darussalam. 2. Science – Brunei Darussalam

Q180.B7 B788 2016

SCIENTIA BRUNEIANA

Publication Ethics Policy

The Editorial Board of *Scientia Bruneiana* is committed to implementing and maintaining the publication standards of a high-quality peer-reviewed scientific journal.

Each manuscript submitted to *Scientia Bruneiana* is examined by a referee with recognised expertise in the manuscript's subject area, and all communications between the referee and the author(s) pass must first through the Editorial Board, so that the identity of the referee remains confidential.

No one will be appointed as the referee of a manuscript if he or she is known to have a potentially compromising relationship with one or more of the authors of the manuscript, as for example in being related through blood or marriage to an author, or in being the research supervisor or research student of an author.

The Editorial Board of *Scientia Bruneiana* makes every effort to ensure that each paper published in the journal is free of plagiarism, redundant or recycled text, and fabricated or misrepresented data. Where possible, plagiarism detection software will be used to check for plagiarised or recycled text.

Provided that a manuscript is free of the ethical lapses described in the previous paragraph, the decision to publish it in *Scientia Bruneiana* is based entirely on its scientific or academic merit, as judged by the referee. The referee's assessment of the merit of the manuscript is final. While a full statement of the reasons behind the referee's decision will be passed on to the author(s), no appeals from the author(s) will be entertained.

Under no circumstances will the referee of a paper published in *Scientia Bruneiana* be credited as one of the authors of the paper, and other papers that have been authored or co-authored by the referee will be admitted to the paper's list of references only after an independent third party with expertise in the area has been consulted to ensure that the citation is of central relevance to the paper.

If a member of the Editorial Board of *Scientia Bruneiana* is listed as an author of a manuscript submitted to *Scientia Bruneiana*, that Board member will play no part whatsoever in the processing of the manuscript.

Where necessary, any corrections or retractions of papers previously published in *Scientia Bruneiana* will be printed in the earliest possible edition of the journal, once the need for a correction or retraction has been drawn to the attention of the Editorial Board.

SCIENTIA BRUNEIANA SPECIAL ISSUE

2016

Research Articles **Page Numbers**

Research Articles **Page Numbers**

Ecological responses to fluctuating and extreme marine acidification: lessons from a tropical estuary (the Brunei Estuarine System)

David J. Marshall[1], Sorya Proum[2,3], M. Belal Hossain[1], Aimimuliani Adam[1], Lee Hoon Lim[2] and Jose H. Santos[2]*

[1]Environmental and Life Sciences, Faculty of Science, Universiti Brunei Darussalam, Jalan Tungku Link, Gadong, BE 1410, Brunei Darussalam
[2]Department of Chemical Sciences, Faculty of Science, Universiti Brunei Darussalam, Jalan Tungku Link, Gadong BE 1410, Brunei Darussalam
[3]Chemistry Department, The Royal University of Phnom Penh, Cambodia

**corresponding author email: david.marshall@ubd.edu.bn*

Abstract

The impact of acidification on marine ecosystems has become a topic of priority research, following realization of unabated ocean acidification (OA), derived from globally-rising atmospheric CO_2. Many coastal and estuarine ecosystems have historically been acidified through various processes, and it is possible that we can learn and make predictions about OA impacts from the ways estuarine species and communities adapt and respond to acidified water. Studying estuarine acidification, nonetheless, aids understanding of the processes that affect ecological structure and functioning, important for coastal conservation and management. A broad-based research programme was implemented at UBD between 2011 and 2015, to investigate how variation in acidity and salinity affected assemblages and species in the Brunei Estuarine System (BES), an ecologically and economically important natural system in the region. This review summarizes studies that investigated for the BES, (*i*) the physical habitats and water physicochemistry, (*ii*) responses of planktonic and benthic microbial and faunal assemblages to exposure to variable and potentially highly acidic water, (*iii*) effects of acidification on ecological processes, such as barnacle dispersal and recruitment, (*iv*) behavioural and physiological mechanisms of organisms to cope with highly fluctuating and extreme pH water, with special reference to the gastropod, *Indothais gradata*, and (*v*) contaminant uptake by *Indothais gradata* under acidified conditions. The significance of the findings to the ecology of the BES, gaps that need addressing, and how estuarine acidification may contribute to predicting responses to OA are evaluated and discussed.

Index Terms: estuarine acidification, ocean acidification, carbonate chemistry, benthic, *Indothais gradata*

1. Introduction

Coastal and estuarine marine systems provide abundant resources, nursery grounds and ecosystem services, yet are increasingly threatened by urbanization and industrialization (more than 60% of the global human population is located along coastlines). The impact on these sensitive ecosystems is exacerbated by anthropogenic climate change, related to increasing CO_2 emissions (IPCC, 2013).[1] There is a direct link between elevated atmospheric CO_2 and warming and acidification of the surface water of the oceans.[2,3] Oceanic acidification (OA) is predicted to greatly adversely affect some of the most biodiverse and functionally significant marine ecosystems (such as the corals), a realization that has motivated innovative research over the past decade.[2,3] Despite such initiatives, referring to gradual pH change (decreasing by fractions of units over decades), our knowledge of

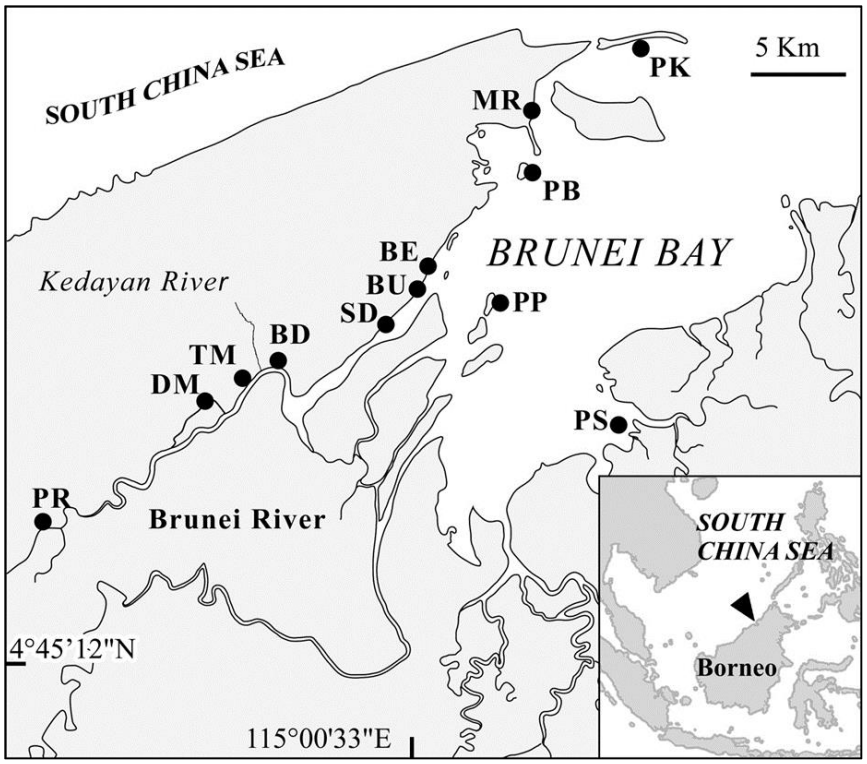

Figure 1. Map of the Brunei Estuary System (BES). Sampling stations for the various studies are shown. Kampong Parit (PR), Damuan (DM), Tamoi (TM), Bandar (BD), Serdang (SD), Sungai Bunga (BU), Sungai Besar (BE), Pulau Bedukang (PB), Muara (MR), and Pulau Keingaran (PK). Also given are locations of Sungai Kedayan, Pulau Pepetan (PP) and P. Selirong (PS).

species and community responses to ongoing dramatic temporal variation in pH (variable by full pH units over hours) in many coastal and estuarine environments is scarce.[4-6] Understanding the nature of pH variation in coastal systems, and how species and communities respond and adapt to it, potentially provides insights into responses of oceans to acidification, but in any event contribute to the conservation and management of such coastal ecosystems.

This review summarizes the findings of several studies undertaken on the Brunei Estuarine System (BES, ***Figure 1***) that aim to assess biological responses to pH change. These studies represent the culmination of research of UBD graduate students, and local and international collaborators, carried out between 2011 and 2015. The BES is ecologically and economically important to Brunei and the region. Historically, it has played a crucial role in the early establishment of the Bruneian people, through provision of food (artisanal fisheries and aquaculture) and habitation (an original water village still exists at Kampong Ayer; ***Figure 1*** and ***Figure 2***). Being fed by four major nutrient-rich rivers (Sungai Brunei, Limbang, Trusan and Temburong), the BES serves as an extensive nursery ground for fish communities, supports highly diverse, unique and pristine mudflats and mangroves, and offers huge potential for ecosystem services provision and scientific research.

Additionally, the BES represents a suitable model system for testing ecological responses to marine acidification. Although estuarine systems are characteristically acidified by sulphate reduction in muddy sediments, acidification in the BES water column is additionally enhanced by highly acidic groundwater inflows and metabolic activity of planktonic and benthic eukaryotes and microbes. The groundwater is extraordinarily acidified by acid sulphate soils (ASS)[7] and to some extent by peat-swamp leachates, whereas decomposition of high detrital input (mangrove leaf litter) elevates metabolic CO_2 production.

Figure 2. Upper: An artisanal fisherman throw-netting from a jetty at the Sungai Besar (BES) mangroves (photo, Roger Bamber). Lower: Sungai Brunei near Bandar showing Kampong Ayer, and characteristically turbid brown water (photo, David Lane).

Consequently, the water column of the BES is characterized by a steep acidity gradient from highly acidic upper estuarine waters (pH = 5.8 at Bandar, BD) to typically marine pH levels at the open ocean extremity that abuts the South China Sea (pH = 8.2 at Muara, MR) **(*Figure 1*)**.[4] The ecological significance of the BES acidification was first reported from observations of gross shell erosion of the intertidal snail, *Indothais gradata* (Jonas, 1846).[4] Because of its ubiquitous distribution in the BES, this snail species has proven to be a valuable model for investigating organism-level responses to variable acidification.[8]

The review first describes (*i*) the physical environment and water physicochemistry of the BES. Then, it summarizes the results of studies investigating, (*ii*) responses of planktonic and microbial and faunal benthic assemblages to exposure to variable and potentially highly acidic water, (*iii*) effects of acidification on some basic ecological processes (such as barnacle dispersal and recruitment), (*iv*) behavioural and physiological mechanisms of organisms to cope with highly fluctuating and extreme pH water (with special reference to *Indothais gradata*), and (*v*) contaminant uptake by *I. gradata* under acidified conditions.[5,6, 8-15]

2. Ocean acidification versus estuarine acidification

Ocean acidification (OA) is a different concept to estuarine acidification, but there are commonalities, which could help understand both phenomena. Below we summarize (subjectively) the state of the art of the immensely rapidly growing field of OA, and suggest similarities and differences between OA and estuarine acidification (EA).

Essentially, OA refers to increased dissolution of CO_2 in the ocean surface water, as a consequence of anthropogenic atmospheric CO_2 elevation. This has two significant chemical outcomes: (*i*) water pH is lowered and (***Equation 1***) and (*ii*) carbonate dissolution increases (***Equation 3***)

$$CO_2 + H_2O \rightleftharpoons HCO_3^- + H^+ \quad (1)$$

$$H^+ + CO_3^{2-} \rightleftharpoons HCO_3^- \quad (2)$$

$$CaCO_3 \rightleftharpoons Ca^{2+} + CO_3^{2-} \quad (3)$$

The destructive potential of OA on marine ecological systems was underscored following observations of shell thinning of pteropod (gastropod) samples during routine oceanic planktonic surveys, in the early 2000s.[2,3] Research that followed centered on key oceanic ecosystems, including corals, and aimed to understand species and community responses. Objectives were largely to identify sensitive species and taxonomic groups, to distinguish 'winners' from 'losers' for century-long acidification.[2] 'Calcifiers', organisms possessing calcified skeletons and structures (including shells), have been repeatedly shown to be more sensitive than moderately

calcified or soft-bodied organisms; the latter two generally fair better in high pCO_2 water. Subtle differences in dissolution have been shown to relate to the $CaCO_3$ crystalline form, such that a higher proportion of calcite relative to aragonite offers greater robustness under elevated pCO_2. A plethora of laboratory studies have now investigated behavioural, physiological and morphological responses, in protocols that compare present-day pCO_2 exposures with experimental treatments that mimic pH and pCO_2 levels around year 2100.[17] Elevated pCO_2 does not always have a negative effect; photosynthesizing organisms may benefit from enhanced productivity in high pCO_2 water. Field studies assessing benthic assemblage responses to naturally high present-day pCO_2 have utilized volcanic vent systems.[18] Although oceanic vent studies continue to produce vast insights into the biological impacts of OA, observations are possibly confounded by other gases or metal contamination associated with vents. How organisms and species might acclimate or adapt to pCO_2 change, variable by fractions of units over decades, is considered a major challenge to future OA work. Other areas requiring urgent investigation include, multi-stressor responses (including effects of interacting temperature, nutrients and hypoxia)[19] and the ways in which acidification and elevated pCO_2 affect ecological interactions, such as predation, competition, etc.

OA and EA differ fundamentally in (*i*) acidification mechanism and (*ii*) timeframe and amplitude of pH change. Whereas OA refers to variation in atmospheric CO_2 over decades, EA is dynamic and usually multifactorial involving, (*i*) biological CO_2 generation, as well as, (*ii*) mineral acidification (with each category constituting further multifactor processes). Additionally, coastal systems are strongly influenced by direct anthropogenic acidification (such as, contaminants and acids released directly into the water). Naturally, contributions to the total acidity by either biological or mineral acidification are likely to vary proportionally at different timescales. For example, mineral acidification relating to acidic freshwater inflow is expected to change seasonally in equatorial regions, being greatest during monsoonal flooding, when freshwater inflow is greatest; biogenic acidification is expected to vary tidally, due to mixing of seawater with poorly-buffered, nutrient-rich brackish water near mangroves and mudflats that supports high benthic microbial activity. To our knowledge, no previous published study has assessed whether different mechanisms of acidification have different ecological outcomes. Probably the best known studies linking OA and EA refer to special cases of penetration of acidic, nutrient-rich, productive estuarine waters (for which pH is biogenically-lowered) into the oceans, often extending hundreds of kilometers out to sea (Pearl River estuarine system).[20-22]

3. Brunei Estuarine System (BES)

The Brunei Estuarine System (BES) comprises complex interacting shallow marine water bodies in northern Brunei (Borneo, South East Asia). It is defined here as the Inner Brunei Bay and the major waterways leading into this, including the Sungai Brunei (Brunei River), S.Temburong and S.Limbang (***Figure 1***). This review focuses on the western perimeter of the BES, that edging Bandar-Maura from Kampong Parit (PR) to Pulau Keingarong (PK) (***Figure 1***). Several islands are found within the Inner Brunei Bay, including the proclaimed Brunei protective area at Pulau Selirong (PS), which reputedly contains some of the oldest mangrove stands in the region, and P. Pepetan (PP) and P. Bedukang (***Figure 1***). The BES supports extensive intertidal mudflats, and its perimeter is predominantly mangrove-fringed. The impact of small-scale aquaculture and artisanal fisheries throughout the system is considered low, though shell-fish harvesting on mudflats has potentially damaging ecological effects. Human-derived impact is presently greatest along the Sungai Brunei, which supports widespread urban settlement, particularly towards Bandar and Kampong Ayer. Tributaries, such as S. Kedayang, which enters the system at Bandar, apparently carry polluted water from the relatively densely-populated Gadong and Kuilap (***Figure 1***). Construction and industrial activities in the Brunei Bay (such a charcoal production at Pepetan) are low key, though the situation could change dramatically with the building of the iconic bridge,

planned to traverse the BES from Sungai Besar to Temburong.

The BES undergoes extreme physicochemical variation. The water is typically brown and turbid, due to high suspended sediment and organic loads, especially during the monsoons (***Figure 2***). Salinity, varying between 4 and 33 psu (Bandar to Muara)[4], is influenced by semi-diurnal tides generated in the South China Sea, stochastic swell forcing, and freshwater inflow. Acidification, as already mentioned, derives from multiple sources, mainly combinations of (*i*) poorly buffered hyposaline water, (*ii*) groundwater permeating acid sulphate soils (ASS), (*iii*) microbial respiration in nutrient enriched waters and (*iv*) direct anthropogenic release of acidic substances.[4] ASS soils are widespread in Brunei[7]; they constitute 'fossilized' pyrite-rich marine sediments (FeS_2) formed during sulphate reduction when the sediments were active marine ecosystems, during periods of global sea-level-rise. Pyrite oxidation, through disturbance of sediments or when flushed, produces iron hydroxide [$Fe(OH)_3$] and sulphuric acid (H_2SO_4). Temporary die-back of local assemblages has been observed along the length of the BES, but communities are seemingly well-adapted to physical extremes and variability[8] (***Figure 3***).

Figure 3. A rich intertidal desmosponge community at Pulau Bedukang was obliterated by extreme sediment loads during January 2014 monsoon flooding.

Although we refer in the review to 'acidification' effects, the BES acidification strongly correlates with other abiotic factors, notably salinity (***Figure 4***), thus, in most cases, the described effects are multifactorial. We use the terms 'acidification' and 'acidity' with reference to the process and the effect, respectively. Both are relevant, as the BES is continually acidified, albeit highly variable in terms of space and time; this differs notably from the linear, slow acidification of the oceans.

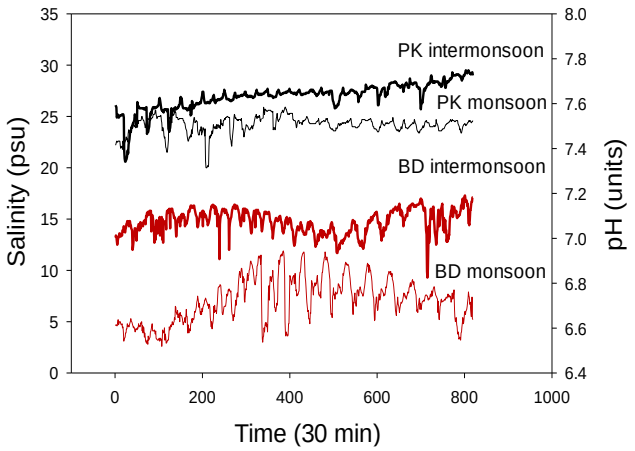

Figure 4. High-resolution temporal recordings of pH and salinity (every 30 min) at Bandar (BD) and Pulau Keingaran (PK) during monsoon (24 Nov -11 Dec 2013, thin line) and inter-monsoon periods (26 Feb – 15 Mar 2014, thick line). Baseline level and tidal amplitude of parameters are shown to vary between stations and seasons.

4. Physical and chemical properties of habitats

4.1 Sediments

Sediment properties of estuarine systems underlie the habitat of functionally-important benthic animals and plants, such as prokaryotes (bacteria), microphytobenthos (benthic diatoms), meiofauna and the macrobenthos (animals with body size <0.05 mm, dominated polychaetes and crustaceans). Hossain et al. studied grain size in the BES.[10] This analysis showed domination of sand fractions in sediments, giving a particle size distribution as follows: sand > clay > silt. Seaward stations yielded a greater sand size fraction and lower organic matter content (< 4 %), compared to the usually low-energy landward stations, which constituted a relatively higher proportion of clay and silt in the sediments, and which were relatively rich in organic content (> 5%). The observed variation in organic matter relative to grain size for the various stations complied with

our prediction and with the general trend for tropical estuaries; in the BES, organic content is elevated by input from dense mangrove stands and anthropogenic eutrophication. Despite the general tendency of seaward increase in grain size[10], a finer spatial resolution of sampling in the BES could reveal more within-station particle size variation, given the highly variable hydrological features over narrow spaces at some stations. As an example, strong outflowing currents must prevail at small tributary confluences in the upper Sungai Brunei (near Bandar), producing patches of more sandy and less nutrient rich sediments than those observed in the study.

4.2 pH, salinity and carbonate parameter variation

The role of carbonate acidification in estuarine systems that are already acidified by mineral processes has been poorly investigated. This question is addressed in a study by Proum et al.[6] Specifically, variation in surface water pH, salinity, temperature, total alkalinity, pCO2, DIC, calcite saturation and aragonite saturation were studied. Hydrologic characteristics measured at three stations, one from each estuarine region (upper, middle, and lower – BD, SD, PK, respectively, ***Figure 1***), confirmed estuarine-wide rapid seaward increase in pH and salinity. High temporal resolution (30 min) data-logging uncovered tidal fluctuations in pH and salinity that were accentuated upstream (landwards), due to variable mixing of the elevated pCO_2 and acidity in the weakly-buffered hyposaline water there (***Figure 4***). A steep decline in baseline pH was observed during monsoons, presumably due to greater ASS flushing in this season; the baseline decline was again more pronounced in the upper estuary (***Figure 4***, BD). The carbonate system analysis (based in discrete water sampling) showed supersaturation of pCO_2 in the upper and middle BES, indicating that these regions are a net source of atmospheric CO_2, whereas the lower estuarine region appeared more like a net CO_2 sink. pCO_2 levels in the upper BES exceeded values reported for many other estuaries, but were similar to data described for other mangrove or ASS-influenced estuaries. Overall, the study showed complex interactions in the BES between acidification parameters, processes, tides and seasons.[5]

5. Community and organism responses

5.1. Planktonic communities

The planktonic community has been characterized in a study by Majewska et al.[11] Samples were collected at four stations (Chermin (near S. Bunga); BU; Pintu Malim (near BD) and S. Kedayan; Fig. 1) between Aug 2011 to June 2012, covering a range in salinity and (0.4 - 28.5 psu) and pH (5.87 - 8.06). The survey recorded a total of 25 algal families (22 genera of diatoms and seven of dinoflagellates) and one ciliate family. Phytoplankton density varied between 7 and 9107 cells ml^{-1}. Diatoms dominated the communities, with species of *Nitzschia*, *Rhizosolenia* and *Leptocylindrus* having highest abundances. Phytoplankton communities varied seasonally (30% of the total variance) among sample stations (20% of total variation). The interactive effects of pH and salinity, and of pH and temperature, explained 16.7% and 17.5% of the total observed variation, respectively.

5.2. Mudflat bacterial diversity

Bolhuis et al.[5] surveyed the surface intertidal mud bacterial diversity for samples collected at six stations over 40 km along the BES (PR; Damuan, DM; BD; S. Besar, BE; PP; MR; ***Figure 1***). The diversity was compared from community fingerprinting analysis using 16S rRNA gene based denaturing gradient gel electrophoresis, and from 16S rRNA gene sequencing and phylogenetic analyses. Results showed functionally conserved, diatom-dominated communities constituting mainly novel species. Species composition at each station was 50-70% unique. Clustering of the sequences commonly occurred, indicating that proteobacterial diversity related to the acidity/salinity gradient of the BES. On the whole, the diversity (considering all phyla) varied in a predictable way with the physical parameters. Mudflat communities comprised typical functional groups of microorganisms associated with photosynthetic carbon flux, sulphur cycling (Gamma- and Deltaproteobacteria) and decomposition (Bacteroidetes). Structurally, however,

communities were discretely distributed along the BES gradient, constituting largely novel bacterial species. This study provides the first insights into patterns of bacterial community structure in a tropical South East Asian estuarine system that experiences highly variable pH and salinity conditions.

5.3. Benthic infaunal communities

Hossain & Marshall[9] investigated infaunal macrobenthic community structure, for samples collected at S. Kedayan, DM, BD, BE and MR (***Figure 1***) between July 2011to June 2012. Sediment pore-water salinity (8.07 to 29.6 psu) was found to decline landwards in accordance with the above-sediment estuarine water salinity (3.58 to 31.2 psu), but interestingly, pore-water pH (6.47- 7.72 units) was remarkably more invariable among stations along the gradient compared to the estuarine water pH (5.78- 8.3 units). The implication is that communities along BES are more strongly influenced by salinity than by pH. Thirty six species were recorded, with neritid polychaetes (*Neanthes* and *Onuphis conchylega*) and a corophiid amphipod dominating. Calcified microcrustaceans (*Cyclopoida* sp. and Corophiidae sp.) were abundant at all stations; there was no clear distinction in BES distribution between calcified and non-calcified infaunal groups. Species richness increased seawards, though abundance (density) showed no distinct directional trend. Diversity indices were largely positively correlated with salinity and pH. Three faunistic assemblages were observed: (*i*) nereid-cyclopoid-sabellid, (*ii*) corophiid-capitellid and (*iii*) onuphid- nereid-capitellid. These assemblages respectively associated with low salinity/pH and muddy sediment, low salinity/pH and sandy sediment, and high salinity/pH and sandy sediment. A multivariate analysis confirmed that species distribution and community structuring are more strongly influenced by sediment particle properties than by water chemistry (either pH or salinity). In conclusion, infaunal estuarine communities are generally well-adapted to cope with highly acidic conditions, and are less likely exposed and probably less vulnerable to estuarine water acidification than epibenthic or pelagic communities.

5.4. Epibenthic faunal communities

Hardsubstrata, such as natural or artificial rocks, concrete or wooden surfaces of mangroves, driftwood, jetties, embankments and bridges, are prevalent in the BES, providing habitat for a variety of animals and plants. Hossain et al.[14] studied variation in species composition, abundance and community structure of BES intertidal epifaunal invertebrates (BD, SD, BU, and PB; ***Figure 1***). Species richness, diversity and abundance were highest at the Bedukang, low in the mid-estuary (Serdang and Bunga) and relatively high again near Bandar. Epibenthic macrofaunal diversity was low (34 in 72 samples), reflecting inadequate taxonomic resolution; however, abundances were high with around 100-300 individuals per 100 cm^2. Three distinct communities were observed: a tanaid-polychaete community in upper estuary, a mussel-dipteran community in mid-estuary and a mussel-amphipod-dipteran dominated community in the lower-estuary. The most seaward station had more than double the abundance of hard substratum macrofauna compared to the other stations. In contrast with infaunal communities, which apparently mainly influenced by salinity variation, the epifaunal communities are likely similarly influenced by both estuarine water pH and salinity. While the seaward diversity probably associates with incursion of typical marine species, the high diversity at Bandar could relate to species favoring nutrient-enriched conditions.

5.5. Ecological processes (barnacle recruitment/settlement on wooden poles)

Barnacles (*Balanus* sp.) are abundant on hard surfaces throughout the BES, settling on natural rocky outcrops, mangrove roots and trunks, and on artificial wooden and concrete walls and jetties. A field study was undertaken by Adam and Marshall[15] to assess whether pH/salinity influenced barnacle recruitment, settlement and early growth in the BES. Wooden poles were embedded into the seabed within the intertidal zone at three locations (DM, S. Kedayan and SD; ***Figure 1***) and barnacle parameters were assessed

following collection every month, over 3 months. The study also investigated vertical distribution and microscale hydrological effects around the poles. Interestingly, the results suggested that acidification is not the dominant factor effecting barnacle settlement and early growth along the BES. Recruitment and settlement are apparently effected by the dynamic combination of conducive environmental conditions and high larval supply. Furthermore, nutrient enrichment was suggested to induce more rapid barnacle growth, despite the stressful environmental conditions in the Kedayan area. Further investigation is required to tease apart the confounding influences of larval supply and nutrient enrichment.[15] The wooden pole approach was nonetheless revealing, and showed that several other key taxa (including the serpulid tubeworms, probably *Hydroides*) colonize the poles at the extremely acidic study sites.

5.6. Ecological processes (barnacle size/density on snail shells)

To assess barnacle age/size structure across the pH/salinity gradient, a novel approach was followed, using barnacle settlement on living gastropod shells (*Indothais gradata*) (***Figure 5***).[16] Snails were collected at three stations along the BES (Tamoi, TM, BD, PB; ***Figure 1***), on two occasions, separated by a seven-year period (2005 and 2012). Barnacle growth differed significantly between years and among stations. Barnacle size (standardized to the same shell age) was lower upstream, suggesting an effect of acidification on growth, an observation contrasting with that for early barnacle growth (see above). An interesting unexpected result was the significant difference in surface area of *Indothais* shells between 2005 and 2012; shell surface area was less at 2012. Differences in width-length ratios of shells suggested a cohort effect, relating to local extinction and new recolonization at some stations. Shell surface area decreased landwards (more acidic sites), which might confound the barnacle growth result, due to crowding (competition for space) on smaller shells.

5.7. Physiological and behavioural responses of snails to acidification

Organism-level responses to extreme and rapid coastal acidification were investigated, with special reference to the physiological and behavioral capacities of *Indothais gradata.*[13] Several very novel findings were revealed when comparing laboratory responses between populations from opposite ends of the BES (BD and PB; ***Figure 1***). The pH range for aerobic performance under acutely increasing mineral acidity (appropriate natural rates) was similar for the populations; however, the lower threshold supporting high aerobic function (4.54 - 5.14 units) was much lower than expected, considering the present and past pH levels experienced. CO_2-acidification raised the threshold to 6.3 units, above that of mineral acidification. Population differences were observed for the time course for behavioral and physiological recovery under stable lowered pH and salinity. Seaward populations showed reduced capacity to recover cardiac performance under chronic pH and salinity reductions, but when free to move under these conditions, they quickly became more active and attempted to escape from the water; in contrast the landward population showed little movement. These capacity differences offer novel insights into physiological mechanisms employed by coastal gastropods to deal with highly fluctuating and different sources of acidification (mineral versus CO_2). They suggest that hypercapnia (rather than pH) associated with elevated pCO2 is the key to regulating snail aerobic physiology. This and other physiological observations have consequences for generalizing of effects of marine acidification across taxonomic, physiological and ecological ambits.[13]

5.8 Snails as indicators of metal contamination

Acidification impacts estuarine ecology, but it can also change availability of contaminants (via metal speciation) to organisms. Proum et al. undertook a metal pollution biomonitoring study in the BES, in particular, assessing the accumulation of Cd, Cr, Cu, Fe, Mn, Ni, Pb, and Zn in *Indothais gradata.*[12] Because this snail inhabits both hard and soft substrata, (sediments, wooden pillars, rocky outcrops, etc.) it was possible to compare metal accumulation (*i*) between substrata (habitats), (*ii*) between the

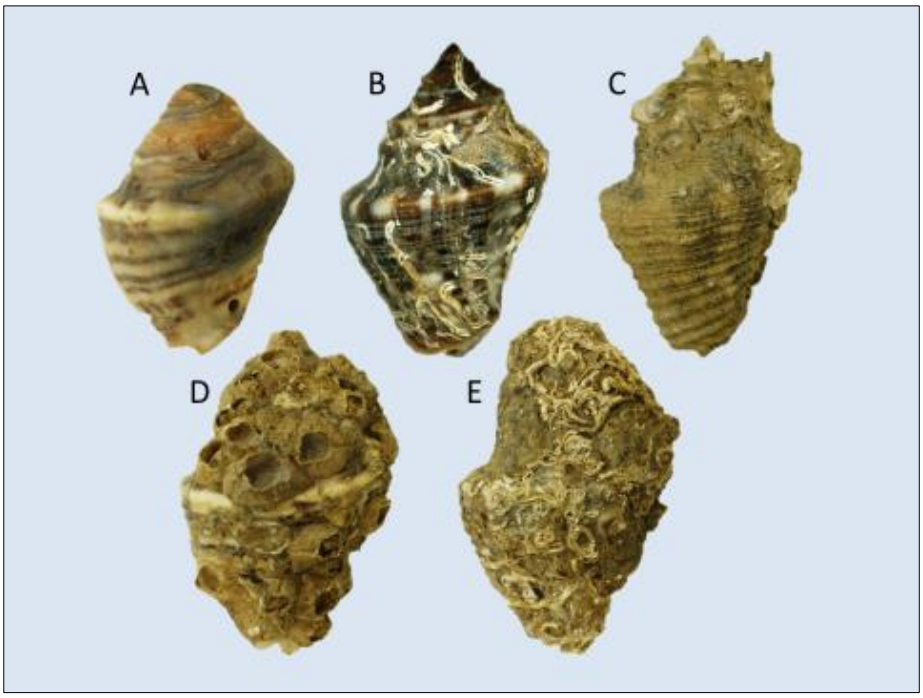

Fig. 5. *Indothais gradata* snails collected from Bandar (A, B), Bedukang (C) and Tamoi (D, E), showing acidic dissolution, epibiont colonization and sediment deposition of shells.

shells and soft tissues of snails and (*iii*) among sample stations along the estuarine gradient. The study found that substratum type had no effect on metal burden. Whereas higher concentrations of essential metals occurred in the tissues relative to the shells, shell metal accumulation was vastly more discriminatory among the sample stations. This and good correlations among different metals, suggest that shells represent better biomonitor tools than tissues for conditions of small estuarine contamination, as in the BES. Domestic pollution was suggested to be most severe, indicated by greatest contamination at Bandar, the entry point of BES tributaries (especially S. Kedayan) feeding from Gadong and Kuilap. Contaminant levels fell off sharply upstream and downstream of Bandar, indicating a limited freshwater mixing or seaward tidal forcing. Fe accumulation in *Indothais* shells was distinctly greater than that of the other metals, consistent with the naturally highly pyritic soils (FeS_2). The effect of acidification in raising the metal burden in the BES, was not clearly shown, when compared with published data for other estuaries; this nonetheless deserves more critical consideration.

6. Concluding remarks

Overall the findings suggest a highly integrated and functional marine ecosystem along the BES to at least Bandar, despite the steep salinity and acidity gradient. Although diversities were relatively low at Bandar, abundances were often high in the case of key marine taxa, presumably largely relating to high nutrient loads. Clearly many taxa are physiologically and behaviourally adapted to the highly dynamically variable salinities and acidities, and supersaturated CO_2 at Bandar and landwards. The fluctuating nature of the physicochemistry suggests periods of amelioration, in which near optimal performance of organisms can be achieved. *Indothais* snails are also well equipped behaviourally to isolate themselves under extreme conditions, reducing exposure. A variety of taxa (mussels, oysters and *Hydroides* – polychaetes that form calcareous tubes) were found to colonize wooden poles at Damuan; whether they are capable of sustaining energetic levels to grow to full size remains to be known. Additional to abilities to behaviorally and physiologically adapt to and secrete calcareous structures under high acidity, communities along the entire BES were found to recover following die-backs during extreme conditions (DJM,

personal observation). Generally, these studies have vastly advanced understanding of organism and community responses to the physical stress characterizing the BES, and show that the BES represents an excellent natural laboratory to explore marine acidification impacts.

Nonetheless cognizance should be given to the limitations with working in estuaries. A major limitation is the pH-salinity correlation, which usually makes it difficult to unravel either effect. Other abiotic factors may be correlated with these, such as contamination. Thus, extrapolation to OA situations from EA observations should be made with reservation; however, much knowledge gained from estuarine studies can be integrated with ocean acidification frameworks. There were several commonalities in benthic community structure variation along the estuarine acidity gradient studied and a pCO_2 gradient associated with vent systems.[9,23] To tease out the effect of acidity on estuarine community structure, comparison could be made between similar kinds of estuaries that are either additionally acidified or show high pH waters. In acidified estuaries, comparisons between infaunal (less acidity variation) and epifaunal (more acidity variation) communities may prove to be useful; though care needs to be made to prevent degassing when sampling and measuring the within-sediment pH. Estuarine species which already experience extreme conditions are excellent models for assessing capacities for adaptation in acidified environments. Different physiological responses of *Indothais* warn against approaches based on CO_2 acidification in OA work, which confounds the effects of acidity and hypercapnia in laboratory experiments[13]; while these factors are correlated naturally under OA frameworks, unraveling mechanisms becomes more difficult when they are confounded in studies.

There are omissions in the BES suite of studies of crucial factors relating to estuarine ecology. This is true especially for turbidity and nutrients. These are important to estuarine structure and functioning; localized nutrient enrichment can possibly be inferred in cases where acidity has no effect on distribution. This was found in the plankton and barnacle studies; nutrient enrichment and planktonic blooms probably increase barnacle growth, regardless of acidification level - these situations are ripe grounds for further investigation. There is also a need for long-term, high-temporal-resolution monitoring of the hydrology of the BES and for relating such data to local weather conditions. Greater understanding of impacts on the BES ecology is especially relevant to the context of the bridge construction over this system. The interconnectivity of the BES and nearby coastal systems (which include sensitive coral reefs) could also potentially yield highly-innovative future research.

Acknowledgements

This research was supported by the Brunei Research Council (UBD/S&T/16). We are thankful for the collaborative efforts of Roger Bamber, Henk Bolhuis, Tapas Chatterjee, Sergey Ermilov, Jason Hall-Spencer, Roksana Majewska, Vladimir Pešić and Henriette Schluepmann.

References

[1] IPCC, 2013. Climate Change **2013**

[2] J.C. Orr, V.J. Fabry, O. Aumont, et al., *Nature* **2005**, 437.

[3] K. Caldeira and M.E. Wickett. *Nature* **2003**, 425.

[4] D.J. Marshall, J.H. Santos, K.M.Y. Leung and W.H. Chak, *Mar. Environ. Res*., **2008**, 66.

[5] H. Bolhuis, H. Schluepmann, J. Kristalijn, J., Z. Sulaiman, and D.J. Marshall, *Aquat. Biosyst.*, **2014**, 10.

[6] S. Proum, J.H. Santos, L.H. Lim and D.J. Marshall, *Cont. Shelf. Res.*, **2016a**, in review.

[7] G. Grealish, R. Fitzpatrick, A.R. Ringrose-Voase, W. Hicks, *Inland acid sulfate soil systems across Australia.* Ed. R. Fitzpatrick and P. Shand. **2008**.

[8] D.J. Marshall, *J. Mar. Biol. Assoc. UK*., **2009**, 89.

[9] M.B. Hossain and D.J. Marshall, *Aquat. Biosyst*. **2014**, 10.

[10] M.B. Hossain, D.J. Marshall and S. Venkatramanan, S., 2014. *Carpathian J. Earth. Environ. Sci*., **2014**, 9.

[11] R. Majewska, A. Adam, N. Mohammad-Noor, P. Convey, M. de Stefano and D.J. Marshall, *J. Trop. Ecol.*, **2016**, in press.
[12] S. Proum, J.H. Santos, L.H. Lim and D.J. Marshall, *Reg. Stud. Mar. Sci.*, **2016b**, in press.
[13] S. Proum, C. D. Harley, M. Steele[1] and D. J. Marshall, *J. Exp. Biol.*, **2016c**, in review.
[14] M.B. Hossain D.J. Marshall and J. Hall-Spencer. **2016**, submitted.
[15] A. Adam and D.J. Marshall. **2016a**, submitted.
[16] A. Adam and D.J. Marshall. **2016b**, submitted.
[17] R. Bibby, P. Cleall-Harding, S. Rundle, et al., *Biol. Lett.*, **2007**, 3.
[18] J. M. Hall-Spencer, R. Rodolfo-Metalpa, S. Martin et al. *Nature*, **2008**, 454.
[19] Y. Sui, H. Kong, X. Huang et al., *Chemosphere*, **2016**, 155.
[20] W.J. Cai, *Annu. Rev. Mar. Sci.*, **2013**, 123–145.
[21] Hu, W.J. Cai, *Geophys. Res. Lett*. **2013**, 40.
[22] W.D. Zhai, M.H. Dai, W.J. Cai, Y.C. Wang et al. *Mar. Chem.* **2005** 93.
[23] K. J. Kroeker, F. Micheli, M. C. Gambi et al., *PNAS*, **2011**, 108.

Appendix. **BES studies published in peer-reviewed journals (2011 to 2016)**

1. Proum, S., Harley, C., Steele, M., & Marshall, D.J. (2016). Physiological flexibility and behavioural isolation help snails flourish in fluctuating acidic estuarine waters. *Marine Biology* (in review).
2. Proum, S., Santos, J.H., Lim, L.H. & Marshall, D.J. (2016). Spatial and temporal variation in carbonate chemistry, pH and salinity in the surface water of a pyrite-acidified, tropical estuarine system. *Coastal Shelf Research* (in review).
3. Proum, S., Santos, J.H., Lim, L.H. & Marshall, D.J. (2016). Metal accumulation in the tissues and shells of *Indothais gradata* snails inhabiting soft and hard substrata in an acidified tropical estuary (Brunei, South East Asia). *Regional Studies in Marine Science* (in press).
4. Majewska, R., Adam, A., Mohammad-Noor, N., Convey, P., de Stefano, M. & Marshall, D.J. (2016). Spatio-temporal variation in phytoplankton communities along a salinity and pH gradient in a tropical estuary (Brunei, Borneo, South East Asia). *Journal of Tropical Ecology* (in press).
5. Hossain, M.B. & Lauren, H. (2016). New species *Victoriopisa bruneiensis* and *Apocorophium acutum* (Chevreux, 1908) from Brunei (Crustacea: Peracarida: Amphipoda). *Zootaxa*, 4117, 375-386.
6. Bamber, R.N. & Marshall, D.J. (2015). Tanaidaceans from Brunei, V. The Leptocheliidae (Crustacea: Peracarida: Tanaidacea), with four new species. *Zootaxa*, 3948, 342-360.
7. Hossain, M.B. & Marshall, D.J. (2014). Benthic infaunal community structuring in an acidified tropical estuarine system, *Aquatic Biosystems*, 10, 11.
8. Hossain, M.B., Marshall, D.J., Senapathi V. (2014). Sediment granulometry and organic matter content in the intertidal zone of the Sungai Brunei estuarine system, northwest coast of Borneo. *Carpathian Journal of Earth and Environmental Sciences*, 9, 231 – 239.
9. Hossain, M.B., Dev Roy, M.K. & Lee, B.Y. (2014). First record of the brachyuran crab, *Baruna trigranulum* Dai and Song, 1986 (Crustacea: Brachyura: Camptandriidae) from Sungai Brunei Estuary, Brunei Darussalam. *Asian Journal of Animal Sciences*, 8, 93-97.
10. Bolhuis, H., Schluepmann, H., Kristalijn, J., Sulaiman, Z. & Marshall, D.J. (2014). Molecular analysis of bacterial diversity in mudflats along the salinity gradient of an acidified tropical Bornean estuary (South East Asia). *Aquatic Biosystems*, *10*(1), 1.
11. Chatterjee, T., Fernandez-Leborans, G., & Marshall, D. J. (2014). New records of ciliate epibionts (Ciliophora: Suctorea) from Brunei Darussalam. *Marine Biodiversity Records*, *7*, e87.
12. Hossain, M.B., Bamber, R.N. (2013). New record of a wood-boring isopod, *Sphaeroma terebrans* (Crustacea: Sphaeromatidae) from Sungai Brunei estuary, Brunei Darussalam. *Marine Biodiversity Records*, 6, e18.
13. Bamber, R. N., & Marshall, D. J. (2013). Tanaidaceans from Brunei III. A New Genus and Two New Species of Shallow-water

sphyrapodids (Crustacea: Peracarida: Tanaidacea) from the South China Sea. *Species diversity*, 18, 255-267.
14. Ermilov, S. G., Chatterjee, T., & Marshall, D.J. (2013). Two new species of oribatid mites of Oripodoidea (Acari: Oribatida) from Brunei. *Annales Zoologici* 63, 393-400.
15. Pešić, V., Chatterjee, T., & Marshall, D.J. (2013). Marine water mites (Acari: Hydrachnidia: Pontarachnidae) from the Brunei Bay, with a description of one new species. *Cahiers de Biologie Marine*, 54, 405-410.
16. Bamber, R.N. (2013). Tanaidaceans from Brunei, IV. The Families Kalliapseudidae, Pagurapseudopsidae, Parapseudidae and Apseudidae (Crustacea: Peracarida: Tanaidacea: Apseudomorpha), with descriptions of a new genus and six new species. *Zootaxa*, 3734, 401-441.
17. Chatterjee, T., Marshall, D. J. & Pešić, V. (2012). New records of *Copidognathus* mites (Acari: Halacaridae) from mangroves in Brunei Darussalam with descriptions of two new species. *Zootaxa*, 3269, 18-30.
18. Chatterjee, T., Marshall, D. J. & Pešić, V. (2012). First record of *Agauopsis* mites (Acari: Halacaridae) from Brunei Darussalam and notes on the distribution of the *Agauopsis brevipalpus* group. *Acta Biologica*, 19, 113-114.
19. Bamber, R. N., Chatterjee, T. & Marshall, D. J. (2012). Inshore apseudomorph tanaidaceans (Crustacea: Peracarida) from Brunei: new records and new species. *Zootaxa*, 3520, 71-88.
20. Chatterjee, T., Marshall, D. J., Guru, B. C., Ingole, B. S. & Pešić, V. (2012). A new species of the genus *Acarothrix* (Acari: Halacaridae) from Brunei Darussalam and India. *Cahiers de Biologie Marine*, 53, 541-546.
21. Pešić, V., Chatterjee, T., Marshall, D. & Pavićević, A. (2011). New records of water mites (Acari: Hydrachnidia) from Brunei Darussalam, Borneo, with descriptions of two new species. *Zootaxa*, 3018, 50-58.

Coral diversity and coral reef environment in Brunei Darussalam

*Yasuaki Tanaka**

Environmental and Life Sciences, Faculty of Science, Universiti Brunei Darussalam, Jalan Tungku Link, Gadong BE1410, Brunei Darussalam

**corresponding author email: yasuaki.tanaka@ubd.edu.bn*

Abstract

This article reviews the coral diversity and coral reef environment in Brunei Darussalam, in comparison with the other regions in the South China Sea (SCS). Extensive surveys on corals had not been conducted in Brunei Darussalam for a long time but the recent efforts of coral identification have revealed that approximately 400 species of scleractinian corals inhabit in Brunei seawaters, which is close to the highest diversity in the SCS. The most dominant coral family in species number was Acroporidae, which accounted for 30% of the coral species inventory. Using the published data on coral diversity in the SCS, multivariate analyses showed that the number of coral species in any tested coral family (Acroporidae, Agariciidae, Fungiidae, Lobophylliidae, Merulinidae, and Poritidae) in a region is significantly correlated with the total number of coral species for that region, indicating that the coral diversity in any family reflects the coral diversity in the whole ecosystem. Although a high coral diversity was confirmed in Brunei Darussalam, several threats to corals have been reported. Regular monitoring of the coral reef status is required to promptly detect undesirable environmental changes in the future.

Index Terms: coral diversity, South China Sea, environmental changes, conservation

1. Distribution of coral reefs in Brunei

Brunei Darussalam (hereafter Brunei) is located at the northwest coast of Borneo and has many submerged patch reefs (***Figure 1***). The total area of coral reefs in Brunei is estimated to be approximately 100 km^2.[1,2,3] Most of the reefs develop 4−30 km offshore from the coast and have a depth of more than 5 m.[2] Coral reefs have not developed extensively on the coast, which is most likely due to high turbidity of seawater caused by suspended particles.

Pelong Rocks (Pulau Pelong-Pelongan) are a series of small islets stretching 500 m north and south (***Figure 1***). Because of the relatively short distance from the coast (ca. 4 km), Pelong Rocks are the most accessible coral reef in this country. The reef has a reef flat with the depth of 3−7 m and the sea bottom is mainly covered with sand, rubble, and hard corals. Two Fathom Rocks is located approximately 8 km off the coast and has three uplifted seafloor regions over an area of 5 km^2. Two of them are shallower (4 m) than the other one (10 m). Pulau Punyit is a rocky island of 100 m long and 30 m wide, which is located 600 m off the coast of Brunei Cliff.

2. Coral diversity in Brunei Darussalam

The first extensive surveys on Brunei's coral reefs was conducted in the 1980s.[2] The researchers studied the diversity of hard corals at Pelong Rocks, Two Fathom Rock, and Pulau Punyit and found 88 coral species in total. The highest diversity (number of coral species) was recorded at Pelong Rocks (60 species) and the lowest diversity was at Pulau Punyit (19 species). The low coral diversity at Pulau Punyit was considered to be due to low visibility of seawater, which was caused by sediment suspension. Acroporidae and Merulinidae were the most dominant coral families found in their study. The coverage of corals occupied 3−40% of the seafloor at Pelong Rocks and Two Fathom Rock, depending on the survey transect, while no survey on coverage was

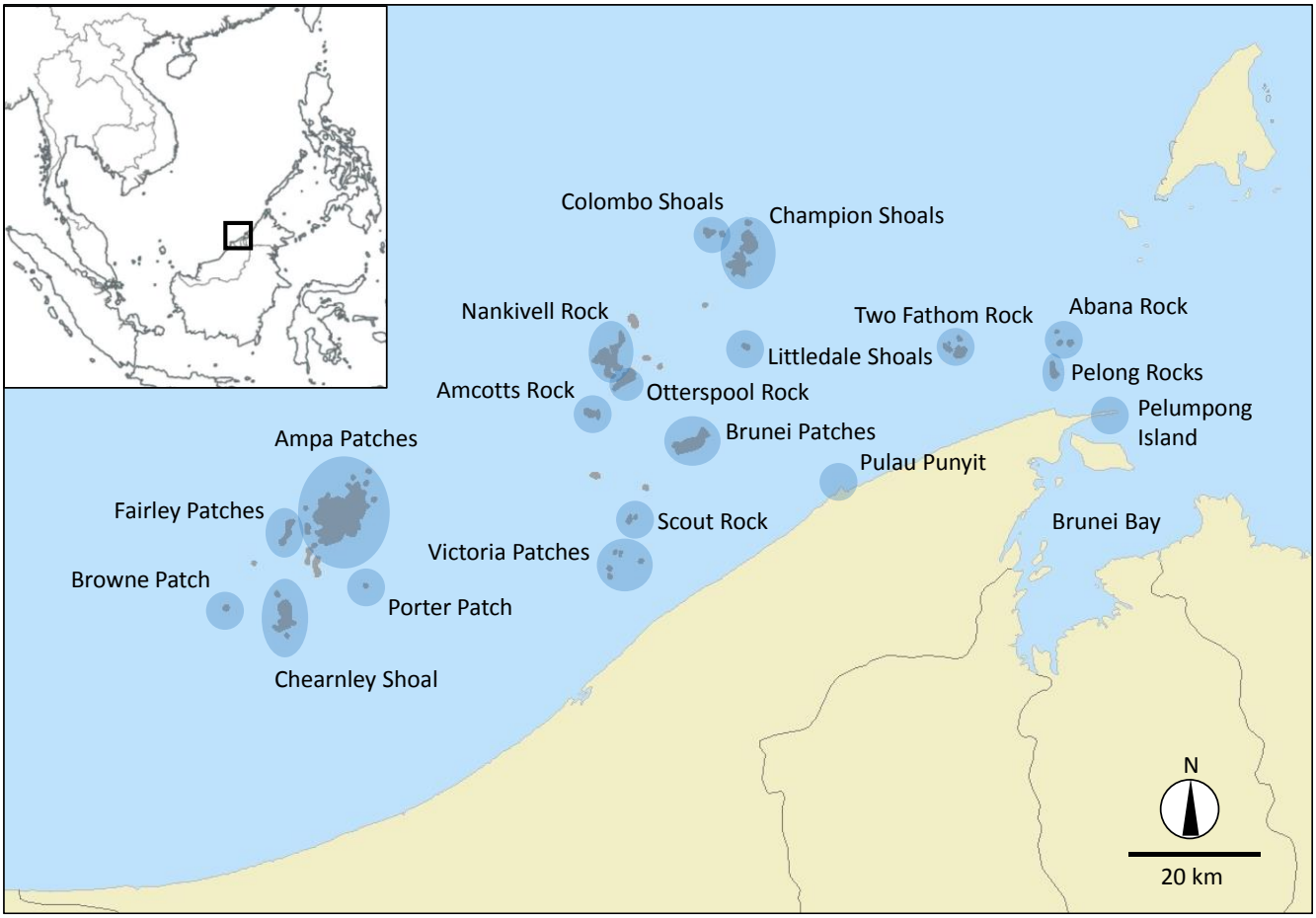

Figure 1. The location of Brunei Darussalam on Borneo (upper left) and major coral reefs in the country. The reef locations and original map was provided by UNEP-WCMC (http://www.reefbase.org/).

performed at Pulau Punyit due to poor coral cover and high turbidity.[2]

Though the total number of coral species in Brunei was lower than those in Singapore or Peninsular Malaysia at the time of the study[4,5], this did not mean that the coral diversity was actually lower than those regions, considering that the study areas were limited to the three sites.[2] Because the studied three sites are located relatively near from the coast, it was expected that offshore reefs could have a higher diversity of corals.

More extensive surveys on Brunei's coral diversity have been conducted and published recently.[3,6,7,8] In addition to many offshore coral reefs, a coral community was also discovered at the mouth of Brunei Bay, Pelumpong Island (***Figure 1***). In total, 404 coral species have been reported from the 14 families.[3,8] The family with the highest number of species was Acroporidae, which had 119 species and accounted for 30% of the total number of coral species. The second and third largest families were Merulinidae (87 species, 22%) and Fungiidae (35 species, 9.0%), respectively (***Figure 2***). Comparing to the surveys in the 1980s, the dominant families of corals, i.e., Acroporidae and Merulinidae, have apparently not changed during the last two decades. However, this cannot be certain because earlier survey coverage was not comparable to recent, more intensive surveys.

The coral diversity seems to show differences among the sites in Brunei. For example, the diversity of Fungiidae (mushroom corals) was relatively high at Brunei Patches (Hornet Reef), Pelong Rocks, and Porter Patch, while it was low at Otterspool Rock, and Colombo and Champion Shoals.[7] The number of coral species found at Pelumpong Island (34) was apparently lower than

the other sites, which is likely due to lower salinity and higher turbidity affected by Brunei River.[6]

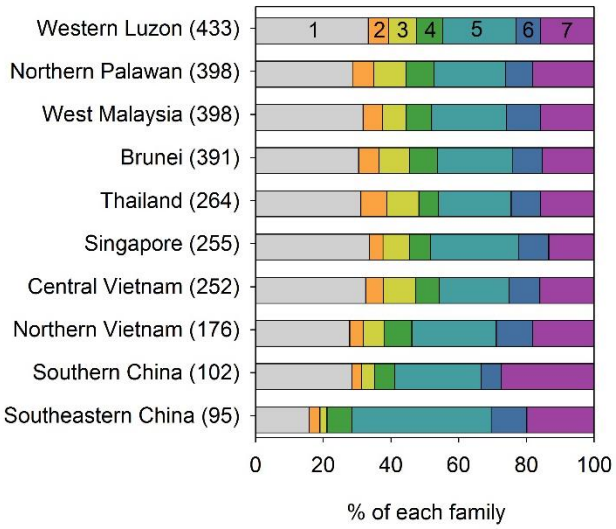

Figure 2. The proportion percentages of each coral family in the regions in the South China Sea. 1: Acroporidae, 2: Agariciidae, 3: Fungiidae, 4: Lobophylliidae, 5: Merulinidae, 6: Poritidae, 7: Others. The number in parantheses shows the total number of coral species found in the region. The original data are obtained from Huang et al.[8]

3. Comparison in the South China Sea

When the coral diversity is compared with the other regions in the South China Sea (SCS), the composition of the Brunei's coral species was most similar to those of Luzon Island and Palawan Island in the Philippines and was significantly distinct from the other regions.[8] The southern coastline of China (e.g., Hong Kong, Hainan) had the lowest number of coral species (151 species) in the SCS and had the lowest similarity compared to Brunei, Luzon, and Palawan Islands (BLP). When the family compositions were compared between these two distinct regions, using the data summarized by Huang et al.,[8] the families Fungiidae (8.3−9.5%) and Agariciidae (6.0−6.3%) accounted for higher percentages in BLP than the southern and southeastern coastline of China (***Figure 2***). On the other hand, the family Merulinidae accounted for lower percentages in BLP. One of the major causes for the difference between these two regions could be the latitude, which changes annual average seawater temperature.[8]

Another cause for the difference in coral diversity in the SCS could be the effect of terrigenous waters: the coastal areas in Brunei and the Philippine islands receive less river water inputs from the land than those in the Asian continental coastline, which results in distinct coastal seawater conditions and coral diversity.[8] Tropical rivers in Southeast Asia often contain high concentrations of nutrients and terrigenous sediment particles.[9] Coral metabolisms and coral reef ecosystem structures are affected by terrigenous waters from various perspectives.[10] For example, high turbidity of seawater (sedimentation) reduces the survival rate of juvenile corals.[11] Nutrient enrichment alters the balance of a symbiotic relationship between a coral animal host and its endosymbiotic algae.[12]

Using the previously published data summarized by Huang et al.,[8] the present review found that the number of coral species in any tested coral family group (Acroporidae, Agariciidae, Fungiidae, Lobophylliidae, Merulinidae, and Poritidae) in a region was significantly correlated with the total number of coral species in the region (***Figure 3***). This indicates that the number of coral species in any family group is strongly and positively related to the whole coral diversity in the region. In other words, the coral diversity in a region can be speculated from the number of coral species in any family. For example, according to the linear regression, the number of Acroporidae species increases by 33 when the total number of coral species in the region increases by 100.

4. Threats to corals in Brunei Darussalam

Because most corals in Brunei inhabit reefs off the coast, they seem not to be affected by terrigenous freshwater discharge of rivers. Nonetheless, some threats to corals have recently been reported in Brunei.[13] The first threat is high seawater temperature, which is a global concern for conserving coral reefs.[14] Under intolerable temperature conditions, many corals lose the endosymbiotic algae and consequently become bleached.[15] Because a coral animal host acquires organic matter from the endosymbiotic algae through photosynthesis, the loss of this symbiotic

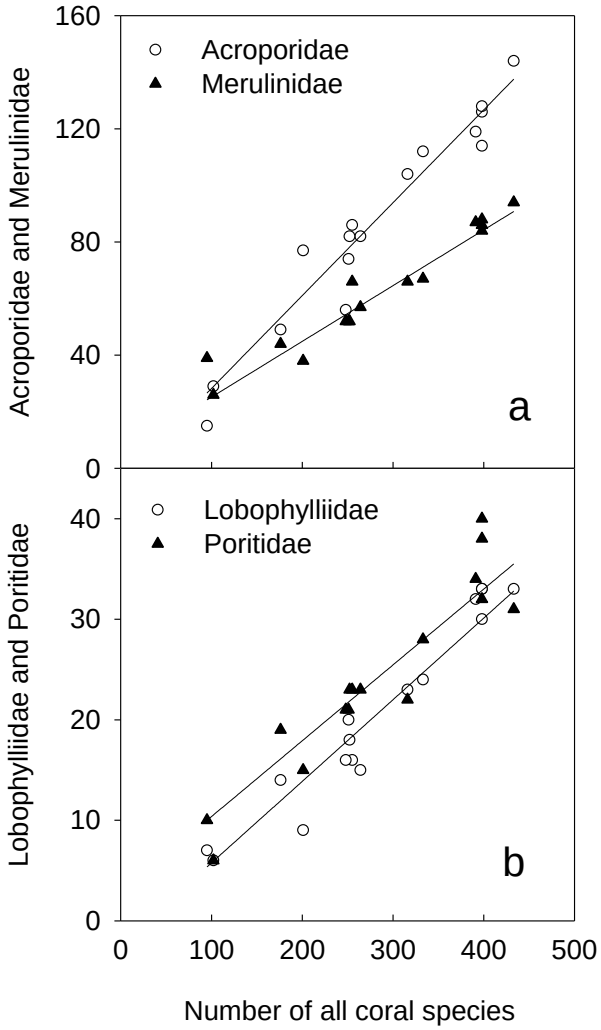

Figure 3. The correlation between the total number of coral species and the number of each family (a: Acroporidae and Merulinidae, b: Lophophylliidae and Poritidae) in various regions in the South China Sea. The two parameters were significantly correlated for all of the coral families ($p < 0.0001$) and the straight lines show linear regressions. The original data are obtained from Huang et al.[8]
Acroporidae: $y = 0.328x - 4.57$ ($r^2 = 0.999$)
Merulinidae: $y = 0.197x + 5.50$ ($r^2 = 0.997$)
Lobophylliidae: $y = 0.0812x - 2.35$ ($r^2 = 0.994$)
Poritidae: $y = 0.0754x + 2.83$ ($r^2 = 0.987$)

partner means the depletion of energy for the coral host.[16] There was no record of major coral bleaching events in Brunei before 2010. In July 2010, a serious coral bleaching event was reported at Littledale Shoal, even though most corals inhabit at the depth of more than 5 m, where the seawater temperature is usually lower than the sea surface temperature.[13] However, the bottom seawater temperature at this site was slightly above 30°C when the bleaching was observed.[13] Concurrently, coral bleaching was also observed over extensive areas in the Indian Ocean and Southeast Asia in response to high seawater temperature[17]. These observations demonstrated that even the deeper Brunei reefs are susceptible to the effects of seawater warming at a relatively extensive regional scale.

Another threat to Brunei corals is predation by other marine animals. The crown-of-thorns starfish *Acanthaster planci* is a major coral-eating echinoderm, which is becoming quite common in many coral reefs of the world. *A. planci* was first found in 2008 in Brunei and during an outbreak episode, the live coral cover was reduced by 50% at Littledale Shoal.[1,13] The muricid gastropod *Drupella* spp. were also reported to prey on corals in Brunei and the number seemed to be increasing.[13] The causes of outbreaks of these coral-eating animals are not fully elucidated yet. One of the proposed causes explains that nutrient enrichment at coastal areas due to human activities enhances the production of phytoplankton, which is a food source for the larvae of *A. planci*, and leads to high growth and survival rates of the starfish (but see ref. [1]).[18]

Though most of the coral reefs in Brunei develop more than 4 km off the coast, some corals inhabit close to the coast near Brunei Bay. Pelumpong Island and Pulau Punyit are two such sites (***Figure 1***). In particular, corals near Pelumpong Island might be affected by terrigenous waters in Brunei Bay, which usually have high turbidity and nutrients, and low salinity and pH.[19] As the coastal terrestrial areas connected to Brunei Bay become urbanized, more human-derived substances such as nutrients might be discharged into the bay and subsequently offshore coral reefs.

5. Summary and future studies

In summary, recent extensive surveys confirmed a high coral diversity in Brunei Darussalam. The species composition was similar to the other east parts of the SCS such as Palawan Island. Brunei is presently excluded from the northwestern boundary of the Coral Triangle[20] but after the extensive surveys of the family Fungiidae, it was

suggested that the boundary might need to be reconsidered.[7]

Studies required for the future management and conservation of Brunei coral reefs would be regular monitoring of the reef status. At the time of writing this article, there was little available published data on regular monitoring and evaluation of the coral reef environment over the long term. Both global and local environmental changes might have altered coral reef seawater conditions in the country as discussed above. Attention also needs to be paid to fishing activities because overfishing causes reduction in the grazing pressure on benthic algae and consequently changes the ecosystem structure. The enhanced growth of benthic algae might outcompete corals and decrease the resilience of corals to other stresses.[21] The conditions of the Brunei coral reef environment need to be monitored and evaluated carefully from these various perspectives.

Acknowledgements
This study was supported by the Brunei Research Council (BRC) grant (S&T-14: Scleractinian Coral Diversity, Reproduction, Growth Processes and Reef Accretion in Relation to Ocean and Coastal Regimes in Bruneian Waters). I am grateful to Dr. David J. W. Lane for reviewing this article.

References

[1] D. J. W. Lane, *J. Mar. Biol. Assoc. U. K.*, **2012**, 803.
[2] L. M. Chou, M. W. R. N. De Silva and A. T. White, *The coastal environmental profile of Brunei Darussalam*, Ed. T-E.Chua, L. M. Chou and M. S. M. Sadorra, **1987**.
[3] E. Turak and L. DeVantier, *Field guide to reef-building corals of Brunei Darussalam*, Ministry of Industry and Primary Resources, Brunei Darussalam, **2011**.
[4] S. H. Chuang, *Proc 3rd Int Coral Reef Symp*, **1977**, 55−63.
[5] C. Betterton, *Malay. Nat. J.*, **1981**, 171.
[6] D. J. W. Lane and G. P. C. Lim, *Galaxea*, **2013**, 166.
[7] B. W. Hoeksema and D. J. W. Lane, *Raffles B. Zool.*, **2014**, 566.
[8] D. Huang, W. Y. Licuanan, B. W. Hoeksema, C. A. Chen, P. O. Ang, H. Huang, D. J. W. Lane, S. T. Vo, Z. Waheed, Y. A. Affendi, T. Yeemin, L. M. Chou, *Mar. Biodiv.*, **2014**, 157.
[9] T. Miyajima, C. Yoshimizu, Y. Tsuboi, Y. Tanaka, I. Tayasu, T. Nagata and I. Koike, *Biogeochemistry*, **2009**, 243.
[10] K. E. Fabricius, *Mar. Poll. Bull.*, **2005**, 125.
[11] R. Babcock and L. Smith, *Proc. 9th Int Coral Reef Symp.* **2000**, 23.
[12] Y. Tanaka, T. Miyajima, I. Koike, T. Hayashibara, H. Ogawa, *Limnol. Oceanogr.*, **2007**, 1139.
[13] D. J. W. Lane, *Scientia Bruneiana*, **2011**, 51.
[14] N. E. Cantin, A. L. Cohen, K. B. Karnauskas, A. M. Tarrant and D. C. McCorkle, *Science*, **2010**, 322.
[15] Y. Tanaka, M. Inoue, T. Nakamura, A. Suzuki and K. Sakai, *J. Exp. Mar. Biol. Ecol.*, **2014**, 220.
[16] Y. Tanaka, T. Miyajima, I. Koike, T. Hayashibara and H. Ogawa, *J. Exp. Mar. Biol. Ecol.*, **2006**, 110.
[17] K. Tun, L. M. Chou, J. Low, T. Yeemin, N. Phongsuwan, N. Setiasih, J. Wilson, A. Y. Amri, K. A. A. Adzis, D. Lane, J. W. van Bochove, B. Kluskens, N. van Long, V. S. Tuan, E. Gomez, Global Coral Reef Monitoring Network, **2010**, 9.
[18] J. Brodie, K. Fabricius, G. De'ath and K. Okaji, *Mar. Poll. Bull.*, **2005**, 266.
[19] M. B. Hossain and D. J. Marshall, *Aquat. Biosys.*, **2014**, 11.
[20] A. L. Green and P. J. Mous, *TNC Coral Triangle Program Report*, **2008**.
[21] P. Houk, C. Musburger, P. Wiles, *Plos One*, **2010**, e13913

Fermented food in Asia as a source of potential probiotics: Properties and beneficial effects

*Nur Bazilah Afifah Matussin, Yeo Yen Chin, Ilisa Ishan and Pooja Shivanand**

Environmental and Life Sciences, Faculty of Science, Universiti Brunei Darussalam, Jalan Tungku Link, Gadong, BE 1410, Brunei Darussalam

**corresponding author email: poojashivanand@outlook.com*

Abstract

Consumption of probiotic food is known to strengthen the human natural microbiome, thereby providing health benefits to the host. Fermented food products are found to be natural sources of probiotics, also known as 'good' bacteria. Fermentation and pickling of food have long been carried out as a means of preservation and long-term storage. They have been associated with human nutrition and social aspects. In this paper, a compilation of some of the staple fermented foods found in the Asian region has been provided. The mode of action of probiotics and the benefits they bring to the host such as production of antimicrobial agents, blocking the adhesion of pathogens and toxins and modulation of immune responses have been outlined. Consumption of probiotics on a regular basis is known to benefit the overall well-being of the host.

Index Terms: Probiotics, immune response, *L. acidophilus*, *Bifidobacterium*, fermented food, belacan

1. Introduction

Probiotics are microorganisms which, when consumed, generally confer a health benefit on humans and this concept of probiotics was introduced by Russian scientist, Elie Metchnikoff 1907, also known as father of probiotics.[1] According to Snydman, probiotics in many different forms are consumed across the world for the health benefits they offer and some of these are shown to be useful in the treatment of certain medical conditions.[2] Most commonly found probiotic bacteria in fermented products are *Lactobacillus acidophilus* and *Bifidobacterium* sp.[3] Other bacteria may also be used as probiotics as well as several species of yeasts such as *Saccharomyces boulardii*. Furthermore, some of the staple fermented foods used in the Asian families are known to be excellent natural sources of probiotics as shown in ***Table 1***.

Diverse groups of both aerobic and anaerobic microbiota are found in the human body. These microbes, predominantly bacteria regulate the gut's epithelial development and function; a disruption of such interactions may result in disease conditions.[4] The colonization of the gastrointestinal tract depends on the ability of the bacteria to tolerate acidic pH of the stomach and bile before it reaches the intestine. Desirable properties in potential probiotics include antimicrobial activity, triggering immune response and good adhesion ability of bacteria to intestinal cells and mucus. Probiotic bacteria can secrete antimicrobial chemicals thereby forming a physical barrier against the invasion of other pathogenic bacteria and yeasts.[5]

L. acidophilus has been largely proposed as the bacterium used for dietary use. The optimum temperature for this organism for growth is 35-40°C. The bacterium grows at an acidic pH of 6.4-4.5 but ceases to grow when pH 4.0-3.6 is reached. In a study reported by Shah, the acid tolerance of this organism with optimum pH at 5.5-6.0 changed from 0.3% to 1.9% titratable acidity. [3] Low concentrations of peptides and free amino acids in milk results in slow growth of *L. acidophilus*.[3] On the other hand, *Bifidobacteria* normally inhabit the gastrointestinal tract of human beings. This group of bacteria has good

Table 1. Asian food that contain probiotics

Name of food	Country	Composition/ constituents	Probiotic/microorganisms present	References
Balao-balao	Philippines	Traditional food generally consumed as a sauce after sautéing with onions and garlic in vegetable oil	*Leuconostoc mesenteroides, Ediococcus cerevisiae* and *Actobacillus plantarum*	[8]
Belacan	Brunei and Malaysia	Fermented food made from shrimp (*Acetes* species).	*Bacillus* spp., *Straphylococcus* spp. and *Pediococcus* spp.	[9]
Belutak	Brunei	Made up of salted minced meat stuffed into casings of cow's or buffalo's small intestines.	*Lactobacillus, Bacillus, Alcaligenes,Pseudomonas* and *Staphylococci*	[10]
Budu Kupang	Brunei	Mussel and salt.	*Lactobacillus, Bacillus, Corynebacterium* and *Staphylococci.*	[10]
Dosa	India	Prepared with rice and black gram and commonly consumed as part of breakfast.	*Leuconostoc mesenteroides, Streptococcus faecalis, Torulopsis candidia* and *Trichosporon pullulans.*	[11]
Dua Muoi	Vietnam	Sour fermented fruit- or vegetable-derived foods.	*Lb. fermentum, Lb. pentosus, Lb. lantarum, Lb. paracasei, Lb. pantheris, P. pentosaceus* and *P. acidilactici.*	[12]
Douchi	China	Salt fermented soybean food.	*Lactobacillus plantarum, L. brevis, L. fermentum, L. alimentarius, Weissella confuse,W. paramesenteroids, W. cibaria, Pediococcus cidilactici, P. pentosaceus, Enterococcus faecalis, Straphylococcus simulans* and *S. capitis.*	[13]
Idli	India	Steamed cake made from a combination of rice and lentils that have been soaked, ground and fermented into smooth dough.	*L. fermentum, L.delbrueckii, L. lactis, Leuconostoc mesenteroides, Lactobacillus coryneformis, Streptococcus faecalis,* and *Pediococcus cerevisiae.*	[14]
Khalpi	Nepal	Fermented cucumber product.	*L. plantarum L. brevis Leuconostoc fallax*	[15]
Kimchi	Korea	The product of fermentation of over a hundred different types of vegetables and many species of *Lactobacillus* are involved in the fermentation of kimchi.	*Lactobacillus casei* spp., *Lactobacillus acidophilus, Lactobacillus plantarum, Lactobacillus lactis* spp., *Lactobacillus curvatus, Lactobacillus debrueckii* spp., *Lactobacillus fermentum, Lactococcus lactis* spp., *Lactobacillus brevis, Weisella paramesenteroides* and *Lactobacillus sakei.*	[16]
Koumiss	China	A fermented milk drink.	*Lactobacillus plantarum, Lactobacillus helveticus, Lactobacillus casei,* and *Lactobacillus kefiri.*	[17]
Miso	Japan	Prepared from fermented rice, rye, beans or barley in hot water.	*Lactobacilli* spp. *Bifidobacterium* spp.	[18]

Table 1. *(cont.)* Asian food that contain probiotics

Name of food	Country	Composition/ constituents	Probiotic/microorganisms present	References
Natto	Japan	Fermented soybean and rich in menaquinone-7.	*Bacillus subtilis* and *Bifidobacterium* spp.	[19]
Puto	Philippines	Steamed bread made from rice.	*L. mesenteroides, S. faecalis* and *Saccharomyces cerevisiae*	[20]
Sayur asin	Indonesia	A fermented mustard cabbage leaf product.	*Leuconostoc mesenteroides, Lactobacillus confuses, Lactobacillus curvatus, Pediococcus pentosaceus* and *Lactobacillus plantarum*	[15]
Tofu	Taiwan	A traditional fermented chinese snack, also known as stinky soybean curd.	*Lactobacillus, Enterococcus, Lactococcus, Streptococcus, Pediococcus, Leuconostoc* and *Weissella*	[17]
Suan tsai	China	Prepared from cabbage or mustard and has a sour flavor.	*Lactobacillus, Leuconostoc, Pediococcus, Pediococcus pentosaceus* and *Tetragenococcus halophilus*	[17]
Tapai	Brunei and Malaysia	Steamed non-waxy rice with ginger and sugar put into the rice alternatively with pulverized laru.	*Amylomyces rouxii Hansenula* spp., *Rhizopus* spp. and *Saccharomycopsis* spp.	[21]
Tempeh	Indonesia	Soybean dish, also made using other substrates e.g. legumes, cereals and soy-blends, non-leguminous seeds and presscake.	*Lactobacillus fermentum, R. oligosporus, Lactobacillus reuteri, Lactobacillus plantarum* and *Lactococcus lactis*	[22]
Tempoyak	Brunei and Malaysia	Fermented condiment prepared from durian pulp (*Durio zibethinus*).	*L. brevis,L. mesenteroides, Lactobacillus mali,* and *L. fermentum*	[15], [23]
Thua nao	Thailand	Fermented soybeans.	*B. licheniformis, Lactobacilli* spp., *B. cereus, B. megaterium, B. subtilis* and *B. pumilus*	[24]

effects on the gut microbiota and some select strains are known to survive the gastrointestinal transit to reach the colon in abundant number. The optimum pH of growth of *Bifidobacterium* is reported to be 6.0-7.0 and the optimum growth occurs at a temperature of 37-41°C. Nowadays, several different strains of bacteria and yeast are found to have probiotic properties which are more pH stable and thus have beneficial effects on human body for example *L. rhamnosus* GG, *L. casei* Shirota and *Saccharomyces cerevisiae* Bouldarii.[3]

Prebiotics, on the other hand are known as non-digestible food ingredients that beneficially affect the host by selectively stimulating the growth of certain specific bacteria in the colon.[6] Prebiotics essentially serve as 'food' for probiotics. The term synbiotic is used when a product contains both prebiotic and probiotic example: a product containing oligofructose and probiotic *Bifidobacteria* content is a synbiotic.[7]

2. Mechanism of action of probiotics

2.1 Production of antimicrobial agents

Several probiotic microbial strains produce at least one antimicrobial substance which includes organic acids, hydrogen peroxide, diacetyl, carbon dioxide, bacteriocins and related molecules.[25,26] However, none of the above listed substances are known to be the vital constituents in in vivo maintenance of health.[26] It has been observed that when some probiotics are consumed, the faecal pH is reduced.[25,26] The anti-infective effects of lactic acid bacterial culture supernatants in humans studies suggests that some of these substances are likely to be produced *in vivo*.[27] Further investigations are required to establish the effect of probiotic bacteria on the production of angiogenin, a potent stimulator of new blood vessels and defensin, the defense peptides active against bacteria, fungi and viruses in the host.[26]

2.2 Blocking the adhesion of pathogens

Probiotic bacteria are known to inhibit adhesion of some particular pathogens in vitro, for example *Escherichia coli, Salmonella enterica, Vibrio, Shigella, Campylobacter* and *Clostridium* sp. to epithelial cells in the gut. The attachment of pathogenic microbes to the cells and the host's mucosal surfaces are the main causes of the majority of infections.[28] A mucus layer of gel-like composition, constituting glycoproteins (mucin) can be found in the gut epithelium. When neurogenic factors are triggered along with the changes in the gut's environment, mucin is produced from the goblet cells and factors including the indigenous flora and microbe-causing infections. The glycoprotein, mucin, plays a role by acting as a barrier to adherence and intrusion of pathogens and toxin, by separating the epithelium from contact directly with the luminal contents. The mucus layer shields the surfaces on the gut against the enteropathogenic bacteria which involve in forming a covering blanket over the epithelial cells, binding competitively through carbohydrate component with pathogens and thereby releasing mucus inside the gastrointestinal tract which might subsequently draw away the contents of the lumen from epithelial cells.[28]

Bifidobacteria are reported to provide dose-dependent inhibition to the adherence of enteropathogenic *E. coli* and *S. typhimurium* in vitro to CaCO-2 cells.[28,29] Additionally, it has also been demonstrated that *Lactobacilli* can inhibit the adhesion and intrusion of epithelial cells by the enteropathogens - *Yersinia paratuberculosis, E.coli* and *Salmonella typhimurium*. The mode of action of this inhibition is not clearly understood, although competitive binding to receptors have been determined.[30,31] Similarly, prebiotic oligosaccharides present in the lumen are reported likely to block receptor sites for gut pathogens.[26] It has not yet been clearly understood how the antibacterial molecules such as bacteriocins are secreted or the secretion of defensin, the antimicrobial substances by the gut cells, are stimulated.[28]

2.3 Modulation of immune response

Oral administration of probiotic strains is found to illicit immune responses, both specific and non-specific to the host in both healthy and unhealthy conditions, including the improvement of phagocytic activity of leukocytes and natural killer cells.[32] Lipoteichoic acids in gram-positive bacteria such as *Bifidobacterium* have a high binding affinity for epithelial cell membranes; they are also reported to serve as carriers for other antigens thus provoking the immune reaction.[33,34] In this section, the two categories of the modulation of immune response are discussed.

2.3.1 Effect on innate immunity

The natural killer cell activity is an example of immune response in the body. Natural killer cells are produced from the bone marrow, which are large granular lymphocytes. It is well known that natural killer cells have a role as cytolytic effector cells.[35] The immune system not only fights against the pathogens by providing first line of defense but also guides the adaptive immune system to bring out an innate immune response by sending biological signals to the targeted area.[36]

The specialized phagocytic cells, macrophages and the dentritic cells are responsible for initiating the innate immune responses that engulf the materials of foreign bodies and also defend against

infection. The pattern recognition receptors, which are developed by the phagocytes, are capable of identifying the specific molecular patterns of a pathogen that is present on the surface and the activation of these receptors happens only by pathogenic microorganisms.[37] The pattern recognition receptors like the Toll-like receptor (TLR) family are studied in-depth. When the pathogenic material exists in the gut, the purpose of the Toll-like receptors is to alert antigen-presenting cells to 'watch-out' for the harmful foreign body.[38]

L. johnsonii LJ-1 and *L. salivarius* UCC 118 stimulated a mucosal IgA response and increased phagocytic activity.[39] The enhancement of the circulating IgA antibody secreting cell response was observed in infants supplemented with a strain of *L. casei* responsible for prevention of diarrhea in the study group compared to the control (placebo). Furthermore, there was an increase in the non-specific immune phagocytic activity of granulocyte populations in the blood of human volunteers after consumption of *L. acidophilus* and *B. bifidum* because phagocytic activity is associated with natural immunity and phagocytes are involved in antibody immune responses as antigen- presenting cells.[40]

2.3.2 Effect on cellular immunity

According to Matsuzaki and Chin, two sections of murine T helper cells are classified depending on the pattern of cytokine production shown: It is reported that Interferon (IFN-γ), interleukin (IL-2), tumour necrosis factor (TNF-β) are produced by type 1 T helper cells while IL-4, IL-5, IL-6 and IL-10 are produced by type 2 T helper cells. In addition, the two types of helper T cells are categorized into two different kind of immunity: the type 1 cytokines contribute to the cellular immunity and type 2 cytokines to humoral immunity. [35,41] Several diseases caused by weak immune system, such as allergies and infections, can appear when the balance of the cell population are interrupted, since cell-balance is vital for the maintenance of homeostasis in each individual.[35]

Exerting an inhibition on the IgE production could be a helpful effect of probiosis on allergic responses.[42] However, the inhibition of IgE production in vivo by the probiotics that are taken in orally through food, are still unsure. The consumption of probiotics by individuals with immune-inflammatory disorders such as atopy and Crohn's disease including those individuals with HIV and immunosuppression has been suggested in few reports.[43,44,45]

3. The benefits of probiotics

Probiotics are known to provide health benefits to humans. However, extensive research needs to be undertaken to provide substantial evidence and account for any side effects. Probiotics contain different strains of bacteria which have different functions in the body, for instance *L. Rhamnosus* GG, which stimulates most of the IgA production whereas *L. acidophilus* contributes in decreasing the amount of enzymes causing cancer.[3] Nevertheless, some of probiotics also provide the same benefit in the body for example *L. helveticus* and *S. cerevisiae Bouldarii* are able to suppress blood pressure.[3,46] The benefits of probiotic strains are summarized in ***Table 2***. The main therapeutic and health benefits of probiotics are: (3.1) Treating acute gastroenteritis/diarrhoea (3.2) improvement of lactose digestion (3.3) prevention of allergy (3.4) Anti-mutagenic (3.5) Anti-carcinogenic (3.6) improvement of vitamin B profile (3.7) reduction of blood pressure (3.8) Decrease cholesterol consumption (3.9) Treatment or prevention of urogenital disease (3.10) reduce the amount of *Helicobacter pylori* in stomach (3.11) Treating inflammatory bowel disease.

3.1 Treating acute gastroenteritis /diarrhea

Diarrhoea caused by *Clostridium difficle* (*C. difficle*) are commonly found in people who consume antibiotic such as metronidazole and vancomycin. This is because *C. difficle* are found in the healthy intestine in small number but there is a distortion of flora that is indigenous, due to antibiotic doses leading to an increased count of *C. difficle* and hence, toxin production.[47] Probiotics are reported to provide a prophylactic regimen with antibiotic-induced diarrhea. Studies have proof that *Lactobacillus* GG and *S. cerevisiae* Bouldarii are very effective in

Table 2. Type of probiotics and their beneficial effects

Type of probiotic strains	Beneficial Effects	References
Bifidobacteria	Decrease the amount of genotoxin from certain compound. Eradication of *H. pylori*. Increase phagocytic activity.	[46], [58], [91]
L. acidophilus	Decrease the level of enzyme that can cause cancer. Produce short fatty acids to inhibit the generation of carcinogenic products. Reduce the total cholesterol concentration by deconjugation of bile acid into free acids. Eradication of *H. pylori*. Increase phagocytic activity.	[3], [40], [72], [92]
L. casei shirota	Enhancement of the circulating IgA antibody secreting cell.	[3], [46]
L. helveticus	Suppress blood pressure.	[76], [81]
L. Johnsonii LJ-1 *L. salivarius*	Stimulate mucosal IgA-response. Increase phagocytic activity.	[39], [40],
L. reuteri CRL 1098	Produce vitamin B	[79], [80]
L. Rhamnosus GG	Effective in termination of diarrhea. Enhance the secretion of IgA-specific antibody. Inhibit the growth and adhesion of enteropathogens. Hydrolyse complex casein to smaller peptides and amino acids.	[40], [48], [49], [62]
L. sporogenes	Reduce the amount of bad cholesterol in the body.	[59], [85]
S. cerevisiae bouldarii	Effective in treatment of diarrhea. Suppress blood pressure. Increase secretory IgA levels in gut.	[3], [48], [81], [82], [95]

cerevisiae Bouldarii are very effective in termination of diarrhea.[3,48]

Diarrhoea caused by rotavirus is a common acute type diarrhea seen in children worldwide. This virus causes the gut permeability of epithelial cell to increase intact protein. Probiotics are claimed to shorten the time span of acute diarrhea as *Lactobacillus Rhamnosus* GG, which is present in yogurt enhancing the secretion of IgA-specific antibody to rotavirus.[49] Moreover, *Lactobacillus Rhamnosus* GG are reported to shorten the duration of rotavirus diarrhoea by inhibiting the adhesion of enteropathogens.[3,50]

Research has been carried out in acute gastroenteritis patients, to note the differences between children receiving yogurt and children consuming placebo (milk formula); duration of hospitalization was shorter in children consuming yogurt and total weight gain also high in these children compared to children receiving placebo (milk formula).[51]

3.2 Improvement of lactose digestion

Lactose malabsorption is a condition where lactose (component of carbohydrate) cannot be hydrolyzed completely to glucose and galactose as a result of deficiency of enzyme β-galactosidase. People with lactose intolerance are often found to experience gastric distress on consumption of unfermented milk or milk products; this is reported to be due to microbial action on undigested lactose forming hydrogen gas in the gut.[3,52] The intolerance symptoms are developed depending on transit rate of lactose in to the large intestine and the ability to ferment lactose by colon microbiota.[46,53]

Yogurt with probiotic bacteria can improve the lactose digestion by fermenting lactose and thereby reducing lactose intolerance.[54] Moreover, microbial lactase from the starter culture also helps the intestine in lactose digestion as microbial lactase can survive in the stomach but will be destroyed in the small intestine by digestive enzymes due to difference in pH.[55] The survival and multiplication of beneficial bacteria in the gastrointestinal tract helps in breaking down the lactose in longer period for example *S. thermophilus* contain more lactase than *lactobacilli* or *bifidobacteria* strains.[56,57] It has been proposed that increase in viscosity of the fermented product could prolong the transit time through the gastrointestinal tract as it slows down gastric evacuation.[46]

3.3 Prevention of allergy

It has been reported that the milk protein casein can trigger the first allergic reaction in some milk-fed infants. There is a higher frequency of allergic diseases especially in western societies over the last 40 years.[58,59] Probiotic are known to be beneficial in lowering inflammation associated with hypersensitivity reactions in patients with food allergy.[59,60,61]

Lactobacillus GG along with other *lactobacilli* are claimed to hydrolyse complex structure of casein to smaller fragments of peptides and amino acids thereby decreasing the production of mitogen-induced human lymphocytes.[40,62] Bacterial host interaction is studied to likely induce the expansion of regulatory T-cells along with the expression of interleukin (IL)-10 and transforming growth factor (TGF-β) which belong to the group of immunomodulatory cytokines .[63] It has been proposed that probiotics might improve barrier mechanisms of the gut, providing a valuable tool for countering food allergic reactions and inflammation of the intestine.[59,64,65]

A study has been demonstrated in a double blind to find the potential of probiotics in atopic disease. Children with high risk of atopic disease were given probiotics and others were given a placebo for a study period of six months. The results show that the children receiving probiotics had reduced occurrence of atopic eczema as compared to children who were given placebo.[66,67]

3.4 Anti-mutagenic

Mutagens are frequently formed due to stress, viral or bacterial infection and phagocytosis.[68] Endogenous DNA damage can be caused by age related degenerative processes in the body. The defense mechanism through leukocytes release several compounds for example NO, O_2^- and H_2O_2 to defend the individual from infection by bacteria and virus however, this mechanism can cause mutation and DNA damage. Anti-mutagenicity developed when the mutation process is stopped or suppressed.[46,68,69]

A study shows that *Lactobacilli* and *Bifidobacteria* decrease the amount of genotoxic from certain compounds. Probiotic organisms are claimed to bind mutagens into the cell surface and thereby reduce the activities of faecal enzymes involved in mutagen activation including nitroreductase, azoreductase and β-glucuronidase.[3] Dead cells shows a low rate in preventing mutation than live bacterial cells suggesting that live bacterial cells are involved in anti-mutagenic metabolism.[46,70]

Neosugar (fructo-oligosaccharide) with probiotics are given to healthy volunteers in chewable form increased *Bifidobacteria* in the intestines and also reduced the faecal enzymatic activities of genotoxic metabolites. This shows the potential of probiotics in prevention of mutation.[33]

3.5 Anti-carcinogenic

Genotoxic compounds such as heterocyclic amines, nitrosamine, ammonia and phenolic compounds are reported to be causative agents for colorectal cancer.[3] Enzymes such as azoreductase, β-glucuronidase and nitroreductase have the potential to convert procarcinogens into carcinogens.[71]

Certain strains of *L. acidophilus* and *Bifidobacterium* spp. contribute to decrease the level of enzyme that can cause cancer such as β-glucuronidase, azoreductase and nitroreductase thereby reducing the risk of tumour

development.[3,72] Furthermore, short fatty acids produced by *L. acidophilus* and *bifidobacteria* are known to inhibit the formation of carcinogenic products and hinder the continuation of cellular growth causing cancer.[73] Other probiotic bacteria also help in balancing the intestinal microbiota and subsequently preventing the absorption of toxins.[3,74] Probiotics can also decrease the inflammatory immune response to inhibit tumour development and enhancing the production of IgA-secreting cells and $CD4^+$ T-lymphocytes found in the lamina propia of the large intestine.[75,76]

3.6 Improvement of vitamin B profile

The action of microorganisms in the intestine can improve the digestibility and absorption of dietary nutrients.[77] The most common vitamin B produced by microbes are riboflavin (Vitamin B_2) and cobalamin (vitamin B_{12}). Riboflavin is the originator of the coenzymes flavin mononucleotide (FMN) and flavin adenine dinucleotide (FAD), which are carriers of hydrogen in cellular reactions. Riboflavin is synthesized through the microbial route from the precursor's guanosine triphosphate (GTP) and D-ribulose 5-phosphate through several enzymatic cascade mechanisms. The only vitamin that is reported to be produced exclusively by microorganisms, mostly anaerobes is cobalamin, a type of cobalt corrinoid. Human, animal and fungi cannot produce cobalamin.[78,79]

Probiotics improve vitamin nutrition by absorption of bacterial synthesized vitamin. Differences in processing technologies and the action of microorganisms can vary the concentration of riboflavin in food products. *Lactobacillus reuteri* CRL 1098 was found to be the first strain that is able to produce a cobalamin like-compound.[79,80]

3.7 Reduce blood pressure

Probiotic bacteria also play a role in blood pressure control as documented by animal and clinical studies.[59] The proteolytic action of some probiotic bacteria on the milk protein, casein results in the generation of bioactive peptides; these peptides such as valine-proline-proline and isoleucine-proline-proline, isolated from yogurt fermentation by *Saccharomyces cerevisea* and *Lactobacillus helveticus* are found to suppress blood pressure. These tripeptides are seen to function on the lines of angiotensin-I-converting enzyme inhibitors thereby reducing blood pressure.[81,82]

3.8 Decrease cholesterol consumption

Cholesterol, a component of cell membranes and nerve cells, is essential for several vital functions in the human body. It acts as a precursor to certain vitamins and hormones in the body. However, increased levels of blood cholesterol are considered risk factors for developing coronary heart disease.[59]

People who consumed probiotics were seen to excrete higher levels of cholesterol in faeces as compared to non-consumers suggesting the influence of probiotics on cholesterol levels. Changes in serum cholesterol have been hypothesized to be caused by alterations in cholesterol synthesis, absorption, conversion into bile acids and also synthesis and degradation of lipoproteins.[82,83] Cholesterol, being a precursor of bile acids converts its molecules to bile acids replacing those lost during excretion leading to a reduction in serum cholesterol. *Lactobacilli* and *Bifidobacteria* have the ability to deconjugate bile acids into free acids more rapidly from the intestinal tract than conjugated bile acids and increasing their rates of excretion.[84]

Results from previous studies demonstrate that probiotic bacteria may have a positive influence on blood cholesterol levels. A study conducted in hyperlipidaemic patients who were given *Lactobacillus sporogenes* reported a mean reduction of 32% in total cholesterol level and a reduction of 35% in low-density lipid over a study period of three months.[82,85] Furthermore, cholesterol levels in one of the studies showed significant decreases within 7 days of consuming yogurt and rose gradually to baseline levels within 4 weeks of resuming a normal diet.[86]

3.9 Treatment or prevention of urogenital infection
Intestinal tract is found to be the major source of pathogenic microbes for urinary tract infections in women. *Trichomonas*, *Candida, Gardnerella vaginalis* and *Mycoplasma hominis* are the examples of pathogenic microbes associated with vaginal infections, whereas urinary tract infections are reported to be caused by anaerobic microbes like *Chlamydia, E. coli* and *Candida*.[82,87]

High populations of *Lactobacilli* in the vaginal tract are found to be sign of good health. *Lactobacilli* reduce infections by replacing the population of other harmful bacteria in the intestine by interfering with the adhesion mechanisms of urinary pathogens. Reduction of *E. coli* colonization by healthy *Lactobacilli* has been proposed to result in lower UTI-associated morbidities. *Lactobacilli* are known to contribute to lower pH levels and thereby inhibiting the growth of *Gardnerella* and other related bacteria.[82,88,89] This shows the usefulness of using oral probiotics in disease management.

In a study done by Sanders, thirty-three women were studied to understand the effect of consuming yogurt on *Candida Vaginitis*. A decrease in *Candida* infection during yogurt consumption was observed compared to subjects who did not receive yogurt. Moreover, thirty-eight other women underwent the study on vaginal *Lactobacilli* present in the yogurt; results show that vaginal *Lactobacilli* contribute significantly to lowering the risk of urinary tract infections.[82]

3.10 Reduce amount of Helicobacter pylori in the stomach
Helicobacter pylori is a gram-negative, spiral bacterium that is reported to survive in acidic environment of the stomach and colonize the lining antrum of the epithelial cells. *H. pylori* is a pathogenic microorganism and increased densities of this bacterium reportedly causes chronic gastritis and peptic ulcer disease.[90,91,]

The use of probiotics has been proposed for countering *H. pylori* infection by exhibiting an inhibitory effect on the pathogen attachment to the gastric epithelial lines.[59] Yogurt containing *Lactobacillus* and *Bifidobacterium* are studied to not only improve the rate of eradication of *H. pylori* substantially but also restore the depleted levels of *Bifidobacterium* in stools. Increase in *Bifidobacteria* is also reported to lower the production of hydrogen gas which commonly produced by *Escherichia coli* and *Clostridium perfringens* which also increased the stomach's colonization by *H. pylori.*[91,92]

In an experiment conducted by Vasiljevic and Shah, intake of yogurt containing *Lactobacillus johnsonii* La1 for three weeks decreased the density of *H. pylori* in humans. Additionally, a decrease in antral inflammation was also observed. [46]

3.11 Treating inflammatory bowel disease
The overlapping phenotypes of Crohn's disease and ulcerative colitis typically characterize inflammatory bowel disease. People with inflammatory bowel disease reportedly have lower numbers of *Lactobacillus* and *Bifidobacterium* in their intestine whereas coccoids and anaerobic bacteria are higher.[3] Boosting the composition of normal microbiota is found to offer immunity against the disease.[67,93,94]

Improvement of intestinal mobility and constipation relief are found to be beneficial effects of lactic acid bacteria through a reduction in gut pH and offering protection against adhesion of pathogenic microbes.[94] *Sacchromyces bouldarii* in patient with Crohn's disease is claimed to reduce relapse rates and extend remission time. *Sacchromyces bouldarii* and *Lactobacillus* GG have been reported to contribute of higher levels of secretory IgA levels in the gut by down regulating TNF-α-induced IL-8 production.[95,96]
In a study conducted by Vasiljevic and Shah, four children with Crohn's disease were investigated for the effect of *Lactobacillus* GG supplementation. The study showed improvement in the clinical outcome of three children who received oral *Lactobacillus* GG. Moreover, additional study has been carried out using large samples in order to support the claim. Forty patients with chronic relapsing pouchitis were

involved in this study and were given a mixture of four species of *Lactobacilli* and three species of *Bifidobacteria* and *S. thermophiles*. After the study period of four months, fewer relapses were observed in the patients receiving probiotics as compared to the control group.[46]

4. Concerns of probiotics

Some potential concerns have been raised with regards to the consumption of probiotics in humans.[2,97,98] Probiotics, according to Salminen and von Wright, can be responsible for four types of side effects: (4.1) systemic infections, (4.2) risk of metabolic disorders, (4.3) risk of adjuvant side effects, (4.4) risk of gene transfer. In addition, (4.5) minor gastrointestinal symptoms have also been reported, as stated by Salminen and von Wright.[99]

4.1 Systematic infections

Probiotics are non-pathogens. Therefore, the risk of infection, if any, should be minimum. However, one of the potential concerns is that some probiotics mainly in commercial products, have been designed or selected to have good adherence to the gastrointestinal lining. According to Boyle et al. (2006), adherence to intestinal mucosa may contribute to bacterial translocation and virulence. Bacterial translocation is a phenomenon caused by a diminished intestinal barrier, which leads to the passage of bacteria across the epithelium and mucous membrane. [100,101]

Bacterial translocation may result in immunodeficiency in the host, intestinal mucosal injury and an abnormal intestinal bacterial flora. [102] The bacteria may be transported through the tunica propria to the mesenteric lymph nodes (MLN) and other organs which is a precursor to bacteremia with the potential to progress into septicemia.[103,104,105]

Reports from cases describe episodes of infection caused by organisms coherent with probiotic strains in patients consuming probiotics. Eight cases of bacteremia associated with *Lactobacilli* including *Lactobacillus acidophilus*, *Lactobacillus casei* and *Lactobacillus* GG have been reported.[106,107,108] Nine cases of overt sepsis have also been observed, associated with *S. boulardii [cerevisiae]*, *Lactobacillus* GG, *Bacillus subtilis*, *Bifidobacterium breve* or combination probiotics.[108,109,110] Furthermore, endocarditis events caused by both *Lactobacillus* and *Streptococcus* probiotics have been documented.[111,112]

4.2. Risk of metabolic disorders

The intestinal microbiota play an essential role in numerous metabolic activities, including carbohydrate and lipid metabolism and glucose homeostasis.[100,113] Thus, there is a potential risk of adverse metabolic effects. However, incidence of significant adverse effects appears to be lower.[100,114]

4.2.1 Excessive degradation of intestinal mucus

It has been documented that some endogenous bacteria including numerous bacteroides species and some *lactobacilli*, as well as some strains of *Bifidobacteria* have the capability to degrade human intestinal mucus.[99] In order to study these effects, Ruseler-van Embden, van Lieshout, Gosselink, and Marteau, have examined the mucus degrading properties of three commonly used probiotic strains such as *L. acidophilus*, *Bifidobacterium* spp. and *L. rhamnosus* GG that were administered in fermented milk. Nevertheless, no mucus degradation was observed in vitro or in gnotobiotic rats mono-associated with the test strains and thus the strains were considered safe for the mucus.[115]

4.2.2 Excessive deconjugation of bile salts

Secondary bile acids are produced by intestinal bacterial actions and can exhibit carcinogenicity by acting on the mucous-secreting cells and stimulating their proliferation. They can also act as promoters of carcinogenesis.[116] A study on hypothetical risk of excessive deconjugation of bile salts in the small bowel by probiotics was carried out in healthy humans, which showed how *L. acidophilus* and *Bifidobacterium* spp. contained in fermented milk could convert conjugated primary bile salts into toxic free secondary bile salts.[99] However, more studies are required to conclusively establish the side effects.

4.3. Risk of adjuvant side effects

Studies on the role of intestinal microbiota in immune development suggest that manipulations caused by probiotics could lead to immunomodulatory effects. Boyle et al., reported that a medium to long-term alteration of the microbiota might be attained in neonatal probiotic supplementation. [100] However, it is difficult to predict the long-term effect of these manipulations on the host. Nevertheless, the consumption of probiotics during pregnancy, in neonates and in children has not been associated with any adverse immunological effects.[2]

According to O'Brien, Crittenden, Ouwenhand and Salminen, probiotic cell was and cytoplasmic material have the potential to trigger the immune effects. [117] Studies have shown that cell wall fragments from *Lactobacilli* can induce arthritis in rats. As stated by Salminen and von Wright, immunological side effects have been observed in rats with systemic uptake of cell wall polymers from the intestinal lumen via colonic injury and during small bowel bacterial overgrowth. [99,118 119] Furthermore, the cell walls from *Bifidobacteria* have the potential to be arthritogenic.[120] Nonetheless, there have been no immunological side effects caused by oral-administered probiotic reported in humans.

4.4. Risk of gene transfer

A major area of concern as stated Salyers et al. and Mathur and Singh has been the potential of transfer of antibiotic-resistance genes in the gastrointestinal tract between probiotic and pathogenic bacteria. [121,122] According to Lin, Fung, Wu, and Chung, in lactic acid bacteria, one can observe the presence of plasmids with antibiotic-resistance genes, including genes exhibiting resistance to a range of antibiotics such as tetracycline, erythromycin, chloramphenicol, lincosamide, macrolide, streptomycin and streptogrammin. [123]

Morelli, Sarra, and Bottazzi reported that several attempts have been done to transfer antibiotic resistance with a broad-host-range plasmid pAMB. Morelli, Sarra and Botazzi also observed that merely one strain each of *L. brevis* and *L. helveticus* accepted the plasmid with low efficiency (10^{-7}), out of 14 strains of *Lactobacillus delbrueckii*, 44 strains of *L. acidophilus*, one strain of *Lactobacillus brevis*, one strain of *Lactobacillus helveticus*, 6 strains of *L. casei rhamnosis*, one strain of *L. fermentum* and 5 strains of *L. plantarum.*[124] Mathur and Singh and Soedings, Kleinschmidt, Teuber and Neve have reported that 7 of 14 strains were capable of transferring resistance from *Lactobacillus* to *Enterococcus* at 10^{-4}–10^{-7} of frequencies. Whereas, two of 14 strains could transfer to *L. lactis* but were not capable to transfer to *Staphylococcus aureus*.[121,125]

There have been molecular identification attempts of vancomycin-resistance genes in lactobacilli where one strain of *L. rhamnosis* and five strains of *L. reuteri* were probed for vanA, vanB, and vanC genes and none were found in the observation according to Klein, Hallmann, Casas, Abad, Louwers, and Reuter.[126] Doron and Snydman reported that *Lactobacillus* GG has been examined precisely and no plasmids have been discovered; there is no verification of vanA, vanB, vanH, vanX, vanZ, vanY, and vanS, by hybridization or polymerase chain reaction products. [108,126,127]

As specified by Doron and Snydman, in spite of the theoretical likelihood of lateral gene transfer between probiotic and other pathogenic microorganisms in sites such as in the gut, there has been no clinical evidence for the transfer of antimicrobial resistance seen. [108]

4.5. Gastrointestinal side effects

Studies have reported minor gastrointestinal symptoms occurring in subjects receiving probiotics, for example abdominal cramping, flatulence, soft stools and taste disturbance. Gastrointestinal side effects happen when the gastrointestinal tract is colonised with a large number of bacteria. The organisms present in high numbers can induce intestinal inflammation mainly through deconjugation and dehydroxylation of bile salts.[128]

5. Conclusion

Probiotic bacteria such as *Lactobacillus* species and *Bifidobacteria*, widely occur in fermented products including local foods in various geographic locations. The bacteria present in the probiotic food products are essentially similar to the gut microbiota. Administration of these probiotic bacteria can provide health benefits to an individual by increasing the amount of good bacteria in the body and also provide therapy for certain diseases. Although, some of the mechanisms of blocking or inhibition of adhesion of pathogenic bacteria remains unclear, probiotic bacteria are well known of their benefits as they can increase the immunity of the host by strengthening the gut microbiota.

References

[1] R. Saini, S. Saini and J. Sughanda, *Cutan. Aesthet. Surg.*, **2009**, 112.

[2] D. R. Snydman, *Clin. Infect. Dis.*, **2008**, *46*, s104-111.

[3] N. P. Shah, *Int. Dairy. J.*, **2007**, *17*, 1262-1277.

[4] Y. Fang and D. B. Polk, *J. Biol. Chem.*, **2002**, *277*, 50959-50965.

[5] H. S. Gill, *Best Pract. Res. Clin. Gastroenterol.*, **2003**, *17*(5), 755-773.

[6] J. Slavin, *Nutrients*, **2013**, *5*(4), 1417-1435.

[7] J. Schrezenmeir and M. D. Vrese, *Am. J. Clin. Nutr.*, **2001**, *73*(2), 361s-364s.

[8] P. C. Sanchez, *Japanese J. lactic acid bact.*, **1998**, *10*, 19-28.

[9] J. A. Bakar, *Belacan. Bruneiana: Anthology of Science Article*, **2002**, *3*, 5-8.

[10] F. Petra, *Studies of Belutak and Budu Kupang Traditional Fermented Products of Brunei Darussalam.* University of Brunei Darussalam, **1999**.

[11] S. Ray, U. Raychaudhuri and R. Chakraborty, *Cereal Foods World*, **2015**, *60*(5), 218-223.

[12] N. La Anh, *Food Sci. and hum. wellness*, **2015**, *67*, 1-15.

[13] C. J. Liu, F-m. Gong, X-r. Li, H-y. Li, Z-h. Zhang, Y. Feng and H. J. Nagano, *J. Biomed. Biotechnol*, **2012**, *13*(4), 298-306.

[14] B. K. Iyer, R. S. Singhai and L. Ananthanarayan, *J. Food Sci. Tech.*, **2013**, *50*(6), 1114-1121.

[15] M. R. Swain, M. Anandharaj, R. C. Ray and R. P. Rani, *Biotechnol. Res. Int.*, **2014**, 1-19.

[16] J. H. Chang, Y. Y. Shim, S. K. Cha, and K. M. Chee, *J. Appl. Microbiol.*, **2009**, *109*, 220-230.

[17] S-n. Liu, Y. Han and Z-j. Zhou, *Food Res. Int.*, **2010**, *44*(2011), 643-651.

[18] K. Gomathy, *Probiotic Foods*, **2013**, 209-211.

[19] T. Hosoi and K. Kiuchi, *Handbook fermented fuctional food*, **2013**, 227-250.

[20] S. J. Rhee, J. E. Lee and C-H. Lee, *Microb. Cell. Fact.*, **2011**, *10*(Suppl 1), 1-13.

[21] J. A. Bakar, *Fermented rice-Tapai.* Department of Biology, *UBD*, N.D, 16-28.

[22] X. M. Feng, A. R. B. Eriksson and J. Schnurer, *Int. J. Food Microbiol.*, **2005**, *104*(3), 249-256.

[23] J. J. Leisner, M. Vancanneyt, G. Rusul, B. Pot, K. Lefebvre, A. Fresi and L. K. Tee, *Int. J. Food Microbiol.*, **2001**, *63*(1-2), 149-157.

[24] E. Chukeatirote, K. Dajanta and A. Apichartsrangkoon, *J. Biol. Sci.*, **2010**, *10*(6), 581-583.

[25] A. C. Ouwehand, P. V. Kirjavainen, C. Shortt and S. Salminen, *Int. Dairy. J.*, **1999**, *9*, 43–52.

[26] R. A. Rastall, G. R. Gibson, H. S. Gill, F. Guarner, T. R. Klaenhammer, B. Pot,…M.E. Sanders, *FEMS. Microbiol. Ecol.*, **2005**, *52*(2), 145-152.

[27] P. Michetti, G. Dorta, P. H. Wiesel, D. Brassart, E. Verdu, M. Herranz,…I. Corthesy- Theulaz, *Digestion*, **1999**, *60*(3), 203-209.

[28] H. S. Gill, *Best. Pract. Res. Clin. Gastroenterol.*, **2003**, *17*(5), 755-773.

[29] M. F. Bernet, D. Brassart, J. A. Neesar, and A. L. Servin, *Appl. Environ. Microbiol.*, **1993**, *59*, 4121-4128.

[30] D. R. Mack, S. Michail, S. Wei, L. McDougall and M. A. Hollingsworth, *Am. J. Physiol.*, **1999**, *276*(4), G941–G950.

[31] Y. K. Lee and K. Y. Puong, *Br. J. Nutr.*, **2002**, *88* (Suppl. 1), S101–S108.

[32] A. E. Wold, *Scand. J. Nutr*, **2001**, 45, 76-85.

[33] G. T. Macfarlane and J. H. Cummings, *B. M. J.*, **1999**, *318*, 999-1003.
[34] A. Dobson, P. D. Cotter, R. P. Ross and C. Hill, *Appl. Environ. Microbiol.*, **2012**, *78*, 1-6.
[35] T. Matsuzaki and J. Chin, *Immunol. Cell. Biol.*, **2000**, *78*, 67-73.
[36] C. M. Galdeano and G. Perdigon, *Clin. Vaccine. Immunol.*, **2006**, *13*(2), 219-226.
[37] S. Akira, K. Takeda and T. Kaisho, *Nat. Immunol.*, **2001**, *2*, 675-680.
[38] S. Dunzendorfer, H. K. Lee, K. Soldau and P. S. Tobias, *J. Immunol.*, **2004**, *22*, 33-54.
[39] M. Saarela, G. Mogensen, R. Fonden, J. Matto and T. Matilla-Sandholm, *J. Biotechnol.*, **2000**, *84*, 197-215.
[40] K. Kailasapthy and J. Chin, *Immunol. Cell. Biol.*, **2000**, *78*, 80-88.
[41] T. R. Mosmann and R. L. Coffman, *Adv. Immunol.*, **1989**, *46*, 111-47.
[42] K. Shida, K. Makino, A. Morishita, A. et al., *Int. Arch. Allergy. Imm.*, **1998**, *115*, 278-87.
[43] M. Malin, H. Suomalainen, M. Saxelin and E. Isolauri, *Scand. J. Gastroenterol.*, **1996**, *36*, 971–974.
[44] B. W. Wolf, K. B. Wheeler, D. G. Ataya and K. A. Garleb, *Food Chem. Toxicol.*, **1998**, *36*, 1085–1094.
[45] P. V. Kirjavainen, S. J. Salminen and E. Isolauri, *J. Pediatr. Gastroenterol. Nutr.*, **2003**, *36*(2), 223-227.
[46] T. Vasiljevic and N. P. Shah, *Int. Dairy. J.*, **2008**, *18*, 714-728.
[47] M. D. A. Guarino, M. D. S. Guandalini and M. D. A. L. Vecchio, *J. Clin. Gastroenterol.*, **2015**, *49*, s37-s45.
[48] E. Biagi, M. Candela, S. Fair-w-Tait, C. Franceschi and P. Brigidi, *Age*, **2012**, *34*, 247-267. doi: 10.1007/s11357-011-9217-5.
[49] G. Boudraa, M. Benbouabdellah, W. Hachelaf, M. Boisset, J-F. Desjeux and M. Touhami, *Gastroenterol. Nutr.*, **2001**, *33*, 307-313.
[50] J. M. Saavedra, N. A. Bauman, I. Oung, J. A. Perman and R. H. Yolken, *Lancet*, **1994**, *344*, 1046-1049.
[51] B. Patro-Golab, R. Shamir and H. Szajewska, *Clin. Nutr.*, **2015**, *34*, 818-824.
[52] M. de Vrese, C. Laue, B. Offick, E. Soeth, F. Repenning, A. Tho and J. Schrezenmeir, *J. Clin. Nutr.*, **2015**, *34*, 394-399.
[53] M. C. Martini and D. A. Savaino, *Am. J. Clin. Nutr.*, **1988**, *47*, 57-60.
[54] O. Adolfsson, S. N. Meydani and R. M. Russell *Am. J. Clin. Nutr.*, **2004**, *80*, 245-256.
[55] L. Morelli, *Am. J. Clin. Nutr.*, **2014**, *99*, 1248s-1250s.
[56] D. D. G. Mater, L. Bretigny, O Firmesse, M-J. Flores, A. Mogenet, J-L. Bresson and G. Corthier, *FEMS. Microbiol. Lett.*, **2005**, *250*, 185-187.
[57] S. ScheinBach, *Biotechnol. Adv.*, **1998**, *16*(3), 581-608.
[58] G. T. Macfarlane and J. H. Cummings, *B. M. J.*, **1999**, *318*, 999-1003.
[59] S. Parvez, K. A. Malik, S. A. Kang and H-Y Kim, *J. Appl. Microbiol.*, **2006**, *100*, 1171-1185.
[60] L. V. McFarland, *Eur. J. Gastroen. Hepat.*, **2000**, *49*, 543-552.
[61] S. H. Murch, *Lancet*, **2001**, *357*, 1057-1059.
[62] Y. Sutas, M. Hurme and E. Isolauri, *Scand. J. Immunol.*, **1996**, *99*, 175-185.
[63] E. Zigmond, B. Bernshstein, G. Friedlander, C. R. Walker, S. Yona, K. K. Kim, O. Brenner, R. Krauthgamer, C. Carol, W. Muller and S. Jund, *Immunity*, **2014**, *40*(5), 720-733.
[64] M. A. Kalliomaki and E. Isolauri, *Immunol. Allergy. Clin. North. Am.*, **2004**, *24*, 739-752.
[65] G. M. D. Miraglia and M. G. D. Luca, *J. Clin. Gastroenterol.*, **2004**, *38*, S85-S86.
[66] M. Kalliomaki, S. Salminen, H. Arvilommi, P. Kero, P. Koskinen and E. Isolauri, *Lancet*, **2001b**, *357*, 1076-1079.
[67] A. C. Ouwehand, S. Salminen and E. Isolauri, *Antonie van Leeuwenhoek*, **2002**, *82*, 279-289.
[68] K. Hirayama and J. Rafter, *Microbes. Infect.*, **2000**, *2*, 681-686.
[69] H. Gaudreau, C. P. Champagne, G. E. Remondetto, L. Bazinet and M. Subirade, *Food Res. Int.*, **2013**, *53*, 751-757.
[70] W. E. V. Lankhaputra and N. P. Shah, *Mutat. Res.*, **1998**, *397*, 169-182.

[71] R. Fonden, G. Mogensen, R. Tanaka and S. Salminen, *I. D. F.*, **2000**, *352*, 1-37.
[72] H. Yoon and D. B. Polk, *J. Biol. Chem.*, **2002**, *277*, 50959-50965.
[73] B. F. Hinnebusch, S. Meng, J. T. Wu, S. Y. Archer and R. A. Hodin, *J. Nutr.*, **2002**, *132*, 1012-1017.
[74] G. Cenci, J. Rossi, F. Throtta and G. Caldini, *Syst. Appl. Microbiol.*, **2002**, *25*, 483-490.
[75] A. de Moreno de LeBlanc and G. Perdigón, *Med. Sci. Monit.*, **2004**, *10*(4), BR96-104.
[76] M. E. Sanders, F. Guarner, R. Guerrant, P. R. Holt, E. M. Quigley, R. B. Sartor, . . . E. A. Mayer, *Gut*, **2013**, *62*, 787-796.
[77] S. C. Resta, *J. Physiol.*, **2009**, *587.17*, 4169-4174.
[78] C. M. Burgess, E. J. Smid and D. V. Sinderen, *Int. J. Food Microbiol.*, **2009**, *133*, 1-7.
[79] J. G. LeBlanc, C. Milani, G. S. de Giori, F. Sesma, D. van Sinderen and M. Ventura, *Biotechnol.*, **2013**, *24*, 160-168.
[80] M. P. Taranto, J. L. Vera, J. Hugenholtz, G. F. De Valdez and F. Sesma, *J. Bacteriol.*, **2003**, *185*, 5643-5647.
[81] Y. Hata, M. Yamamoto, M. Ohni, K. Nakajima, Y. Nakamura and T. Takano, *Am. J. Clin. Nutr.*, **1996**, *64*, 767-771.
[82] M. E. Sanders, *J. Nutr.*, **2000**, *130*, 384s-390s.
[83] M. du Toit, C. M. A. P. Franz, L. M. T. Dicks, U. Schillinger, P. Harberer, B. Warlies, . . . W. H. Holzapfel, *Int. J. Food Microbiol.*, **1998**, *40*, 93-104.
[84] M. Kumar, R. Nagpal, R. Kumar, R. Hemalatha, V. Verma, A. Kumar, C. Chakraborty, B. Singh, F. Marotta, S. Jain and H. Yadav, *Exp. Diabetes Res.*, **2012**, 1-14.
[85] J. C. Mohan, *Indian J. Med. Res.*, **1990**, *92*, 431-432.
[86] G. Hepner, R. Fried, S. S. Jeor, L. Fusetti and R. Morin, *Am. J. Clin. Nutr.*, **1979**, *32*, 19-24.
[87] G. Reid, A. W. Bruce and V. Smeianov, *Int. Dairy. J.*, **1998**, *8*, 555-562.
[88] B. Mombelli and M. R. Gismondo, *Int. J. Anitimicrob. Agents*, **2000**, *16*, 531-536.
[89] A. E. Stapleton, M. Au-Yeung, T. M. Hooton, D. N. Fredricks, P. L. Roberts, C. A. Czaja, . . . W. E. Stamm, *Clin. Infect. Dis.*, **2011**, *52*, 1212-1217.
[90] J. Parsonnet, G. D. Friedman and D. P. Vandersteen, *N. Engl. J. Med.*, **1991**, *325*, 1127-1131.
[91] K-Y. Wang, S. N. Li, C. S. Liu, D. S. Perng, Y. C. Su, D. C. Wu, . . .W. M. Wang, *Am. J. Clin. Nutr.*, **2004**, *80*, 737-741.
[92] W. Zhen-Hua, G. Qin-Yan and F. Jing-Yuan, *J. Clin. Gastroenterol.*, **2013**, *47*(1), 25-32.
[93] J. Hamillton-Miller, *J. Infect.Dis.*, **2001**, *3*, 83-87.
[94] M. J. Saez-Lara, C. Gomez-Llorente, J. Plaza-Diaz and A. Gil, *BioMed. Res. Int.*, **2014**, 1-15.
[95] L. Zhang, N. Li and J. Neu, *J. Nutr.*, **2005**, *135*, 1752-1756.
[96] E. Distrutti, L. Monaldi, P. Ricci and S. Fiorucci, *World. J. Gastroenterol.*, **2015**, *22*(7), 2219-2241.
[97] A. C. Senok, A. Y. Ismaeel and G. A. Botta, *Clin. Microbiol. Infect.*, **2005**, *11*, 958-966.
[98] R. J. Boyle, R. M. Robins-Browne and M. L. K. Tang, *Am. J. Clin. Nutr.*, **2006**, *83*, 1256-1264.
[99] S. Salminen and A. V. Wright, *Microb. Ecol. Health Dis.*, **1998**, *10*, 68-77.
[100] R. J. Boyle, R. M. Robins-Browne and M. L. K. Tang, *Am. J. Clin. Nutr.*, **2006**, *83*, 1256-1264.
[101] N. Ishibashi and S. Yamazaki, *Am. J. Clin. Nutr.*, **2001**, *73*(Suppl 2), 465s-470s.
[102] R. D. Berg, E. Wommack and E. A. Deitch, *Arch. Surg.*, **1988**, *123*, 1359-1364.
[103] Berg, R. D., *Exp. Anim.*, **1985**, *34*, 1-16.
[104] [104] C. Vaishnavi, *Indian J. Med. Microbiol.*, **2013**, *31*(4), 334-342.
[105] P. A. M. Van Leeuwen, M. A. Boermeester, A. P. J. Houdijk, C. H. C. Ferwerda, M. A. Cuesta and S. Meyer, *Gut*, **1994**, *35*(suppl), s28-34.
[106] C. Tommasi, F. Equitani, M. Masala, M. Ballardini, M. Favaro, M. Meledandri, . . . E. Nicastri, *J. Med. Case. Rep.*, **2008**, *2*, 315.
[107] E. Vahabnezhad, A. B. Mochon, L. J. Wozniak and D. A. Ziring, *J. Clin. Gastroenterol.*, **2013**, *47*, 437-439.

[108] S. Doron and D. R. Syndman, *Clin. Infect. Dis.*, **2015**, *60*(S2), 129-134.
[109] A. Ohishi, S. Takahashi, Y. Ito, K. Tsukamoto, Y. Nanba, N. Ito, . . . T. Nakamura, *J. Pediatr.*, **2010**, *156*, 679-681.
[110] E. F. Zein, S. Karaa, A. Chemaly, I. Saidi, W. Daou-Chahine and R. Rohban, *Ann. Biol. Clin.*, **2008**, *66*, 195-198.
[111] A. D. Mackay, M. B. Taylor, C. C. Kibbler and J. M. Hamilton-Miller, *Clin. Microbiol. Infect.*, **1999**, *5*, 290-292.
[112] E. Presterl, W. Kneifel, H. K. Mayer, M. Zehetgruber, A. Makistathis and W. Graninger, *Scand. J. Infect. Dis.*, **2001**, *33*, 710-714.
[113] F. Backhed, R. E. Ley, J. L. Sonnenburg, D. A. Peterson and J. I. Gordon, *Science*, **2005**, *307*, 1915-1920.
[114] J. M. Saavedra, A. Abi-Hanna, N. Moore and R. H. Yolken, *Am. J. Clin. Nutr.*, **2004**, *79*, 261-267.
[115] J. G. Ruseler-van Embden, L. M. van Lieshout, M. J. Gosselink and P. Marteau, *Scand. J. Gastroenterol.*, **1995,** *30(7)*, 675-80.
[116] P. Y. Cheah, *Nutr. Cancer*, 1990, *14*, 5-13.
[117] J. O'Brien, R. Crittenden, A. C. Ouwehand and S. Salminen, *Trends Food Sci. Tech.*, **1999**, *10*(12),418-424.
[118] M. A. McConnel, A. A. Mercer and G. W. Tannock, *Microb. Ecol. Health Dis.*, **1991**, *4*, 343-355.
[119] V. Blancuzzi, E. D. Roberts, D. Wilson, L. R. Fryer, E. M. O'Byme and G. DiPasquale, Agents Actions. *Special conference*, **1993**, *39*, 183-185.
[120] A. J. Severijnen, R. van Kleef, M. P. Hazenberg and J. P. van de Merwe, *J. Rheumatol.*, **1989**, *16*, 1061-1068.
[121] A. A. Salyers, A. Gupta and Y. Wang, *Trends Microbiol.*, **2004**, *12*, 412-416.
[122] S. Mathur and R. Singh, *Int. J. Food Microbiol.*, **2005**, *105*, 281-295.
[123] C. F. Lin, Z. F. Fung, C. L. Wu and T. C. Chung, *Plasmid*, **1996**, *36*, 116-124.
[124] L. Morelli, P. G. Sarra and V. J. Botazzi, *J. Appl. Bacteriol.*, **1988**, *63*, 371-375.
[125] B. Soedings, J. Kleinschmidt, M. Teuber and H. Neve, *Syst. Appl. Microbiol.*, **1993**, *16*, 296-302.
[126] G. Klein, C. Hallman, I. A. Casas, J. Abad, J. Louwers and G. Reuter, *J. Appl. Microbiol.*, **2000**, *89*, 815-824.
[127] S. Tynkkynen, K. V. Singh and P. Varmanen, *Int. J. Food Microbiol.*, **1998**, *41*, 195-204.
[128] P. Marteau, M. F. Gerhardt, A. Myara, E. Bouvier, F. Trivin and J. C. Rambaud, *Microb. Ecol. Health Dis.*, **1995**, *8*, 151-157.

Current status and concerns on tropical anguillid eel stocks

*Takaomi Arai**

Environmental and Life Sciences, Faculty of Science, Universiti Brunei Darussalam, Jalan Tungku Link, Gadong BE1410, Brunei Darussalam

**corresponding author email: takaomi.arai@ubd.edu.bn*

Abstract

Freshwater eels of genus *Anguilla* have fascinated biologists for centuries due to the spectacular long-distance migrations between the eels' freshwater habitats and their spawning areas far out in the ocean and the mysteries of their ecology. The spawning areas of Atlantic eels and Japanese eel were located far offshore in the Atlantic Ocean and the Pacific Ocean, respectively, and their reproduction took place thousands of kilometres away from their growth habitats. Phylogenetic studies have revealed that freshwater eels originated in the Indonesian region. However, remarkably little is known about the life histories of tropical freshwater eels despite the fact that tropical eels are key to understanding the nature of primitive forms of catadromous migration. Recently, the juvenile abundance has declined dramatically: by 99% for the European eel and by 80% for the Japanese eel. Recruitment of the American eel near the species' northern limit has virtually ceased. Other eel species, including Australian and New Zealand eels, also show indications of decline. The main problem is that all young eels used in cultivation are wild juveniles (glass eels and elvers), which are captured in estuaries. Almost all (90 %) of the total world eel supply comes from aquaculture. Therefore, the supply of eel resources for human consumption is completely dependent on wild catch. Commercial eel industries are now considering tropical eels as possible replacement for European and Japanese eels to compensate for declining stocks. However, useful scientific research and information on the biology and stock assessments of tropical eels are lacking, a situation quite different from that for other temperate freshwater eels, which have been well studied for several decades with trends and recruitment patterns being on record. Nevertheless, the present tropical eel catch has been reported as being less than half that of 20 years ago. The present trends in eel stocks and utilization for human consumption suggest that all eel populations will decline to numbers that fall outside safe biological limits and will be seriously threatened with extinction without protection and conservation from strict enforcement of local and international laws.

Index Terms: Anguilla, Life history, Overfishing, Population, Stock assessment, Tropical eels

1. World eel stocks

Freshwater eels are exotic animals, and despite a huge number of scientific studies conducted on eels, the crucial aspects of their biology remain a mystery. No one has yet observed eels spawning in the natural environment, as spawning areas are located in the open ocean. This distinctly contrasts with other animals, such as anadromous salmon fish whose biology is well studied and better understood because localized spawning stocks are relatively easy to survey when the adults return to freshwater to spawn. Freshwater eels are the most important of the eel families from a conservation standpoint because they have a unique catadromous life history (***Figure 1***) and are utilized as food resources. Recently, however, juvenile abundance (***Figure 2***) has declined dramatically by 99% for the European eel and by 80% for the Japanese eel,[1,2,3,4] while recruitment of the American eel near the species' northern limit has virtually ceased.[4]

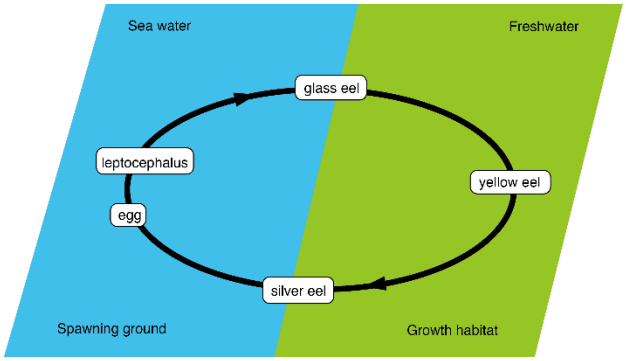

Figure 1. Typical life history of freshwater eels of Genus *Anguilla.*

Other eel species, including the Australian and New Zealand eels also show indications of decline.[4] The main problem is that all young eels used in aquaculture are wild juveniles (glass eels and elvers) captured in estuaries. Since almost all (90%) of the total world eel supply comes from aquaculture,[5] therefore, the supply of eel resources for human consumption is completely dependent on wild catch.

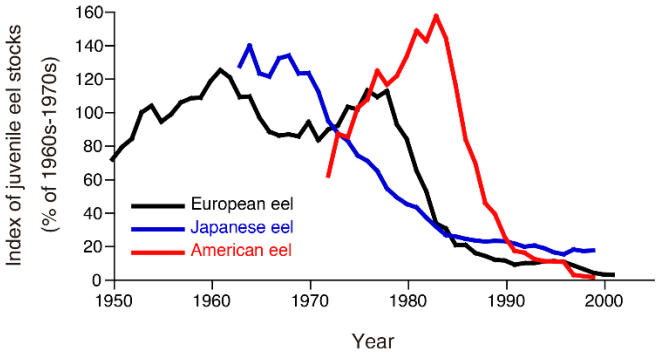

Figure 2. Trends in juvenile stocks of the European, American and Japanese eels. Note: Data for European and Japanese eels are shown as landings of juveniles in each area and for the American eel as recruitment data from Lake Ontario at the northern limit of its distribution, the abundance of juvenile eels shows sharp decline after peaks, *i.e.* the European eel by 99%, the Japanese eel by 80%, and recruitment of the American eel has virtually ceased. Source: Figure reference materials came from Dekker *et al.*[4] and was drawn using original data provided by Dr. Willem Dekker.[6]

The population size of wild juveniles has linearly decreased from over 200 metric tons in the early 1960s to 20 metric tons at present, and in Japanese eels, shortage of fry has become a serious problem for fish culture in recent years.[6] Eel stocks throughout Europe are also declining,[1] and eel fishery yields have decreased in most European countries.

Populations of the European, American and Japanese eels are considered to be outside safe biological limits, and current fisheries are not sustainable.[2,4,6] Under such circumstance, the European eel was recently categorized as critically endangered by the European Union (EU) and the United Nations,[7] although other eel species have not yet been seriously considered for protection. Since the early 1980s, juvenile recruitment has decreased, dropping to 1.0% that of the levels in 1970s. Nonetheless, the causes of decline in stock and recruitment are not well understood, although overfishing, habitat loss and migration barriers, increased natural predation, parasitism, ocean climate variations, and pollution might have some impacts.[8,9,10,11]

Since the European eel was listed by CITES under Appendix II and came under protection in March 2009, and considering that export/import ban was already issued by the EU in 2010, the international trade of juvenile eels has changed. Species other than the European and Japanese eels, such as several tropical species, seem to have replaced the European eel on the international market. In addition, countries including Canada, the USA, Dominican Republic, Morocco, Madagascar, Philippines, and Indonesia have now entered the market by supplying juvenile eels for the farming industry in China, Japan, Taiwan, and South Korea.[12,13,14] Since fewer studies had been conducted on tropical eels than those of the European, American, Japanese, Australian, and New Zealand eels, the unavailability of information on basic life history, stock and population on the tropical eels could lead to further serious declines in such eel resources. Therefore, before tropical eel juveniles are used to replace and augment the European and Japanese eels stocks, stock assessments and recruitment studies of source stocks are necessary to determine the sustainability of tropical eels. However, consumers in the East Asian countries do not pay

much attention to protection, conservation and enhancement of tropical eel populations, concentrating instead on having a stable eel supply and trade as they did with European and Japanese eels. If such *ad hoc* eel resource utilization would continue, eels around the world would become extinct in the near future, considering that artificially induced breeding techniques for eel species are not yet firmly established, unlike for salmon, blue fin tuna and livestock. This situation could accelerate the status of wild eel stocks from threatened to declining. The inadequacy of scientific research, assessment and protection would lead to the collapse of tropical eel populations and affect the sustainability of the European, American, Japanese, Australian, and New Zealand eel resources. Therefore, rapid stock assessment and continuous monitoring of recruitment in tropical eels are necessary before fully utilizing this resource to avoid eel extinctions around the world.

2. History of eel aquaculture

The global demand for eels has been met largely through the aquaculture production of essentially two eel species, the Japanese eel and the European eel (***Figure 3***). Consumers in East Asia and Europe value the nutritional properties of these eels, making it a high-value aquaculture commodity. In fact, FAO[5] mentioned that almost all (90%) of the world's eel supply comes from aquaculture.

Aquaculture of eels has been pioneered by countries where eels are a delicacy. Eel culture in Japan began in 1879[15] and at approximately the same time in Italy and France.[16,17,18] Initially, eel was raised in polyculture systems,[16] but large-scale commercial production started in the early 1960s when formulated feeds became available.[19] Eel farming depends completely on the collection from the wild of juvenile stages such as the glass eel and elvers (***Figure 4***).

Therefore, the annual recruitment of the glass eel is very important to the eel aquaculture industry. However, recent recruitments of the glass eel stage of the Japanese eel have fallen to 10% that of the early 1960s rate.[20] For the European eel, recruitment has also fallen, on average to <5% of the peak levels of the late 1970s and early 1980s[3] as shown in ***Figure 2***, and the ICES continues to advise that the stock is outside of safe biological limits and that current fisheries are not sustainable.[21]

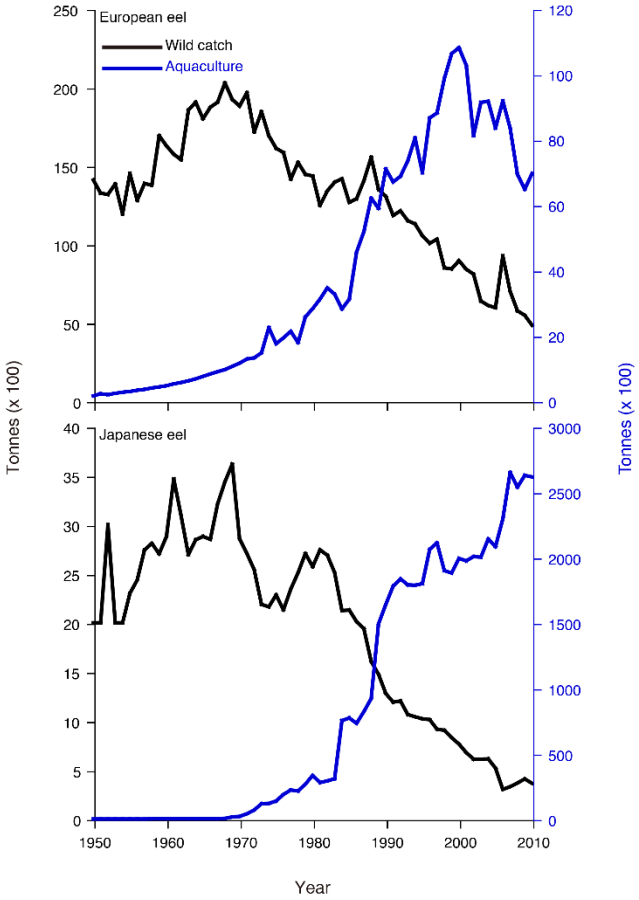

Figure 3. Trends in global capture and aquaculture production between 1950 and 2010 for the European eel (*top*) and Japanese eel (*bottom*). Source: Arai 2014,[6] figure was drawn using the FAO FishFinder of the Food and Agriculture Organization of the United Nations (http://www.fao.org/fishery/fishfinder/contacts/en). Note: Sharp declines in wild European and Japanese eel populations correspond to drastically increasing aquaculture demands for these eels after the 1970s, where peak capture of Japanese eels is less than the lowest captures of European eels, indicating a relatively low virgin biomass of Japanese eels.

The unstable supplies and prices for glass eels are serious concerns that confront the eel aquaculture industry. Therefore, the development of eel artificial breeding techniques is urgently necessary. In Japan, attempts to induce the

artificial maturation of the Japanese eel started in the 1960s.[22] Yamamoto and Yamauchi[23] were the first to successfully obtain fertilized eggs and larvae from the Japanese eel using hormone treatments, and after a two-week rearing period the preleptocephalus larvae reached 7 mm TL.[24] However, the larvae did not feed, and the transition into leptocephalus larvae did not occur. Although many researchers have henceforth succeeded in obtaining eel preleptocephali,[25,26] larval feeding and the production of leptocephali were not successful until 2001.[27]

Figure 4. Newly recruited glass eels to Indonesian coasts (approximately 50 mm in total length), the complete dependence of eel aquaculture on wild glass eels could lead to serious declines in eel stocks.

For other eel species, such as the European eel[28] and the New Zealand short- and long-finned eels (*A. australis* and *A. dieffenbachii,* Anguillidae) experimentally produced larvae have only survived for few days,[29] and as with the Japanese eel, did not develop into leptocephali. After much trial and error, Tanaka *et al*.[27] found that preleptocephali were strongly attracted to and actively fed on shark egg powder. Thereafter, leptocephali have been successfully reared in aquaria using this diet for 100 days and have been raised to 22.8 mm TL, and the morphological characteristics and age of the reared leptocephali overlap with those of wild leptocephali.[27] Soon after this study was performed, Tanaka *et al*.[22] reported further progress in rearing larvae to the glass eel stage and even further to the yellow eel stage in 2003.[20] After succeeding in rearing the eels to the leptocephalus stage,[27] their diet was improved by supplementation with krill hydrolysate, soybean peptide, vitamins and minerals.[22] The leptocephali that fed on this new diet grew to 50 to 60 mm TL and had begun to metamorphosis into glass eels approximately 250 days after hatching.[22] The artificially produced glass eels could be grown and were artificially matured.[20] Thereafter, a second generation of larvae was produced in 2010.[20] However, the techniques for producing glass eels are not yet firmly established.[22] The egg quality is unstable, and the survival rates of the larvae are usually extremely low. In addition, the growth of the larvae is slower in captivity than in the wild by approximately 100 days.[30] Under such conditions, the mass production of glass eels for use in aquaculture has not succeeded until present day.

3. Current status of trading and biological studies of tropical freshwater eels

The present target tropical eel species is *Anguilla bicolor* from Indonesia (*A. bicolor bicolor*) and the Philippines (*A. bicolor pacifica*).[13,14] China, Japan, Taiwan and South Korea have been importing these cultured tropical eels and selling it to consumers, using it to replace and compensate for the declining European and Japanese eel supply. Although Indonesia and the Philippines prohibit the export of juvenile eels, *i.e.* less than 150 g in weight from Indonesia and less than 15 cm in length from the Philippines to protect their resources, no regulations are enforced for juvenile fisheries in these countries.[13,14]

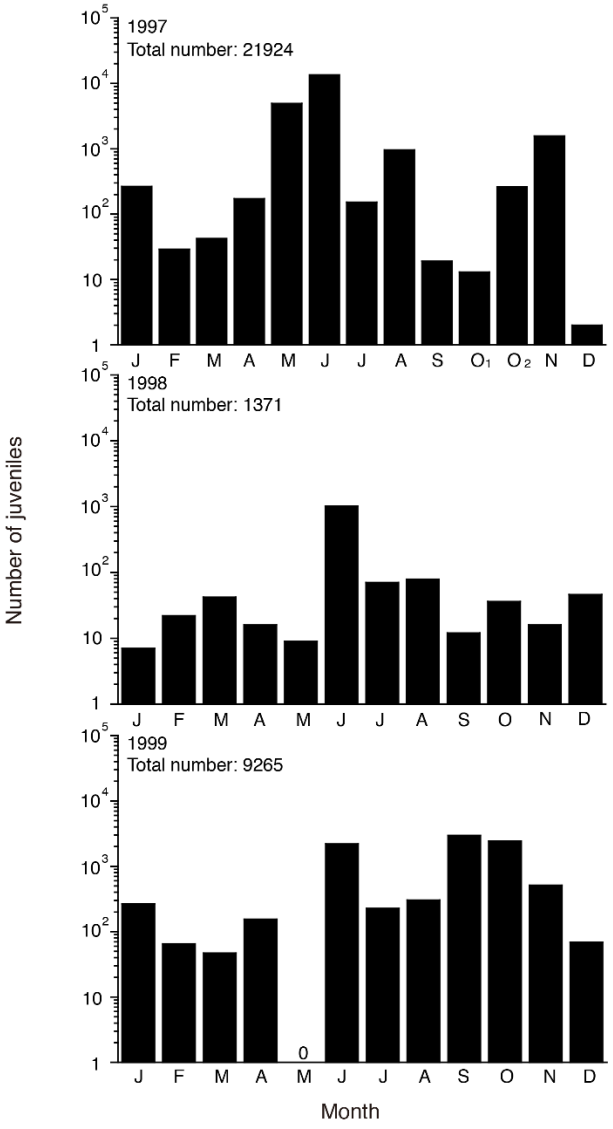

Figure 5. Fluctuations of recruitment in tropical juvenile eels in Indonesia between 1997 and 1999.
Notes: Monthly abundance of 3 tropical juvenile eels collected at the new moon in the Poigar River estuary, north Sulawesi Island of Indonesia from 1997 to 1999, where for October 1997 samples: 1 = early, 2 = late.[31,32] Juvenile eels were collected at the mouth of the tropical river, and were caught along a 10 m transect at the beach within 1.5 m from shore using 2 triangular scoop nets (mouth 0.3 m^2, 1 mm mesh), where the nets were fished simultaneously at depths of 25 to 50 cm in 10 replicate passes at hourly intervals;[31,32] where the temporal patterns of juvenile catches suggest tropical juveniles recruit to the estuary throughout the year with considerable inter-annual variation in the recruitment patterns, such recruitment patterns are clearly different from those of European, American, Japanese, Australian and New Zealand eels, which have much shorter seasonal ranges in recruitment period during about half the year or less.[15,31,32,33,34,35,36]

All marked eels are either wild-caught eels or cultured eels from wild juveniles. Since there are no historical stock or juvenile recruitment data for eels available in these countries, fluctuation in the abundance of eels could not be well understood. The only available data in tropical eels show the trend for recruitment for 3 years from 1997 to 1999 from quantitative sampling from an estuary in Indonesia,[31,32] where juveniles were found to occur throughout each year (***Figure 5***) with the highest recruitment occurring at the time of the new moon.[33]

More than 30,000 glass eels were collected quantitatively in the Poigar River estuary on north Sulawesi Island, Indonesia, in monthly collections from 1997 to 1999.[31,32] The specimens were identified three species, *Anguilla celebesensis*, *A. marmorata*, and *A. bicolor pacifica*, were found each year in fluctuating abundances (***Figure 6***).

A. celebesensis was the most abundant species and comprised 73.5 %, 79.5 %, and 81.9 % of all glass eels recruiting to the estuary of the Poigar River in 1997, 1998, and 1999, respectively (***Figure 6***).[31, 32]

This species was relatively abundant in all three years with peaks during June in 1997 and 1998 and during September in 1999 (***Figure 6***). *A. marmorata* was the second most abundant species and comprised 23.8 %, 18.8 %, and 17.7 % of the yearly catches, respectively, and reached peaks in abundance during June in 1997 and 1998, and during January 1999 (***Figure 6***). *A. bicolor pacifica* comprised only 2.7 %, 1.7 %, and 0.3 % of the yearly catches respectively, with peak catches in June 1997, in January 1998, and in January and February 1999 (***Figure 6***). *A. celebesensis* and *A. marmorata* were collected almost throughout the year in 1997, 1998, and 1999, suggesting that in contrast to the temperate eels that recruit during half the year from winter to spring, these tropical eel species recruit to some degree throughout the year.

The temporal patterns of glass eels catches near the mouth of the Poigar River differed among species and years suggesting that there was

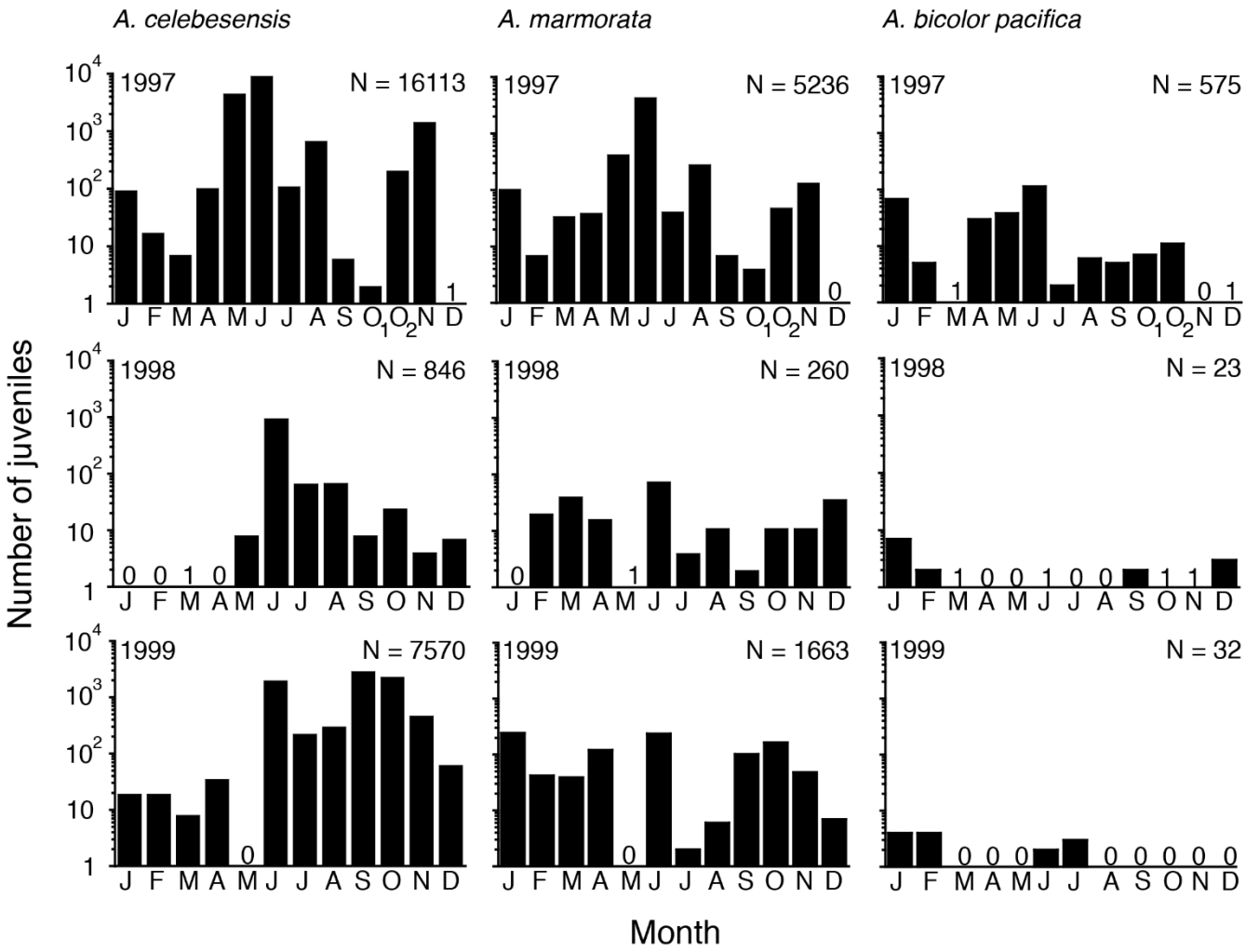

Figure 6. Fluctuations of recruitment in tropical eels *Anguilla celebesensis*, *A. marmorata* and *A. bicolor pacifica* in Indonesia between 1997 and 1999.[31,32] Note: Monthly abundance of glass eels of each species collected at new moon in the Poigar River estuary from 1997 to 1999 (for October 1997 samples: O_1 = first new moon, O_2 = second new moon). This figure was drawn using the original data from Arai *et al*.[31] and Sugeha *et al*.[32]

considerable inter-annual variation in the recruitment patterns of glass eels in the region. However, such systematic surveys for tropical glass eels have never been conducted in other tropical regions. Further long-term surveys should be urgently needed to understand natural (*e.g*. ambient environments such as global climate change and oceanic circulation system) and anthropogenic impacts (*e.g*. overexploitation, habitat degradation and pollution) on the recruitment of glass eels in tropical regions. The natural reproductive ecology and spawning patterns of both tropical and temperate eel species remain a mystery, and it is thus extremely difficult to determine the nature of the migrations of freshwater eels.[37]

Recently, Arai[37] found that tropical freshwater eels in Lake Poso, located in central Sulawesi, Indonesia, had higher gonadosomatic index values than did temperate eels that were collected in coastal waters preparing for spawning migration and showed histologically fully developed gonads (***Figure 7***).

The results suggested that, in contrast to the long-distance migrations made by the Atlantic and Japanese eels, freshwater eels originally migrated only short distances, perhaps less than 100 km to local spawning areas adjacent to their freshwater growth habitats.[37]

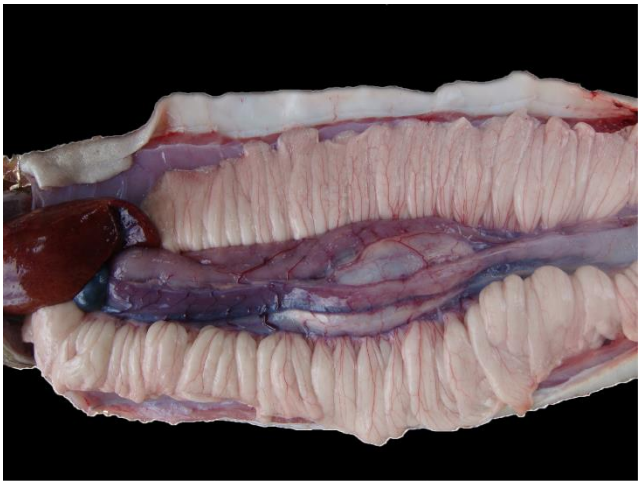

Figure 7. Gonadal morphology of a spawning-condition tropical freshwater eel *Anguilla celebesensis* (754 mm in TL) that were collected from Lake Poso, central Sulawesi, Indonesia.

The first description of a spawning period of a tropical eel that extends throughout the year (***Figure 8***), as revealed by gonadal development and histology.[38]

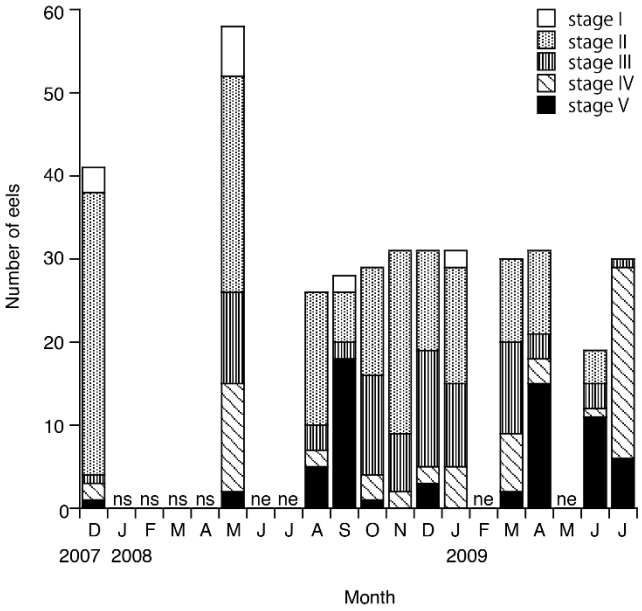

Figure 8. Monthly fluctuation of maturation stage in a tropical freshwater eel *Anguilla bicolor bicolor* collected in Segara Anakan, central Java of Indonesia between December 2007 and July 2009.[38] ns: no study for eel sampling was conducted that month. ne: study was conducted, but no eels were collected. Eels in more developed stages, such as Stages IV and V, were found every month, although the frequency differed among months. These findings suggest that *A. bicolor bicolor* carries out seaward migration for spawning throughout the year.

Until recently, considerably less research has examined the spawning migration of tropical eels in comparison with that of temperate eel species. The findings described in this report indicate that tropical eels have life history characteristics that differ markedly from those of temperate eels. Temperate anguillid species make their spawning migration as silver eels during the fall and winter. The year-round spawning migration of tropical species and constant larval growth extend the period of recruitment to estuarine habitats to year-round in tropical eels. The spawning seasons of tropical eels were found to extend throughout the year by back calculation of otolith daily increment in *A. celebesensis*, *A. marmorata* and *A. bicolor pacifica* in North Sulawesi of Indonesia[39] where is close to central Java Island of Indonesia. Additionally, the present results support a year-round spawning period, as evidenced by the monthly occurrence of matured eels in *A. bicolor bicolor*.

In tropical region, several eel species are living sympatrically in a river system. Chino & Arai[40,41] found that the migratory patterns of *A. bicolor bicolor* were mainly of the switch type involving moving from fresh water to sea water environments (75%). The other eels resided consistently in either sea water (20 %) or brackish water (5%). There were no eels that showed constant freshwater resident in Segara Anakan, central Java, Indonesia. In the Philippines, some *A. bicolor bicolor* eels showed freshwater resident (37%), while most showed estuarine resident (63%).[42] Thus, *A. bicolor bicolor* in the Philippines preferred to live in a brackish water environment. However, this finding is quite different from that of Indonesia, which showed only a 5% estuarine resident in Segara Anakan. In Segara Anakan, there was a wide range of salinity environments in which eels may live. Interspecific competition for food and space is one of the reasons for the dissimilarity of habitat use in this species. In central Java there were three species, *A. bicolor bicolor*, *A. marmorata* and *A. nebulosa nebulosa*, and in the Philippines, three species were also found, *A. bicolor bicolor*, *A. bicolor pacifica* and *A. marmorata*. Chino & Arai[40,41] discovered *A. bicolor bicolor* in either brackish

water or sea water area, although they did not collect eels from the upstream area of the river where there was no influence of a tidal effect. In the Philippines, *A. bicolor bicolor* also occurred in the downstream area of the river.[42] Therefore, interspecific competition may occur between (among) eel species at each site, and each species has a restricted distribution in either fresh water, brackish water or sea water habitats. In *A. marmorata*, the habitat preference in terms of salinity environment may depend on the habitat where there are either multiple or mono species of anguillid eels. In the Philippines and Taiwan, *A. marmorata* tends to live in fresh water environments,[42,43] while they live in brackish water environments in Ogasawara Island of Japan.[44] There were *A. bicolor bicolor*, *A. bicolor pacifica* and *A. marmorata* in the Philippines and *A. marmorata* and *A. japonica* in Taiwan, while only *A. marmorata* was observed in Ogasawara Island. In Ogasawara Island, *A. marmorata* could live in every environment with no interspecific competition,[44] and thus estuarine-dependent eels may be more abundant than in the Philippines and Taiwan. The results suggest that the determination of the distribution of eels at each site may occur by interspecific competition.

4. Current status of stocks in temperate eels

In contrast to the tropical eels, historical stock data for wild eels are available for European, American, Japanese, Australian and New Zealand eels. For European and Japanese eels, wild catches fell gradually after the peak levels of the late 1970s and early 1980s in accordance with the increasing demand for eels in aquaculture (***Figure 3***). Trends in juvenile abundance of the major eel stocks for European, American and Japanese eels also suggest that juvenile populations have declined dramatically and clearly lie outside of safe biological limits (***Figure 2***). Recruitment of European and Japanese eels in each distribution range declined by 99% and 80%, respectively. Recruitment of American eel at the northern limit of its distribution has ceased (***Figure 2***).

5. Decline of eel populations in the world

The worldwide decline of freshwater eel populations is a major concern for animal conservation and diversity. European, American and Japanese eels have experienced sharp declines across their ranges over the last 30–40 years[3,4,21,45,46] (***Figure 2*** and ***Figure 3***). In spite of the seriousness of the situation for juvenile eel recruitment, eel consumption is still increasing. To continue to supply large amounts of eels to consumers, the replacement and compensation have started to import eels from foreign countries, mainly the Philippines, Indonesia and Madagascar.[13,14,47] The main problem with consumption of this animal is that artificial propagation has not yet succeeded as it has with other common animals, such as salmon, blue fin tuna and livestock; therefore, juvenile eels are high-value aquaculture commodities that put high fishing pressure on a natural environment. Almost all (90 %) of the world's eel supply comes from aquaculture,[5] and the present eel aquaculture completely (100 %) depends on wild juveniles. More than 90 % of the world production of eels is cultured in East Asia, primarily Japan, Taiwan and China.[48] Thus, wild juvenile eel catch will be needed in the future for these countries due to the increasing demands of aquaculture (***Figure 3***). To enhance natural eel stocks and continue their commercial usage for human consumption, studies related to the establishment of commercial juvenile production are urgently required and should focus on this goal as a means of protecting wild eel stocks.

6. Lack of stock assessment and enhancement in freshwater eels

For the European eel, as a consequence of these concerns, the European Commission has agreed to an eel recovery plan, the aim of which is to return the European eel stock to sustainable levels of adult abundance and juvenile recruitment.[49] In 2007, the European eel was listed in Appendix II of CITES (the Convention on International Trade in Endangered Species of Wild Fauna and Flora) and Appendix II ''includes species not necessarily threatened with extinction, but in which trade must be controlled to avoid utilization incompatible with their survival''.[7] Although stock assessment and management of the European eel have received increasing attention from both the scientific community and fisheries

agencies in recent years,[21] such assessment and management of the Japanese eel have not yet been well studied. Such studies would help with the development of a concrete conservation policy and management applications for stock enhancement. Please note that despite the high demand for the product, the peak capture of Japanese eels is less than the lowest captures of European eels (***Figure 3***).[50] This fact indicates a relatively low virgin biomass of Japanese eels. To make matters worse, trade in tropical eels started with no scientific assessment and management before usage in spite of our experience with severely declining stocks in European, American, Japanese, Australian and New Zealand eels. Until now, there has been no information available on historical fishing records in tropical eels and only limited biological information compared with European, American, Japanese, Australian and New Zealand eels.

7. Conclusion

Although European, American, Japanese, Australian and New Zealand eels appeared to have much shorter seasonal ranges during the recruitment period for about half of the year or less,[15,33,34,35,36] at least a few juveniles of the tropical eels recruited year round. The temporal pattern of tropical juvenile recruitment was found to have considerable interannual variation (***Figure 5*** and ***Figure 6***).[31,32] Thus, continuous long-term research is needed to determine the causes of the variation. Such year-round recruitment in tropical eels might be more convenient in aquaculture, which would enable eel aquaculture throughout the year. In fact, 70 tonnes of eels were exported to Japan from one eel farm in Indonesia in 2013, and this amount is estimated to double in 2014.[14] Because the present market price of juvenile eels is 150 times higher than 20 years ago, a number of village people near juvenile eel fishing grounds in Indonesia tend to concentrate on eel fishing only, whereas they used to focus on farming and fishing.[14] However, the juvenile eel catch is now reported to be half that of 20 years ago,[14] although the estimated decline has never been evaluated based on scientific research. The causes of decline in eel stocks and recruitment are not well understood. One of the main reasons must be overfishing, as sharp declines in wild European and Japanese eel populations correspond to drastically increased aquaculture demands for these eels since the 1970s (***Figure 3***). Now, tropical eels may have begun to follow the same trends as the European and Japanese eels. This suggests that we cannot rule out overfishing in tropical countries. Thus, if the wild juvenile eel catch of tropical eels continues to increase without assessment and protection of the stock and regulation of the catchment, all eel populations will decline to numbers outside safe biological limits.[51] Currently, European, American and Japanese eels are seriously threatened with extinction due to eel consumption, and demand is still increasing. After the stocks and recruitment collapse in the present target eel species and areas, we will have to seek other targets for replacement and compensation to continue eel consumption.[51] We may not be able to see such a unique animal on the earth in the near future.

Acknowledgements

This work was partially supported in part by the Ministry of Higher Education *Malaysia under* the Fundamental Research Grant Scheme (Vot No. 59406).

References

[1] W. Dekker, *Can. J. Fish. Aquat. Sci.* 2003a., 60:787–799.

[2] W. Dekker, *Fish. Manag. Ecol.* **2003**, 10: 365–376.

[3] W. Dekker, M. Pawson and H. Wickström, Is there more to eels than slime? *ICES J. Mar. Sci.,* **2007**, 64:1366–1367.

[4] W. Dekker, J. M. Casselman, D. K. Cairns, K. Tsukamoto, D. Jellyman and H. Lickers, *Fisheries,* **2003**, 28:28–30.

[5] FAO (Food and Agriculture Organization of the United Nations). *The state of world fisheries and aquaculture*. Food and Agriculture Organization of the United Nations, Rome; 197 p. **2010**.

[6] T. Arai, *Rev. Fish Bio. Fish.,* **2014**, 24:75-88.

[7] CITES, Convention on International Trade in Endangered Species of Wild Flora and Fauna. Fourteenth meeting of the Conference of the Parties, The Hague,

Netherlands, 3–15 June 2007 CoP14, Prop. 18. **2007**.
[8] B. Knights, *Sci. Total Environ.,* **2003**, 310: 237–244.
[9] L.A. Marcogliese and J. M. Casselman, *Am. Fish. Soc. Symp.*, **2009**, 58:197–206.
[10] S. Bonhommeau, E. Chassot and E. Rivot, *Fish. Oceanogr.,* **2008**, 17:32–44.
[11] K. D. Friedland, M. J. Miller and B. Knight, *ICES J. Mar. Sci.* **2007**, 64:519–530.
[12] V. Crook, *Traff. Bull*., **2013**, 25. http://www.traffic.org/bulletin-download
[13] Anonymous. Competition on eel fishery and trading in Asia. **2013**. http://www.nhk.or.jp/ohayou/marugoto/2013/08/0801.html (accessed March 19 2014).
[14] Anonymous. Eel battle in tropical area. **2014**.
[15] I. Matsui, *J. Shimonoseki Coll. Fish.*, **1952**, 2:1–245.
[16] B. Gousset, *Aquaculture*, **1990**, 87:209–235.
[17] L. T. N. Heinsbroek, *Aquacult. Fish. Manag.*, **1991**, 22:57–72.
[18] E. Ciccotti and G. Fontennelle, *Abstracts of the 3rd East Asian Symposium on Eel Research—Sustainability of Resources and Aquaculture of Eels*. Keelung: Taiwan Fisheries Research Institute, pp 9–11, **2000**. http://www.cites.org/common/cop/14/raw_props/EDE04-Anguilla%20anguilla.pdf (accessed 8 Aug 2007)
[19] I. C. Liao, Y. K. Hsu, W. C. Lee, *Rev. Fish. Sci.*, **2002**, 10:433-450.
[20] S. Ijiri, K. Tsukamoto, S. Chow, H. Kurogi, S. Adachi and H. Tanaka, *Aquacult. Eur*. **2011**, 36:13–17.
[21] ICES. Report of the Joint EIFAC/ICES Working Group on Eels. ICES Document CM 2006/ACFM: 16: 367 p. **2006**.
[22] H. Tanaka, H. Kagawa, H. Ohta, T. Unuma and K. Nomura, *Fish Physiol. Biochem.*, **2003**, 28:493-497.
[23] K. Yamamoto and K.Yamauchi, *Nature*, **1974**, 251:220-222.
[24] K. Yamauchi, M. Nakamura, H. Takahashi and K. Takano, *Nature*, **1976**, 263:412.
[25] H. Satoh, *Iden*, **1979**, **33:**23–30.
[26] Y. Wang, C. Zhao, Z. Shi, Y. Tan, K. Zhang and T. Li, *J. Fish. China*, **1980**, 4:147–156.
[27] H. Tanaka, H. Kagawa and H. Ohta, *Aquaculture*, **2001**, 201:51-60.
[28] G. A. Prokhorchik, *J. Ichthyol.,* **1986**, 26: 121–127.
[29] P. M. Lokman and G. Young, *NZ J. Mar. Freshw. Res.*, **2000**, 34:135–145.
[30] T. Arai, T. Otake and K. Tsukamoto, *Mar. Ecol. Prog. Ser.*, **1997**, 161:17–22.
[31] T. Arai, J. Aoyama, D. Limbong and K. Tsukamoto, *Mar. Ecol. Prog. Ser.*, **1999**, 188:299–303.
[32] H. Y. Sugeha, T. Arai, M. J. Miller, D. Limbong and K. Tsukamoto, *Mar. Ecol. Prog. Ser.,* **2001**, 221:233-243.
[33] A. J. Haro and W. H. Krueger, *Can. J. Zool.* **1988**, 66:528:2533.
[34] G. Gandolfi, M. Pesaro and P. Tongiorgi, *Oebalia*, **1984**, 5:17–35.
[35] R. D. Sloane, *J. Mar. Freshw. Res.*, **1984**, 35:325–339.
[36] D. J. Jellyman, *NZ J. Mar. Freshw. Res.* **1977.** 11:193–209.
[37] T. Arai, *Ecol. Evol.*, **2014**, 4:3812-3819.
[38] T. Arai, S. R. Abdul Kadir and N. Chino, *Mar. Biol.*, **2016**, 163:2, 1-7.
[39] T. Arai, D. Limbong, T. Otake and K. Tsukamoto, *Mar. Ecol. Prog. Ser.*, **2001**, 216:253-264.
[40] N. Chino and T. Arai, *Mar. Biol.*, **2010**, 157:1075-1081.
[41] N. Chino and T. Arai, *Environ. Biol. Fish.*, **2010b**, 89: 571-578.
[42] A. A. Briones, A. V. Yambot, J. C. Shiao, Y. Iizuka and W. N. Tzeng, *Raffl. Bull. Zool.*, **2007**, 14:141-149.
[43] J.C. Shiao, Y. Iizuka, C.W. Chang and W. N. Tzeng, *Mar. Ecol. Prog. Ser.,* **2003**, 261: 233-242.
[44] N. Chino and T. Arai, *Ecol. Freshw. Fish*, 2010c, 19:19-25.
[45] M. W. Aprahamian, A.M. Walker, B. Williams, A. Bark and B. Knights, *ICES J. Mar. Sci.,* **2007**, 64:1472–1482.
[46] M. Castonguay, P.V. Hodson, C. Moriarty, K. F. Drinkwater and B. M. Jessop, *Fish. Oceanogr.*, **1994,** 3:197–203.
[47] Anonymous. The danger zone for eel. **2013**. http://weekly.japantimes.co.jp/ed/the-

danger-zone-for-eels. (accessed March 28 2014) http://bulo.hujiang.com/menu/110460/item/862115/ (accessed March 19 2014).
[48] S. Ringuet, F. Muto and C. Raymakers, *Traff. Bull.*, **2002**, 19:2–27.
[49] H. Svedäng and L. Gipperth, *Mar. Pol.*, **2012**, **36**:801–808.
[50] P. Halpin, Unagi: Freshwater ‘‘Eel’’. *Anguilla japonica*, *A. anguilla*, *A. rostrata*. Seafood Watch, Seafood Report. Monterey Aquarium, Monterey, **2007**. http://www.seafoodwatch.org/cr/cr_seafoodwatch/content/media/MBA_SeafoodWatch_UnagiReport pdf. (accessed March 28, 2013)
[51] T. Arai, *SpringerPlus*, **2014**, 3:534.

Antimicrobial activities of soaps containing *Senna alata* leaf extract

Muhammad Fairuz Aminuddin, Aida Maryam Basri, Hussein Taha[*]*, Adlan Mursyid Abidin and Norhayati Ahmad*

Environmental and Life Sciences, Faculty of Science, Universiti Brunei Darussalam, Jalan Tungku Link, Gadong, BE1410, Brunei Darussalam

**corresponding author email: hussein.taha@ubd.edu.bn*

Abstract

Senna alata is an important ethnomedicinal plant and is often used traditionally to treat skin diseases. Hence, it can be a potential attractive ingredient for natural skincare products. In this study, we determined the potential of producing antimicrobial soaps by using *S. alata* leaf extract, either aqueous crude extract or essential oil, as the key ingredient and also virgin coconut oil as the base. Although *S. alata* essential oil is not feasible yet to be considered for soap production due to its poor extraction yield, the aqueous leaf crude extract had shown promising potential. Our antimicrobial assays showed the aqueous extract exhibited antifungal activity but did not show any antibacterial activity under the conditions tested. Similarly, the prototypes of *S. alata* soap containing the aqueous extract also showed an antifungal activity against *Saccharomyces cerevisiae*. Therefore, the potential use of *S. alata* for antimicrobial soaps warrants further consideration and study.

Index Terms: antimicrobial, *Senna alata*, medicinal plant, soaps

1. Introduction

Senna alata (L.) Roxb. (synonym *Cassia alata*) or candlestick is considered an important ethnomedicinal plant, as it has been used traditionally to treat fungal infections such as ringworm, and to relieve other skin diseases such as itchiness and eczema. It can also be used to treat constipation and intestinal worm infestation.[1] The plant has been previously reported to have antibacterial and antifungal activities.[2-6] Furthermore, it is also reported to have antioxidant, anticancer, anti-allergic and laxative activities.[7-10]

S. alata has the potential to be used as an attractive ingredient for natural soaps, as natural and organic skincare products have been gaining in popularity. However, many of the commercially available natural soaps in the market have not been scientifically proven for their ethnomedicinal claims. Thus, it is vital for any skincare product(s) to be scientifically validated. In this study, we presented prototypes of *S. alata* soaps with scientific validation on their antifungal activities (no antibacterial activities were detected).

2. Experimental approach

Sample collection and preparation

S. alata leaves were collected from Jalan Madang, Brunei Darussalam in March 2015. The samples were ground into powdered form after being air-dried for three weeks.

Extraction of aqueous crude extract

Ultrasound extraction was employed.[11] Powdered samples were mixed with distilled water in the ratio of 1 g to 10 ml. The mixture was ultrasonicated (Soltec Sonica Ultrasonic Cleaner) for 30 mins at 25°C. It was subsequently centrifuged and filtered to remove solid residues, and the filtrate was used directly for antimicrobial assays and soap preparation.

Extraction of essential oil

Hydrodistillation was used to extract *S. alata* essential oil.[12] Powdered samples (100 g) were

boiled in distilled water, and the distillate was collected. To obtain the essential oil, 10% hexane was subsequently added. The resulting oil-containing solvent was collected and gently evaporated to remove hexane, leaving behind the essential oil.

Soap preparation

Prototypes of *S. alata* soap were prepared as described elsewhere [13], to contain virgin coconut oil (as the soap base) and sodium hydroxide in the ratio of 1 g to 0.178 g, respectively. The latter was initially dissolved in distilled water before mixing with the former and also the aqueous extract in different volumes. The mixture was heated with continuous stirring until it became thick. It was subsequently poured into a moulding tray and allowed to solidify. For antimicrobial assays, the solidified soaps were dissolved at 100 µg/ml with distilled water.

Antimicrobial assays

Antimicrobial activities were determined by agar-well diffusion method.[14] Four bacterial strains were studied, *Bacillus subtilis* ATCC-11774, *Escherichia coli* ATCC-11775, *Pseudomonas aeruginosa* ATCC-27853, and *Staphylococcus aureus* ATCC-29213, and one fungal strain, *Saccharomyces cerevisiae*. An overnight nutrient broth culture of the microorganism was uniformly spread onto a Mueller-Hinton agar plate. The agar was bored to create wells with 4-mm diameter, in which the extract was introduced for testing. For positive and negative controls, streptomycin sulfate and distilled water were also tested, respectively. The plate was incubated at 37°C for 18 hours. Antimicrobial activity was detected by a zone of clearance around the well. The diameter of this zone of inhibition was measured.

3. Results and Discussion

S. alata aqueous crude extract was successfully obtained, which had a brownish colour and a mild tea-like aroma, whereas the *S. alata* essential oil had an aroma similar to green tea. However, the percentage yield of extraction was low (<1%) under the conditions tested, suggesting higher starting plant material and/or different extraction technique might be required for viable extraction of essential oil. Alternatively, other parts of the *S. alata* plant could also be tested such as the flowers, roots or seeds.

Under the conditions tested, the aqueous extract of *S. alata* leaf extract did not show any antibacterial activity against Gram-negative bacteria (*E. coli* and *P. aeruginosa*) and Gram-positive bacteria (*B. subtilis* and *S. aureus*) (data not shown). However, it showed an antifungal activity against *S. cerevisiae* with a zone of inhibition of 21 ± 1 mm (mean ± standard deviation, SD of 4 replicates). Similarly, the prototypes of *S. alata* soap containing different fractions of the aqueous extract also did not exhibit any antibacterial activity but also showed an antifungal activity against *S. cerevisiae* (***Table 1***). Although the study could be improved further by also testing other important fungal species, it nicely complementes the ethnomedicinal uses of *S. alata* as antifungal remedy.[1]

Table 1. Antimicrobial activities of *S. alata* soaps. Antibacterial activities were not detected for *E. coli*, *P. aeruginosa*, *B. subtilis* and *S. aureus* (data not shown). Negative control did not show any detectable activity as expected. [a] Concentration is calculated as the volume to volume fraction of the aqueous extract in the soap. [b] Mean values (±SD) of four replicates were presented.

Concentration of *S. alata* aqueous extract (%)[a]	**Zone of inhibition for *S. cerevisiae* (mm)[b]**
0	41 ± 3
3	45 ± 5
6	41 ± 1
20	39 ± 1
40	40 ± 2
60	42 ± 2
80	38 ± 3

Our statistical analysis using one-way ANOVA did not find any significant differences ($P>0.05$) between the means for the different extract concentrations. This means increasing the aqueous extract concentration in the soap did not show any detectable improvement in the antifungal activity. Although the size of the inhibition zone could indicate the potency of the plant antimicrobial, the zone of inhibition test

itself is considered as a qualitative method. Moreover, the soap with 0% aqueous extract also showed similar zone of inhibition compared to the other concentrations, suggesting the observed antifungal activity of these soaps could be contributed solely by or in synergy with virgin coconut oil and/or sodium hydroxide, which were also the other components of the soaps. Virgin coconut oil has been reported to have antimicrobial activities.[15]

In light of the possible synergy, virgin coconut oil should also be further studied. In view of making the soap, it would not only be commercially attractive but also might increase the bioactive potency of any soap that contained different combinations of plant extracts or oils. Thus, it should be taken into consideration when designing future soaps.

A lack of detectable antibacterial activity in this study does not necessarily mean the absence of potential antibacterial in *S. alata*, as the outcomes of the test could be condition-dependent. The use of low concentration of aqueous crude extract could be a limiting factor, and hence, for future studies, freeze drying or lyophilisation could be considered to enable analysis with concentrated aqueous extract. Apart from water, the use of other solvents to generate different *S. alata* extracts could also be considered for future analyses, as different solvents would generally extract a variety of different phytochemicals.

Fractionation of the crude extract by column chromatography could also be considered for the isolation of active fraction(s) containing specific bioactive compound(s), which could be used directly in the soap making instead of the whole crude extract itself. However, in view of a commercial local production, this would only escalate the cost of the soaps but low-priced products are more attractive and competitive.

Finally, other vital tests such as toxicity test should also be taken into account before *S. alata* soaps could be made available in the market, as it might cause unwanted side effect.[16] The effect of *S. alata* leaf extract on the natural microbiome present on the skin surface should also be studied to gain more insight into its antimicrobial efficacy. The prototypes of *S. alata* soaps presented here arguably warrant further consideration and study.

4. Conclusion

Aqueous crude extract from *S. alata* leaves had shown a promising potential to be used for commercial antifungal soap production.

Acknowledgements

The research was supported by the Brunei Research Council (JPKE/BRC/UBD/BRC6) and Universiti Brunei Darussalam.

References

[1] Department of Agriculture, *Medicinal Plants of Brunei Darussalam*, MIPR, Brunei Darussalam, **2000**.
[2] O. Adedayo, W. A. Anderson, M. Moo-Young, et al., *Pharm. Biol*., **2001**, 39.
[3] O. Adedayo, W. A. Anderson, M. Moo-Young, et al., *Pharm. Biol*., **1999**, 37.
[4] M. Wuthi-Udomlert, S. Prathanturarug, N. Soonthornchareonnon, *Acta Hort.*, **2003**, 597.
[5] J. A. Owoyale, G. A. Olatunji, S. O. Oguntoye, *J. Appl. Sci. Environ. Mgt*., **2005**, 9.
[6] S. Y. Timothy, C. H. Wazis, R. G. Adati, I. D. Maspalma, *J. Appl. Pharm. Sci*., **2012**, 2.
[7] J. Okpuzor, H. Ogbunugafar, G. K. Kareem, et al., *Res. J. Phytochem*., **2009**, 3.
[8] B. Singh, J. R. Nadkarni, R. A. Vishwakarma, et al., *J. Ethnopharm*., **2012**, 141.
[9] V. E. Fernand, J. N. Losso, R. E. Truax, et al., *Chem. Biol. Interact*., **2011**, 192.
[10] A.A. Elujoba, A. T. Abere, S. A. Adelusi, *Niger. J. Nat. Prod. Med*., **1999**, 3.
[11] B.Trusheva, D. Trunkova, V. Bankova, *Chem. Cent. J.*, **2007**, 1.
[12] V. I. Njoku, B. O. Evbuomwan, *Greener J. Chem. Sci.*, **2014**, 1.
[13] P. G. Kareru, J. M. Keriko, G. M. Kenji, et al., *Afr. J. Trad. CAM*, **2010**, 7.
[14] N. S. Ncube, A. J. Afolayan, A. I. Okoh, *Afr. J. Biotechnol.*, **2008**, 7.

[15] D. O. Ogbolu, A. A. Oni, O. A. Daini, A. P. Oloko, *J. Med. Food*, **2007**, 10.
[16] M. T. Yakubu, A .O. Adeshina, A. T. Oladiji, et al., *J. Reprod. & Contracept.*, **2010**, 21.

First record and conservation value of *Periophthalmus malaccensis* Eggert from Borneo, with ecological notes on other mudskippers (Teleostei: Gobiidae) in Brunei

*Gianluca Polgar**

Environmental and Life Sciences Programme, Faculty of Science, Universiti Brunei Darussalam, Jalan Tungku Link, Gadong, BE 1410, Brunei Darussalam

**corresponding author email: gianluca.polgar@ubd.edu.bn*

Abstract

The mudskipper *Periophthalmus malaccensis* is first reported from two mangrove areas of Brunei Darussalam, on the island of Borneo. This species has a relatively restricted geographic distribution and have been reported from Singapore, Philippines, Maluku Islands, western New Guinea, and northern Sulawesi. In Brunei, this species occurs at low population density in high intertidal habitats, which are highly impacted by anthropogenic destruction and fragmentation. For these reasons, the conservation status of this species should be evaluated. The distribution and habitat types of species belonging to *Periophthalmus* and *Periophthalmodon* in Brunei are also described.

Index Terms: mudskippers, Brunei Bay, mangrove destruction, extinction risk

1. Introduction

The genus *Periophthalmus* (Perciformes: Gobioidei: Gobiidae; '*Periophthalmus* lineage'[1]) presently includes 18 species with amphibious lifestyles, known as mudskippers.[2,3] Four species were previously recorded from Borneo[2]: *P. argentilineatus* Valenciénnes, 1837 (Malaysia: Sarawak); *P. gracilis* Eggert, 1935 (Sarawak); *P. chrysospilos* Bleeker, 1852 (Indonesia, Kalimantan: Sebatic Island = Pulau Sebatik), and *P. novemradiatus* (Hamilton, 1822) (= *P. variabilis* Eggert, 1935, sensu[5]; Malaysia: Sabah, Sarawak; Pulau Sebatik). *Periophthalmus argentilineatus* (USNM 356813-356814) and *P. gracilis* (USNM 366713) were collected in Brunei in 1997[4] (Sandra Raredon, pers. comm., ***Appendix 1***). However, I could not confirm the taxonomic status of USNM 366713.

Molecular data suggest that the morphospecies *P. argentilineatus* is a complex of three cryptic or pseudocryptic species.[6] These molecular clades are morphologically similar to three morphospecies revised by Eggert[7] (GP, unpublished data), that Murdy[2] synonymised as *P. argentilineatus*. Two of these species, *P. vulgaris* Eggert (clade F in Polgar et al.[6]) and *P. argentilineatus* Valenciénnes (clade K), occur sympatrically in Southeast Asia; *P. sobrinus* Eggert (clade I) occurs in Eastern Africa, Seychelles and Madagascar. A taxonomic revision of *P. argentilineatus* is beyond the scope of this contribution. Therefore, I will here record specimens of *P. argentilineatus* that are morphologically similar to those in clade F[6] as *Periophthalmus* cf. *vulgaris* Eggert, 1935. No specimens similar to clade K[6] were found during this study.

Periophthalmus malaccensis is known from the Philippines, Maluku Islands, western New Guinea[2,8], and northern Sulawesi[6]. In northern Sulawesi[6], *P. malaccensis* occurs in riverine mangrove forests, up to 1.5 km from the coast (unpublished data). The type locality of this species is Singapore, and the species was named after the Strait of Malacca, between Sumatra and the Malay Peninsula[7] (***Figure 1***). However, this species has not been recorded in this area since its description, in spite of extensive sampling efforts.[9,10,11,12] In fact, both the coastal wetlands along the west coast of the Malay

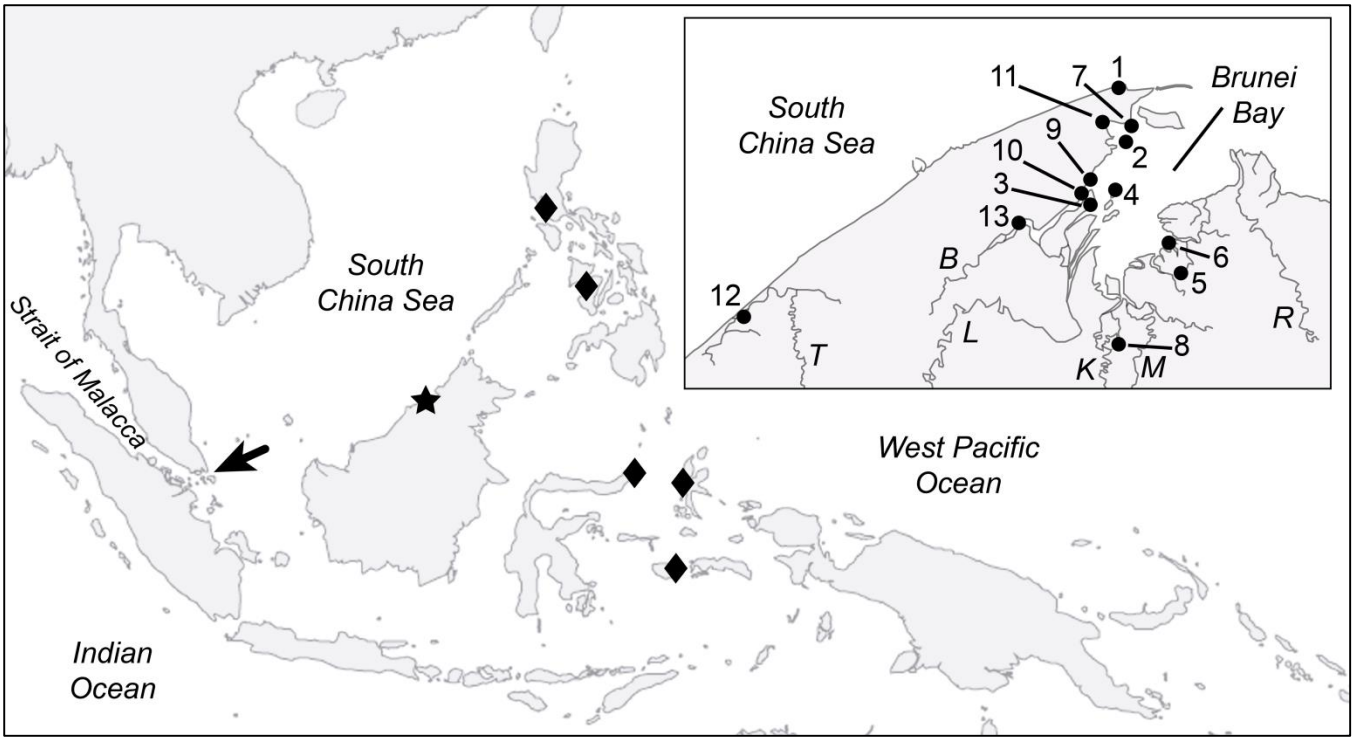

Figure 1. Study sites in Brunei Darussalam (inset, numbered black dots; see ***Table 1***; ***Appendix 2***) and geographic distribution of *P. malaccensis*; some major river systems in the study area are illustrated: B = Brunei river; K = Kibi river; L = Limbang river; M = Temburong river; R = Batang Tarusan river; T = Tutong river; *black arrow* = type locality, *black diamonds* = previous records[2,6,8]; *black star* = new record and geographical position of the map in the inset.

Peninsula[13] and Singapore[14] underwent extensive deforestation, which severely impacted the higher intertidal and supratidal zone, and could have extirpated *P. malaccensis* in Singapore.[15]

The genus *Periophthalmodon* includes three species ecologically and systematically closely related to *Periophthalmus* species.[2] *Periophthalmodon schlosseri* (Pallas, 1770) was recorded in northern Borneo (Sarawak; Sebatic Island)[2]; *Periophthalmodon septemradiatus* (Hamilton, 1822) was also collected in Sarawak[2]. A first record of *P. malaccensis* from Borneo is here documented from two mangrove areas in Brunei Darussalam, with notes on the presence and habitat of the species of the genera *Periophthalmus* and *Periophthalmodon*. The potential conservation interest of *P. malaccensis* is also briefly discussed.

2. Experimental approach

Study sites

Brunei Darussalam (***Figure 1***) is characterised by a tropical climate, with an average annual temperature of 27 °C, and an average annual rainfall of 2,880 mm (mean from 1966 to 2006), with two peaks in correspondence of Southwest monsoon (May), and the Northeast monsoon (December) (Brunei Meteorological Service, Department of Civil Aviation).

The Brunei Bay occupies an area of ~ 2,500 km^2; several rivers flow into the bay, such as the Brunei, Limbang, Temburong River, and Batang Trusan (Yau 1991; ***Figure 1***). Twenty-eight sampling surveys of gobioid fishes were conducted in coastal areas and tidally-influenced rivers where *Periophthalmus* species were found, at 13 sites, from May 2013 to August 2015 (***Figure 1***; ***Table 1***; ***Appendix 2***). All surveys were conducted during the day and ± 2 hours around low tide (TideComp v. 7.04 © Mike Harris; tidal reference stations: Bandar Limbang 4°45'0.0" N 114°59'60.0" E; Dato Gandi 4°54'0" N 114°58'60" E; Kuala Limbang 4°50'60.00" N 115°1'0" E).

Table 1. Study sites where *Periophthalmus* and *Periophthalmodon* mudskippers were found, number of surveys (n), and species occurrence (X). Pulau = island; Sungai = river. Abbreviations: a = *P.* cf. *vulgaris*; g = *P. gracilis*; m = *P. malaccensis*; s = *Pn. schlosseri*.

	Site	Coordinates	n	Species occur.			
				a	g	m	s
1	Pemburongunan Creek	5°02'36.8"N 115°03'21.1"E	2	X			
2	Pulau Bedukang	4°58'45.7"N 115°03'40.4"E	5	X	X		X
3	Pulau Berambang	4°54'13.0"N 115°01'15.8"E	1		X		
4	Pulau Pepataan	4°59'40.5"N 115°03'59.2"E	1	X*	X		
5	Pulau Selirong site A	4°49'30.9"N 115°07'51.9"E	1			X	
6	Pulau Selirong site B	4°51'18.7"N 115°6'47.9"E	1	X	X		
7	Serasa jetty	4°59'40.5"N 115°03'59.2"E	1	X			
8	Sungai Belayang	4°44'22.9"N 115°2'59.2"E	1		X		
9	Sungai Besar	4°55'39.8"N 115°00'52.0"E	3	X			
10	Sungai Bunga	4°55'0.5"N 115°00'25.0"E	6	X	X	X	X
11	Sungai Salar	4°59'59.1"N 115°1'51.8"E	1	X	X		
12	Sungai Tutong	4°46'10.8"N 114°36'23.4"E	2	X	X		
13	Ujong Bukit	4°53'17.9"N 114°56'07.5"E	3				X

*examined specimens were not deposited in the UBDM collection (***Appendix 2***)

Table 2. Morphometric measurements of *P. malaccensis* (n = 4) from Brunei. %SL = percentage of standard length.

Total length (mm)	71.5-113.9
Standard length (mm)	54.2-90.3
In % SL	
Head length	25.3-27.2
Head depth	16.8-19.5
Head width	15.5-17.6
Body depth	14.9-16.5
Body width	15.9-17.7
Length of D1 base	17.0-23.7
Length of D2 base	18.1-21.5
Length of anal-fin base	16.1-18.6
Least caudal-peduncle depth	8.8-9.4
Pectoral-fin length, base included/not included (left)	25.2-28.4 / 16.2-17.7
Pectoral-fin height, base included/not included (left)	10.3-11.7 / 6.9-9.0
Pelvic-fin length	13.0-14.6
Caudal-fin length	25.2-31.9

Table 3. Meristic measurements of *P. malaccensis* (n = 4) from Brunei.

Fin-ray counts	
First dorsal fin	10-12
Second dorsal fin	12
Anal fin	12
Pectoral fin (left/right)	13-14 / 13
Principal-caudal rays	16
Scale counts	
Number of lateral-scale rows	54-58
Transverse scales counted ventrally backward	16-21
Transverse scales counted dorsally backward	17-21
Transverse scales counted ventrally forward	17-23
Predorsal scales	25-27
Number of interdorsal-scale rows	3-8

Sampling, preservation and measurements
Specimens were sampled with hand nets, transported alive to the laboratory, anesthetised placing them in a refrigerator at 4°C for 1 hour, euthanised by rapid cooling at -20°C, and then fixed and preserved in 70% undenatured ethanol. Measurements were taken with a digital calliper to the nearest 0.1 mm, and are reported as a percentage of the specimens' standard length (SL), unless stated. Counts were made under a dissecting microscope. All measurements followed Polgar et al.[16] Soft and spinous fin rays were counted together.

Several specimens were deposited in the zoological collection of the Universiti Brunei Darussalam Museum (UBDM; ***Appendix 2***). Specimens from other museum collections were examined, to confirm taxonomic discrimination of species potentially present in the region, and verify previous records (***Appendix 1***). The heads of some specimens of *Pn. schlosseri* (UBDM MUb131013sch) and *P. malaccensis* (UBDM MBu111013mal) were fixed in Karnovsky fixative solution for histological preparations, and left pectoral fins were fixed in absolute ethanol for molecular analyses.

3. Results and Discussion
The specimens' morphology and colouration patterns corresponded to the available taxonomic descriptions[2,7] (***Tables 2, 3***). To my knowledge, there are no mudskippers' records from Brunei in the literature, therefore all the species recorded here are first records for Brunei. *P. malaccensis* is also a first record for the island of Borneo, near the western limit of the longitudinal range of this species (***Figure 1***).

The examined specimens of *P. malaccensis* were characterised by (***Figure 1***): (i) squared-shaped pelvic fins, with prominent pelvic frenum, partially united by a basal membrane, both ventrally and dorsally pigmented, and with white margin; (ii) presence of dark pigmentation of anal interradial membranes; (iii) sky blue speckles on cheeks and opercula; (iv) prominent transversal crease on snout; and (v) elongate first spine of D1 in both males and females (***Figures 2, 3***).

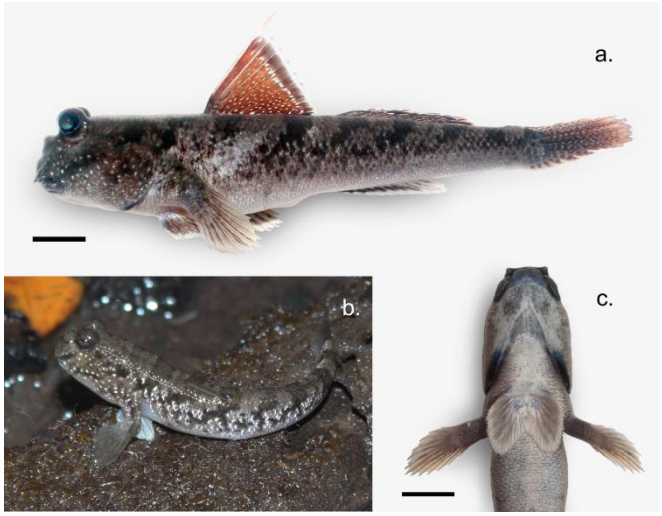

Figure 2. *Periophthalmus malaccensis* collected in Sungai Bunga, Brunei (UBDM MBu081013mal); a. freshly dead specimen, lateral view; b. live specimen; c. freshly dead specimen, ventral view, detail (scale bars are 10 mm long).

In the field, *P. malaccensis* can be discriminated from other congeners in Brunei by the presence of an elongated first spine in the first dorsal fin, a prominent crease on the snout, and small sky blue speckles on cheeks and opercles. In this study, *P. malaccensis* reached 90 mm SL (***Table 2***). The collected *P.* cf. *vulgaris* were 32-61 mm SL, and *P. gracilis* were 25-40 mm SL (***Appendix 2***). Like *P. malaccensis*, *Pn. schlosseri* (109.8, 205.0 mm SL, ***Appendix 2***) also possesses sky blue speckles on the head, but differs from *P. malaccensis* in the presence of a black stripe coursing posteriorly from behind the orbits to the caudal peduncle (not always visible), absence of white spots on the interspinous membranes of the first dorsal fin, and absence of series of dark brown speckles on the caudal interradial membranes (***Figure 3***).

P. variabilis and *P. chrysospilos* were not found in Brunei during these surveys, but I found these species in Sarawak, in the Kuching area (unpubl. data). *Pn. septemradiatus* was also not found in Brunei. *P.* cf. *vulgaris* and *P. gracilis* are the most common mudskipper species in Brunei, and occurred at several sites, in a variety of habitats; *Pn. schlosseri* was only found in three sites (***Table 1***, ***Appendix 3***).

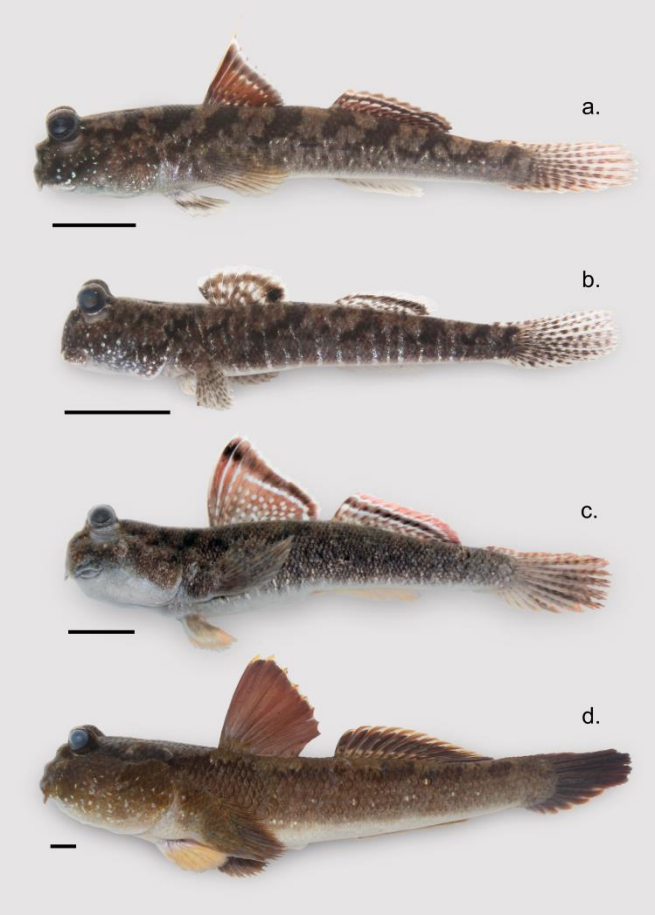

Figure 3. Mudskippers of Brunei of the genera *Periophthalmus* and *Periophthalmodon*. a. *Periophthalmus malaccensis* (UBDM MSe170414mal); b. *Periophthalmus gracilis* (UBDM MBm050514gra); c. *Periophthalmus* cf. *vulgaris* Eggert (UBDM MBe070513arg, female); and d. *Periophthalmodon schlosseri* (UBDM MUb131013sch, female); lateral view of freshly dead specimens; scale bars are 10 mm long.

The highest recorded richness of mudskipper species was in Sungai Bunga (***Table 1***), a small mangrove forest adjacent to a mud bank 30-50 m wide during spring low tide, in front of Berambang Island (***Figure 1***; ***Table 1***; ***Appendix 3***). The mudskipper species *Boleophthalmus boddarti* (Pallas, 1770), *Boleophthalmus* cf. *pectinirostris* (Linnaeus, 1758), and *Scartelaos histophorus* (Valenciénnes, 1837) were also observed in Sungai Bunga, on the exposed and unvegetated mud bank. However, these sightings were irregular, suggesting high seasonal variability of larval recruitment[17]. *Boleophthalmus* species were also always observed in very low numbers (< 3 individuals per survey). In general, mudskippers appear to be less diverse and much less abundant in Brunei than in other neighbouring areas in the region, such as western Peninsular Malaysia[9], and Sarawak (pers. obs.).

Among the surveyed sites, *P. malaccensis* was found only in Sungai Bunga and in Pulau Selirong (where only a single sighting was made), in the high intertidal zone[10]. The mangrove habitats of *P. malaccensis* were dominated by large trees of *Rhizophora apiculata* Blume; in the higher portion of this habitat, several *Thalassina* mounds occurred, up to several m wide and 0.5-1 m high, colonised by the sesarmid crabs *Episesarma chentongense* Serene and Soh, *E. mederi* A. Milne-Edwards, and *Acrostichum* ferns[18]. The *Acrostichum* zone was adjacent to a backforest supratidal swamp (sites 5 and 10, ***Appendix 3***).
The rather limited distribution of *P. malaccensis*, its probable recent extirpation from its type locality, its rarity in Brunei and its exclusive presence in the highly impacted high intertidal zone of mangrove forests[15] prompt for a conservation assessment of this species throughout its distributional range[19].

4. Conclusion

The mudskipper *P. malaccensis* Eggert is recorded for the first time in Borneo. Three other mudskipper species (Teleostei, Gobiidae, '*Periophthalmus* lineage'[1]) were recorded in Brunei Darussalam in several sites, and three more species in a single site. Notes on the habitat of *P. malaccensis* are provided. It is suggested that this species is of high conservation interest.

Acknowledgements

Thanks to the Forestry Department of the Ministry of Industry and Primary Resources for permits to conduct research in the study sites. Thanks to Sandra Raredon, Smithsonian National Museum of Natural History, Division of Fishes Collections for providing high resolution images of USNM mudskipper lots from Brunei. Thanks also to Laura Ribero, Claas Damken and Rossana Bottone for their help in the field during the surveys, and to Zeehan Jaafar for her revision of the manuscript.

References

[1] Agorreta, D. San Mauro, U. Schliewen, J. L. Van Tassell, M. Kovačić, R. Zardoya and L. Rüber, *Mol. Phylogenet. Evol*., **2013**, 69(3).

[2] E. O. Murdy, *Rec. Aust. Mus.*, **1989**, Suppl. 11.

[3] Z. Jaafar and H. K. Larson, *Zool. Sci.*, **2008**, 25.

[4] Smithsonian National Museum of Natural History, Division of Fishes Collections, http://collections.nmnh.si.edu/search/fishes/ . Accessed: May **2016**.

[5] Z. Jaafar, M. Perrig and L. M. Chou, *Zool. Sci.*, **2009**, 26.

[6] G. Polgar, L. Zane, M. Babbucci, F. Barbisan, T. Patarnello, L. Rüber and C. Papetti, *Mol. Phylogenet. Evol.*, **2014**, 73.

[7] Eggert, *Zool. Jahrb. Jena, Abt. F Syst.*, **1935**, 67.

[8] M. Kottelat, A. J.Whitten, S. N. Kartikasari and S. Wirjoatmodjo Ed., *Freshwater Fishes of Western Indonesia and Sulawesi*, Periplus, Hong Kong, **1993**, 344.

[9] G. Polgar and V. Bartolino, *Mar. Ecol. Progr. Ser.*, **2010**, 409.

[10] G. Polgar and G. Crosa, *Mar. Biol.*, **2009**, 156(7).

[11] H. K. Larson, Z. Jaafar, K. K. P. Lim, *Raffles Bull. Zool.*, **2008**, 56(1).

[12] T. Takita, Agusnimar, Ahyudin B. Ali, *Ichthyol. Res.*, **1999**, 46(2).

[13] G. Polgar and A. Sasekumar, *Ecotourism: Management, Development and Impact*, Ed. A. Krause and E. Weir, Nova Science Publ., Hauppage, **2010**.

[14] A.T.K. Yee, W. F. Ang, S. Teo, S. C. Liew and H. T. W. Tan, *Nat. Singap.*, **2010**, 3.

[15] G. Polgar, *Wetl. Ecol. Manag.*, **2009**, 17(2).

[16] G. Polgar, Z. Jaafar and P. Konstantinidis, *Raffles Bull. Zool.*, **2013**, 61(1).

[17] K. A. Townsend and I. R. Tibbetts, *Mem. Qld. Mus.*, **1995**, 38(2).

[18] P. B. Tomlinson Ed., *The Botany of Mangroves*, Cambridge University Press, London, **1986**.

[19] IUCN, *The IUCN Red List of Threatened Species. Version 2015-4.* http://www.iucnredlist.org/technical-documents/categories-and-criteria, **2016**.

Appendix 1. **List of examined museum specimens)**

Periophthalmodon freycineti (Quoy and Gaimard, 1824): MCZR VP1018, VP1019, Papua New Guinea, Western Province, southern Fly river delta, Toro Pass. MSNG 54691, Papua New Guinea, Western Province, Fly river delta, Purutu Island, 2007. NTM S.15545-001, Australia, Northern Territory, Wildman river, Ten Inch Creek.

Periophthalmodon schlosseri (Pallas, 1770): MSNG 54125, Malaysia, Selangor, Kuala Selangor.

Periophthalmodon septemradiatus (Hamilton, 1822): BMNH 2009.4.23.29, Myanmar, Rakhine State, Mee Chaun, close to its mouth at Dalet Chaung. MSNG 54643, Malaysia, Selangor, Kampong Kuantan.

Periophthalmus argentilineatus Valenciénnes, 1837 (clade K, Polgar et al. 2014): MSNG 55637 (A,B), Indonesia, North Sulawesi, Bunaken island, 2005. MSNG 55638, Indonesia, North Sulawesi, Bunaken island, 2005.

Periophthalmus chrysospilos Bleeker, 1852: [1]FMNH 117467, 117468, Malaysia, Johor, mouth of Muar river, south side. MCZ 33228, Java Sea. MSNG 52024, Malaysia, Selangor, Pulau (= Island) Kelang. MSNG 54127, Malaysia Negeri Sembilan, Tanjung (= Cape) Tuan. MSNG 54128, Malaysia, Selangor, Morib. RMNH 4760 (syntypes), Indonesia, Banka Island (East of Sumatra). USNM 151130, Malaysia, Penang Island. USNM 244031, southeast Thailand, north of Chonburi Chachoengsao Province, Maenam Bang Pakong. USNM 278428, 278435, 279331, Malaysia, Johor, Muar, Southside Muar River. ZMUC P.781480, P.781481, Indonesia, Java, Soetji. [2]ZMUC P.781616, P.781617, P.781618, Thailand, Phuket Island.

Periophthalmus darwini Larson and Takita, 2004: MCZR VP1012, VP1013, Papua New Guinea, Western Province, Fly river delta, Purutu Island, 2007. MSNG 54692, Papua New Guinea, Western Province, Fly river delta, Purutu Island, 2007. NTM S.10554-004 (holotype), Australia, Northern Territory, Shoal Bay, Mickett Creek. NTM S.10694-

022 (paratype), Australia, Northern Territory, Gunn Point. NTM S.11360-015 (paratype), Australia, Northern Territory, Milingimbi, Darbilla Creek. NTM S.14400-006 (paratype), Australia, Northern Territory, Melville Island, beach south of Picker-Taramoor.

Periophthalmus gracilis Eggert, 1935: MSNG 54129, Malaysia, Selangor, Kuala Selangor. MSNG 54130, Malaysia, Selangor, Pulau (= Island) Kelang. MSNG 54131, Malaysia, Selangor, Morib. MSNG 54132, Malaysia, Negeri Sembilan, Tanjung (= Cape) Tuan. MSNG 55639, Indonesia, North Sulawesi, Bajo, Talawan River, 2005.

Periophthalmus kalolo Lesson, 1831: RMNH 4593 (in part), Indonesia, west Sumatra, Padang; east Flores, Larantuka. RMNH 4754 (in part), Indonesia, Ambon. MSNG 55640 (A-C), Indonesia, North Sulawesi, Bajo, Talawan River, 2005. MSNG 55641 (A,B), Indonesia, North Sulawesi, Bunaken Island, 2005. MSNG 55642, Indonesia, North Sulawesi, Mantehage, Buhias, 2005. MSNG 55643, Indonesia, North Sulawesi, Likupang, 2005.

Periophthalmus malaccensis Eggert, 1935: USNM 112908, Philippines, Luzon, Manila Bay. USNM 148591, Philippines, Iloilo. USNM 268451, Indonesia, Halmahera Island, Jailolo District, Kampong (= village) Pasir Putih. [3]USNM 278471, Philippines, Luzon, Bataan, Mariveles. MSNG 55644, Indonesia, North Sulawesi, Likupang, 2005. MSNG 55645 (A,B), Indonesia, North Sulawesi, Likupang, Marawuwung River, 2005. MSNG 55646 (A,B), 55647, 55648, Indonesia, North Sulawesi, Wawontulap, Talonka River, 2005.

[4]*Periophthalmus minutus* Eggert, 1935: AMS I.24684-001, Australia, Northern Territory, Melville Island. ZMUC P.781609, Thailand, Phang Nga, North East of Phuket Island. ZRC 52261, Thailand, Phuket Island, Rassada harbor.

Periophthalmus novaeguineaensis Eggert, 1935: MCZR VP1003, VP1004, VP1005, Papua New Guinea, Western Province, Fly river delta, Purutu Island. AUM 47699, Papua New Guinea, Western Province, 40.7 km NE of Daru. MSNG 54693, 54694, Papua New Guinea, Western Province, Fly river delta, Purutu Island. NTM S.10426-002 (paratype of *Periophthalmus murdyi*, Larson and Takita 2004), Australia, Northern Territory, Shoal Bay, Buffalo Creek. NTM S.11193-004 (5 paratypes of *P. murdyi*), Australia, Northern Territory, Adelaide river, bend northeast of Harrison Dam, Boustead's Barramundi farm. NTM S.14024-013 (paratype of *P. murdyi*), Australia, Northern Territory, Roper river. NTM S.14467-006 (paratype of *P. murdyi*), Australia, Northern Territory, East Alligator river, Smith's landing. NTM S.15800-001 (paratype of *P. murdyi*), Australia, Western Australia, Derby jetty.

Periophthalmus spilotus Murdy and Takita, 1999: AMS I.39049-001 (paratypes), Indonesia, Sumatra, Tebing Tinggi Island. NSMT-P 56864, NTM S.14699-001 (paratypes), Indonesia, Sumatra, Tebing Tinggi Island. USNM 352414 (paratypes), Indonesia, Sumatra, Tebing Tinggi Island. MSNG 54644, Malaysia, Selangor, Sementa.

Periophthalmus takita Jaafar and Larson, 2008: AMS I.34341-028, Australia, Queensland, Mangrove channel, Port Clinton. MCZR VP1002, Papua New Guinea, Western Province, Fly river delta, Purutu Island, 2007. MSNG 54695, Papua New Guinea, Western Province, Fly river delta, Sisikura Island. MSNG 54696, Papua New Guinea, Western Province, Fly river delta, Purutu Island. NTM S.10798-011, Australia, Northern Territory, Bathurst Island, Buchanan Island. NTM S.14637-032 (paratypes), Australia, Northern Territory, south end of Field Island, mouth of South Alligator river.

Periophthalmus variabilis Eggert, 1935: MCZ 54404, Malaysia, Sarawak, Kuala Samunsam (= mouth of the Samunsam river). MSNG 54133, 54134, Malaysia, Selangor, Kuala Selangor. MSNG 54135, Malaysia, Pulau (= Island) Kelang. MSNG 54136, Malaysia, Negeri Sembilan, Tanjung (= Cape) Tuan. NSMT-P 54453, Malaysia, Selangor, Kuala Selangor. NSMT-P 54464, Indonesia, Sumatra, Tebing Tinggi Island. USNM 139372, Indonesia, north Borneo, Sebatic (=

Sebatik) Island. USNM 222971, Thailand, Central Merram Chao Phya (= Chao Phraya), Paknam. USNM 278470, Malaysia, Sabah, mangrove swamps on island opposite Sandakan, Borneo. USNM 279318, Malaysia, Johor, Muar, Indian Temple Creek. ZMA 113.702, Malaysia, Selangor, Kuala Langat. ZMUC P.781597-1608, 1610, 1611, Thailand, Phang Nga, northeast of Phuket Island.

Periophthalmus weberi Eggert, 1935: AUM 47584, Papua New Guinea, Western Province, Fly river, 15.8 km SW of Sturt Island. MCZR VP1011, Papua New Guinea, Western Province, lower Fly river. MSNG 54682, Papua New Guinea, Western Province, Fly river, Suki. MSNG 54683, Papua New Guinea, Western Province, Sturt Island. MSNG 54684, Papua New Guinea, Western Province, Fly river delta, Purutu Island.

Periophthalmus cf. *vulgaris* Eggert, 1935 (clade F in Polgar et al. 2014): MSNG 55627 (A-D), Indonesia, North Sulawesi, Bajo, Talawan River, 2005. MSNG 55628 (A-C), Indonesia, North Sulawesi, Bunaken Island, 2005. MSNG 55629, 55630, 55631, Indonesia, North Sulawesi, Likupang, 2005. MSNG 55632, Indonesia, North Sulawesi, Likupang, Marawuwung River. MSNG 55633, 55634, Indonesia, North Sulawesi, Wawontulap, Talonka River, 2005.

Periophthalmus cf. *vulgaris* Eggert (morphologically similar to the specimens of clade F in Polgar et al. 2014): USNM 356813, Brunei Darussalam, Sungai Penabai, where it enters Sungai Tutong, 1997. USNM 356814, Brunei Darussalam, Lubok Api-Api, Kuala Tutong, 1997.

Periophthalmus sp.: USNM 366713, 3 ex., Brunei Darussalam, Sungai Dalit, just above where it enters Sungai Belait, 1997 (catalogued as *P. gracilis*).

[1]Cited in Murdy (1989) as "FMNH uncatalogued" (Mary Ann Rogers, pers. comm.).

[2]Cited in Murdy (1989) as "ZUMC 78616-18" (Tammes Menne, pers. comm.).

[3]Determined as *P. novemradiatus* (= *P. variabilis sensu* Jaafar *et al.* 2009) by Murdy (1989).

[4]The lot of *P. minutus* ZMA 113.218 (in part), reported by Murdy (1989) from Java, is in fact from Flores, Mbawa (= Ma'u Mbawa) (Hielke Praagman, pers. comm.).

Appendix 2. **List of deposited museum specimens** (all specimens were collected by G. Polgar in Brunei Darussalam, were fixed and preserved in 70% ethanol).

Periophthalmus cf. *vulgaris* Eggert (morphologically similar to the specimens included in clade F in Polgar et al. 2014): UBDM MMe011213arg, 1 female, 50.5 mm SL; Meragang lagoon, Pemburongunan Creek, 01 Dec 2013. UBDM MBe131013arg (A), 1 male, 43.3 mm SL; Pulau (= island) Bedukang, logs and debris in the mangrove pioneer shore (*Sonneratia* sp.); (B), 1 male, 48.3 mm SL; same site, high forest *Acrostichum* sp. ferns on *Thalassina* mounds, 13 Oct 2013. UBDM MBe070513arg (A), 1 female, 61.3 mm SL; Pulau Bedukang, mangrove pneumatophore zone; (B), 1 male, 48.4 mm SL; same site, pioneer mangrove forest, 07 May 2013. UBDM MBe270513arg, 1 ex., 34.8 mm SL; Pulau Bedukang, pioneer mangrove forest, 27 May 2013. UBDM MSe070813arg, 1 ex., 39.7 mm SL; Pulau Selirong, pioneer mangrove shore (*Rhizophora apiculata*), 07 Aug 2013. UBDM MSr300115arg, 1 male, 39.3 mm SL, Serasa, artificial jetty with rock breakwaters, 30 Jan 2015. UBDM MBs101013arg (A), 4 ex., 32.5-36.0 mm SL, Sungai (= river, creek) Besar, pioneer mangrove forest (*Sonneratia* sp.); (B), 2 ex., 32.9, 33.6 mm SL; same site, backforest and plant debris, 10 Oct 2013. UBDM MBs240513arg, 1 male 52.5 mm SL, Sungai Besar, pioneer mangrove forest, 24 May 2013. UBDM MBu081013arg, 2 males, 1 female, 46.3-53.7 mm SL; Sungai Bunga, *Rhizopora apiculata* forest, 08 Oct 2013. UBDM MSa150815arg, 1 ex., 40.3 mm SL; Sungai Salar, mangrove forest (*Rhizophora apiculata*, *Xylocarpus granatum*) along a tributary creek, 15 Aug 2015. UBDM MTu210214arg (A), 1 female, 50.9 mm SL,

Sungai Tutong, *Rhizopora apiculata* forest, near tide pools; (B), 1 male, 36.6 mm SL; same site, *Nypa fruticans* forest, 21 Feb 2014. UBDM MTu300713arg, 1 male, 1 ex., 37.6-43.1 mm SL, Sungai Tutong, *Nypa fruticans* forest, 30 Jul 2014.

Periophthalmus gracilis Eggert: UBDM MBe070513gra, 2 males, 32.6, 34.8 mm SL; Pulau Bedukang, high mangrove inlet, 07 May 2013. UBDM MBe131013gra (A), 1 female, 40.5 mm SL; Pulau Bedukang, logs and debris in the mangrove pioneer shore (*Sonneratia* sp.); (B), 2 males, 32.4, 32.8 mm SL; same site, high forest *Acrostichum* ferns on *Thalassina* mounds, 13 Oct 2013. UBDM MBm050514gra, 1 male, 35.3 mm SL; Pulau Berambang, 05 May 2014. UBDM MPe270513gra, 1 ex., 25.2 mm SL; Pulau Pepataan, pioneer mangrove shore, 27 May 2013. UBDM MSe070813gra, 1 ex., 30.2 mm SL; Pulau Selirong, pioneer mangrove shore (*Rhizopora apiculata*), 07 Aug 2013. UBDM MTm151013gra, 1 female, 38.2 mm SL; Sungai Belayang, tide pools on the vegetated banks (*Nypa fruticans*) of the river, 15 Oct 2013. UBDM MBu081013gra, 1 male, 1 female, 34.1, 35.5 mm SL; Sungai Bunga, high mangrove shore, 08 Oct 2013. UBDM MSa150815gra, 1 ex., 38.5 mm SL; Sungai Salar, mangrove forest (*Rhizophora apiculata*, *Xylocarpus granatum*) along a tributary creek, 15 Aug 2015. UBDM MTu210214gra, 1 female, 37.8 mm SL; Sungai Tutong, *Nypa fruticans* forest, 21 Feb 2014.

Periophthalmus malaccensis Eggert: UBDM MSe170414mal, 1 ex., 54.7 mm SL; Pulau Selirong vegetated creek banks (*Rhizophora apiculata*), 17 Apr 2014. UBDM MBu081013mal, 1 female, 83.0 mm SL; Sungai Bunga, high mangrove shore (*Rhizopora apiculata*), 08 Oct 2013. UBDM MBu111013mal, 2 males, 83.1, 90.3 mm SL (head dissected); Sungai Bunga, high mangrove shore (*Rhizopora apiculata*), 11 Oct 2013.

Periophthalmodon schlosseri (Pallas): UBDM MUb131013sch (A), 1 female, 109.8 mm SL; Ujong Bukit, mudflat with sparse *Avicennia* sp. trees, around stilt houses; (B), 1 male 205.0 mm SL (head dissected), same site and habitat, 13 Oct 2014.

Museums' abbreviations: AMS = Australian Museum, Sydney, New South Wales, Australia. AUM = Auburn University Natural History Museum, Auburn, Alabama, U.S.A. BMNH = Natural History Museum, London, U.K. FMNH = Field Museum of Natural History, Chicago, Illinois, USA. MCZ = Museum of Comparative Zoology, Harvard University, Ichthyology Department, Cambridge, Massachusetts, U.S.A. MCZR = Museo Civico di Zoologia, Comune di Roma, Roma, Italy. MSNG = Museo Civico di Storia Naturale di Genova 'Giacomo Doria', Genova, Italy. NSMT = National Science Museum, Zoology Department, Division of Fishes, Tokyo, Japan. NTM = Museums and Art Galleries of the Northern Territory, Ichthyology, Darwin, Northern Territory, Australia. RMNH = Naturalis - National Natuurhistorisch Museum, Leiden, Netherlands. UBDM = Universiti Brunei Darussalam Museum, Zoological Collection. USNM = Smithsonian Institution National Museum of Natural History, Department of Vertebrate Zoology, Division of Fishes, Washington D.C., U.S.A. ZMA = Universiteit van Amsterdam, Faculty of Science, Zoologisch Museum, Amsterdam, The Netherlands. ZMUC = Københavns Universitet, Zoologisk Museum, Vertebrater, Fiskesamlingen, Copenhagen, Denmark. ZRC = Zoological Reference Collection, Department of Life Sciences, Faculty of Science, National University of Singapore, Singapore.

Appendix 3. **Study sites** (***Figure 1***; ***Table 1***).

Site 1. Pemburongunan Creek. Mangrove creek, 10-20 m wide at its mouth, flowing into the South China Sea. The creek crosses the Meragang coastal lagoon, which is almost completely isolated from the sea by a ~ 100 m-wide coastal ridge.

Site 2. Pulau (= island) Bedukang. Transect (~ 100 m) along the intertidal gradient, positioned on the west coast of the island. The transect included a pioneer mangrove shore dominated by *Sonneratia* sp., and a mangrove-creek network dominated by *Rhizophora apiculata*, and halophytic ferns of the genus *Acrostichum* colonising mud mounds built by crustaceans of the genus *Thalassina* (*Thalassina* mounds).

Site 3. Pulau Berambang. Patch of nypah forest (*Nypa fruticans*) with *Thalassina* mounds colonised by *Acrostichum* ferns, at ~ 300 m from the northeastern coast of the island.

Site 4. Pulau Pepataan. Pioneer mangrove forest (*Avicennia alba, Rhizopora apiculata*) along the northern coast of the island, at 5-20 m from the first line of trees.

Site 5. Pulau Selirong, site A. Banks of the Sungai Melimbai creek, at ~ 5 km from its confluence with the creek Aloh Besar, which delimits the southern coast of Selirong island. The site was ~ 4 km from the coastline. The creek banks were colonised by a ~ 30 m-wide stand of *Rhizopora apiculata*, followed by patches of *Acrostichum* ferns, and a steep transition (2-3 m wide) to a backforest swamp with *Pandanus* palms.

Site 6. Pulau Selirong, site B. Area ~ 1 km south of the mouth of the Aloh Besar, along the marine fringe of a stand of *Rhizopora apiculata*, at 5-10 m from the first line of trees.

Site 7. Serasa jetty. Artificial strip of land ~ 5 m wide, projecting for ~ 100 m into the sea, and protected on both sides by 2-3 m of rocky breakwaters.

Site 8. Sungai (= river) Belayang. Bank of a tributary of the Belayang river, which is a tributary of the Kibi river. The bank was covered by a ~ 50 m fringe of *Nypa fruticans*, and was positioned at ~ 8 km from the coastline.

Site 9. Sungai Besar. Tract of coast on the western bank of the Brunei Bay, colonised by a 100 m-long and ~ 15 m-wide mangrove fringe (*Sonneratia* sp.), located ~ 100 m north of the mouth of a small river (= Sungai Besar).

Site 10. Sungai Bunga. Tract of coast on the western bank of the Brunei Bay, at the mouth of the Brunei river and in front of the northern tip of Berambang island. The area included a 50-350 m intertidal zone, including an unvegetated mudbank; a pioneer mangrove fringe (*Sonneratia* sp. and *Rhizopora apiculata*); a middle mangrove forest dominated by *Rhizopora apiculata*; a high forest dominated by *Acrostichum* ferns and *Thalassina* mounds; and a transition to the backforest, with thorny palms, *Pandanus* sp. and *Hibiscus* sp.

Site 11. Sungai Salar. Mangrove forest (*Rhizophora apiculata*, *Xylocarpus granatum*) and mud banks of a tributary of Sungai Salar, at < 5 m from the water's edge.

Site 12. Sungai Tutong. *Nypa fruticans* forest, forming a ~ 100 m-wide fringe, along the southern bank of the mouth of the Tutong river.

Site 13. Ujong Bukit. Mud bank on the western bank of the Kedayan river, which after ~ 450 m flows into the lower tract of the Brunei river, at ~ 12 km from the western coast of the Brunei Bay. The area is occupied by a small village made of stilt houses.

Biology of aerial parasitic vines in Brunei Darussalam: *Cuscuta* and *Cassytha*

Kushan U. Tennakoon[1, 2], Roshanizah Rosli[1] and Quang-Vuong Le[1,3]*

[1]Institute for Biodiversity and Environmental Research, Universiti Brunei Darussalam, Jalan Tungku Link, Gadong, BE 1410, Brunei Darussalam
[2]Environmental and Life Sciences, Faculty of Science, Universiti Brunei Darussalam, Jalan Tungku Link, Gadong, BE 1410, Brunei Darussalam
[3]Biology Faculty, Vinh University, 182-Le Duan, Vinh, Nghe An, Vietnam

**corresponding author email: kushan.tennakoon@ubd.edu.bn*

Abstract

Plants of the genus *Cuscuta* (Convolvulaceae) have often been mistaken as *Cassytha filiformis*, an unrelated genus in the family Lauraceae in Brunei Darussalam. Large majority of *Cuscuta* species are holoparasitic and all species of *Cassytha* are obligate stem hemiparasites. Also, *Cassytha* is perennial, whilst *Cuscuta* is annual. The chlorophyll content in *Cassytha* is generally influenced by the physiology of host, passive /dormant hosts usually increase the greening of *Cassytha*. Field observations conducted over 7 years have revealed that a novel method of *Cuscuta* infestation exist in Brunei Darussalam where a large majority of *Cuscuta* populations produce seeds vary rarely, and the infestations and spread are more often due to perennating structures. The nastic movements that allow both these parasitic species to "forage" hosts are still not totally understood, but there is strong evidence to suggest the involvement of chemical cues released by host plants trigger parasite's growth and attachment to the host. Both *Cuscuta* and *Cassytha* species have shown extremely broad host ranges in Brunei where a single parasite can even attach to many different hosts. Studies on the impacts of both these parasitic angiosperms on the community structure, diversity and vegetation cycling under both natural and agricultural systems will be useful to assess the impacts the parasitic plants on agricultural crops and native plants in tropical Brunei Darussalam.

Index Terms: parasitic plants, convergent evolution, parallelism, haustoria

1. Introduction

Have you seen a mass of orange spaghetti rashly thrown over shrubs and herbs? This can well be the parasitic plant dodder (*Cuscuta* spp. of the morning glory family - Convolvulaceace) or woe vine (*Cassytha* spp. of the laurel family - Lauraceae). Species of both these genera are commonly known as *Cuscuta* and *Cassytha* species ("love vines") and look similar with haphazard appearance in nature. In Brunei, both parasitic vines are generally referred to as "akar janjang", directly translates to 'stringy roots'. However, they are highly ordered and taxonomically different. Thus, these species cause confusion to many naturalists[1] but provide an excellent example of convergent evolution in parasitic plants[2]. It is one of the most remarkable examples of a phenomenon known as parallelism as shown in ***Figure 1*** - the development of similar structures in entirely unrelated organisms existing in tropical Brunei Darussalam.

Genus *Cuscuta* Yuncker includes about 170 species[3], while genus *Cassytha* L. is composed of 20 species with a worldwide distribution[4]. Both genera have thin, light greenish yellow stems, with scaly leaves and are virtually rootless as shown in ***Figure 1a*** and ***Figure 1b***. Young *Cassytha* stem is often green (photosynthetic) and turns yellowish when mature. However *Cuscuta* spp.

Figure 1. General habit of (a) *Cuscuta* (Cu) and (b) *Cassytha* (Ca) *parasitizing* host plants. One of the most convenient methods of correct identification of these two species showing parallelism in the field is by close examination of the vegetative body. Stem appearance of *Cuscuta* is smooth (c), while *Cassytha* has a coarse stem due to the presence of waxy plates (d).

have smooth, shiny appearance whereas *Cassytha* spp. have coarse and ridged stems due to the presence of numerous waxy plates as shown in ***Figure 1c*** and ***Figure 1d***. When stems are crushed, while *Cuscuta* is generally odourless, most *Cassytha* spp. release a pungent odour due to the presence of a range of essential oils, which is a characteristic feature of family Lauraceae.

Confusion has been infused to all species of "love vines" because sometimes in literature both genera are introduced as stem holoparasites (completely dependent on host plants for their water and nutritional requirements). In reality, large majority of *Cuscuta* species are holoparasitic and all species of *Cassytha* are obligate stem hemiparasites (only some of its sustenance derives from the host as it has chlorophyll for synthesis of some of its carbon requirements). Visser (1981)[5] has suggested that the chlorophyll content in *Cassytha* is generally influenced by the physiology of host *viz*. dormant hosts increase the greening of *Cassytha*. It is worthwhile to mention the fact that even though most dodders are holoparasitic, some *Cuscuta* species (ie. *C. reflexa*) have retained little chloroplast plastid genome and functional RUBISCO activity to become hemiparasitic to some extent. [6, 7]

Here we summarise some unusual field discoveries that we have made over the past six years when trying to unravel the biological and behavioural mystiques of love wines in Brunei Darussalam. In this research note, one of our main aims is to bring attention of a wider scientific community about this novel group of tropical parasitic plants least investigated in Borneo.

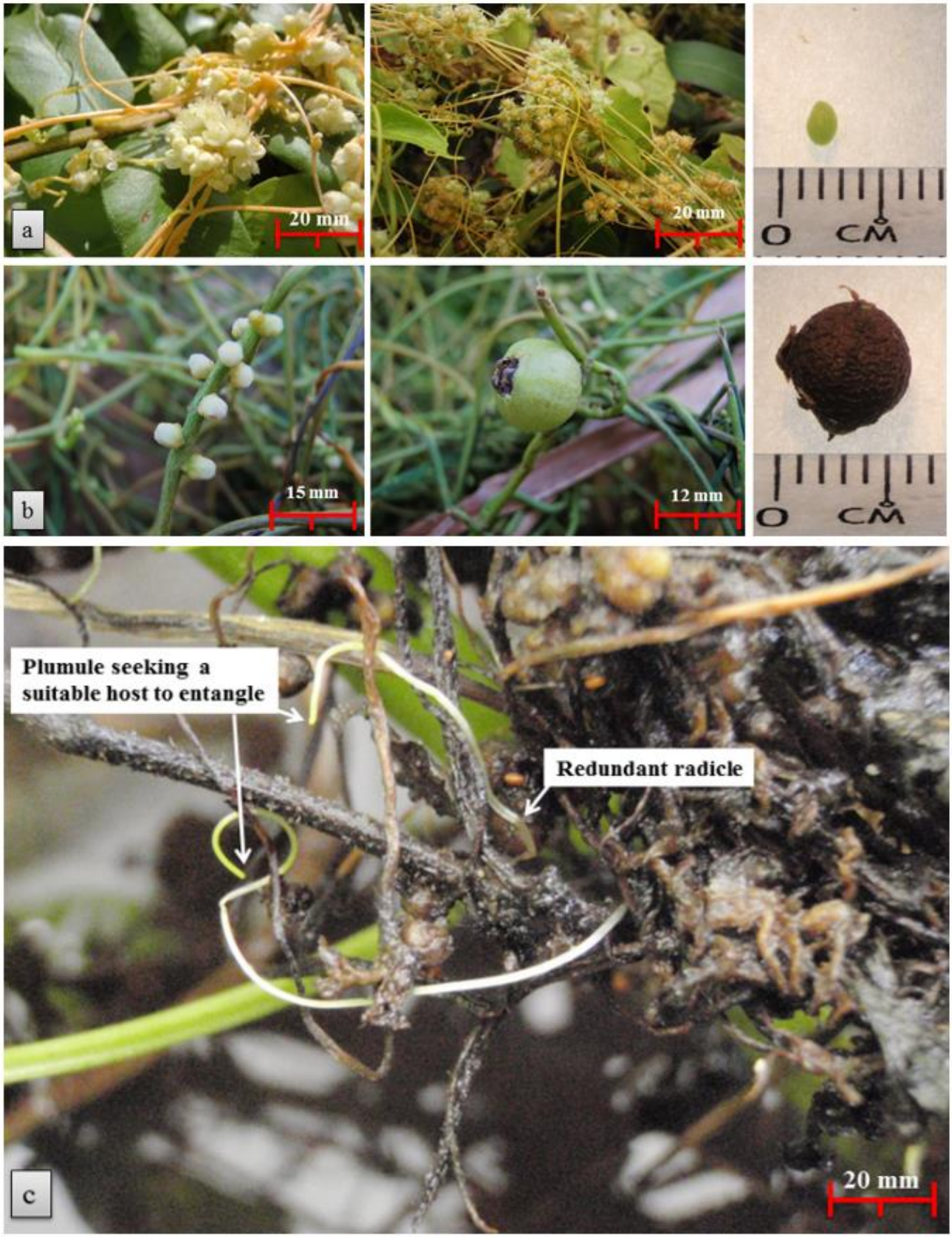

Figure 2. Distinguishable flower, fruit and seed characters of (a) *Cuscuta* spp., (b) *Cassytha filiformis and* (c) Geminating *Cuscuta* seeds – note the lack of development of radicle and the elongating plumule in search of a suitable host plant for immediate attachment.

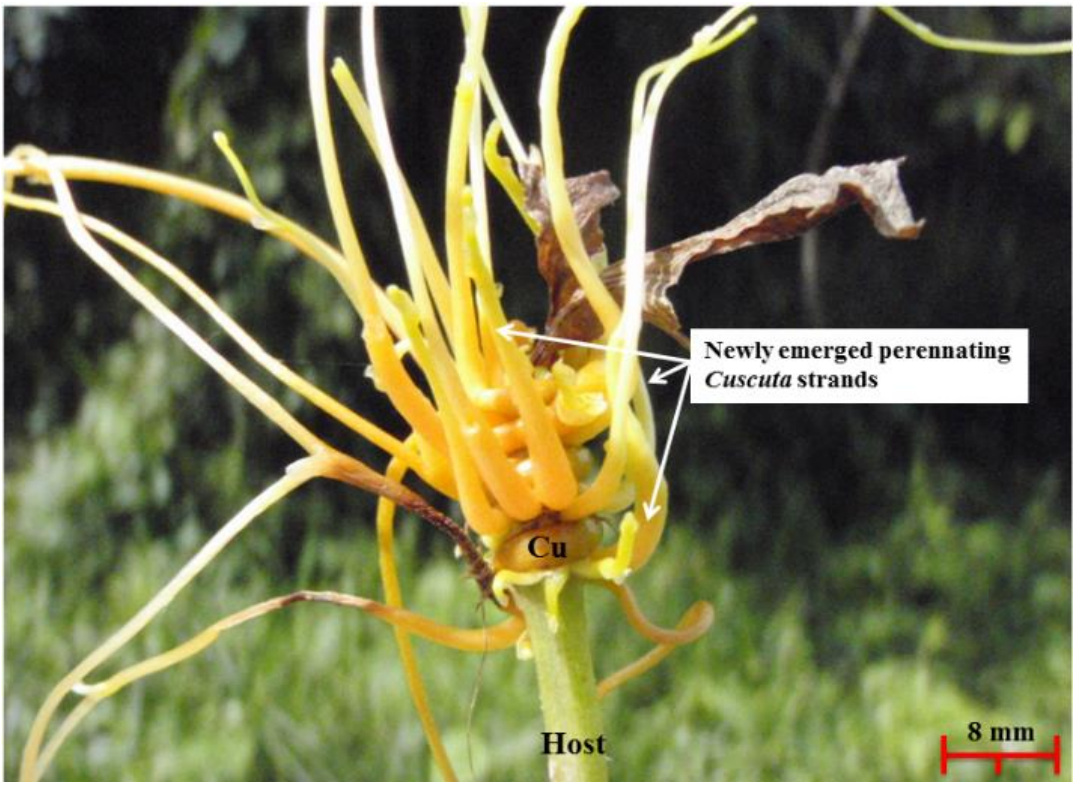

Figure 3. Perennating structures emerging from a mature strand of *Cuscuta* vegetative body (Cu) that has remained alive on a host found in Brunei Darussalam where flowering has not being recorded for over 4 years continuously.

2. Experimental approach

Field observations of *Cuscuta* and *Cassytha* spp. were conducted in Brunei-Muara, Tutong and Belait districts of Brunei Darussalam between January 2010 and January 2016, with localities recorded using a Global Positioning System (Garmin GPSMap 60CSx, Taiwan). Descriptions of study sites are elaborated recent studies.[8,9,10,11] The branching patterns, stem colours, haustorial developmental stages, emergence of new shoots from perennating tissues and flowers of both species were recorded for each site at least once in three months over the six year observation period.

3. Results and Discussion

Cassytha is perennial, whilst *Cuscuta* is annual. Both genera are twining parasites and both species have the ability to overwinter on host tissue or debris and re-emerge.[8] However, the most obvious mode of dispersal of both these love vines is by seeds (***Figure 2c***). *Cuscuta* produces a dehiscent capsule carrying four seeds with very hard seed coat, requiring mechanical or chemical scarification to induce germination. *Cassytha* fruit is a drupe with pulp, brightly coloured when mature to attract fruit eating birds as dispersal agents. Each drupe carries a solitary seed with hard seed coat. Seeds can remain dormant on soil for a long duration until it is scarified.[4,11,12,13]

A novel method of *Cuscuta* infestation has been reported in Brunei Darussalam[8], where a large majority of *Cuscuta* populations produce seeds vary rarely, and the continuation of *Cuscuta* infestations is more often due to perennating structures. After the entire *Cuscuta* population completely disappears at the end of its life cycle, few swollen fully mature *Cuscuta* strands that remain alive give rise to a number of new *Cuscuta* shoots early in the next growing season to continue its existence (***Figure 3***).

Stems of both genera actively move to find its host. Even though the stem movement is not evident to casual observer, if you mark the location of the dodder or woe vine stem tip of any species of these two genera and return the next day, you will find that stem has moved noticeably.

Figure 4. Nastic movement of *Cuscuta* stems in search of potential hosts; (inset) Young vegetative stems of *Cuscuta* inadvertently entangling among themselves when foraging towards the preferred host plants for establishing successful parasitic connections via numerous haustoria.

Field observations have revealed that dodders appear mostly along the banks of streams, degraded watersheds and wastelands while woe vines distribute mainly in coastal vegetation. Dodders also grow at a much faster rate than woe vines in search of host plants.[9] It was reported that dodders usually make the attachments with hosts within 3 days upon germination. The movement of parasite stem is from side to side to facilitate contact with vertically growing hosts.

The nastic movements (in response to a host stimulus) that allow these parasitic species to "forage" (move towards) hosts are still not totally understood (***Figure 4***). Albert et al. (2008) and Runyon et al. (2006) have suggested the involvement of chemical cues released by host plants trigger parasite growth and attachment to the host[14,15]. *Cuscuta* and *Cassytha* both studiously avoid parasitizing some of the monocotyledonous plants (especially grasses), even though they may only twine about as supporting structures to reach neighbouring (potential) host plants with their growing tips.

Both *Cuscuta and Cassytha* species usually have extremely broad host ranges (total number of different species that can be parasitized), and can even be attached to many different hosts at once. But in nature, the host preference (choice of the most desirable host for optimal growth) typically is much narrower and the parasite can often be located by first finding the preferred host. Similar patterns are observed for both genera in Brunei.[8,10,16] If a suitable host stem is not available within reachable distance, *Cuscuta* and *Cassytha* will inadvertently twine about an intimate object. Due to the parasitic nature of both genera, seedlings will die if a suitable host is not found within a few days.

Upon successful contact with a suitable host, both parasites coil indiscriminately around the host stem and penetrate into host tissues (mostly the stems) by a specialized structure known as the haustorium (***Figure 5***). After the initial host-parasite connection (adhere) phase is completed, haustorium penetrates into host tissue and intimate connections are made with both xylem (mostly direct lumen - lumen connections) and phloem

(from absorbing hyphae abutting host phloem sieve tubes) tissues of host.[17,18]

Figure 5. Successful haustorial establishment of (a) *Cuscuta* (Cu) and (b) *Cassytha* (Ca). (c) Longitudinal sections at the haustorial interface clearly show the orderly tissue contacts made by the haustorium (ha) to tap nutrients and waters from the host vascular tissue.

Absorption system of all species of "love vines" for host substance appears to be very efficient. Albert et al. (2008) and Wolswinkel (1984) have reported that during host plant fruit development, dodders compete for assimilates and act as a much stronger sink than the host plants fruits itself.[14,19] Both *Cuscuta* and *Cassytha* species usually have extremely broad host ranges (total number of different species that can be parasitized), and can even be attached to many different hosts at once. But in nature, the host preference (choice of the most desirable host for optimal growth) typically is much narrower and the parasite can often be located by first finding the preferred host. Similar patterns are observed for both genera in Brunei.[8,10,16]

In natural communities, love vines are capable of affecting the community composition by influencing the host growth, biomass allocation, and reproductive output, thus changing the ability of a range of host plants to successfully compete with neighbours. Due to its ability of reducing host performance, love vines clearly affect the community structure, diversity and vegetation cycling. Furthermore, they perform a valuable role in natural ecosystems by attracting birds and other seed dispersing agents to communities they inhabit.[10,11]

4. Conclusion

In spite of its fascinating biology, physiology and scientific interest, *Cuscuta* species (especially *C. australis* and *C. campestris* found in Brunei Darussalam) often considered as one of the most damaging pests in agriculture. It is widely reported that *Cuscuta* parasitism can reduce the production of a range of cash crops such as tomato, chilli, onion, cowpea, beans, corn and a range of other leafy vegetables by more than 50%.[20] *Cuscuta* is listed as one of the top ten weeds by the United States Department of Agriculture. However there has not been many reports on the detrimental effects of *Cassytha* on agricultural crop production, especially in Brunei Darussalam.[11]

In spite of their parasitic behaviour, many biological aspects of the love vines are yet to be unravelled. New research frontiers related to

bioprospecting (both genera of love vine seeds reported here are commonly used in traditional herbal medicines for various ailments), ability of these plants used as biological control of noxious weeds and a tool to transfer pathogens and genetic material from plant to plant will no doubt provide more prominence to this special group of nature's scroungers in the future.

Acknowledgements
Research funding provided by the Brunei Research Council (S&T Research Grant No. 8) for studies on angiosperm parasitic plants in Brunei Darussalam is gratefully acknowledged.

References

[1] J. Thurman and I.P.-A Cheong, *Some common plants and animals in Brunei Darussalam*, Universiti Brunei Darussalam (Brunei Darussalam), **2008,** 127.
[2] J. Kuijt, *The Biology of Parasitic Flowering Plants*. Berkeley, CA: University of California Press. **1969.**
[3] J.H. Dawson, *Cuscuta* (Convolvulaceae) and its control. In: Weber HC, Forstreuter W (eds). Parasitic Flowering Plants. Phillips – Universitat, Marburg, **1987,** 137-149.
[4] U. Molau, *Reproductive ecology and biology. In: Parasitic Plants* (eds. M.C. Press and J.D. Graves), Chapman and Hall, New York, **1995,** 141- 173.
[5] J. Visser, *South African parasitic flowering plants*, Juta & Co. Ltd. Cape Town, **1981.**
[6] M.A. Machado and K. Zetsche,Planta, **1990,** 181: 91-96.
[7] G. Haberhausen and K. Zetsche, Plant Molecular Biology, **1994**, 24: 217-222.
[8] W. H. Chak, K. U. Tennakoon and L. J. Musselman, *Folia Malaysiana,* **2010,** 11 (1):13-24.
[9] Q. V. Le, K. U. Tennakoon, F. Metali, L. B. Lim and J. F. Bolin, *Weed Biology and Management*, **2015,** 15(4): 138-146.
[10] Q.V. Le, Physiology and biochemistry of selected parasitic plants in Brunei Darussalam, PhD Thesis, Universiti Brunei Darussalam, **2015**: 104
[11] R. Rosli, *Biology and physiology of the hemiparasitic Cassytha filiformis L*., MSc Thesis, Universiti Brunei Darussalam, **2014**: 102.
[12] O. B. Lyshede, Annals *of Botany*, **1992**, 69: 365-371.
[13] J. H. Dawson, *Reviews in weed Science,* **1994,** 6: 265-317.
[14] M. Albert, X. Belasteggui-Macadam, M. Bleischwitz and R. Kaldenhoff, *Progress in Botany*, **2008,** 69: 267-277.
[15] J. B. Runyon, M. C. Mescher and C. M. De Moraes, *Science*, **2006,** 313: 1964-1967.
[16] R. Rosli, K.U. Tennakoon, L.B. Lim, J.F. Bolin and L.J. Musselman, An ecophysiological study of *Cassytha filiformis* L. (Lauraceae) in Brunei Darussalam, Borneo. Abstract proceedings from 13th World Congress on Parasitic Plants, Kunming, China, **2015**.
[17] D. Balasubramanian, K. Lingakumar and A. Arunachalam, *Taiwania*, **2014**, 59(2): 98-105.
[18] C. Jayasinghe, D.S.A Wijesundara, K.U. Tennakoon and B. Marambe, *Tropical Agricultural Research,* **2004,** 16: 223-241.
[19] P. Wolswinkel, Plant Growth and Regulation, **1984,** 2: 309-317.
[20] C. Parker and C. Riches. *Parasitic weeds in the world: biology and control*. CABI, Wallingford, **1993,** 332.

Beneficial effects of tropical fruit-derived polyphenols against lipid-mediated stress *in vitro*

*Chiew Jia Chi[1], Gan Yi Ling[1], Asgar Ali[1], Zairi Bin Jaal[2], Adanan Bin Che Rus[2]and Monowarul Mobin Siddique[3]**

[1]School of Biosciences, Faculty of Science, University of Nottingham Malaysia Campus, 43500 Semenyih, Selangor, Malaysia
[2]School of Biological Sciences, University of Science Malaysia, 11800 Penang, Malaysia
[3]Environmental and Life Sciences, Faculty of Science, Universiti Brunei Darussalam, Jalan Tungku Link, Gadong, BE1410, Brunei Darussalam

**corresponding author: mobin.siddique@ubd.edu.bn*

Abstract

Fatty liver formation is a consequence of hyperlipidemia, associated with an imbalance between lipid uptake and its metabolism. Persistent lipid load in the liver cells results in lipid-mediated toxicity or lipotoxicity which leads to the pathogenesis of several metabolic diseases. Recent studies suggest that activation of autophagic pathway might be useful to remove excess hepatic fat. Dietary polyphenols present in fresh fruits and vegetables are able to induce autophagy apart from their well-known anti-oxidative property. Our preliminary observation suggests that fruit-derived polyphenols might be effective to prevent hepatic fat accumulation by inducing autophagy. Total phenolic contents from dragon fruit and mangosteen have been used to address the beneficial properties of these two tropical fruits. Results showed that these polyphenols protect cells against lipotoxicity and oxidative stress. Expression levels of several key genes that are involved in lipid metabolism and energy expenditure were upregulated in presence of these polyphenols. This preliminary study suggests that the underutilized tropical fruits might be useful to develop functional foods, especially those containing beneficial phenolics.

Index Terms: Autophagy, glucotoxicity, hepatocyte, lipotoxicity, polyphenols

1. Introduction

Functional foods are receiving increased attention due to the fact that apart from nutrients, they contain a number of active ingredients that are beneficial for human health. The incident of non-communicable diseases are increasing and becoming one of the main concerns for health care sector and policymakers. The rising epidemic of obesity, obesity-related cardiovascular diseases (CVDs), and cancers has prompted the search for novel and feasible approaches to tackle the situation. High prevalence of these diseases in Asia concerns immediate attention from both healthcare and economic perspectives. One promising alternative therapeutic area comprises functional foods. In this regard, the bioactive properties of fresh fruits and vegetables in preventing metabolic diseases are being investigated extensively. Tropical fruits and vegetables are often underutilized and their beneficial properties are either underestimated or not investigated enough to convince the consumers to use them as a means of maintaining good health. Polyphenols are the known beneficial phytochemicals present in fruits and act as an important determinant of their nutritional quality.[1] Polyphenols, with at least two phenol subunits, are the main classes of phenols found in plants along with their bioactive properties. According to the number of phenol rings, polyphenols are grouped into phenolic acids, stilbenes, flavonoids, tannins and lignans.[1] The health benefits of polyphenols are well established, especially as antioxidants. Consumption of polyphenol-rich foods has shown

to increase antioxidant capacity in plasma with reduced oxidative stress in liver. Several studies have reported that polyphenols help to prevent the development of cancers, CVD, diabetes, neurodegenerative diseases[2], chronic obstructive pulmonary disease[3], lung diseases[4], osteoporosis[5, 6], adverse effect on aging[7-9] and protect skin damages from UV radiation.[10] The anti-carcinogenic properties of polyphenols are partly due to their ability to scavenge free radicals and ROS. Polyphenols present in green tea, such as catechin or epigallocatechin-3-gallate (EGCG), protects from obesity, insulin resistance, hypertension and obesity-related fatty liver diseases.[11-13] All these beneficial properties of polyphenols are believed to explain the "French paradox", the lower CVD occurrence in France despite having relatively higher saturated fat intake and it is believed that this is because of consumption of higher dietary polyphenols.[14] Tropical fruits contain a wide number of polyphenols that have been found to prevent several cellular abnormalities which often lead to the development of cardiovascular and metabolic diseases. Polyphenolic compounds such as phenolic acids, flavonoids and lignans can modulate carbohydrate and lipid metabolism, reduce hyperglycaemia and insulin resistance, thus preventing long-term diabetes complications.[15-17]

In hyperglycaemia, chronic elevated level of plasma glucose damages insulin-targeted tissues and induces insulin resistance due to glucose-mediated toxicity or glucotoxicity. Elevated level of glucose efflux through constitutive glucose transporters into the cell overwhelms the mitochondrial electron transport chain which often results in the generation of reactive oxygen species (ROS) and induces cell death. Chronic hyperglycaemia causes type II diabetes (T2D) which contributes to the progression of long-term complications in vital organ such as blood vessels, heart, nerves, eyes and kidneys. In prolonged hyperglycaemia, pancreatic β-cells are often subjected to glucolipotoxicity which leads to the development of type I diabetes. T2D is often associated with obesity where individuals suffer from high level of circulatory lipids, a condition also known as hyperlipidaemia. A consequence of hyperlipidaemia is the ectopic fat deposition where lipids accumulate in non-adipose tissue and impair cellular function. Excess lipid accumulation in peripheral tissues including pancreatic β-cells and liver results in lipotoxicity, further leads to insulin resistance and T2D.[18-20]

The term "glucolipotoxicity" is widely used to describe the combined effects of glucotoxicity and lipotoxicity. Removal of damaged organelles, metabolizing excess lipids and cellular storage by catabolic processes reduce glucolipotoxicity. Among the well described phenomenon, autophagy is believed to be most effective catabolic process that helps to reduce intracellular fat and other lipid metabolites that exert lipotoxicity; while removal of damaged organelles and detoxifying free radicals reduce glucotoxicity.

Recycling and reusing of cellular metabolites are a well-conserved adaptive response in the living beings during unfavourable condition. Autophagy is such a mechanism that degrades unnecessary components to help maintain cellular energy needs during stress conditions (***Figure 1***). Stress conditions such nutrient deprivation, mitochondrial damages and metabolic stresses are known to induce autophagy.[21-24] Autophagy is necessary for embryonic development as this process maintains cellular homeostasis by eliminating misfolded proteins, unwanted or damaged organelles.[25,26] This process was initially thought to be adaptive in nature. However, recent advancement in science suggests that this recycling process could be beneficial to prevent lipid accumulation in the cells. The role of autophagy in lipid metabolism has thus gained attentions for the interplay between autophagy and metabolic syndromes.

Several recent findings suggest that autophagy is also involved in intracellular lipid break down to provide free fatty acids, a process known as lipophagy.[27,28] Sinha et al (2013) reported that hepatic lipid can be removed by inducing autophagy, suggesting an interesting role of this degradative process in preventing lipid accumulation in cells.[29] Bioactive food

constituents such as polyphenolics, triterpenoids, isothiocyanates, selenium as well as vitamins C, D, E and K2 were found to be inducers of autophagy.[30] These compounds are abundant in functional foods that induced autophagy and are listed in human diet for a long time. The best examples are tea, coffee, cocoa, red wine and nuts. The beneficial properties of these food ingredients are well known, however the molecular mechanism behind this beneficial effect remains to be illustrated.

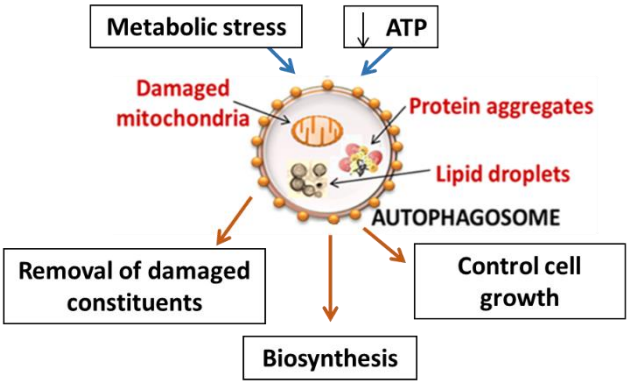

Figure 1. The autophagic process is an adaptive response, initiated mainly by stressed conditions.

A recent animal study indicated that caffeine significantly reduces hepatosteatosis and concurrently increase autophagy and lipid uptake in lysosomes. The lipolytic actions of caffeine via autophagy may contribute to its ameliorative effects on NAFLD.[31] This suggests that induction of autophagy might be effective strategy to prevent lipid accumulation or lipid-mediated disorders. Nowadays, natural supplements and synthetic drugs that induce autophagy are widely developed for therapeutic purposes[32-34] and individual plant-derived polyphenols have been studied as potential therapeutic agents to treat metabolic syndromes.[35]

In this regard, we have used two tropical fruit-derived polyphenols which are known to induce autophagy and speculated that glucose and lipid-mediated toxicity might be mitigated in our experimental *in vitro* model.

2. Experimental approach

Extraction of polyphenol

Total polyphenolic content was extracted from *H. undatus* and *G. mangostana* using the standard liquid-liquid extraction protocol. Freshly harvested fruit samples were lyophilized and extracted with methanol-water (60:40, v/v), at a ratio of solute to solvent of 1:10, at 35°C for one hour. The solvent was separated by centrifugation at 4°C, 2000 g for 10 minutes and then concentrated using a Buchi Rotavapor R-200 (Buchi, Switzerland) at 50°C. Extracts were filtered using 0.45µM nylon membrane filter (Agilent, Germany) to obtain clear hydrophilic solution. The filtrate was stored at -20 °C.

Cell culture and treatments

Human liver carcinoma cells, HepG2 (ATCC HB-8065) have been used in this study as an *in vitro* model. The cells were cultivated in Dulbecco's Modified Eagle Medium (DMEM), supplemented with 10% fetal bovine serum, 10U/ml penicillin-streptomycin, 100 mM sodium pyruvate, and 100 X MEM non-essential amino acids solution (Gibco, New York, USA). Cells were cultured in tissue culture flasks or dishes kept in a water jacket incubator at 37°C and in the presence of 7.5% carbon dioxide (CO_2).

Cell proliferation assay (MTS)

Cell viability was measured by MTS reagents, (CellTiter 96® AQueous Non-Radioactive Cell Proliferation Assay, Promega ,Wisconsin, USA) according to the manufacturer's protocol. 5000 cells per well were platted in 96-well plates containing 100 µl of culture medium and treated with food dyes as indicated in the figure legends. To analyze cell viability, 20 µl of the MTS solution was added to each well and the plates were incubated at 37°C in a humidified (5% CO_2) incubator until it developed desired color. Absorbance of the reaction mix was measured at OD490 nm using a microplate reader (Varioskan Flash Multimode Reader, Thermo Scientific, USA).

Oil Red O staining

To detect intracellular lipid accumulation, the cells were cultured in 24-well plates according to the experimental conditions indicated in the figure

legends. After treatment, the cells were washed with 1X PBS and then fixed with 10% formalin for one hour at room temperature. The cells were then washed twice with distilled water followed by 60% isopropanol for 5 minutes at room temperature and let it dry at room temperature. Once dried, the cells were stained with 0.21% Oil Red O solution (Sigma-Aldrich, Missouri, USA) for 10 minutes. The cells were then washed with distilled water for 4 times and dry at room temperature. 100% isopropanol was added to each well and incubated for 10 minutes under gentle shaking to elute lipid bound dye. The intensity of oil-red-o measured using a microplate reader at OD 500 nm.

Extraction of RNA from cultured cells

The cultured cells were washed with sterile PBS twice before lysed in 1.5 ml of QIAzol Lysis Reagent (Qiagen, Germany) and incubated at room temperature for 5 minutes. The lysate was transferred into 2 ml microfuge tubes. 300 µl of chloroform was added into each tube and centrifuged at 12,000 x g for 15 minutes at 4°C. The supernatant was transferred to a new microfuge tube and mixed with 0.75 ml isopropanol. The RNA was precipitated at room temperature for 10 minutes followed by centrifugation at 12,000 x g for 10 minutes at 4°C. The supernatant was discarded and RNA pellet was washed once with 75% ethanol.

Real Time PCR

1st strand cDNA was synthesised using the QuantiTect Reverse Transcription Kit (Cat. No. 205311, Qiagen) following manufacturer's protocol. Briefly, 2.5 µg of total RNA was mixed with 2 µl of gDNA buffer and top up to 14µl with RNase-free water. After 2 minutes incubation at 42°C, the sample mix was chilled on The reverse-transcription master mix was added and the reaction volume was brought up to 20 µl. This reaction mix was incubated at 42°C for 30 minutes and finally the reverse transcriptase was inactivated by heating the samples at 95°C for 3 minutes. The prepared cDNA was used as a template for real time PCR using QuantiFast SYBR® Green RT-PCR Kit (Cat. No. 204154, Qiagen, Germany) following manufacturer's prtocol. Briefly, 1 µl of 1st strand cDNA, 0.5 µl of each set of primers and 10µl of QuantiFast SYBR® Green RT-PCR Master Mix were mixed and topped up to a total reaction volume of 20µl with DNase free water. The cDNA was amplified and quantified using Eco Real-Time PCR System (Illumina, California, USA).

Acridine orange staining

27 µg/µl acridine orange solution (Sigma-Aldrich) was dissolved in PBS as suggested. 48 hours before treatment, one coverslip was placed in each well of a 6 well plate and cells were cultured at 37°C in a humidified (5% CO_2) incubator. After treated with polyphenols (75 µM and 150 µM) for 72 hours, cells were stained with acridine orange solution. Each sample was mixed gently and images were captured immediately using fluorescence microscope (Nikon AZ100). Images were taken according to the recommended filter for green and red fluorescence and then merged using *Image J* software.

Statistical analysis

The data were expressed as mean ± standard error (SE) for all experiments, except for the results for gene expression levels that were presented as mean ± standard deviation (SD). Statistical analysis was performed using SPSS Statistic 22.0 (IBM, USA). One-way analysis of variance (ANOVA) and post hoc Dunnett's test were applied in all independent experiments to compare values between control and treated groups. The values depicting $p<0.05$ were considered as statistically significant.

3. Results and Discussion

To mimic the physiological condition of hyperlipidaemic condition, cells were cultured in in saturated fat (palmitate) containing medium. The percentage of cell viability is presented in ***Figure 2***. MTS assay was performed after treating the cells with palmitate either in presence of extracted polyphenols (treated) or without polyphenols (untreated). The data showed a clear opposite trend in cell survival rate between treated and untreated groups. Cells that were treated with polyphenols (blue line) showed a pro-survival characteristic that increased gradually along with

the increase of palmitate concentrations. On the other hand, untreated cells (red line) underwent cell death that was also increased with the increase of palmitate concentrations. Compared to 20mM glucose (***Figure 2B***), the effect of polyphenol on viability was more obvious in 5mM glucose containg medium (***Figure 2A***). In presence of 20mM glucose and palmitate, cell viability was remarkably increased in presence of polyphenols (***Figure 2B***), suggesting the protective role of these polyphenols against glucose and lipid mediated stresses.

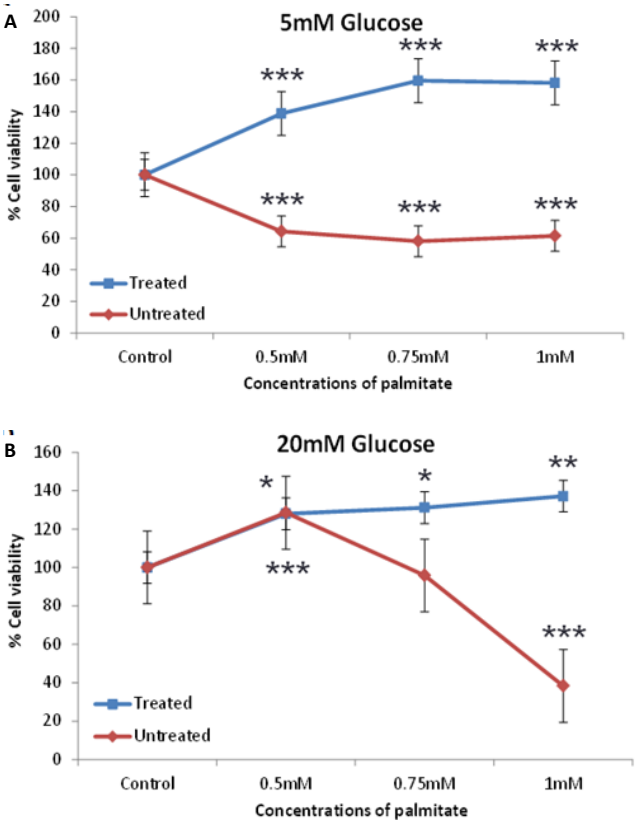

Figure 2. Polyphenols affect cell viability at different palmitate and glucose concentrations. 2000 cells/well was distributed before 48 hours of incubation and the percent of cell survivability was measured by MTS assay. Values are mean ± SE of four replicates. Polyphenols (75µM) significantly increased cell viability, while cell survivability in the untreated group is significantly decreased. (*P<0.05, **P<0.001, ***P<0.0001 vs control)

Induction of autophagy in the form of lipophagy (that selectively degrades cellular lipids) is known to reduce metabolic stresses by removing hepatic lipid droplets. Hence, the amount of lipid accumulated in these cells in hyperlipidemic condition was measured to explain the previous initial observation (as shown in ***Figure 2***). Lipid accumulation was evaluated by oil-red-o (ORO) staining in presence of palmitate along with polyphenols at different concentrations. Interestingly, intra cellular lipid level was reduced in all experimental units (***Figure 3***). Dragon fruit derived polyphenols are effective in preventing lipid accumulation in hyperglycaemic condition (***Figure 3B***) while mangosteen derived polyphenols significantly reduced lipid accumulation at all different polyphenol concentrations in both hypoglycaemic and hyperglycaemic conditions (***Figure 3C*** and ***Figure 3D***).

To confirm the pro-autophagic properties of these polyphenols, cells were treated with rotenone to impair mitochondrial function and cell survivability was measured. Rotenone increases reactive oxygen species (ROS) generation by blocking oxidative phosphorylation and subsequently inhibiting mitochondrial respiration.[36] When mitochondria are affected, cells that undergo extensive autophagy manage to survive.

The effects of polyphenols on cell viability during rotenone-induced oxidative stress were evaluated by MTS assay as shown in ***Figure 4***. The data indicated that rotenone significantly reduced cell survivability in the absence of polyphenol supplementation (red line). In contrast, cells that were treated with polyphenols exhibited higher survival rate compared to control in 25mM and 40mM glucose (***Figure 4B*** and ***Figure 4C***). This data suggest that apart from nullifying oxidative stress, polyphenol-induced autophagy might help the cells to survive better when their mitochondria are affected by recycling cellular reserves. Autophagy may also help these cells to remove damaged mitochondria and thus increases cell survivability.

To confirm the presence of autophagic vesicles, cells were stained with acrydine orange. In neutral pH, acrydine orange produces green fluorescence, while it results orange-red fluorescence in presence of acidic autophagic vesicles. As

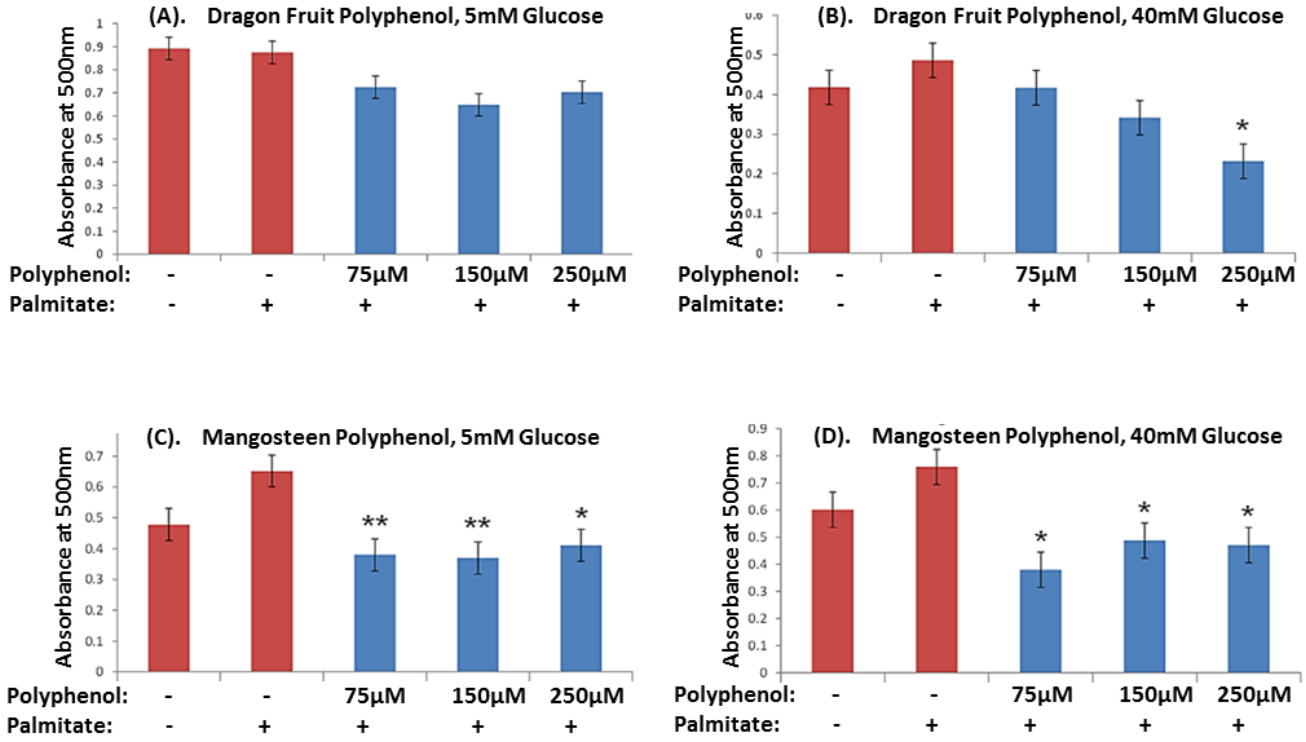

Figure 3. The effects of polyphenols on cellular lipid accumulation were measured by ORO staining. Absorbance was taken after 72 hours incubation. Values are mean ± SE of three replicates. Both types of polyphenols reduced the amount of lipid accumulated in the hepatocytes, however mangosteen derived polyphenols is more effective than dragon fruit-derived polyphenols. (*P<0.05, **P<0.001)

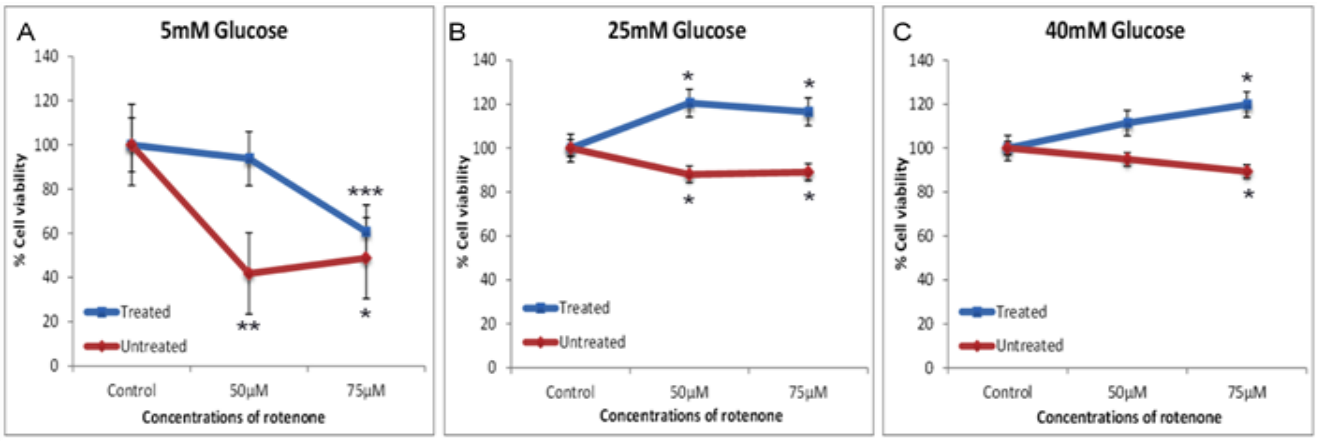

Figure 4. Polyphenols influence cell growth at different concentrations of glucose and rotenone. 2000 cells/well were distributed and treated with polyphenols and rotenone accordingly. MTS reagents were added after 48 hours incubation and absorbance were taken at the second hour. Values are mean ± SE of four replicates. In 25 mM and 40 mM glucose, polyphenols significantly protect cell from oxidative stress. (*P<0.05, **P<0.001, **P<0.0001)

illustrated in ***Figure 5***, due to the formation of autophagosomes, cells that were treated with polyphenols exhibited the presence of acidic autophagic vesicles and their number was highest in 150 µM polyphenol treated cells.

To elucidate the beneficial effects of these polyphenols, we have investigated the expression pattern of genes involved in lipid metabolism upon exposing the cells to different concentrations of polyphenols (***Figure 6***). mRNA expression level of peroxisome proliferator-activated

receptors alpha (PPAR-α), peroxisome proliferator-activated receptors gamma coactivator-1 alpha (PGC-1α), uncoupling protein 1 (UCP1), and sterol regulatory element binding protein 2 (SREBP-2) were determined by Real-Time PCR (***Figure 6***). These are the key genes involved in glucose and lipid metabolism and energy expenditure in the liver. The mRNA expression level of all these genes (SREBP-2, PPAR-α, PGC-1α, and UCP1) was significantly up-regulated in the samples treated with 250μM of experimental polyphenols (***Figure 6***).

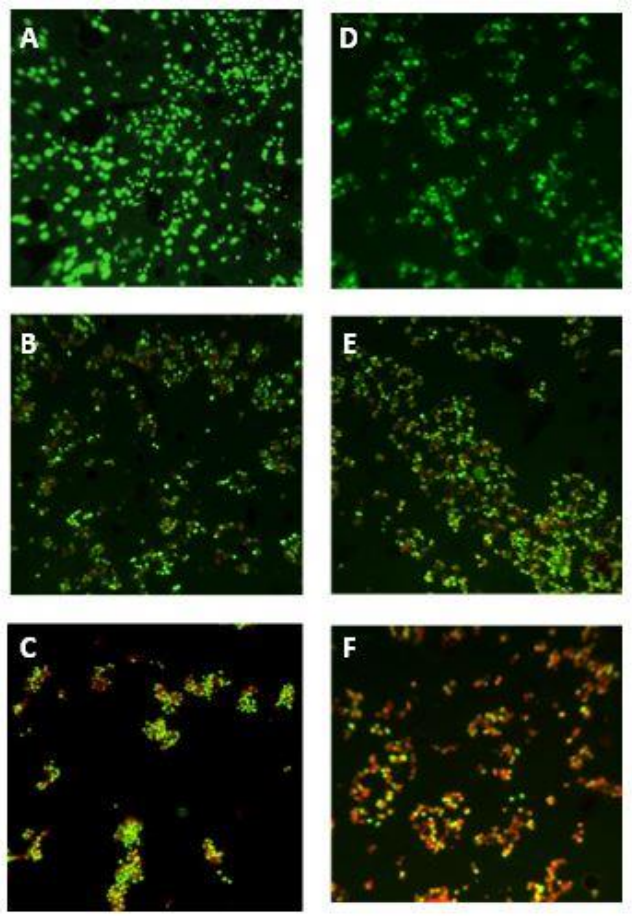

Figure 5. Polyphenols induced massive autophagy in hepatic cancer cells. Microphotographs were captured using a fluorescence microscope (30X magnification). A, B, C: control, 75 μM, and 150 μM polyphenol, respectively in 5mM glucose. D, E, F: the same group of cells in 40 mM glucose.

We have used human liver cell line (HepG2) in order to assess the beneficial properties of these fruit-derived polyphenols. Liver is the central organ of metabolism and hepatocytes are special cells that deal with high level of glucose and lipids in hyperlipidemia and hyperglycemia. Glucolipotoxicity often affects these cells that causes insulin resistance, cellular damage due to xenotoxic stress, and induces cell death. All these cellular events are associated with non-alcoholic fatty liver disease (NAFLD) and its advanced form such as NASH or cirrhosis. Inhibition of ROS and intracellular lipids is a proposed alternative strategy to combat this situation. Both glucose metabolism and lipid peroxidation generate ROS, excess amount of this metabolic byproduct eventually induces cellular stress or cell death. Polyphenols are known antioxidants and are believed to be effective in protecting cells from glucolipotoxicity, though the precise mechanism is not well illustrated. Apart from anti-oxidative property, certain polyphenols are believed to be efficient inducers of autophagy. This self-degradative catabolic process might help to remove defective mitochondria and other cellular metabolites such as lipid droplets during hyperglycemia and hyperlipidemia. Autophagy deficient mice developed hepatomegaly due to increased TAGs and cholesterol accumulation.[37] Autophagy (mainly lipophagy) exerts its protective effects by breaking down lipids to produce ATP, promote metabolism of toxic lipid molecules and prevent energy depletion which results in apoptosis or necrosis during mitochondrial impairment.[38]

In this experiment, cells treated with polyphenols exhibited higher viability in presence of palmitic acid (***Figure 2***), suggests that polyphenols might protect these cells from glucolipotoxicity by inhibiting ROS as well as inducing autophagy. This was further supported by staining the cells with lipid-specific oil-red-o staining. Mangosteen derived polyphenol (***Figure 4C*** and ***Figure 4D***) is more effective to clear hepatic lipid than dragon fruit derived polyphenol (***Figure 4A*** and ***Figure 4B***). Mangosteen is rich in xanthones, a class of polyphenolic compounds, which is responsible for its bioactive properties. Previous studies reported that mangosteen-derived xanthones can inhibit cell growth through induction of autophagy by suppressing mTOR pathway. This suggests that the reduction of hepatic lipid accumulation could

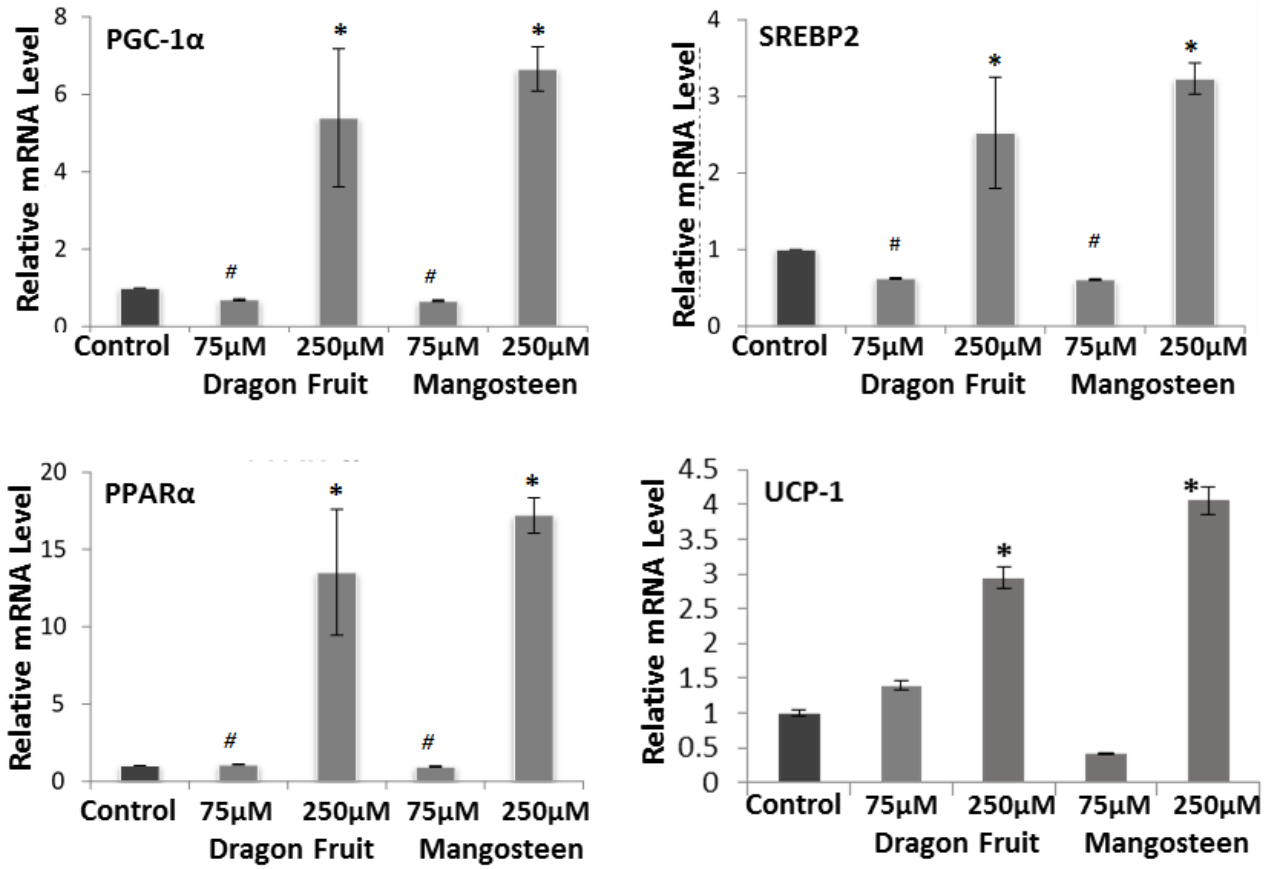

Figure 6. mRNA expression of indicated genes detected by Real-Time PCR. Data are expressed as mean ± SD of three replicates. DF: polyphenol from dragon fruit; MNG: mangosteen polyphenol. (*P<0.001, **P<0.0001).

be due to the induction of autophagy by xanthones or other similar polyphenols present in these fruits. On the other hand, hydroxycinnamates are the main phenolic compound in dragonfruits [39]. So far, their role in autophagy has not yet been illustrated. However, based on this study, both polyphenols are able to induce autophagy as detected by staining acrydine orange (***Figure 5***).

Mitochondria are most vulnerable organelles in glucolipotoxicity that often leads to decrease cellular ATP level which leads to necrosis or triggers mitochondria-mediated (intrinsic) apoptotic cell death. Autophagy, in form of mitophagy, plays a protective role in cells with defective mitochondria by recycling and removing the damaged mitochondria from cytoplasm. As stated earlier, autophagic process helps to protect cells from such stress which we have observed in our experiment. To confirm this speculated phenomenon, we have treated cells with rotenone, a known mitochondrial poison that impairs ATP production[40], a situation that occurs during glucolipotoxicity. High survival rate in the rotenone-treated cells in the presence of polyphenol was most probably attributed to autophagy (mitophagy and lipophagy). The result supports the hypothesis that pro-autophagic property of polyphenols improves cell survivability by recycling cellular organelles or cellular reserves.

Finally, the expression pattern of certain genes involved in lipid metabolism and induction of autophagy was investigated. SREP2, involved in cholesterol metabolism, was upregulated in all experimental units upon treating cells with polyphenols. Existing evidences suggest that SREBP2 contributes to the activation of autophagy inducing genes[41] and SREBP2 knockout mice exhibited decreased autophagosome formation and along with reduced

LC3 expression, a known molecular marker of autophagy.[42] Similarly, expression level of PGC-1α and its downstream targets such as PPARα and UCP1 were significantly high in cells treated with these extracted polyphenols. Expression of these genes induces mitochondrial biogenesis and fatty acid oxidation that ultimately helps to reduce cellular lipid level. Anti-obesity drugs often target this pathway, such as upregulating UCP1 to accelerate uncoupling mitochondrial respiration, leading to the elevated heat production by dissipating oxidation energy.[43]

5. Conclusion

This study is a part of our ongoing research project where we are investigating the molecular mechanisms that drive the beneficial effects of phytonutrients, especially polyphenols that are present in our tropical fruits. Though the findings need to be confirmed using *in vivo* or other *in vitro* models, this preliminary observation suggests that increased consumption of these tropical fruits might be beneficial to our local population who are at high risk of developing obesity or obesity-related disorders. Amongst these two fruits, total phenolic contents from mangosteen are beneficial for releasing hepatic lipid load and mediating lipid metabolism. Further *in vivo* studies are necessary to determine the bioactive compounds that exert these beneficial effects.

Acknowledgements

The authors acknowledge the FRGS grant (FRGS/1/2014/SG05/UNIM/02/2) awarded to Dr. Md Monowarul Mobin Siddique.

References

[1] I. Ignat, I. Volf and V. I. Popa, *Food chemistry*, 2011, **126**, 1821-1835.

[2] K. B. Pandey and S. I. Rizvi, *Oxidative medicine and cellular longevity*, 2009, **2**, 270-278.

[3] C. Tabak, H. A. Smit, D. Heederik, M. C. Ocke and D. Kromhout, *Clinical and experimental allergy : journal of the British Society for Allergy and Clinical Immunology*, 2001, **31**, 747-755.

[4] M. J. Bao, J. Shen, Y. L. Jia, F. F. Li, W. J. Ma, H. J. Shen, L. L. Shen, X. X. Lin, L. H. Zhang, X. W. Dong, Y. C. Xie, Y. Q. Zhao and Q. M. Xie, *Nutrition*, 2013, **29**, 235-243.

[5] C. Puel, A. Quintin, J. Mathey, C. Obled, M. J. Davicco, P. Lebecque, S. Kati-Coulibaly, M. N. Horcajada and V. Coxam, *Calcified tissue international*, 2005, **77**, 311-318.

[6] D. Nakajima, C. S. Kim, T. W. Oh, C. Y. Yang, T. Naka, S. Igawa and F. Ohta, *Journal of physiological anthropology and applied human science*, 2001, **20**, 285-291.

[7] U. Uysal, S. Seremet, J. W. Lamping, J. M. Adams, D. Y. Liu, R. H. Swerdlow and D. J. Aires, *Current pharmaceutical design*, 2013, **19**, 6094-6111.

[8] A. F. Fernandez and M. F. Fraga, *Epigenetics*, 2011, **6**, 870-874.

[9] M. Reinisalo, A. Karlund, A. Koskela, K. Kaarniranta and R. O. Karjalainen, *Oxidative medicine and cellular longevity*, 2015, **2015**, 340520.

[10] M. Nadim, D. Auriol, L. N. Lamerant-Faye, F. Lefevre, L. Dubanet, G. Redziniak, C. Kieda and C. Grillon, *International journal of cosmetic science*, 2014, **36**, 579-587.

[11] Y. K. Chen, C. Cheung, K. R. Reuhl, A. B. Liu, M. J. Lee, Y. P. Lu and C. S. Yang, *Journal of agricultural and food chemistry*, 2011, **59**, 11862-11871.

[12] M. Bose, J. D. Lambert, J. Ju, K. R. Reuhl, S. A. Shapses and C. S. Yang, *The Journal of nutrition*, 2008, **138**, 1677-1683.

[13] L. Gan, Z. J. Meng, R. B. Xiong, J. Q. Guo, X. C. Lu, Z. W. Zheng, Y. P. Deng, B. D. Luo, F. Zou and H. Li, *Acta pharmacologica Sinica*, 2015, **36**, 597-605.

[14] S. Renaud and M. de Lorgeril, *Lancet*, 1992, **339**, 1523-1526.

[15] D. D. Mellor, L. A. Madden, K. A. Smith, E. S. Kilpatrick and S. L. Atkin, *Diabetic medicine : a journal of the British Diabetic Association*, 2013, **30**, 478-483.

[16] S. A. Palma-Duran, A. Vlassopoulos, M. Lean, L. Govan and E. Combet, *Critical reviews in food science and nutrition*, 2015, 0.

[17] L. U. Thompson, J. H. Yoon, D. J. Jenkins, T. M. Wolever and A. L. Jenkins, *The American journal of clinical nutrition*, 1984, **39**, 745-751.

[18] H. M. Roseman, *Journal of managed care pharmacy : JMCP*, 2005, **11**, S3-11.
[19] W. I. Sivitz, *Postgraduate medicine*, 2001, **109**, 55-59, 63-54.
[20] C. Brons and A. Vaag, *The Journal of physiology*, 2009, **587**, 3977-3978.
[21] J. J. Lemasters, A. L. Nieminen, T. Qian, L. C. Trost, S. P. Elmore, Y. Nishimura, R. A. Crowe, W. E. Cascio, C. A. Bradham, D. A. Brenner and B. Herman, *Biochimica et biophysica acta*, 1998, **1366**, 177-196.
[22] J. J. Wu, C. Quijano, E. Chen, H. Liu, L. Cao, M. M. Fergusson, Rovira, II, S. Gutkind, M. P. Daniels, M. Komatsu and T. Finkel, *Aging*, 2009, **1**, 425-437.
[23] N. Pallet, D. Anglicheau and E. Thervet, *Nephrology, dialysis, transplantation : official publication of the European Dialysis and Transplant Association - European Renal Association*, 2009, **24**, 3891; author reply 3891.
[24] J. Fu, C. J. Shao, F. R. Chen, H. K. Ng and Z. P. Chen, *Neuro-oncology*, 2010, **12**, 328-340.
[25] X. Qu, Z. Zou, Q. Sun, K. Luby-Phelps, P. Cheng, R. N. Hogan, C. Gilpin and B. Levine, *Cell*, 2007, **128**, 931-946.
[26] Z. Yue, S. Jin, C. Yang, A. J. Levine and N. Heintz, *Proceedings of the National Academy of Sciences of the United States of America*, 2003, **100**, 15077-15082.
[27] H. Weidberg, E. Shvets and Z. Elazar, *Developmental cell*, 2009, **16**, 628-630.
[28] C. W. Wang, *Biochimica et biophysica acta*, 2015.
[29] R. A. Sinha, S. H. You, J. Zhou, M. M. Siddique, B. H. Bay, X. Zhu, M. L. Privalsky, S. Y. Cheng, R. D. Stevens, S. A. Summers, C. B. Newgard, M. A. Lazar and P. M. Yen, *The Journal of clinical investigation*, 2012, **122**, 2428-2438.
[30] K. Singletary and J. Milner, *Cancer epidemiology, biomarkers & prevention : a publication of the American Association for Cancer Research, cosponsored by the American Society of Preventive Oncology*, 2008, **17**, 1596-1610.
[31] R. A. Sinha, B. L. Farah, B. K. Singh, M. M. Siddique, Y. Li, Y. Wu, O. R. Ilkayeva, J. Gooding, J. Ching, J. Zhou, L. Martinez, S. Xie, B. H. Bay, S. A. Summers, C. B. Newgard and P. M. Yen, *Hepatology*, 2014, **59**, 1366-1380.
[32] S. Chen, S. K. Rehman, W. Zhang, A. Wen, L. Yao and J. Zhang, *Biochimica et biophysica acta*, 2010, **1806**, 220-229.
[33] S. Sarkar, *Drug discovery today. Technologies*, 2013, **10**, e137-144.
[34] B. Levine, M. Packer and P. Codogno, *The Journal of clinical investigation*, 2015, **125**, 14-24.
[35] E. P. Cherniack, *Nutrition*, 2011, **27**, 617-623.
[36] K. Radad, W. D. Rausch and G. Gille, *Neurochemistry international*, 2006, **49**, 379-386.
[37] R. Singh, S. Kaushik, Y. Wang, Y. Xiang, I. Novak, M. Komatsu, K. Tanaka, A. M. Cuervo and M. J. Czaja, *Nature*, 2009, **458**, 1131-1135.
[38] K. Liu and M. J. Czaja, *Cell death and differentiation*, 2013, **20**, 3-11.
[39] K. Mahattanatawee, J. A. Manthey, G. Luzio, S. T. Talcott, K. Goodner and E. A. Baldwin, *Journal of agricultural and food chemistry*, 2006, **54**, 7355-7363.
[40] T. K. Lin, C. H. Cheng, S. D. Chen, C. W. Liou, C. R. Huang and Y. C. Chuang, *International journal of molecular sciences*, 2012, **13**, 8722-8739.
[41] Y. K. Seo, T. I. Jeon, H. K. Chong, J. Biesinger, X. Xie and T. F. Osborne, *Cell metabolism*, 2011, **13**, 367-375.
[42] J. D. Horton, J. L. Goldstein and M. S. Brown, *The Journal of clinical investigation*, 2002, **109**, 1125-1131.
[43] S. Rousset, M. C. Alves-Guerra, J. Mozo, B. Miroux, A. M. Cassard-Doulcier, F. Bouillaud and D. Ricquier, *Diabetes*, 2004, **53 Suppl 1**, S130-135.

Bat diversity in two lowland forests of Brunei Darussalam

Huwaida Hj Masmin[1], Kathleen Collier[2], Pallavi Sirajuddin[3] and T. Ulmar Grafe[1]*

[1]Environmental and Life Sciences, Faculty of Science, Universiti Brunei Darussalam, Jalan Tungku Link, Gadong BE 1410, Brunei Darussalam
[2]School of Biological Sciences, The University of Auckland, Private Bag 92019, Auckland 1142, New Zealand
[3]Department of Forestry and Environmental Conservation, Clemson University, South Carolina, 29634–0310, USA

**corresponding author email: grafe@biozentrum.uni-wuerzburg.de*

Abstract

The forests of Brunei Darussalam harbour rich bat assemblages. In this study we update current knowledge of the abundance and distribution of bats in Brunei by comparing bat diversity between two lowland forest sites: Temburong and Tasek Merimbun. We recorded 27 bat species with three new locality records for each of the two sites surveyed. Temburong had higher bat diversity than Tasek Merimbun, suggesting that it has more diverse habitat types. This study highlights the need for further bat surveys as full inventories of bat communities have not yet been reached and little is known about the ecology and conservation status of bat populations.

Index Terms: Chiroptera; Conservation; Range extension; Tasek Merimbun; Temburong

1. Introduction

Bats have their highest diversity in the tropics where more than 60 species can be found at a single locality.[1,2] Bat populations have recently been declining due to factors such as global climate change, habitat disturbance, water pollution, environmental toxins, overhunting, and the spread of diseases.[3]

Bats play key roles in many ecosystems as pollinators, seed dispersers, and insect eaters. They are the primary pollinator for important agricultural plants such as bananas, durian, and mango.[4] Currently, approximately 250 genera of plants are known to rely on bats for pollination.[5] In addition, they play a role in restoring rainforests that have been cleared or damaged due to forest fires by dispersing the pollen or seeds.[6] They also provide many ecosystem services[7], for example by controlling insect pests on farmland.[8]

Bats can be used as bio-indicators to assess the health of an ecosystem because they are relatively easy to identify and most species have been described.[3] In addition, they are widely distributed and the effects of short and long-term forest disturbance on their populations can be monitored with relative ease.

The tropical rainforests of Brunei Darussalam have high levels of biodiversity and endemism.[9] Struebig et al.[10,11] reported 36 bat species from eight families surveyed at seven Bruneian study sites. The communities were dominated by forest-insectivorous species, including *Kerivoula papillosa*, *K. minuta* and *K. intermedia*. The highest number of species was found in Temburong and Andulau. By contrast, Merimbun had the fewest species.

In this study, bat diversity was resampled in two forests: Ulu Temburong National Park, Temburong and Tasek Merimbun Heritage Park, Tutong as part of a long-term monitoring program.

The objective of this study was to re-assess bat species richness and abundance in two lowland mixed-dipterocarp rainforests in Brunei separated

by only 50 km. However, long-term studies are needed to provide full inventories of bat communities and information on conservation status, rarity, threats and population trends of bat populations.

Based on previous surveys by Streubig et al.[10], we hypothesised that bat diversity would be higher in the never-logged Ulu Temburong forest because of the higher mosaic of microhabitats there. Furthermore, we hypothesised that that the composition of bat species differs between the two sites depending on the foraging strategies/roosting ecology of the affected species Finally, we expected to find additional bat species at these two sites as bat inventories in the tropics are notoriously incomplete.

2. Experimental approach

Bat diversity was sampled in two forests in Brunei Darussalam: Ulu Temburong National Park (N 4° 31', E 115° 08') and Tasek Merimbun Heritage Park (N 4° 34', E 114° 38'). Sampling in Temburong was done behind the Kuala Belalong Field Studies Centre, specifically along the Ashton trail. No logging activity has taken place in this forest. Sampling in Tasek Merimbun took place in the C2 sector of the forest, which has been subject to selective logging.

Both Ulu Temburong and Tasek Merimbun are categorised as mixed-dipterocarp rainforests. However, their forest structure is significantly different, leading Anderson & Marsden[12] to place them in two different subcategories (***Figure 1***). The sampling area in Ulu Temburong has dense, uneven canopy that is primarily made up of large crowns. By contrast, Tasek Merimbun has an uneven or moderately open canopy, with some medium and large emergents. Tasek Merimbun is also surrounded by padang forest and land under urban and industrial use.

Bat surveys in Temburong were caried out in 2015 during four periods: 8-21 March, 13-26 May, 8-12 July, and 20-23 September. Sampling in Tasek Merimbun was conducted from 2-12 October 2015. Bats were captured and collected in the early morning from 6-7am, and at night between 7-10pm.

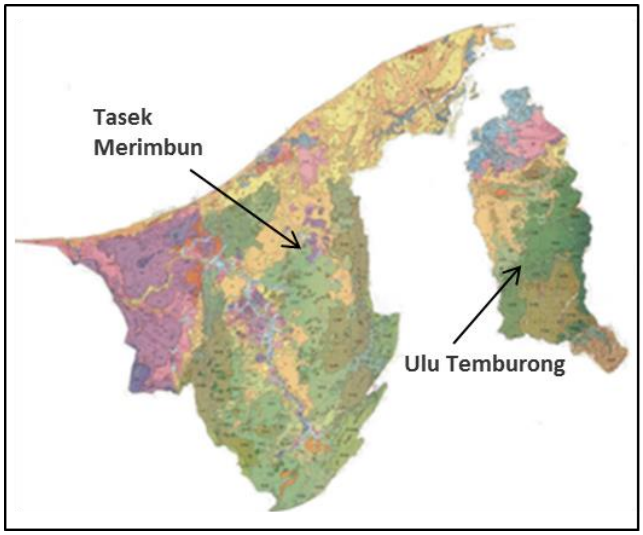

Figure 1. Forest map of Brunei Darussalam modified from Anderson & Marsden[11]. Different forest types are coded by colour: shades of green for mixed-dipterocarp forest, orange for Kerangas, purple for peat swamp, blue for mangrove or fresh water swamp, yellow for secondary forest, and ochre for urban or cleared land.

Bats were captured using harp traps placed perpendicular to established forest trails, preferably with overhanging tree branches to increase the probability of the bats being captured. This method was chosen because many bat species use established trails to move between roost sites and foraging sites. Harp traps were chosen over mist nets as they have been shown to be more effective in catching bats.[10,13,14] In addition, they cause less distress to the bats and need to be checked less frequently[14]. Bats fly against the strings and fall into cloth bags attached beneath the trap where they can be collected easily and without harming the animals.

Between 2-4 traps were moved between sites on forest trails each day to increase trapping efficacy for species that might be spatially limited to staying nearby a certain resource and to prevent capture rate from decreasing due to bats learning to avoid traps.[13] Bags were only attached to the aluminum frame of the trap in the late afternoon to prevent bats or non-target species from being trapped in the daytime. The traps were checked

twice a day, at 6-9 am and 7-10 pm. Each day, the traps were transferred approximately 50-150 m along the trail from the previous location.

Captured bats were processed and identified *in situ* according to unpublished keys by Matthew J. Streubig based on Payne and Francis.[15] As a precaution to protect against bites lightweight leather gloves were used while handling the bats.

Forearm length was measured using calipers to help identify the bat species.[16] Other measurements such as the length of tibia, tail, ear and tragus were also taken. Body mass was measured using a Pesola spring balance and the gender and reproductive condition was noted.

Catch rates were calculated by determining the mean number of bats captured per trap night. We controlled for recaptures by punching a small hole into the wing membrane of each captured bat. A trap night was defined as a single trap/night. We used the open access statistical software R with Vegan package and Fossil package to analyse the data. The Fossil package was used to calculate Simpson's index, abundance based estimators (Chao 1 and abundance based coverage (ACE)), Morisita-Horn index and the rarefied species accumulation curves.

The rarefaction method was used to standardise the sampling effort, since the sample size in Temburong was higher than in Tasek Merimbun. We used the Simpson's index to compare the diversity of the two study sites since it is less sensitive to small sample sizes than the Shannon-Wiener index.

The Simpson's index was calculated by measuring the probability that two individuals randomly selected from a sample belonged to the same species. Therefore, when the value is higher, diversity is lower.[17] Simpsons's measure of evenness was used to determine assemblage evenness. A high value means even species abundance regardless of the number of species.[9]

We also calculated the abundance-based estimators Chao 1 and the abundance-based coverage estimator (ACE). Chao 1 estimates the total number of species present in a community based on the number of rare classes. ACE uses abundance data sets to estimate the total number of species.

Chi-square tests were conducted to test for significant differences in foraging strategy and roosting ecology of bats among the two sample sites. Yates' correction was applied to roosting ecology to improve the accuracy of the test since it only has one degree of freedom.

The Morisita-Horn index was used to determine beta diversity, i.e. the spatial turnover of bat communities in the landscape.[18]

3. Results and Discussion

A total of 27 species were identified from both study sites. From 81 trap nights and a total of 189 individuals, 144 individuals belonging to 24 species were caught in Temburong. Another, 45 individuals of 18 species were caught in Tasek Merimbun over 35 nights (***Table 1***). Catch rates in Temburong were similar to those in Tasek Merimbun. However, the total number of species was higher in Temburong.

Table 1. Number of trap nights, number of bats captured, catch rates, and total number of species for both Ulu Temburong (UTNP) and Tasek Merimbun (TMHP) study sites

Site	Trap nights	Number of bats captured	Catch rate	Species richness
UTNP	81	144	1.78	24
TMHP	35	45	1.28	18

Members of the subfamily Kervoulinae and the family Hipposideridae were commonly found in both Temburong and Tasek Merimbun (***Figure 2***). The most abundant species at both sites, *Kerivoula papillosa*, accounted for 25.7% and 17.8% of all individuals captured in Temburong and Tasek Merimbun, respectively. Other dominant species from Temburong were *Hipposideros ater, Kerivoula lenis and Kerivoula minuta.* In Tasek Merimbun, *Hipposideros ridleyi* was the second most dominant species.

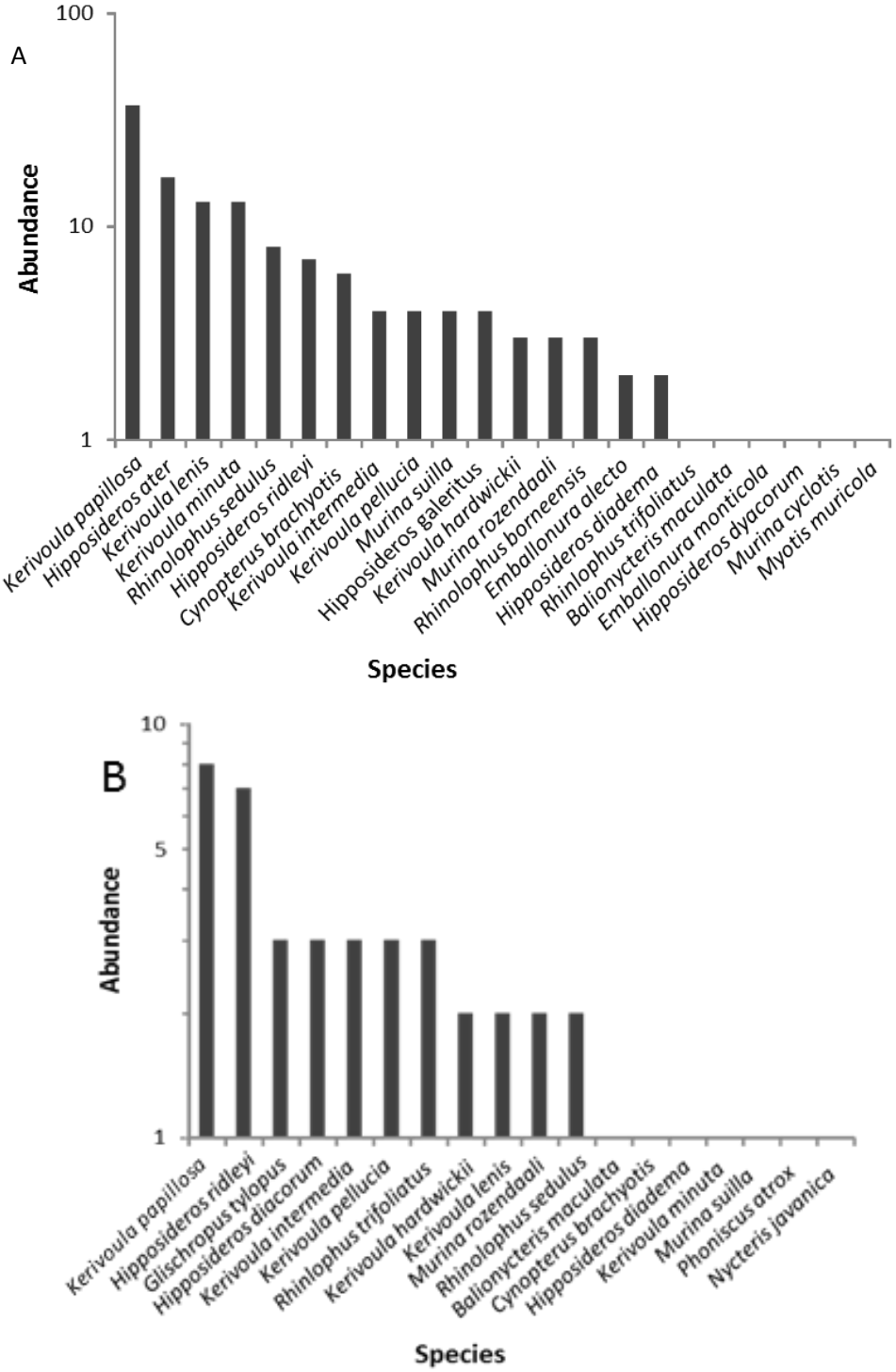

Figure 2. Rank abundance (log-scaled) of bat species found in Temburong (A) and Tasek Merimbun (B).

Six apparently rare species (singletons) sighted in Temburong were *Balionycteris maculata, Emballonura monticola, Hipposideros dyacorum, Macroglossus minimus, Murina cyclotis and Myotis muricola*. Three species were new records for Ulu Temburong National Park: *Cynopterus brachyotis, Hipposideros galeritus,* and *Murina rozendaali.* In Tasek Merimbun, seven species were found only once: *Balionycteris maculata, Cynopterus brachyotis, Hipposideros diadema, Kerivoula minuta, Murina suilla, Phoniscus atrox and Nycteris javanica*. Of particular interest were *G. tylopus, M. rozendaali* and *P. atrox* as they

were not recorded as being present at Tasek Merimbun in a previous survey by Struebig et al.[10]

The species accumulation curves suggest that sampling was far from complete (***Figure 3***). The diversity estimators Chao 1 and ACE suggest that the true number of species would be between 26-30 and 21-24 species in Temburong and Tasek Merimbun, respectively (***Figure 3***). The Chao 1 index indicated a greater number of bat species predicted than the actual number of species obtained.

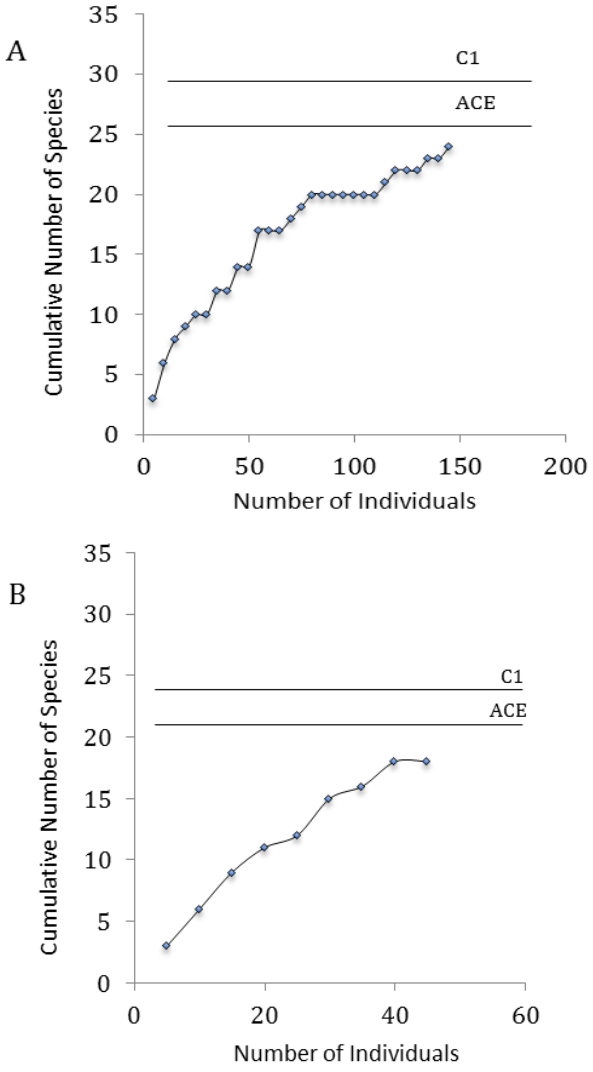

Figure 3. Species accumulation curves of bats species found in Temburong (A) and Tasek Merimbun (B). The straight lines above the curve indicate the diversity estimators C1 = Chao 1 & ACE = the abundance-based coverage estimator.

The species accumulation curve derived from sample-based rarefaction shows that Tasek Merimbun had higher species richness than Temburong (***Figure 4***). The rarefied values for Temburong and Tasek Merimbun, with the sample size standardised to 45 individuals, were 16 and 18 species, respectively. However, since the rarefaction curve for the Tasek Merimbun assemblage falls within the 95% confidence interval of the Temburong assemblage, species richness between the two sites was not significantly different.[19]

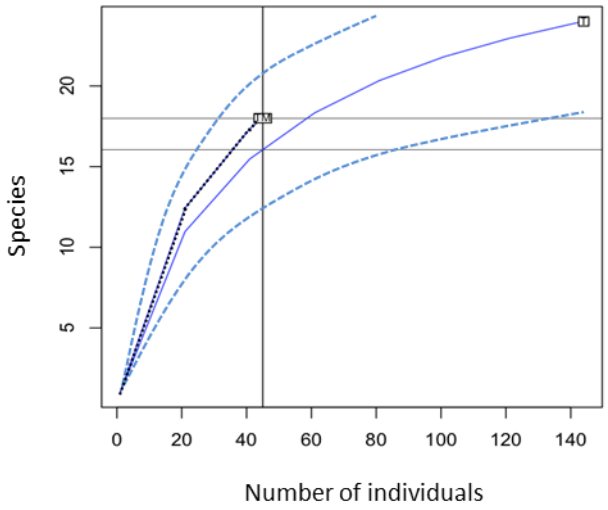

Figure 4. Sample-based rarefied species accumulation curve for Temburong and Tasek Merimbun. At 45 individuals species counts were 16 and 18 in Temburong (grey) and Tasek Merimbun (dotted black), respectively. Dashed grey lines are the 95% confidence intervals for Temburong.

The Simpson's index indicated that there might be higher bat diversity in Temburong (***Table 2***). Furthermore, Simpson's measures of evenness ($E_{1/D}$) were: 0.07 for Temburong and 0.06 for Tasek Merimbun. Thus, both of the sites had a similar degree of evenness.

Table 2. Simpson's index (D) and Simpson's measure of evenness ($E_{1/D}$) for Temburong (UTNP) and Tasek Merimbun (TMHP)

Site	D	$E_{1/D}$
UTNP	0.89	0.07
TMHP	0.91	0.06

The Morisita-Horn index was 0.704 suggesting that the two communities were quite dissimilar in composition. Insectivorous bats dominated the assemblage, with Kervoulinae and Hipposideridae being the most abundant taxa in both study sites.

Most of the bats in both study sites typically forage in narrow spaces or clutter inside the forest (Ni) (***Figure 5***)[2]. There were no frugivorous or insectivorous bats that forage in open areas and over large distances (Of and Oi) in either study site. There was no significant difference in the foraging strategy of bats between Temburong and Tasek Merimbun ($\chi^2 = 3.1841$; df = 2; p = 0.204).

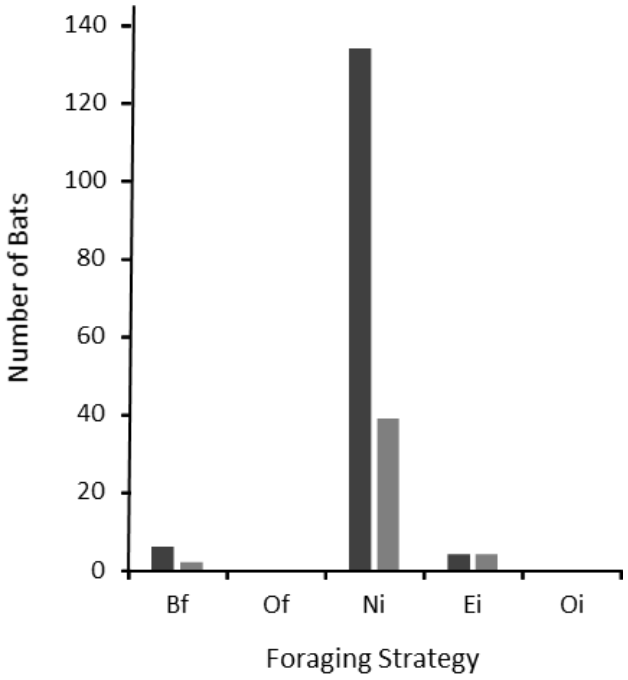

Figure 5. Foraging strategy of bats based on wing morphology captured in Temburong (black bars) and Tasek Merimbun (grey bars) following Streubig et al.[12]. Bf, frugivorous or nectarivorous species that forage in clutter within the forest; Of, frugivorous or nectarivorous species that forage in open areas over large distances; Ni, forest-interior insectivorous species that typically forage in narrow spaces; Ei, insectivorous species that forage in clutter within the forest; Oi, insectivorous species that forage in open areas and over large distances.

Most individual bats (81%) found at the two study sites are known to predominantly roost in trees, hollows or other foliage. The remainder were classified as roosting in caves or under boulders. There was a significant difference in roosting ecology between the two sites with Temburong having proportionally more cave/boulder-dwelling bats than Tasek Merimbun ($\chi^2 = 4.9586$; df = 1; p = 0.026).

A total of 27 bat species were recorded from the two study sites. We recorded three new records for each of the two sites Ulu Temburong and Tasek Merimbun, bringing the total number of bat species recorded from this and previous studies for these localities to 42 and 28, respectively.[10] The Brunei bat list contains 64 species out of 93 known to occur on Borneo.[10,11,20,21]

Our study, although small in scale and with unequal sampling effort between sites, indicates that the coastal, nutrient-poor forest at Merimbun has a more depauperate bat fauna than Ulu Temburong.[10] Although the rarefied species estimates at a sample size of 45 were not significantly different for the two forests, the species accumulation curve for Tasek Merimbun is likely to level off much faster than in Temburong as shown in the more extensive study by Struebig et al.[10] Clearly, a larger sampling effort for Tasek Merimbun would be most revealing.

Both sites had similar bat diversity as indicated by the Simpson's index. Likewise, Simpson's measure of evenness showed that both sites had similar evenness. However, unequal distributions of species among subfamilies and families in the two communities translated into a relatively low Morisita-Horn value suggesting that the two bat communities were dissimilar in composition.

This study has shown that Temburong and Tasek Merimbun have dissimilar bat assemblages. Although both are lowland mixed-dipterocarp rainforests, they are of different subtypes, with Temburong having much higher canopy than Tasek Merimbun.[12] In addition, the sites in Merimbun have experienced selective logging and are in close proximity to major economic activities such as rice and rubber plantations.[22] Fukuda et al.[23] observed low bat diversity in disturbed forests on Borneo. Moreover, canopy height and

tree-cavity availability, both of which are associated with minimally-disturbed old-growth forests, were recently identified as predictors of interior-forest bat assemblage composition.[24]

About 96% of the bats sampled in Temburong and Tasek Merimbun were insectivorous. Struebig et al.[10] also recorded mostly insectivorous bats (27 out of 35 species) across six sites in Brunei using harp traps set along forest interior trails. Frugivorous bats tend to move seasonally to disturbed habitat to find food[25] and are often found in higher numbers in disturbed forests.[26] The abundance of frugivorous bats was higher in Tasek Merimbun, suggesting a greater availability of flowering and fruiting plants; possibly locally-cultivated ones such as *Durio spp*.[22]

The woolly bat, *K. papillosa*, was the dominant species in both study sites, suggesting that both forests experience only low levels of disturbance.[10] *K. papillosa* is a forest specialist that can inhabit primary forests of different altitudes.[27] They also prefer to roost in hollows of small standing trees less than 20m in height.[28] They are dependent on the forest, restricting their range to forest-interior areas near their roosts.[29] Habitat disturbances such as logging are a threat to *Kerivoula*, and to other forest-specialist species. This sensitivity, combined with their relative abundance, makes *K. papillosa* a useful indicator of forest disturbance.[30]

Our study was biased towards capturing forest-interior insectivorous bats within the families/sub-families Hipposideridae, Kervoulinae, and Murininae as they are more susceptible to capture in harp traps than other species.[2] Genera such as *Tylonycteris*, *Hesperoptenus*, and *Pipistrellus* are not well represented in bat surveys that use harp traps because they forage around edges, above forest canopies, and open spaces.[10] A comprehensive survey of bat communities would thus require the use of multiple trap types such as mist nets, harp traps, and canopy nets as well as bioacoustic methods.

Some of the vulnerable and near threatened species listed by the IUCN[31] were captured in relatively high numbers, such as *Murina rozendaali, Hipposideros ridleyi, Rhinolophus sedulus, Kerivoula intermedia, K. minuta* and *K. pellucida*, suggesting that the forests surveyed are highly suitable for these species and thus should be protected.

This study also informs on the turnover of diversity across the landscape or beta diversity. Struebig et al.[10] found low bat landscape-level beta diversity across a spatial scale of 500km in northwestern Borneo. Low beta diversity, due to homogeneity of bat species across sites, indicates that biogeographical processes are likely to be irrelevant in shaping community structure at this scale. The distinct differences in community composition between Temburong and Tasek Merimbun, indicated in this study, however, suggests that bat communities across northwestern Borneo might be less homogeneous than previously thought. Less well studied forest types such as peatswamp forests or heath forests are likely to contain specialised forest-interior species, such as *Murina rozendaali* that may play key ecological roles in these habitats.

The availability and type of roosting sites can influence bat community composition and structure.[26] The difference in species composition between sites is commonly driven by the presence or absence of cave-roosting species. A higher proportion of cave-roosting bats (Hipposideridae and Rhinolophidae) were found in Temburong than in Tasek Merimbun. This is probably due to the higher availability of boulders in Temburong under which bats can roost in a cave-like manner[9].

Out of the 27 species recorded in this study, the majority were insectivorous bats that forage in the forest interior. These species were described by Kingston et al.[2] as intolerant to habitat disturbance. Frugivorous bats were not well represented in this study because they mostly forage at canopy level and shift their activity patterns in response to tree fruiting and flowering.[25,32]

The presence of six apparently rare species in Temburong and seven apparently rare species in

Tasek Merimbun shows that these sites should receive high conservation priority. Further research on bat roosting sites, foraging behaviour, and diets should be conducted to better understand bat abundance and distribution. Moreover, multiple sites across the landscape need protection to ensure that not only high biodiversity sites are protected but also areas with complementary fauna.

4. Conclusion

Our survey adds new records of bats to two rainforest sites in Brunei (Temburong and Tasek Merimbun) and shows high and complementary diversity. This leads us to the conclusion that both sites are of significant conservation value. Differences in bat community composition are likely to be driven by variation in canopy height and tree-cavity availability.

Acknowledgements

We gratefully thank Mhd. Dhiyaul Haziq and Hakeem Julaihi for field assistance; rangers at Tasek Merimbun Heritage Park; staff and management of Kuala Belalong Field Studies Centre, Universiti Brunei Darussalam (UBD) and The University of Auckland (UoA). We thank Stuart Parsons and Roger Coles for facilitating field work and Michael Schöner for reviewing the manuscript. Kathleen Collier was supported by a graduate scholarship from UoA. Research was funded by a grant from UBD (URG 193).

References

[1] E.K.V. Kalko, C.O. Handley and D. Handley, *Long-term Studies in Vertebrate Communities*, Eds. M. Cody and J. Smallwood, Academic Press, Los Angeles, **1996**, 503–553.

[2] T. Kingston, C. Francis, Z. Akbar, and T. Kunz, *Journal of Tropical Ecology*, **2003**, 19, 67-79.

[3] G. Jones, D. Jacobs, T. Kunz, M. Willig, and P. Racey, *Endangered Species Research*, **2009**, 8, 93-115.

[4] E. Gould, *Biotropica*, **1978**, 10, 184-193.

[5] T.H. Fleming, C. Geiselman and W.J. Kress, *Annals of Botany*, **2009**, 104:1017-1043.

[6] T.W.B. Horsley, J.E. Bicknell, B.K. Lim,. and L.K. Ammerman, *Acta Chiropterologica*, **2015**, 17, 331-336.

[7] T.H. Kunz, E.B. de Torrenz, D. Bauer, T. Lobova and T.H. Fleming, *Annals of the New York Acamdey of Sciences*, 2011, 1223,1-23.

[8] T.C. Wanger, K. Darras, and S. Bumrungsri, *Biological Conservation*, **2014**, 171, 220-223.

[9] E. Cranbrook and D.S. Edwards, *Belalong a Tropical Forest*, Sun Tree Publishing, Singapore, **1994**.

[10] M.J. Struebig, M. Bożek, J. Hildebrand, S.J. Rossiter and D.J.W. Lane, *Biodiversity Conservation*, **2012**, 21, 3711-3727.

[11] M.J. Struebig, J.C.-C. Huang, N.Z. Mohamed, S. Noerfahmy, C.R. Schöner, M.G. Schöner and C.M. Francis, *Mammalia*, **2016**.

[12] J.A.R. Anderson and J.D. Marsden, *Brunei Forest Resource and Strategic Planning Study*, **1984**.

[13] C. Francis, *Journal of Mammalogy*, **1989**, 70, 865-870.

[14] T. Kingston, *Behavioral and Ecological Methods for the Study of Bats*, Ed. T. Kunz and S. Parsons, Smithsonian Institution Press, Washington, **2009**, 195-215.

[15] J. Payne and C. Francis, *A Field Guide to the Mammals of Borneo*, The Sabah Society, Kota Kinabalu, **2005**.

[16] P. Richardson, *The Heart of Borneo*, London: Smithsonian Institution Press, London, **2002**.

[17] P. Hunter and M. Gatson, *Journal of Clinical Microbiology*, **1988**, 26, 2465-2466.

[18] M. Amaral, P. Netto, C. Lingnau and A.F. Figueiredo, *Applied Ecology and Environmental Research*, **2015**, 13, 361-372.

[19] C.J. Numa, R. Verdú, and P. Sánchez-Palomino, *Biological Conservation*, **2005**, 122,151-158.

[20] J. Payne, C.M. Francis, K. Phillips and S.N. Kartikasari, *Wildlife Conservation Society*, Indonesia Program, Jakarta, **2000**.

[21] C.P. Kofron, *Mammalia*, 2002, 66,259-274.

[22] J. Sidhu, *Historical Dictionary of Brunei Darussalam*, Scarecrow Press, Plymouth, **2009**.

[23] D. Fukuda, O.B. Tisen, K. Momose and S. Sakai, *The Raffles Bulletin of Zoology*, **2009**, 57, 213-221.
[24] M.J. Struebig, A. Turner, E. Giles, F. Lasmana, S. Tollington, H. Bernard and D. Bell, *Advances in Ecological Research*, **2013**, 48, 183-224.
[25] S. Bumrungsri. W. Leelapaibul and P. Racey, *Biotropica*, **2007**, 39, 241-248.
[26] I. Castro-Arellano, S. Presley, L. Saldanha, M. Willig and J. Wunderele, *Biological Conservation*, **2007**, 269-285.
[27] L. Joann, C. Fletcher, H. Salim, K. Abdul Rahman, R. Harrison and M. Potts, *Malayan Nature Journal*, **2011**, 63, 569-576.
[28] T. Kingston, B.L. Lim and Z. Akbar, *Bats of Krau Wildlife Reserve*, Penerbit Universiti Kebangsaan Malaysia, **2006**.
[29] M. Struebig, T. Kingston, A. Zubaid, S. Le Comber, A. Mohd-Adnan, and A. Turner, *Biological Conservation*, **2009**, 142, 2089-2096.
[30] M. Struebig, M. Harrison, S. Cheyne, and S. Limin, *Orxy*, **2007**, 14, 390-393.
[31] IUCN. Red list of threatened species: 2015. Retrieved April 14, 2016, from http://www.iucnredlist.org
[32] M. Struebig, L. Christy, D. Pio and E. Meijaard, *Biodiversity Conservation*, **2010**, 449-469.

Nutritional attributes of hemiparasitic mistletoe *Scurrula ferruginea* in Brunei Darussalam

Tang Yuan Pin[1], Linda B. L. Lim[1] and Kushan U. Tennakoon[2]*

[1]Department of Chemical Sciences, Faculty of Science, Universiti Brunei Darussalam, Jalan Tungku Link, Gadong, BE1410, Brunei Darussalam
[2]Department of Biological Sciences, Faculty of Science, Universiti Brunei Darussalam, Jalan Tungku Link, Gadong, BE1410, Brunei Darussalam

**corresponding author email: yuan_pin86@hotmail.com*

Abstract

Three different associations of *Scurrula ferruginea* parasites on three different hosts, namely *Tabebuia pallida*, *Acacia holosericea* and *Acacia auriculiformis* were collected from the Brunei-Muara District, Brunei Darussalam. Moisture content and chemical analyses (ash content, total carbohydrate content, crude protein, proline and mineral content composition) were determined to explain the host-parasite physiological biochemistry. *Scurrula ferruginea* contained relatively higher moisture content (47-65%) and ash content (2.1-2.5%, dry basis) than the hosts (0.7-1.4%, dry basis). High nutrient and moisture contents in *Scurrula ferruginea* make it more preferred food source than its hosts for generalist herbivores in a given community. The mistletoe exhibited differential storage profile of total carbohydrate (1.9-6.4%, dry basis) and total nitrogen (1.2-3.0%, dry-basis) when compared to hosts (total carbohydrate 2.3 - 3.0 % dry basis; total nitrogen 1.6-2.1%). Meanwhile the proline content was found to be in the range of 24.9-56.0 mg/kg, dry basis, in *Scurrula ferruginea*. Among all the minerals analysed, potassium was the most abundant mineral present in all mistletoe-host associations. Data indicated that certain host desired solutes are preferentially absorbed and stored in mistletoe.

Index Terms: mistletoe-host associations, parasitic plants, solute processing, plant nutrients

1. Introduction

Mistletoes are angiosperm obligate stem hemiparasites that inhabit branches (shoots) of completely independently growing woody trees or shrubs. Mistletoes do not produce functional roots and their photosynthetic efficiency is usually much inferior to other angiosperms. Hence, they are adapted to withdraw almost all water requirements and at least part of their nutritional requirements (by means of organic and inorganic solutes) from the hosts they parasitize.[1,2]

Studies conducted on water relations and nutrition of a range of temperate and Mediterranean mistletoe-host associations have shown that the potassium and proline contents of mistletoes were the highest among other major nutrients and osmotically active solutes, thus playing a vital role in osmotica of the parasite.[1,3-9] However, the phytochemistry of tropical mistletoes remains unclear due to paucity of studies except for a few studies conducted on *Scurrula ferruginea*[10,11], *Scurrula oortiana*[12], *Dendrophthoe falcata*[13] *Tapinanthus lugardii*, *Erianthenum ngamicum*, *Viscum rotundifolium*, and *Viscum verrucosum.*[14]

Scurrula ferruginea Danser [syn.: *Loranthus ferruginea* Roxb. (Loranthaceae)] attaches itself to a host by highly modified root known as the haustorium. Water and solutes are transported to the mistletoe thorough direct xylem-xylem or parenchyma cells connection present in the haustorium. Many countries including Malaysia, Indonesia, Australia and New Zealand have reported its distribution.[15] This species has been widely used in traditional medicine for the

treatment of hypertension and gastrointestinal complaints, gerontological effect and other therapeutic uses such as for treatment of ulcers and cancer.[16]

Huaxing and Michael[17] reported that the recorded hosts for *Scurrula ferruginea* include *Citrus grandis*, *Ficus hispida*, *Phyllanthus emblica* and *Prunus salicina*. Here we attempt to identify the solute partitioning and flux interaction between this tropical mistletoe and its common hosts. By comparing these variations among mistletoe-host partnerships with a single host we hope to reveal the selective manner in which nutrients are absorbed, transported and partitioned in tropical mistletoes where results are scarce.

2. Experimental approach

Samples

This study was conducted on three *S. ferrruginea*-host associations, viz: *S. ferruginea-Tabebuia pallida*, (Lindl.Miers, Bignoniaceae), *S. ferruginea- Acacia holosericea* (A. Cunn. ex G. Don, Mimosoideae) and *S. ferruginea- Acacia auriculiformis* (A. Cunn. ex Benth, Mimosoideae). These associations were grown in edges of heath forest patches (N 04˚55, E 114˚56) in Brunei Darussalam. The samples were collected where mistletoes have successfully established on host trees. From the leaves of the parasite, and leaves from parasitized hosts and non-parasitized hosts were collected and stored in the freezer for further analyses.

Chemicals

Phenol (Sigma-Aldrich), glucose (Fluka), concentrated sulfuric acid (Merck), sodium hydroxide pellets (Merck), boric acid (BDH), Concentrated hydrochloric acid (Merck), ninhydrin (Merck), 2-propanol (Fluka), proline (Sigma), concentrated nitric acid (Ajax), formic acid (Fluka), ethylene glycol monomethyl ether (Riedel-de Haën).

Instruments

VIRTIS Specimen Freeze Dryer, Memmert Laboratory Oven, GALLENKAMP muffle furnace, Shidmadzu UV-1601PC UV spectrophotometer, GERHARDT automated digestion system and distillation system and Shidmadzu AA-6701F atomic absorption spectrometer.

Sample preparation

Two types of drying methods were used: oven-drying and freeze-drying. For oven-drying, leaf samples were dried at 45 °C until a constant weight was attained. While for freeze-drying, samples were freeze-dried using VIRTIS Specimen Freeze Dryer. Each analysis was carried out in duplicates. Dried samples were separately weighed and the change in mass of each samples were used to determine the moisture content.

Sample extraction

The leaf samples collected were cleaned to remove any dirt on the leaf surface. The slightly modified AOAC Official method 920.149[18] was used. Fresh leaf samples (about 10.00 g) from the parasite, parasitizing host and non-parasitizing part of each tree were blended with doubly distilled water (100 mL) at room temperature and the mixture was gravity filtered. The filtrate was then kept in the freezer prior to analysis. These sample extracts in duplicates were used for total carbohydrate and proline contents.

Determination of ash content

Fresh samples (about 1.00 to 2.00 g) were placed in the GALLENKAMP muffle furnace and ignited to 600 ˚C and maintained at this temperature for about 4 to 6 hours until samples turned white due to complete combustion. The change in mass was used to determine the ash content of the samples. The ash was subsequently used for the determination of mineral nutrient analyses. Each sample was carried out in duplicates.

Determination of total carbohydrate

The phenol-sulfuric acid method (AOAC Method 44.1.30), as stated in the Food Analysis Laboratory Manual[19] with slight modifications, was used for the determination of total carbohydrate content in leaf samples. A series of 6 calibration standard glucose solutions was prepared from the glucose stock solution with the concentrations ranging from 0 µg/2 mL to 100

µg/2 mL. The absorbance of each of the solutions was then measured using a Shidmadzu UV-1601PC UV spectrophotometer at wavelengths between 450-550 nm. The standard solution with 0 µg/2mL was used as reference.

The absorbance for each of the standard and sample solutions was recorded at 490 nm to plot a graph of absorbance against different concentrations of glucose. Each sample was carried out in duplicates.

Determination of total nitrogen

Total nitrogen was determined by using the standard block digestion Kjeldahl method.[18,20-21] Protein content in both freeze-dried and oven-dried leaf samples was determined using GERHARDT automated digestion and distillation systems. Each sample was carried out in duplicates.

Determination of proline

The method was based on the original method of Ough.[22] The blended sample solutions, as described in Section 4.3, were used for the determination. The absorbances were measured using the Shidmadzu UV-1601PC UV/VIS spectrophotometer at wavelength between 400 and 800 nm. The absorbance at 510 nm was recorded for each of the tubes. The proline content was determined from the ratio of the sample solution and the proline standard solution at the wavelength of 510 nm. Each sample was carried out in duplicates.

Determination of minerals

Mineral determinations were carried out in duplicate. The ash obtained was dissolved in concentrated hydrochloric acid (2.5 mL) followed by concentrated nitric acid (2.5 mL). The mixture was then left at room temperature until all the ash had dissolved. Each replicate mixture was diluted to 50 mL using ultrapure water respectively. The solution was kept in the refrigerator until further analysis using Shidmadzu AA-6701F atomic absorption spectrometer. Each sample was carried out in duplicates.

Statistical Analyses

All data presented are means of two determinations. Statistical analysis was done using ANOVA single factor, Microsoft Excel 2010 Data analysis Program. The level of statistical significant was set as $p < 0.05$.

3. Results and Discussion

There is a significant difference in the moisture content obtained using both freeze drying method and oven drying method ($p<0.05$). Moisture content data obtained in duplicates by freeze-drying method showed lower values than oven drying method (***Figure 1***). This might be probably due to the presence of volatile compounds in the leaves that vaporize when temperature was increased beyond 45 °C. Volatile compounds such as esters, terpenes and alcohols are commonly present in plant matter and can be responsible in making the cell sap of mistletoe more concentrated than host thus allowing the mistletoe to absorb host derived water and dissolved solutes along a favorable water potential gradient. General pattern of high moisture content shown in mistletoe indicates that they are more palatable for generalist herbivores than the host leaves.[23]

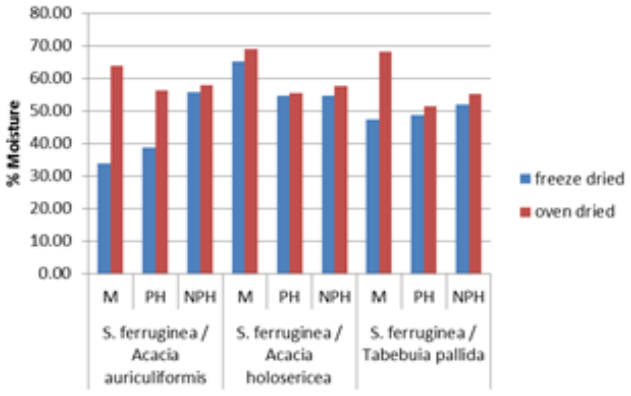

Key: M – Mistletoe, PH – Parasitized host, NPH – Non-parasitized host

Figure 1. Percentage moisture content in *Scurrula ferruginea* and its hosts

In order to ensure uniformity, subsequent comparisons will be based on oven-dried method. Ash content reflects the total mineral content. The mean ash content in *S. ferruginea* parasitizing on the three different hosts do not show an

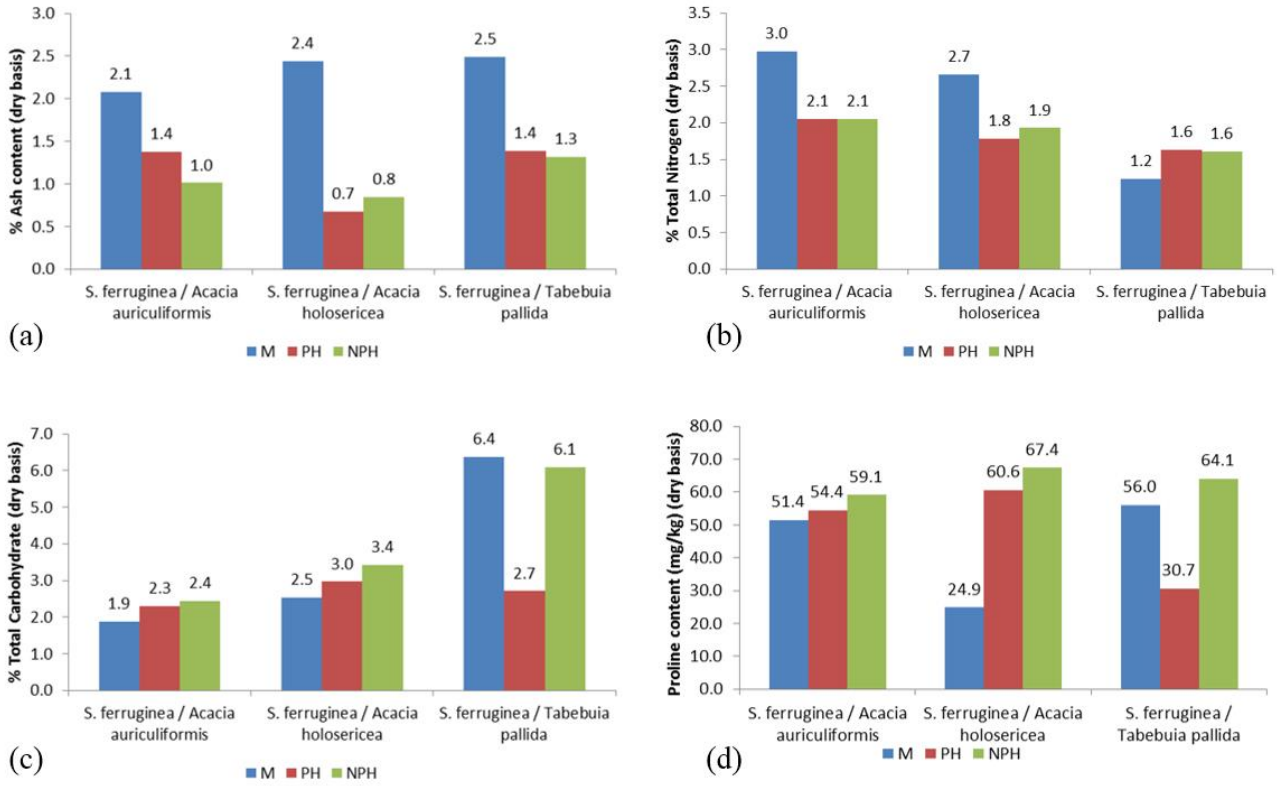

Figure 2. Percentage ash content (a), total carbohydrate (b), total nitrogen content (c) and proline content (d) of *Scurrula ferruginea* parasitizing on *Tabebuia pallida, Acacia holosericea* and *Acacia auriculiformis* respectively. Each sample was carried out in duplicates.

appreciable difference ranging from 2.1 to 2.5 % dry basis (***Figure 2a***). The values of the mistletoes showed a generally higher value than the comparable hosts[24], thus we expect generally low ash content in mistletoe. However, it can be argued that mistletoes have absorbed and retained a large content of nutrients along the host derived xylem flux *via* the haustoria. Hence, the phenomenon of the presence of high ash content is generally in agreement with the physiology of mistletoes.

Hull and Leonard[25] stated that it is important to maintain sufficient carbohydrate reservoir in mistletoes for the survival and production of new foliage during the unfavorable periods. There was a significant difference among all the total carbohydrate contents analysed ($p<0.05$). The tropical mistletoe *S. ferruginea* shows generally lower carbohydrate contents (1.9-6.4% dry basis) than the corresponding non-parasitized (2.4-6.1 % dry basis), (***Figure 2b***). This can be attributed to generally favorable environmental conditions prevailing in tropical Brunei in contrast to results reported for arid and temperate species.

There is significant difference among the three associations of *S. ferruginea* ($p<0.05$). The nitrogen content (***Figure 2c***) indicates that *S. ferruginea* parasitizing the nitrogen fixing *A. holosericea* and *A. auriculiformis* have higher nitrogen content than those parasitizing on non-nitrogen fixing *T. pallida.* The nitrogen concentrations in mistletoe leaves are dependent on the type of host it parasitizes.[24,26-27] Results of nitrogen partitioning clearly are in agreement with the literature that storage of some nutrients in mistletoe is influenced by host species. Furthermore, nitrogen profile on *S. ferruginea* reflecting those of hosts may be interpreted as little solute processing related to nitrogenous compounds taking place in the haustorium.

Ehleringer *et al.*[28] have stated that proline often serves as an essential role in osmotic relations of

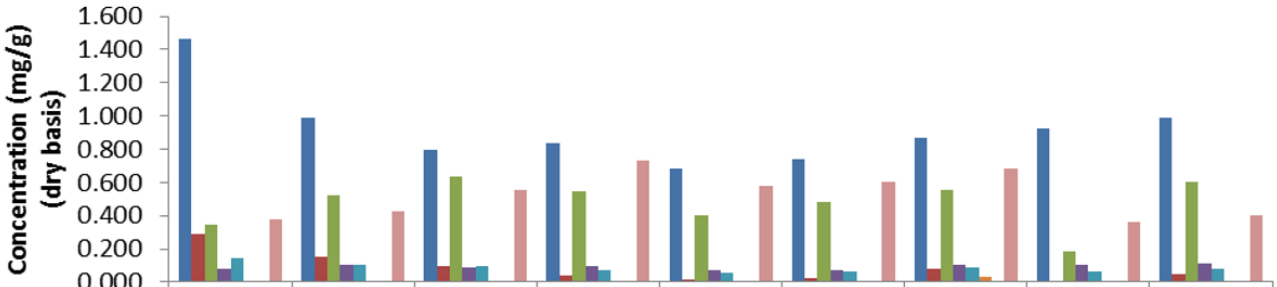

	M	PH	NPH	M	PH	NPH	M	PH	NPH
	S. ferruginea / Acacia auriculiformis			S. ferruginea / Acacia holosericea			S. ferruginea / Tabebuia pallida		
K	1.461	0.991	0.793	0.840	0.683	0.737	0.865	0.923	0.992
Na	0.293	0.155	0.099	0.042	0.016	0.021	0.081	0.011	0.048
Ca	0.346	0.525	0.638	0.543	0.401	0.486	0.553	0.188	0.600
Mg	0.083	0.102	0.085	0.094	0.070	0.074	0.102	0.105	0.110
Fe	0.142	0.107	0.093	0.073	0.060	0.063	0.091	0.064	0.078
Zn	0.010	0.010	0.011	0.007	0.007	0.007	0.032	0.008	0.009
Mn	0.002	0.010	0.011	0.003	0.004	0.005	0.007	0.004	0.003
Cu	0.374	0.428	0.559	0.729	0.581	0.605	0.687	0.361	0.402

Key: PL – Parasite leaves, PHL - parasitized host leaves, NPHL - non-parasitized host leaves

Figure 3. Concentration of potassium, calcium, sodium, magnesium, copper, zinc, manganese, iron of *S. ferruginea* and its hosts. Each sample was carried out in duplicates.

parasitic plants and it is expected that mistletoes would have higher concentrations of proline than the hosts. However, a reverse effect was observed as where the non-parasitized host showed the highest proline content in our investigation. Even though the total nitrogen content of *S. ferruginea* is always higher than the hosts, the proline content of the mistletoe *S. ferruginea* was always lower than the non-parasitizing host partner (***Figure 2d***). Leaf nitrogen can be attributed to the storage of polyphenol[29]. Hence, this implies that proline is not the major component of nitrogen in the leaf of *S. ferruginea.* However consistent with the literature the mistletoe had higher proline content than the parasitized host in the *S. ferrugina-T. pallida* association, interestingly this was the only host that was not a N fixer.

As a consequence to the absence of retranslocation of solutes between the mistletoe and host due to lack of phloem links in the haustorium that connects these two separate plants, mistletoes rely exclusively on host xylem for their water and mineral requirements.[1] The major and minor mineral nutrients profiles are in ***Figure 3***. Potassium was the major mineral found in the all samples investigated. As reported by Glatzel,[1] potassium enrichment in mistletoe is directly linked to the absence of retranslocation between mistletoe and host because of the lack of phloem links. Mistletoes have the ability to divert a steady stream of potassium from the xylem-phloem cycle of the host. The second most abundant mineral found in the samples was calcium followed by sodium. The distribution of other minerals between the mistletoe and the parasitized host were not consistent.

Mistletoes lack a usual plant-root system capable of active uptake. They rely upon a host connection through the haustorium for nitrogen and mineral nutrients. Both the host leaves and mistletoe leaves draw from the same xylem sap[30]. Nevertheless, whether or not the mistletoe should have higher mineral content than the host may be dependent on as of yet unresolved factors as Lamont[4] reported the calcium levels were lower in the mistletoe than in the host, while McDowell[3]

reported that the mistletoes have higher concentrations of nitrogen, phosphorus, potassium and magnesium than the host.

Furthermore, Singh and Carew[6] did not detect meaningful differences in macronutrient or micronutrient concentrations for any plant parts analyzed in a range of mistletoe-host association. Such variations might be due to the age of the plant analysed, the growing environment of these tropical mistletoe-host association, the type of parasite and the specific host and the time chosen for sample collection.[4,7] In addition, loss of nutrients can also occur to the older part of the host plant and mistletoe independently by the phloem-mediated cycling or remobilization from senescing leaves.[1]

Some evidence suggest that the complex nature of solute partitioning between mistletoes and hosts due to selective (active) transportation of solutes across the haustoria. The haustorium cells at the interface have enhanced concentrations of mitochondria and show signs of being able to mobilize energy. The main function of these cells is to pump unwanted materials back to the host. However, the mechanisms behind these processes are only partly understood.[31]

4. Conclusion

Results of this study revealed that solute partitioning of the mistletoes is likely to be complex, but interacts in a highly ordered fashion in relation to the composition of host derived solutes. The compositional changes shown across the mistletoes, parasitized and non-parasitized host branches occur in favor of the successful continuation of mistletoe-host association partnership. Further studies on nutritional partitioning of tropical mistletoes at molecular level must take into account the haustorial anatomy, co-evolutionary strategies adopted by both host and mistletoe that ensures successful co-habitation, and the confounding tropical environmental conditions that many influence physiological biochemistry of mistletoes.

Acknowledgements

The authors would like to thank Aywen Wang H. Chak for field assistance and the Universiti Brunei Darussalam for logistic support. Financial assistance for this study was provided by Universiti Brunei Darussalam, Science and Technology Grant No. 8.

References

[1] G. Glatzel, *Oecologia*, **1983**, 193.
[2] J. Kujit, *The Biology of Parasitic Flowering Plants*, University of California Press, Berkeley, **1969**, 45.
[3] L. C. McDowell, *Physiological relationships between dwarf mistletoe and ponderosa pine*, Oregon State University, Corvallis, OR, Oregon State University, **1964**, 68.
[4] B. Lamont, *Mineral nutrition of mistletoes*. *The biology of mistletoes*, M. Calder and P. Bernhardt, **1983**, 185.
[5] W. H. Chak, *Preliminary investigation on the mineral nutrition and water relations of tropical hemiparasitic mistletoes found in Brunei-Muara District (Brunei Darussalam)*, Universiti Brunei Darussalam. **2009.**
[6] P. Singh and G. C. Carew, *Euro. J. Forest Pathology*, **1989**, 305.
[7] K. U. Tennakoon and J. S. Pate, *Plant, Cell & Environ.*, **1996**, 517.
[8] M. Popp, R. Mensen, A. Richter, H. Buschmann and D. J. Willert, *Trees*, **1995**, 303.
[9] J. M. Hibberd and W. D. Jeschke, *J. Exp. Botany*, **2001**, 2043.
[10] D. F. Lohézic-Le, A. Bakhtiar, C. Bézivin, M. Amoros and J. Boustie, *Fitoterapia*, **2002**, 400.
[11] O. Z. Ameer, I. M. Salman, M. J. Siddiqui, M. F. Yam, R. N. Sriramaneni, A. Sadikun, Z. Ismail, A. M. Shah and M. Z. Asmawi, *The American J. Chinese Med.*, **2009**, 991.
[12] C. Kirana, *Bioactive compounds isolated from mistletoe (Scurulla oortiana (Korth).Danser) parasitizing tea plant (Camellia sinensis L.)*, University of Adelaide, South Australia. **1996**.

[13] D. N. Raut, C. P. Subodh and C. M. Subhash, *Int. J. Pharmaceutical Res. Develop*., **2009**, 6.
[14] O. R. Madibela, M. Letso, W. S. Boitumelo, M. Masedi and K. Alton, *Animal Feed Sci. Technol.*, **2002**, 159.
[15] B. A. Barlow, *Flora Malesiana Bull.*, **1991**, 335.
[16] O. Z. Ameer, I. Salman, M. Yam, A. H. Allah, M. Abdulla, A. Shah, A. Sadikun and M. Asmawi, *Int. J. Pharmacology*, **2009**, 44.
[17] Q. Huaxing Q and G. G. Michael, *Flora of China*. **2003**, 220.
[18] P. Cunniff, *Methods of Analysis of AOAC International*. AOAC International, USA. **1998**, 37.
[19] S. S. Nielsen, *Food Analysis Laboratory Manual*, Indiana, **2003**, 39.
[20] L. S. P. Madamba, *Laboratory Instruction Manual: Technical analysis I - Foods and Feeds*, The Philippines, **2000**, p 28-31.
[21] S. S. Nielsen, *Food Analysis Laboratory Manual*, Indiana, **2003**, 33.
[22] C. Ough, *J. Food Sci.*, **1969**, 228.
[23] D. V. Canyon and C. J. Hill, *Australian J. Ecology*, **1997**, 395.
[24] J. Ehleringer, E. Schulze, H. Ziegler, O. Lange, G. Farquhar and I. Cowan, *Science*, **1985**, 1479.
[25] R. J. Hull and O. A. Leonard, *Plant Physiology*, **1964**, 996.
[26] P. Bannister and G. L. Strong, *Oecologia*, **2001**, 10.
[27] E. D. Schulze, O. Lange, H. Ziegler and G. Gebauer, *Oecologia*, **1991**, 457.
[28] J. R. Ehleringer, C. Craig and L. T. Larry, *Oecologia*, **1986**, 279.
[29] J. C. Rambourg and B. Monties, *Plant Foods for Human Nutrition*, **1983**, 169.
[30] G. Glatzel and B. Geils, *Canadian J. Botany*, **2009**, 10.
[31] H. Shen, W. Ye, L. Hong, H. Huang, Z. Wang, X. Deng, Q. Yang and Z. Xu, *Plant Biol.*, **2006,** 175.

Rapid detection of pork DNA in food samples using reusable electrochemical sensor

*Hafizah Munirah, Sharmili Roy, Jean L.Z. Ying, Ibrahim A. Rahman and Minhaz U. Ahmed**

Biosensors and Biotechnology Laboratory, Department of Chemical Sciences, Faculty of Science, Universiti Brunei Darussalam, Jalan Tungku Link, Gadong BE 1410, Brunei Darussalam

**corresponding author email: minhaz.ahmed@ubd.edu.bn*

Abstract

This study aims to demonstrate the potential use of reusable electrochemical sensor for detecting pork DNA in solution. The approach was based on electrochemical principle in which the electrostatic interaction between DNA and redox species will generate detectable signal upon introduction of electrical charge. In this study, Ruthenium Hexaamine (RuHex) was used as the redox species and result was based on the output current. Coupled with highly specific Polymerase Chain Reaction (PCR) primers designed for pork DNA, this study has successfully demonstrated the reliability of proposed novel detection approach that utilized reusable electrochemical sensor and can potentially be developed into a rapid detection tool for halal and kosher food industry.

Index Terms: Pork DNA, Halal, Kosher, Electrochemical Sensor, PCR, Ruthenium Hexaamine

1. Introduction

The concept of "halal" and "kosher" have been well acknowledged and put into practice by Muslims and Jews respectively. These two terms are frequently mentioned in their respective scriptures and are commonly practiced amongst the Muslims and Jews as part of their food law. When applies in food law, the term "halal" is referring to permissible food consumed by Muslim that does not contain any prohibited component.[1]

PCR, a DNA-based technology, has been successfully performed to detect pig meat and fat. It has also been deemed as one of the most effective and reliable detection methods.[2,3] Conventionally, agarose gel electrophoresis is subsequently performed to detect the PCR amplicons. However, this detection method possesses several drawbacks arisen from its requirement for time consuming post-PCR sample preparation, high voltage, bulky instruments and may yield a rather vague qualitative result. Moreover, the long-term cost of using agarose is relatively expensive when compared to the cost of a reusable sensor and this method has also been proven to display poor separation on samples with low molecular weight.[4-7]

Several alternative methods have been well applied in place of gel electrophoresis to avoid the above mentioned drawbacks, electrochemical method being one of them. Modern electrochemical method often uses a three-electrode electrochemical system that has been re-designed into miniature forms and integrated onto a biochip to increase its compatibility as an electrochemical sensor.[8] The sensor requires minimal current flow in nanoampere (nA) range and small sample volume in microlitre (μL) range for the electrode reaction to occur.

The detection of pork DNA profoundly relied on the capability of redox active compound to interact with DNA to initiate electrochemical reaction. RuHex being electrochemically active and capable of binding to DNA via electrostatic interaction made it an ideal redox species candidate for this study [9-11]. Moreover, this approach requires no modification to the electrode surface. Electrostatic interaction occurs between DNA and redox species when the cationic RuHex

binds to the anionic phosphate group in DNA backbone (***Figure 1***).

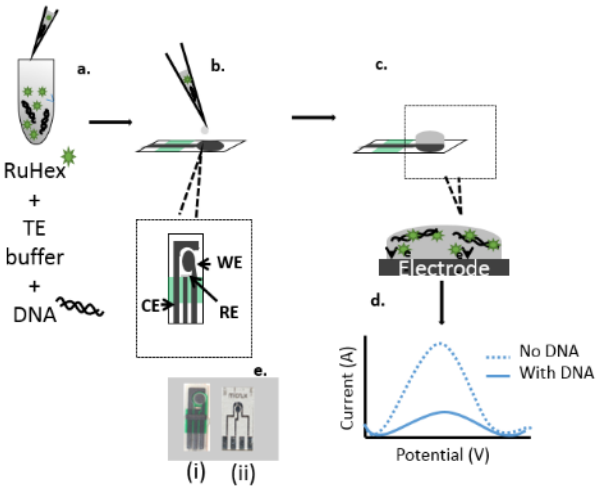

Figure 1. Schematic diagram of DNA detection in solution using electrochemically active RuHex on carbon screen printed electrode (SPE) chip. (a) solution composition mixture comprises of amplicons (dsDNA) : RuHex : buffer in a ratio of 2:1:1 respectively; (b) solution spiked onto the surface, covering the whole area of working electrode; (c) Electrostatic interaction between RuHex and dsDNA; (d) peak current generated where solution of free RuHex gives higher peak current than solution containing dsDNA which gives lower peak; (e) two types of electrodes used; (i) SPE chip made from carbon ink and (ii) thin film microelectrode (ME) made of platinum or gold.

Although electrostatic interaction achieved via the use of RuHex was applied in this study, but the innovativeness was profoundly focused on PCR amplicons, carbon screen-printed electrodes (SPE chip) and thin-film microelectrodes (ME) as the mediator. A novel pork-specific primer set was employed in PCR to amplify a specific region of pork mitochondrial DNA.

This modern electrochemical sensor equipped with different substrate materials was utilized in this analytical study as a detection device. The major aims of this study are namely: a) to develop new PCR primers for pork DNA amplification, b) to detect pork DNA in food samples using two types of reusable electrochemical sensors, the thin film microelectrodes and screen printed chip and c) to make comparison on efficiency, rapidity, sensitivity and cost for the two types of electrochemical sensors employed.

2. Experimental approach

Meat samples

23 food products, including raw meat, processed meat and canned food of different brands and origins were collected from various local supermarkets. These include raw meats of six species that are commonly consumed by the locals, namely pork (*Sus scrofa*), goat (*Capra hircus*), chicken (*Gallus gallus*), ostrich (*Struthio camelus*), beef (*Bos indicus*) and duck (*Anas platyrhynchos*). Out of the 23 samples, 8 samples analysed were pork samples, 6 were beef samples including beef gelatin from marshmallows, 4 chicken samples, 3 goat samples, 1 ostrich and 1 duck sample (***Table 1***).

DNA extraction and quantification

DNA was extracted from meat samples using Biokits DNA extraction kit (Neogen Corporation, Lansing, Michigan, USA). The kit isolation method was based on the use of magnetic beads. The extracted DNA was quantified using Nanophotometer P-Class (Implen, München, Germany). Five measurements were taken to obtain the average DNA concentration to be used as final DNA concentration. Subsequent to quantification, PCR amplification was carried out.

Primer selection and PCR amplification

Primers were designed in our laboratory and synthesized by Integrated DNA Technologies (Coralville, Iowa, USA). The forward primer (5'-CAC ATC AGA CACA AAC AAC -3') and the reverse primer (5'- CCT ACG TGG ATG AAT AGG -3') generated amplicon of 132 base-pair (bp) in length at annealing temperature of 56^{o}C.

PCR amplification was executed in a 25 µL volume reaction mixture, which contained autoclaved water, 10× PCR buffer II, 25 mM $MgCl_2$, 10 mM dNTP mix, 20 µM forward and reverse primer, 0.625 U AmpliTaq DNA Polymerase (Thermo Fisher Scientific, USA) and 10 ng of template DNA. PCR was then run using a Veriti® thermal cycler (Applied Biosystems, Thermo Fisher Scientific, USA). The PCR cycling conditions used include an initial denaturation at

Table 1. Samples of different species from different brand and origin for the development of pork-specific PCR

No	Name	Brand	Origin
1	Negative control	-	-
2	Wild boar	-	-
3	Spiced pork cubes	Narcissus	China
4	Pork mince with beans paste	Narcissus	China
5	Chopped pork and ham	Greatwall	China
6	Pork and bamboo shoot	Gulong	China
7	Pork meat	-	Brunei
8	Sliced ham	Pinoy Fiesta	Philippines
9	Pork short sausages	-	Unknown
10	Corned beef	Banquet	Brazil
11	Beef loaf	CDO	Philippines
12	Curry beef	Amocan	Singapore
13	Canned beef luncheon meat	Mei Ning	China
14	Mallow bakes (beef gelatin)	Betta	Australia
15	Marshmallow (beef gelatin)	Haribo	Turkey
16	Chicken luncheon meat	Mei Ning	China
17	Chicken luncheon meat	Tulip	Denmark
18	Chicken luncheon meat	Hana	United Arab Emirates
19	Chicken luncheon meat	Golden Bridge	Singapore
20	Duck meat	Perak Duck Food	Malaysia
21	Mutton luncheon with chicken	El-Dina	Singapore
22	Corned mutton	Carters	Australia
23	Lamb curry with potatoes	Adabi	Malaysia
24	Corned ostrich	Mulaut Abbatoir	Brunei

95ºC for 2 min, followed by 35 cycles of three steps of denaturation at 95ºC for 20 s, primer annealing at 56ºC for 30 s and extension at 72ºC for 1 min. The final extension was performed at 72ºC for 5 min. The PCR products were held at 4ºC until further analysis. For initial confirmation, PCR amplicons were ran on 1.0% agarose gel submerged in a 10x Tris-Borate EDTA (TBE) electrolyte buffer for 75 minutes at 80 V, 400 mA using Bio-Rad Sub-Cell FT (Bio-Rad Laboratories, USA). The agarose gel was visualized under UV illuminator (UVP, USA). The length of the amplicons was measured against a 50 bp ladder (New England BioLabs Inc., Ipswich, USA).

Specificity, sensitivity and real samples analysis

Specificity was analyzed with 7 genomic DNA of non-specific species, namely sheep (*Ovis aries*), goat (*Capra hircus*), buffalo (*Bubalus bubalis*), horse (*Equus caballus*), duck (*Anas platyrhynchos*), ostrich (*Struthio camelus*) and turkey (*Meleagris*). Wild boar (*Sus scrofa*) was used as positive control for every PCR reaction. These non-specific species and all the 23 samples were further diluted to 10 ng prior to PCR amplification. For sensitivity, 10-fold serial dilutions of wild boar DNA were prepared, ranged from 10 ng to 10^{-5} ng.

RuHex preparation

1 mM of RuHex stock solution was prepared from 2.7315 mg of RuHex dissolved in 10 mL of water in a 15 mL polypropylene tube. The tube was wrapped up with aluminium foil to prevent RuHex from light exposure as ruthenium complexes are found to have resemblance as chlorophyll which is capable of absorbing light.[12] This stock solution was stored at 4ºC until usage.

Electrochemical sensors

Two kinds of electrodes were used in this detection method; Screen-Printed Electrodes chip (SPE chip) and thin-film microelectrodes (ME). SPE chip made from carbon ink with a working

electrode (WE) area of 2.64 mm^2 was obtained from Biodevice Technology, Co. (Ishikawa, Japan). This SPE chip has an external dimension of 12.5 mm by 4 mm, with cell diameter of 2 mm. The chip requires sample volume of 10 - 30 μL. Two MEs were attempted in this study, having noble metal substrate materials such as platinum and gold based.

These microelectrodes were obtained from MicruX Technologies (Asturias, Spain), with area of WE of 0.79 mm^2, external dimension of 10 mm by 6 mm and cell diameter of 1 mm. These microelectrodes only require sample volume of 1 - 10 μL. Prior to electrochemical analysis, the electrochemical sensors were cleaned for each reaction to avoid background interferences. Sulfuric acid (H_2SO_4) was used to clean the platinum and gold microelectrode, whereas phosphate-buffered saline (PBS) buffer was used as cleaning solvent for SPE chip. For PCR amplicons detection, all the electrodes were optimized based on their measuring condition for SWV, pH of Tris-EDTA buffer (TE buffer) and final concentration of RuHex. Salmon DNA was used for optimization purposes prior to amplicons analysis.

Measuring condition for Square Wave Voltammetry (SWV)

The measuring technique opted was square wave voltammetry (SWV). In this electrochemical analysis, potentiostat (Autolab system PGSTAT 101, Metrohm, Netherlands) was connected to a computer. The program used to process the data was NOVA 1.10. Three readings were taken and the average of the peak current (A) was calculated and regarded as the final peak current expressed in μA. The measurement condition for SWV varies for each electrode after optimization. The measurement condition for SPE chip were frequency = 25 Hz; amplitude = 0.0495 V; scan rate = 0.04875 Vs^{-1}; step potential = 0.00195 V. The potential range was slightly shifted from -0.5 to -0.1 V to -0.7 to -0.2 V, whereas the rest of the variables were maintained. The shift was made due to the availability of peak response. This measurement was also used in platinum ME but only differ by their potential range (-0.5 to 0.5 V). For gold ME, the measuring condition was personally optimized based on peak response obtained. The measurement condition for gold ME were frequency = 24 Hz; amplitude = 0.2 V; scan rate = 0.5 Vs^{-1}; step potential = 0.02 V with a potential range of -1 to 0 V.

The detection of PCR amplicons on the electrode was carried out in amplicon-buffer-RuHex mixture with composition ratio of 2:1:1 respectively. The mixture was spiked onto the electrode surface of SPE chip, platinum and gold ME, covering the area of working electrode. These electrodes were inserted into their respective connectors which were connected to the potentiostat and detector computer. The instrument setup for platinum and gold ME used drop-cell connector (MicruX Technologies, Asturias, Spain).

3. Results and Discussion

PCR-based method and pig-specific primers

The newly designed pork-specific primers targeted the mitochondrial pork DNA sequences and yielded amplicons of 132 bp in length. The amplification can also be achieved using several other PCR-based methods such as real time PCR and probes such as TaqMan or SyBr-Green. [13-15] However, real time PCR instrumentation is known to be not economical when compared to conventional PCR.[16] Our approach in this study using PCR-based method is not only cost-effective but also highly specific with the use of novel primers.

Following the optimization, cross-reactivity with non-specific species was performed with seven non-specific species. The primers did not cross-react with any of the mentioned non-specific species and only amplified the DNA sequence from wild boar. After the cross-reactivity analysis, sensitivity analysis was tested with sample concentration of 10 ng - 10 pg. The designated primers set has successfully amplified detectable wild boar DNA of as low as 5 ng and hence 5 ng was determined as the limit of detection (LOD) for this approach.

pH working condition of TE buffer

The optimum pH determined by this study was pH 9.23 for the two electrodes used (platinum ME and carbon SPE chip). At a higher pH range, destabilization of DNA may have occurred. The bonds that hold the two strands of DNA bound together might have instantly ruptured at high pH, causing the double stranded DNA to be unwound and denatured into a single stranded.[17] In addition, nitrogenous bases of DNA molecules; guanine's N (1) and thymine's N (3), could become deprotonated in basic condition and as a result the charge of the whole DNA could become negative.[18] An electrostatic interaction became possible when negatively charged DNA interacted with positively charged RuHex. The interaction of RuHex is commonly reported with double stranded DNA. The ratio of RuHex to DNA in this case was 1:1. As discussed, it is essential to keep the pH of the TE buffer used to store amplicons or DNA constant throughout the analysis. Depurination of DNA tends to occur at acidic and neutral pH leading to lose of purine bases and eventually breaking the DNA chain.[19-20] The chain breaking induces the free distribution of RuHex in solution thus giving contradicting results when detected using SWV. Therefore the detection mode was not executed at a lower pH range.

Optimized RuHex concentration for DNA sensor

When fixed measuring conditions for SWV were applied (scanning range= -0.7 to -0.2 V; step potential=0.00195 V; amplitude=0.04950 V; frequency=25 Hz; scan rate=0.04875 Vs^{-1}) at pH 9.23, the final concentration of RuHex was determined to be 10 μM according to the best signal-to-noise ratio (S/N ratio) when compared with lower RuHex concentration of 5 and 1 μM. S/N ratio was calculated based on the differences of peak current height between the blank and the amplicon. The S/N ratio obtained for 10, 5 and 1 μM RuHex was 2.369, 1.749 and 1.724 respectively.

Carbon SPE chip as the preeminent electrochemical sensor

An extensively used electrode substrate of carbon can be fabricated into many forms due to its soft properties, such as carbon SPE chip (made from carbon paste) glassy carbon electrode (GCE), graphene biochip etc. This carbon material was found to be chemically inert, showing a rich surface chemistry and can generate low background current.[21] These superior features offer a great support in yielding a more reliable and reproducible outcome. In addition, carbon SPE chip is more economical than ME due to fabrication cost. When these noble metals ME were experimentally compared to carbon SPE chip, the carbon SPE chip managed to scan at a more negative potential. Therefore as predicted, the response peak was observed at a more negative potential range. Ultimately, carbon SPE chip was opted as the preeminent electrochemical sensor due to its low-cost and tendency to give a promising conclusion.

During optimization, many problems were encountered when using the metal based microelectrodes. Both of the electrodes, platinum and gold ME, gave contradictory readings at some point and failed to present reproducible outcome. The quality of these particular electrodes was highly doubted and incapable to meet the expectation of the study. The discrepancy may arise from irreversible adsorption of significant amounts of DNA onto a scratched thin metal film surface.[22] This adsorption may generate inconsistent results. Therefore, platinum and gold ME were exempted in this study for further analysis.

Comparisons were established between platinum ME and carbon SPE chip by retaining SWV parameters, using final RuHex concentration of 10 μM and pH of TE buffer of 9.23. It turned out that the SPE chip gave a higher R^2 value of 0.9794 (***Figure 2a***) than R^2 value of Platinum ME 0.7961 (***Figure 2b***). After careful consideration based on the overall quality of performance from the aspect of its reproducibility and sensitivity, SPE chip was chosen as the final electrochemical detection tool for this study.

Cross-reactivity, sensitivity and real samples electrochemical analysis

Carbon SPE chip was used throughout the analysis. After optimization, cross-reactivity analysis, sensitivity analysis and analysis with real

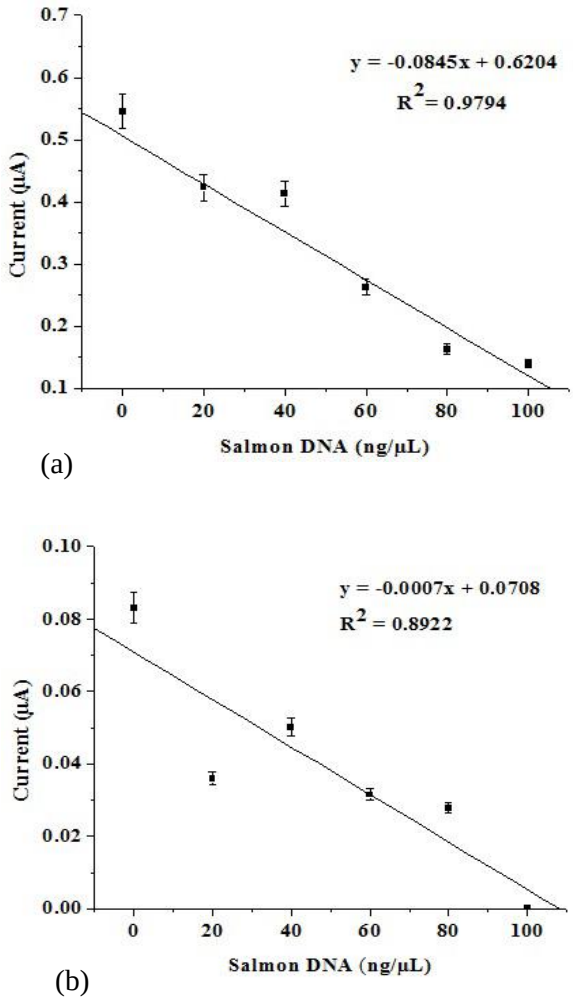

Figure 2. Electrochemical detection of 0, 20, 40, 60, 80 and 100 ng/µL of Salmon DNA using (a) carbon SPE chip and (b) platinum ME at 10 µM RuHex and pH 9.23. Measuring condition for SWV; scanning range=-0.7 to -0.2 V; step potential=0.00195 V; amplitude= 0.04950 V; frequency= 25 Hz; scan rate= 0.04875 Vs^{-1}

samples were conducted using electrochemical detection approach. For blank which comprised of RuHex and TE buffer, the peak current height was expected to be the highest. Positive control and samples that contain pork DNA significantly reduced the current flow and therefore expected to be yielding lower peak current height. Negative control and samples without pork DNA were expected to give higher peak than the one contained pork DNA but slightly lower than blank. The reason for such observation was because even amplicons of the negative control contains primers which consist of DNA fragments. Even without the presence of pork DNA, the primers can also develop electrostatic interaction with RuHex hence insignificantly reduced the current.

In cross reactivity analysis, specific species wild boar gave the lowest peak whereas non-specific species gave higher peaks (***Figure 3a***). For sensitivity analysis, 10 ng/µL of wild boar DNA gave the lowest peak than 5 ng/µL of wild boar (***Figure 3b***).

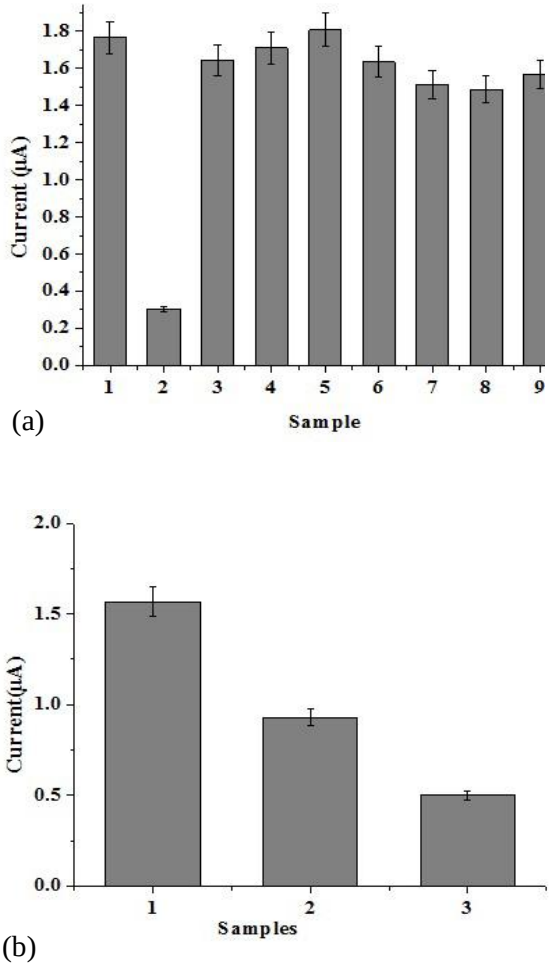

Figure 3. SWV behaviour of 10 µM RuHex with carbon SPE chip using pork primers for (a) specificity. Sample 1: Negative control, 2: Wild boar, 3: Duck, 4: Ostrich, 5: Turkey, 6: Buffalo, 7: Goat, 8: Horse and 9: Sheep; (b) sensitivity. Sample 1: Negative control, 2: 5 ng/µL wild boar and 3: 10 ng/µL wild boar.

For that reason, concentration of DNA and current response can be correlated. The linearity followed

increasing DNA concentration with decreasing peak current and vice versa. For sample analysis, the presence of pork DNA was indicated by lowest peak, whereas the absent of pork DNA gave higher peak. The extracted values from current response of 23 food samples in SWV were translated and illustrated in ***Figure 4***.

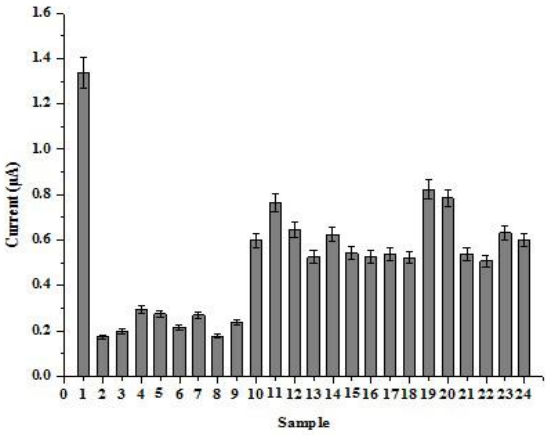

Figure 4. SWV behaviour of 10 µM RuHex with carbon SPE chip for all 23 real sample analysis (concentration of 10 ng/µL) using pork primers as mentioned in table 1. Sample 1: Negative control, 2-9: pork; 10-15: beef; 16-19: chicken; 20: duck; 21-23: goat and 24: ostrich.

Diffusion coefficient of Ruthenium Hexaamine

The current signal was proportional to the diffusion rate of molecules. The diffusion rate or diffusion coefficient can be determined using the Randles-Sevcik equation by entering the extracted data of current peak into the equation $i_p = 2.69 \times 10^5\ n^{3/2}\ A\ D^{1/2}\ v^{1/2}\ C$, where i_p = peak current in ampere A, n = no of electrons, A = electrode area in cm^2, D = diffusion coefficient in $cm^2\ s^{-1}$, v = scan rate in Vs^{-1}, C = concentration in mol cm^{-3}.

To verify that the diffusion activity of RuHex was hindered by the presence of DNA, diffusion coefficient using Randles-Sevcik equation was calculated for blank and positive control of PCR amplicons. Based on the calculation, the diffusion coefficient for blank (only RuHex) was determined to be 0.03762 cm^2s^{-1}. The diffusion coefficient of positive control (RuHex and DNA) was determined to be 0.001835 cm^2s^{-1}. In the solution where DNA was absent, RuHex in the solution rapidly diffuse onto the electrode surface. Being an electrochemically active species, such high diffusion activity increased the tendency to yield an intense current peak. However, when DNA is present, the electrostatic interaction took place between RuHex and DNA which showed slow diffusion of RuHex in the solution.[10] Slow diffusion reduced the current peak and hence reduced the current peak intensity as predicted. As a result, the expected diffusion coefficient of RuHex has been confirmed the presence and absence of DNA in the solution.

4. Conclusion

In conclusion, a PCR-based method to detect pork in food samples was successfully developed using rapid and reusable electrochemical sensor. With the newly designed primers, the primers were able to amplify as low as 5 ng/µL of pork DNA. It was highly recommended to use carbon SPE chip as a detection tool to detect the presence of specific species DNA. The reason for such recommendation was that, the outcome reported was highly reproducible when compared to metal film microelectrodes due to the existing broad characteristics of carbon materials. Moreover, the detection method was found to be rapid, sensitive and cost effective as it can be reused after several rounds of testing. As discussed above, since PCR amplicons were generally used in this study to detect via electrochemical detection, a further improvement using novel and high throughput reusable integrated microfluidic device is imminent for on-site food analysis. Our group is currently working on the development of field deployable and cost-effective system for point-of-care analysis.

Acknowledgements

Hafizah Munirah wishes to acknowledge the Ministry of Education, Negara Brunei Darussalam. Sharmili Roy wishes to acknowledge the UBD Graduate Research Scholarship (GRS) for her Ph.D. fellowship.

References

[1] M. Riaz and M. Chaudry, *Halal Food Production*, **2004,** 2.

[2] A. Aida, Y. B. C. Man, C. Wong, A. Raha and R. Son, *Meat Sci.*, **2005.** 47.

[3] N. Fadzlillah, Y. B. C. Man, M. Jamaludin, S. A. Rahman and H. Al-Kahtani *Proceedings of the 2nd International Conference on Humanities, Historical and Social Sciences*, **2011**.162.

[4] M. Ahmed, K. Idegami, M. Chikae, K. Kerman, P. Chaumpluk, S. Yamamura and E. Tamiya, *Analyst*, **2007**, 431.

[5] M. Ahmed, M. Saito, M. M. Hossain, S. R. Rao, S. Furui, A. Hino, Y. Takamura, M. Takagi and E. Tamiya, *Analyst*, **2009**, 966.

[6] M. Ahmed, Q. Hasan, M. M. Hossain, M. Saito and E. Tamiya, *Food Control*, **2010**, 599.

[7] P. Barril and S. Nates, In Magdeldin, S *Rijeka: InTech*, **2012, 4.**

[8] M. Ahmed, M. M, Hossain, M. Safavieh, Y. L. Wong, I. A. Rahman, M. Zourob and E. Tamiya, *Critical Rev. Biotechnol.*, **2015**, 495.

[9] P. Ho, C. Frederick,, D. Saal,, A. Wang and A. Rich, *J. Biomol. Structure Dynamics*, **1987**, 521.

[10] M. Ahmed, S. Nahar, M. Safavieh and M. Zourob, *Analyst*, **2013**, 907.

[11] S. Roy, I. Rahman, J. Santos and M. Ahmed, *Food Control*, **2015**, 70.

[12] R. Lewin. *New Scientist*, **1976**, 651.

[13] J. J. Dooley, K. E. Pain, S. D. Garrett and H. M. Brown, *Meat Sci.*, **2004**, 431.

[14] Z. Kesmen, A. Gulluce, F. Sahin and H. Yetim, *Meat Sci.*, **2009**, 444.

[15] I. Martin, T. Garcia, V. Fajardo, M. Rojas, N. Pegels, P. E. Hernandez, I. González and R. Martín, *Meat Sci.*, **2009**, 252.

[16] N. Karabasanavar, S. Singh, D. Kumar and S. Shebannavar, *Food Chem.*, **2014**, 530.

[17] M. Ageno, E. Dore and C. Frontali, *Biophys. J.*, **1969**, 1281.

[18] J. Stenesh, *Nucleic acids. Biochemistry*, USA: Springer US, **2013**, 190.

[19] C. Tamm, M. Hodes and E. Chargaff, *J. Biol. Chem.*, **1952**, 49.

[20] S. Greer and S. Zamenhof, *J. Mol. Biol.*, **1962**, 123.

[21] G. Li and P. Miao, *Theoretical background of electrochemical analysis*, Berlin: Springer, **2012**. 5.

[22] T. Schalkhammer, *Analy. Biotechnol.*, **012**.191.

Parkia speciosa (Petai) pod as a potential low-cost adsorbent for the removal of toxic crystal violet dye

Linda B. L. Lim[1], Namal Priyantha[2,3], Hui Hsin Cheng[1] and Nur Afiqah Hazirah Mohamad Zaidi[1]*

[1]Department of Chemical Sciences, Faculty of Science, Universiti Brunei Darussalam, Jalan Tungku Link, Gadong, BE1410, Brunei Darussalam
[2]Department of Chemistry, University of Peradeniya, Peradeniya, Sri Lanka
[3]Postgraduate Institute of Science, University of Peradeniya, Peradeniya, Sri Lanka

**corresponding author email: linda.lim@ubd.edu.bn*

Abstract

This study focused on the use of *Parkia speciosa* (Petai) pod as a potential adsorbent for the removal of crystal violet (CV) dye. Batch adsorption isotherm experiments carried out under optimized conditions were fitted to six isotherm models, namely Langmuir, Freundlich, Temkin, Dubinin-Radushkevich, Redlich-Peterson and Sips. Of these, the Sips model best described the adsorption isotherm of Petai pod for the removal of CV dye, giving a desirable maximum adsorption capacity (q_{max}) of 163.2 mg g^{-1}. Adsorption kinetics was found to follow the pseudo-second order, and further, intra-particle diffusion played a significant role. This study also revealed that the adsorption of CV by Petai pod is influenced by the ionic strength of the medium. However, Petai pod showed resilience towards changes in medium pH.

Index Terms: Parkia speciosa, adsorbent, adsorption isotherm, crystal violet dye

1. Introduction

The past few decades have seen a rise in industries to cater to the rapidly increasing world population. As a result, the amounts of industrial wastes being discharged into water systems have resulted in detrimental problems to both the ecosystem and human health. Hence, there is an urgent need to remove these pollutants and to provide clean water. Various methods have been devised over the years, of which adsorption has gained popularity as it utilizes low-cost materials and unused wastes, which would otherwise be disposed of, to remove toxic environmental pollutants.[1-4]

Of the pollutants being discharged into water systems, dyes cause not only health problems, but also destroy aesthetic nature of water. A common dye widely used in textile, paint and printing industries is crystal violet (CV), or methyl violet 10B, which belongs to the triarylmethane class of dyes. Being non-biodegradable and poorly metabolized by microbes, CV would be persistent in a variety of environments. If present in the human cells, this dye is highly cytotoxic and carcinogenic. CV has been reported to cause skin and digestive tract irritation, and may also cause respiratory and kidney failure.[5]

This study focuses on the use of the pod of a popular local vegetable, *Parkia speciosa*, locally known as Petai, for the removal of CV dye. In South East Asia, this vegetable is usually cooked with spicy prawn paste or "sambal" as a vegetable dish. The pods, being inedible, are discarded as waste. To date, there have been limited reports on the use of Petai as adsorbents for the removal of pollutants. Seeds of Petai were successfully used for the removal of methylene blue dye,[6] while Petai pods have been used to remove Coomassie Brilliant Blue R-250 dye.[7]

2. Experimental approach

Sample preparation

Petai pods were separated from the edible seeds and dried in an oven at 80 ^{o}C until a constant mass

was obtained. The dried sample was then blended and sieved using stainless steel brass laboratory test sieves to obtain the desired particle size of 355-850 µm which was used throughout this study.

Instrumentation

Thermo Scientific, MaxQ 3000 orbital shaker, set at 250 rpm, was used to agitate the mixture of solution, unless otherwise stated. pH was measured using EDT Instruments, GP 353 pH meter. Concentration of CV dye solutions was determined using Shimadzu, UV-1601PC spectrophotomer set at the wavelength of 590 nm. Shimadzu, IRPrestige-21 spectrophotometer was used for functional group characterization. Surface morphology of adsorbent's surface was analysed using Tescan Vega XMU scanning electron microscope (SEM) and the adsorbent was sputter coated with gold using SPIMODULETM Sputter Coater for 60s.

Optimization of parameters

The effects of contact time, medium pH and ionic strength were investigated following the methods as described by Cheing *et al.*[8] with slight modifications. Briefly, 100 mg L^{-1} CV was used and the adsorbent:adsorbate ratio was kept at 1:500 (wt:vol). For medium pH, the range used was from pH 3 to 10. Ionic strength effect was studied using KNO_3 with concentration ranging from 0.01 M to 1.0 M.

Adsorption studies

Adsorption isotherm and kinetics studies were carried out using similar methods as reported by Dahri *et al.*[9] with slight modifications. Briefly, batch adsorption isotherms were performed with dye concentration in the range of 0 – 1000 mg L^{-1} under optimized contact time. Kinetics of the adsorption of CV dye onto Petai pod was investigated using 500 mg L^{-1} CV dye.

Regeneration studies of spent adsorbent

Regeneration studies were carried out based on the method reported by Lim *et al.*[10] with some modifications. The Petai pod was first treated with 100 mg L^{-1} CV dye. Four desorption methods were used on the spent Petai pods *i.e.*, treatment with 1 M HCl, 1 M NaOH, distilled water and heat (200 ^{o}C).

3. Results and Discussion

Effect of contact time

Establishing the contact time required for the adsorbate-adsorbent system to reach equilibrium is an important parameter in adsorption studies. As shown in ***Figure 1***, rapid uptake of CV dye was observed within the first 30 minutes, which then became unchanged during the period of investigation up to 4.0 h. Such observation can be attributed to the immediate occupation of the limited number of available adsorption sites of the adsorbent. In this study, a contact time of 2.5 h was used for all subsequent experiments.

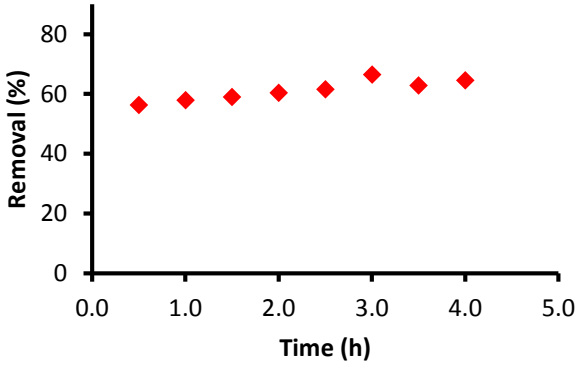

Figure 1. Effect of shaking time for the removal of crystal violet dye using Petai pod

Effect of pH

Another important parameter in adsorption studies is the medium pH. Any change in pH would cause surface characteristics of the adsorbent to alter, thereby affecting its ability to adsorb adsorbates. From ***Figure 2***, it is observed that the ability of Petai pod to attract CV is very resilient to the change in pH, maintaining its constant ability to adsorb CV over a pH range from 3 to 10. This demonstrates the superior adsorption ability of the adsorbent under investigation in contrast to many adsorbents which show pH-dependent dye removal abilities. For example, breadfruit skin[11] reported 60% reduction in removal of CV at pH 2 while adsorbents such as water lettuce,[12] breadnut core[10] and dragon fruit skin[13] displayed drastic reduction with cationic dyes at low pH. In this study, no adjustment of pH was necessary since

the untreated (ambient) pH of dye solution (pH = 5.2) gave a reasonably high extent of removal of CV.

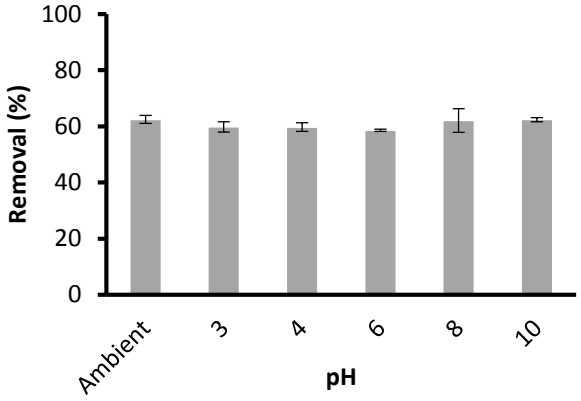

Figure 2. Effect of medium pH on the removal of crystal violet dye by Petai pod

Effect of ionic strength on adsorption of CV

The maximum reduction of approximately 50% in the removal of CV was observed in 0.4 M KNO_3 (***Figure 3***). Clearly, Petai pod's ability to adsorb CV is influenced by the concentration of salt solution. The reduction in dye removal could be due to competition between K^+ with the cationic CV dye for the limited active sites on the adsorbent's surface. Beyond 0.4 M, no further reduction of dye removal was observed which suggests that the inner Helmholtz plane of adsorbent particles gets saturated with 0.4 M KNO_3.

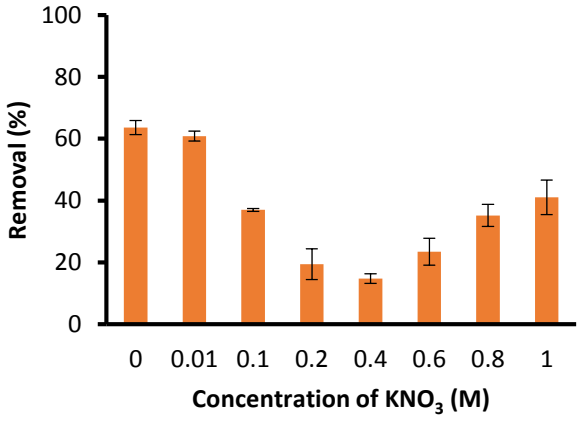

Figure 3. Effect of ionic strength on the removal of crystal violet dye by Petai pod

Adsorption isotherm for the removal of CV by Petai Pod

Adsorption isotherm studies (***Figure 4***) on the removal of CV by Petai pod, carried out over 0 to 1000 mg L^{-1} dye concentration range, indicate the gradual buildup of the adsorbate layer until the initial dye concentration of 400 mg L^{-1} at which the monolayer coverage is complete. Based on the solution analysis, the number of adsorbate dye molecules, more than what is required for monolayer coverage, has been transferred to the adsorbent phase after the initial concentration of 800 mg L^{-1}. This is attributed to the transfer of CV molecules that had been initially present in the monolayer to the interior of the adsorbent phase, probably through inter-particle and intra-particle diffusion with the concomitant transfer from the solution phase to the adsorbent surface. This process would lose adsorbate molecules from the solution phase demonstrating the behavior observed in ***Figure 4***.

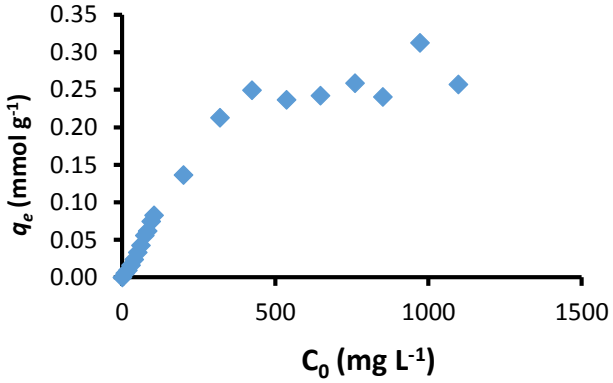

Figure 4. Adsorption isotherm for the removal of crystal violet dye using Petai pod

In an attempt to further understand the adsorption behavior, the data on the extent of adsorption of CV and equilibrium concentrations were fitted to six different isotherm models, namely, Langmuir,[14] Freundlich,[15] Temkin,[16] Dubinin-Radushkevich (D-R),[17] Redlich-Peterson (R-P)[18] and Sips,[19] and analyzed using four different error functions. The isotherm equations and error functions are presented in ***Table 1*** and ***Table 2***, respectively.

Table 1. Linearized equations of the six isotherm models used

Isotherm model	**Linear**
Langmuir	$\frac{C_e}{q_e} = \frac{1}{k_L q_{max}} + \frac{C_e}{q_{max}}$
Freundlich	$lnq_e = \frac{1}{n} ln\, C_e + ln\, k_F$
Temkin	$q_e = B\ lnk_T + B\ lnC_e$
D-R	$lnq_e = lnq_s - \beta\varepsilon^2$
R-P	$ln\left(k_R \frac{C_e}{q_e} - 1\right) = g\ lnC_e + ln\, a_R$ *where* $0 \leq g \leq 1$
Sips	$ln\left(\frac{q_e}{q_{max} - q_e}\right) = {}^1/_n\, ln\, C_e + ln\, k_s$

where k_L, k_F, k_T, k_R and k_S are the adsorption isotherm constants for the Langmuir, Freundlich, Temkin, Redlich-Peterson and Sips models, respectively. C_e is the equilibrium dye concentration, q_e is the amount of dye adsorbed and q_{max} is the maximum adsorption capacity. *n* in the Freundlich equation represents the empirical parameter which is related to the strength of the adsorption process and if it falls within 1 to 10, this indicates the adsorption process is favourable. Constant *B* is related to the heat of adsorption, R is the gas constant (8.314 J K^{-1} mol^{-1}), T is absolute temperature in Kelvin, β gives the mean free energy of sorption per molecule of sorbate. a_R is the Redlich-Peterson constant and g is the exponent which lies between 0 and 1. The 1/n is the Sips model exponent.

Table 2. Four error functions used

Type of errors	**Equations**
Average relative error (ARE)	$\frac{100}{n}\sum_{i=1}^{n}\left\lvert\frac{q_{e,meas} - q_{e,calc}}{q_{e,meas}}\right\rvert_i$
Sum square error (SSE)	$\sum_{i=1}^{n}(q_{e,calc} - q_{e,meas})_i^2$
Hybrid fractional error function (HYBRID)	$\frac{100}{n-p}\sum_{i=1}^{n}\left[\frac{(q_{e,meas} - q_{e,calc})^2}{q_{e,meas}}\right]_i$
Marquardt's percent standard deviation (MPSD)	$\sqrt{\frac{1}{n-p}\sum_{i=1}^{n}\left(\frac{q_{e,meas} - q_{e,calc}}{q_{e,meas}}\right)_i^2}^{100}$

Based on R^2 values, error analyses (***Table 3***) and simulation of data with the above six isotherm models (Figure not shown for brevity), it was concluded that even though the Temkin model gave the highest R^2 value, its large errors clearly indicate that this model does not fit with the experimental data. The D-R and R-P models were also ruled out due to similar arguments. The Langmuir and Freundlich models gave lower R^2 values and slightly higher errors. The Sips isotherm model, a three-parameter isotherm model that combines both the Langmuir and Freundlich models, which gave a high R^2 value with the lowest errors, is thus selected as the most suited model to explain the adsorption of CV on Petai pod.

Table 3. R^2 and their error values of Adsorption isotherm models

Model	R^2	**ARE**	**SSE**	**HYBRID**	**MPSD**
Langmuir	0.901	26.74	0.02	0.60	37.80
Freundlich	0.865	40.76	0.09	2.36	53.49
Temkin	0.951	66.72	0.01	2.63	202.30
D-R	0.850	400.04	0.24	64.68	790.05
R-P	0.506	40.76	0.09	2.51	55.13
Sips	0.928	26.82	0.02	0.69	37.64

Table 4 shows all the parameters obtained for the six isotherm models used in this study. The maximum adsorption capacity (q_{max}) of CV determined from the Sips adsorption isotherm is 163.2 mg g^{-1}, which is superior to many natural adsorbents, as shown in ***Table 5***. As this is relatively higher, surface modification methods were not attempted.

Table 4. Adsorption isotherm parameters

Model	Parameters	Values
Langmuir	q_{max} (mg g^{-1})	141.3
	K_L (L $mmol^{-1}$)	0.01
Freundlich	K_F (mg g^{-1})	1.42
	n	1.39
Temkin	K_T (L $mmol^{-1}$)	0.10
	b_T (kJ mol^{-1})	38249
D-R	q_{max} (mg g^{-1})	79.17
	B (J mol^{-1})	2.27E-06
	E (kJ mol^{-1})	469.7
R-P	K_R (L g^{-1})	3.00
	α	0.28
	a_R (L $mmol^{-1}$)	864.3
Sips	q_{max} (mg g^{-1})	163.2
	K_S (L $mmol^{-1}$)	0.00
	n	1.01

Table 5. Comparison of maximum adsorption capacity of various adsorbents for the removal of crystal violet dye

Adsorbent	q_{max} (mg g^{-1})	Reference
Parkia speciosa	163	This work
Breadfruit skin	150	[11]
Peat from Brunei	108	[5]
Yeast-treated peat	18	[20]
Tarap skin (TS)	118	[21]
NaOH-treated TS	195	[21]
Pumice stone	7	[22]
Biomass combustion residue	19	[23]

Adsorption Kinetics of Petai Pod on the removal of CV dye

Adsorption mechanism for the removal of 500 mg L^{-1} CV by Petai pod was investigated, and the data obtained were fitted to the Lagergren pseudo-first order (***Equation 1***) and pseudo-second order (***Equation 2***) models.[24,25]

Linearized equation of Lagergren pseudo-first order:

$$log(q_e - q_t) = log(q_e) - \frac{k_1}{2.303}t \quad (1)$$

Linearized equation of Pseudo-second model:

$$\frac{t}{q_t} = \frac{q}{k_2 q_e^2} + \frac{1}{q_e}t \quad (2)$$

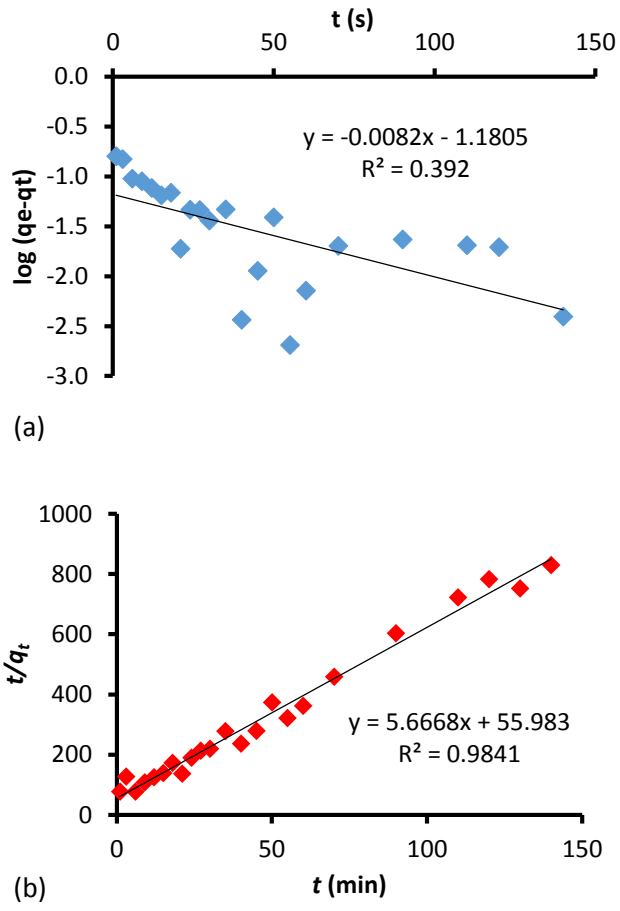

Figure 5. Adsorption kinetics of Petai pod for the removal of crystal violet dye showing pseudo-first order (a) and pseudo-second order (b).

From ***Figure 5***, it is clearly observed that the kinetics follows the pseudo-second order mechanism with high R^2 close to unity. Further, the adsorption capacity determined from experiment (0.24 mmol g^{-1}) and that determined by the pseudo-second order model (0.18 mmol g^{-1}) are comparable. On the other hand, the pseudo-first order model led to the R^2 value of 0.392 with the adsorption capacity of 0.07 mmol g^{-1}, which is much deviated from the value obtained from the isotherm studies. The validity of the pseudo-second order model provides the condition that the possibility of having two reactive moeties for adsorption of CV molecules.

To investigate diffusion mechanisms in the adsorption of CV by Petai Pod, the Weber-Morris intra-particle diffusion (***Equation 3***) and Boyd (***Equation 4***) models were applied.[26,27]

Weber Morris intraparticle diffusion:

$$q_t = k_{id} t^{1/2} + C \qquad (3)$$

Boyd model:

$$F = 1 - \frac{6}{\pi^2} exp(-B_t) \qquad (4)$$

where F = q_t / q_e, F is the fraction of solute adsorbed at any time, t and B_t is mathematical function of F.

The Weber-Morris plot shown in ***Figure 6*** indicates two regions. The initial region involves gradual surface adsorption of CV due to intra-particle diffusion, followed by a slow equilibrium region reaching a plateau. According to the Weber Morris model, intra-particle diffusion is the rate-determining step, if the linear segment passes through the origin. The very small intercept of 0.007 in the plot given in ***Figure 6*** is in support that the intra-particle diffusion providing a significant contribution to mass transfer. The rate constant determined from this model, k_{id} is 0.027 mmol g^{-1} min^{-1}.

In order to determine whether film or particle diffusion also contributes to the adsorption process, the Boyd model was applied. According to the model, if the linear plot passes through the origin, the diffusion is governed by particle diffusion, or otherwise, film diffusion takes control. From ***Figure 6***, the linear plot shows a very small intercept of 0.082, suggesting that particle diffusion is the rate-determining step.

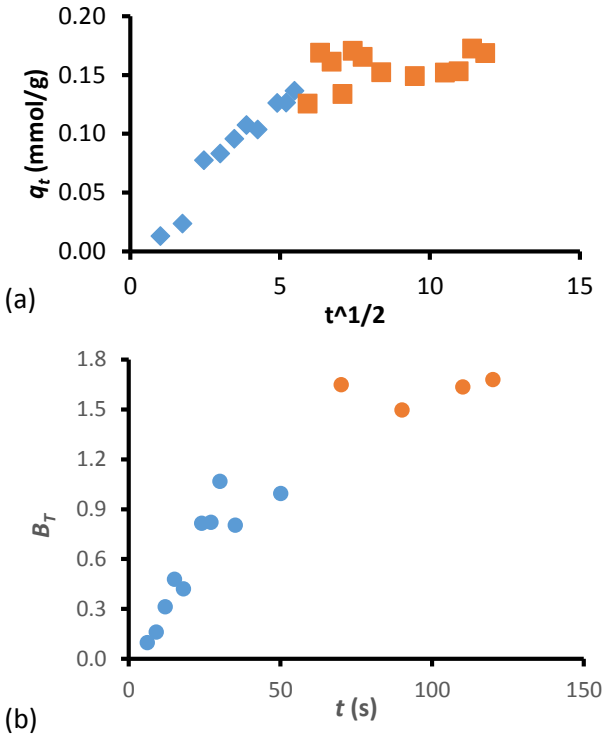

Figure 6. Weber Morris Intraparticle diffusion (top) and Boyd model (bottom) of Petai pod for the removal of crystal violet dye.

Regeneration of spent Petai Pod

Spent adsorbents which are of no use need to be disposed of as wastes. These can pose problems as they can be toxic, inflammable, hazardous and even explosive if incinerated. Therefore, to minimize problem, one way is to regenerate and reuse spent adsorbents. In this study, spent Petai pod was regenerated using various methods. Of these, it was found that NaOH treatment was not only able to retain its adsorption capacity but enhanced the adsorption of CV by 35% even after the 4th cycle (***Figure 7***). On the other hand, treatment with HCl and washing with water reduced the adsorption by 20% and 40%, respectively by the 4th cycle. Heating proved to be the most unfavorable method as 60% reduction was observed as early as the first cycle. It can thus

be concluded that spent Petai pod can be regenerated and reused through NaOH treatment, maintaining high adsorption capacity.

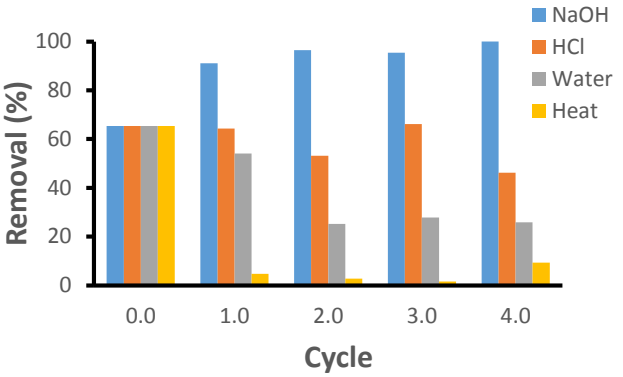

Figure 7. Regeneration studies of Petai pod.

Characterization of Petai pod

Surface morphology from ***Figure 8*** of SEM imaging clearly shows a distinct change upon adsorption with CV dye. The point of zero charge (pH_{pzc}) of Petai pod was determined to be at pH 4.6 indicating, that at this pH, the surface charge is zero. Below this pH, the surface of Petai pod would be predominantly positively charged, while the converse is true for $pH > pH_{pzc}$.

4. Conclusion

It is concluded that Petai pod has the potential to be used as a low-cost adsorbent for the removal of CV dye. Its high adsorption capacity compared to most reported adsorbents coupled with its resilience to medium pH support it being used in real life wastewater treatment. Another attractive feature is its ability to be regenerated and reused through base treatment while being able to maintain very high percentage removal of CV dye even after four consecutive cycles.

Acknowledgements

The authors would like to thank the Government of Negara Brunei Darussalam and the Universiti Brunei Darussalam for their financial support as well as CAMES and Department of Biological Sciences for the use of SEM instrument.

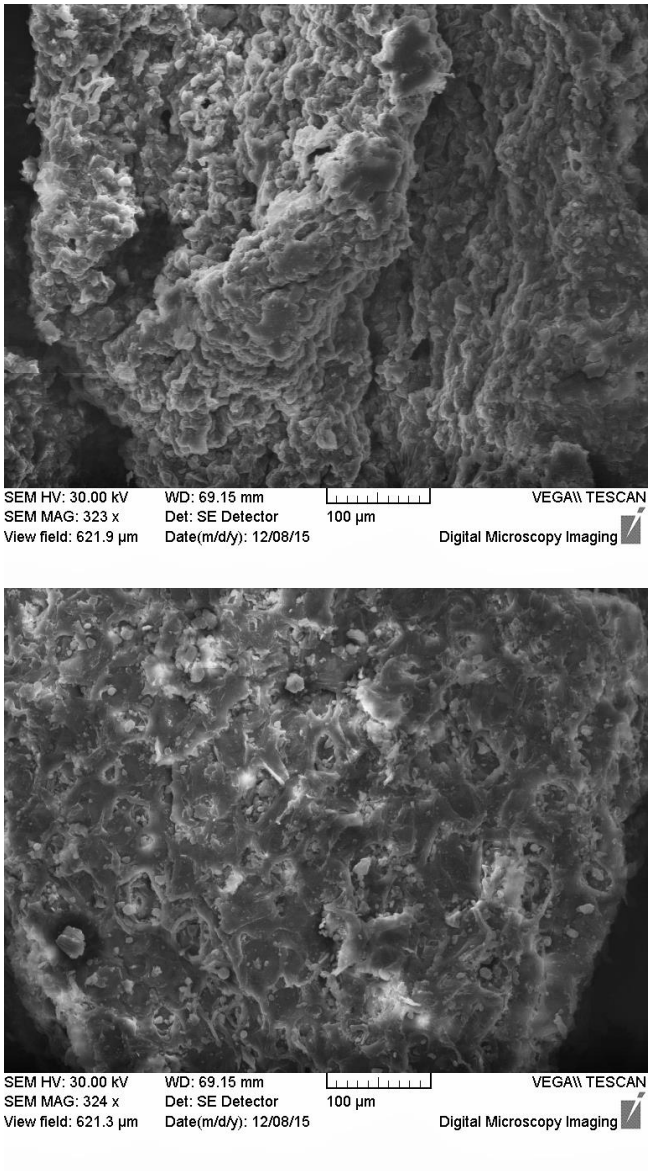

Figure 8. Surface morphology of Petai pod before (top) and after (bottom) adsorption with CV

References

[1] Bhatnagar, M. Sillanpää and A. Witek-Krowiak, *Chem. Eng. J.* **2015**, 270: 244-271.

[2] T. Zehra, N. Priyantha, L. B. L. Lim and E. Iqbal, *Desalin. Water Treat.*, **2015**, 54(9), 2592-2600.

[3] M. K. D. Nordin, M. R. R. Kooh and L. B. L Lim, *ISRN Environ. Chem.*, **2013**, Article ID 619819.

[4] K. A. Adegoke and O. S. Bello, *Water Resource Ind.*, **2015**, 8.

[5] H. I. Chieng, L. B.L. Lim, N. Priyantha and D. T. B. Tennakoon, *Int. J. Earth Sci. Eng.*, **2013**, 791.

[6] A. Ahmad, A. Idris and D. K. Mahmoud, *J. Adv. Sci. Eng. Res.*, **2011**, 261.
[7] Y. Y. Ngoh, Y. H. Leong and C. Y. Gan, *Int. Food Res. J.*, **2015**, 2351.
[8] H. I. Chieng, N. Priyantha and L. B. L. Lim, *RSC Adv.*, **2015**, 34603.
[9] M. K. Dahri, M. R. R. Kooh and L. B. L. Lim, *J. Environ. Chem. Eng*., **2014**, 1434.
[10] L. B. L. Lim, N. Priyantha, H. I. Chieng and M. K. Dahri, *Desalin. Water Treat.*, **2016**, 5673.
[11] L. B. L. Lim, N. Priyantha and N. H. Mohd Mansor, *Environ. Earth Sci.*, **2015**, 3239.
[12] L. B. L. Lim, N. Priyantha, C. M. Chan, D. Matassan, H. I. Chieng and M. R. R. Kooh. *Desalin. Water Treat.*, **2016**, 8319.
[13] N. Priyantha, L. B. L. Lim and M. K. Dahri, *Int. Food Res. J.*, **2015**, 2141.
[14] Langmuir, *J. Am. Chem. Soc.*, **1916**, 2221.
[15] H. M. F. Freundlich, *J. Phys. Chem.*, **1906**, 385.
[16] M. I. Temkin and V. Pyzhev, *Acta Physiochimica USSR.*, **1940**, 327.
[17] M. M. Dubinin and L. V. Radushkevich, *Proc. Acad. Sci.*, 1947, 327.
[18] O. Redlich and D. L. Peterson, *J. Phys. Chem.*, **1959**, 1024.
[19] R. Sips, *J. Chem. Phy.*, **1948**, 490.
[20] T. Zehra, N. Priyantha, and L. B. L. Lim. *Environ. Earth Sci.*, **2016,** doi: 10.1007/s12665-016-5255-8
[21] L. B. L. Lim, N. Priyantha, T. Zehra, W. T. Cheow and C. M. Chan, *Desalin. Water Treat.*, **2016**, 10246.
[22] H. Shayesteh, A. Rahbar-Kelishami and R. Norouzbeigi, *Desalin Water Treat.*, **2015**, doi:10.1080/19443994.2015.1054315
[23] S. Roy, S. K. Ghosh and A. Bandyopadhyay, *Environ. Quality Manage*., **2015**, 55.
[24] S. Lagergren, *Kungliga Svenska Vetenskapsakademiens Handlingar*, **1898**, 1.
[25] Y. S. Ho and G. McKay, *Process Biochem.*, **1999**, 451.
[26] W. Weber and J. Morris, *J. Sani. Eng. Div.*, **1963**, 31.
[27] G. E. Boyd, A. W. Adamson and L. S. Myers, *J. Am. Chem. Soc.*, **1947**, 2836.

Clustering cardiac rehabilitation data: a preliminary study

Daphne T. C. Lai[1], Syazwina Yasmin[1], Seng Khiong Jong[2], Sok King Ong[3] and Chean Lin Chong[2]*

[1]Faculty of Science, Universiti Brunei Darussalam, Jalan Tungku Link, Gadong, BE1410, Brunei Darussalam
[2]Raja Isteri Pengiran Anak Saleha Hospital (RIPASH), BE1518, Brunei
[3]Ministry of Health, BB3910, Brunei

**corresponding author email: daphne.lai@ubd.edu.bn*

Abstract

In this paper, a clustering framework is used on cardiac rehabilitation data to discover meaningful patterns. The data were collected in three phases. Kmeans clusters were generated and evaluated for stability. Visual assessment of the clusters using PCA plots was also done. A scoring system was developed to quantify improvement in the patients' health across the three phases. With the scores, association and correlation measures were employed to assess the meaningfulness of the clusters. Two distinct clusters were found and they were shown to have moderate clinical association (Cramer's V score=0.27) with the improvement scores.

Index Terms: data clustering, longitudinal data, cardiac rehabilitation

1. Introduction

Clustering is widely used to discover hidden structures in unlabeled datasets using a pre-defined similarity measure. Its application covers a wide range of data types such as numerical, binary, image, textual, videos, ordinal and so on. While its application was predominantly on static data, it has long gained grounds in time-based ones such as time series[1] and longitudinal[2] data. It is worth noting that they are different. Time-series data contains uni- or multi-variate data of an incident (such as unemployment, earthquakes), often collected at regular time intervals while longitudinal data contains multivariate data collected from the same subjects with repeated measurements at different time intervals.

Liao[1] has provided an extensive piece on the different clustering algorithms applied to time series, univariate and multivariate data. According to him, there are three different clustering approaches; raw-data-based, feature-based and model-based. Heggeseth[2] has described two main approaches for longitudinal data; nonparametric and model-based. For both time-based datatypes, Kmeans was employed.

For this reason, as preliminary work, we applied a nonparametric approach using Kmeans on a longitudinal patient dataset acquired from a cardiac rehabilitation programme (CRP). So far, statistical techniques have been applied on this dataset (publication is in preparation) but, no clustering techniques have been tried. The aim of this work is to discover clinically meaningful clusters in the dataset. The clusters generated were assessed for stability and clinical relevance.

In this work, two stable clusters were found with moderate clinical relevance (Cramer's V score=0.27)[3,4] to improvement scores based on a collective measure of patients' parameters. Interestingly, these scores were found to have little correlation to each individual parameter but, was able to represent the time-based nature of the data to be used for statistical assessment of the clusters.

2. Experimental approach

Dataset

The dataset contains 180 records of RIPASH CRP patients enrolled between the years 2009-2013. It consists of the following parameters: Short Form

36 Health Survey (SF36), Exercise Test Time (ETT), Resting Blood Pressure (SBP/DBP), Resting Heart Rate (HR), Fasting Blood Sugar (FBS), Total Cholesterol (TC), High Density Lipoprotein (HDL), Low Density Lipoprotein (LDL), Triglyceride (TG), Weight (WT), Waist Circumference (WC) and smoking status (SS). The data is considered longitudinal as the mentioned parameters were recorded from the same patients at enrolment (P1), end of Phase II (P2), which last 8 weeks and end of Phase III (P3), which last another 18 months.

Methodology

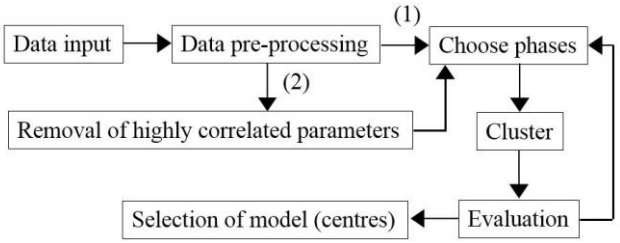

Figure 1. Clustering Framework using (1) raw-data-based and (2) feature-based approaches.

Figure 1 illustrates the steps taken to discover and assess meaningful clusters in the data set. After data pre-processing, we obtained 63 complete and normalised data records, out of the original 180 records. Next, we experimented using the raw-data-based and feature-based approaches. In the later approach, Pearson's correlation was applied on all parameters across the three phases and those that were highly correlated were removed.

To determine clustering solutions of interest, data from different individual phase or combination of phases were chosen to be clustered using Kmeans.

The number of clusters is determined by looking at the "elbow" in the sum of squared error (SSE) scree plot, and the clustering is performed for several runs. The stability of the clusters found across the runs was assessed using the within-sum-of-square (WSS) measure.

As part of clinical evaluation, a scoring system involving parameter comparison between those in 1) P1 and P2 and 2) P2 and P3 is used. For the parameters DBP, HR, FBS, WC, LDL, TG, SS, SBP, WT, BMI and TC, a decrease between two compared phases is regarded as an improvement. The opposite is true for the parameters: ETT, SF36 and HDL. A score of '1' assigned for improvement while a score of '0' indicates otherwise. The scores are then summed for each patient. The Cramer's V coefficient is used to measure clinical association between two nominal variables; cluster assignments and improvement scores of patients. If the level of association is low (<0.2),[3] a new experiment was conducted using different phases. PCA plots were also used to assess the clinical relevance of the clusters.

Experiments

Five experiments on different phases were carried out to find clustering solutions of interest:

1. Clustering individual phases
2. Clustering differences between phases
3. Clustering phase 1 and phase 2 without highly correlated parameters
4. Clustering phase 1 and phase 2 with all parameters
5. Clustering three phases together with all parameters

For each experiment, we conducted 10 runs. All experiments are implemented in **R**.[6]

3. Results and Discussion

In this section, we will present results from experiment 4 and 5 in greater detail, as they are found to be most interesting.

For experiment 1 to 3, the "elbow" on the scree plot was at k=3. For this reason, we test running Kmeans 10 times with k=2, 3 and 4. Solutions with k=2 are most stable. Further investigation into experiments 1 to 3 were stopped because, either clusters found were from individual phases and did not demonstrate observable trend across the phases. Furthermore, the removal of highly correlated parameters prior to clustering means the parameter for a particular phase is not represented. More complex approaches such as those detailed[1,2] are required to be investigated in order to proceed with such experiments.

Table 1. Phase comparison for cluster centres 1 and 2 based on P1 and P2.

Clus1	***ET***	***SF36***	***SBP***	***DBP***	***HR***	***FBS***	***WT***	***BMI***	***WC***	***TC***	***HDL***	***LDL***	***TG***	***SS***
P1	8.26	69.49	132.51	81.54	72.37	6.05	77.27	29.93	38.38	4.19	1.05	2.38	1.65	0.57
P2	9.88	78.26	122.57	74.86	69.31	5.89	77.33	29.85	37.81	3.85	1.04	2.09	1.58	0.06
P1vsP2	↑H	↑	↓H	↓	↓	↓H	↑H	↓H	↓H	↓	↓	↓	↓H	↓
Clus2	***ET***	***SF36***	***SBP***	***DBP***	***HR***	***FBS***	***WT***	***BMI***	***WC***	***TC***	***HDL***	***LDL***	***TG***	***SS***
P1	7.19	73.21	115.57	74.14	73.61	5.36	65.46	26.04	34.84	4.10	1.23	2.30	1.25	0.11
P2	8.79	76.11	119.93	76.43	69.04	5.27	65.69	26.14	34.42	4.09	1.21	2.34	1.19	0.00
P1vsP2	↑	↑	↑	↑	↓	↓	↑	↑	↓	↓	↓H	↑	↓	↓

Table 2. Improvement score (Total) between P1 and P2, showing only for three patients.

	ET	***SF36***	***SBP***	***DBP***	***HR***	***FBS***	***WT***	***BMI***	***WC***	***TC***	***HDL***	***LDL***	***TG***	***SS***	***Total***
1	1	0	1	1	1	0	0	0	1	1	0	1	0	0	7
2	1	1	0	1	1	0	0	0	1	0	1	1	0	1	8
3	1	0	1	0	0	0	0	0	0	1	1	1	1	0	6

Clustering P1 and P2 with all parameters

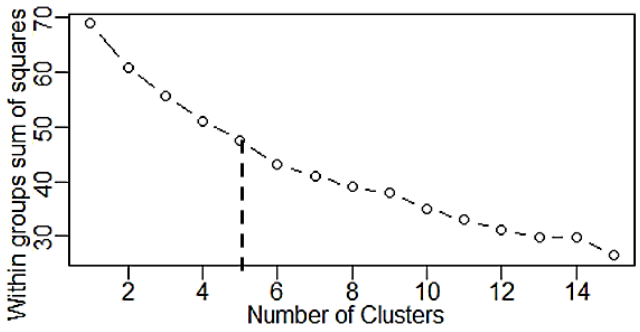

Figure 2. Scree plot of WSS against number of clusters

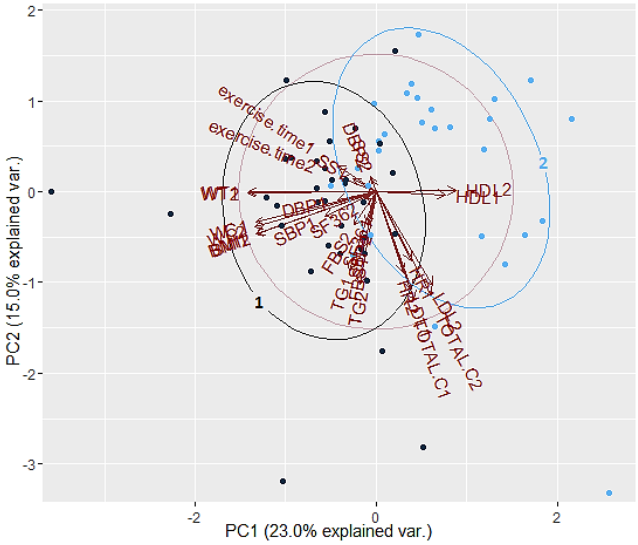

Figure 3. Two clusters found from P1 and P2 data

Based on the scree plot in ***Figure 2***, there appears to be an "elbow" at k=5. Thus, we experimented using k=2,3,4 and 5. Using WSS measure and PCA plots, we found that k=2 produced the most stable clusters across the 10 runs.

Figure 3 shows the cluster plot of the two clusters. Based on the arrows, it appears that cluster 2 is highly characterised by high HDL values while those in cluster 1 by WT and TG. These trends are consistent with the cluster centres tabulated in ***Table 1***, indicated with 'H'. However, what was not observable from the PCA plot is that patients belonging to cluster 1 has more favourable outcomes with lower (↓) SBP, DBP, BMI and LDL in P2, highlighted in green.

To evaluate the clinical associations of the clusters, scores were given for parameters that improved between P1 and P2, as shown in ***Table 2***. In ***Table 3***, it can be observed that there are more patients with total scores above 9 in cluster 1 than 2.

Table 3. Total (T.) scores of patients in cluster 1 and 2.

	T.Scores	***2***	***4***	***5***	***6***	***7***	***8***	***9***	***10***	***11***	***12***
Cluster	**1**	0	0	3	6	4	5	9	3	4	1
	2	1	1	2	9	7	6	0	1	0	1

Table 4. Phase comparisons for cluster centres 1 and 2 based on 3 phases.

Clus1	***ET***	***SF36***	***SBP***	***DBP***	***HR***	***FBS***	***WT***	***BMI***	***WC***	***TC***	***HDL***	***LDL***	***TG***	***SS***
P1	6.43	65.71	126.29	78.57	79.71	6.83	66.44	27.86	35.96	5.05	1.18	3.11	1.69	0.14
P2	8.46	70.00	125.71	72.14	75.71	6.79	66.96	27.90	35.45	5.17	1.17	3.07	2.00	0.00
P3	7.20	69.79	130.71	80.57	77.07	7.99	67.16	28.14	36.18	5.51	1.21	3.51	1.72	0.00
vs	↑↓	↑↓	↓↑ H	↓↑	↓↑ H	↓↑ H	↑↑	↑↑	↓↑	↑↑ H	↓↑ H	↓↑ H	↑↓ H	↓↓
Clus2	***ET***	***SF36***	***SBP***	***DBP***	***HR***	***FBS***	***WT***	***BMI***	***WC***	***TC***	***HDL***	***LDL***	***TG***	***SS***
P1	8.17	72.69	124.61	78.16	70.98	5.43	73.61	28.30	37.05	3.89	1.12	2.13	1.41	0.43
P2	9.66	79.39	120.16	76.53	67.33	5.28	73.64	28.29	36.55	3.61	1.10	1.95	1.24	0.04
P3	8.83	78.82	123.00	78.18	69.33	5.77	74.34	29.29	37.24	3.80	1.19	2.07	1.31	0.04
vs	↑↓ H	↑↓ H	↓↑ L	↓↑	↓↑ L	↓↑ L	↑↑ H	↓↑ H	↓↑ H	↓↑ L	↓↑	↓↑ L	↓↑ L	↓=

Table 5. Total (T.) scores of patients in cluster 1 and 2 based on P1,P2 and P3 data.

	T.Scores	***6***	***7***	***8***	***9***	***10***	***11***	***12***	***13***	***14***	***15***	***16***	***17***
Cluster	**1**	0	0	0	2	4	2	1	1	1	2	1	0
	2	1	1	1	4	6	7	9	6	3	6	4	1

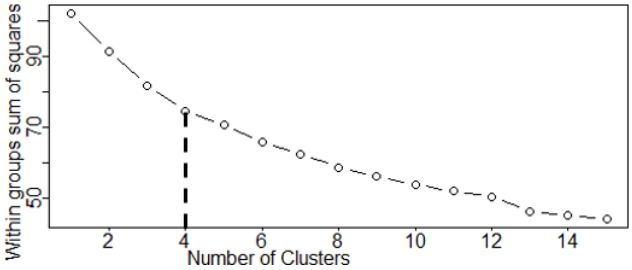

Figure 4. Scree plot of WSS against number of clusters.

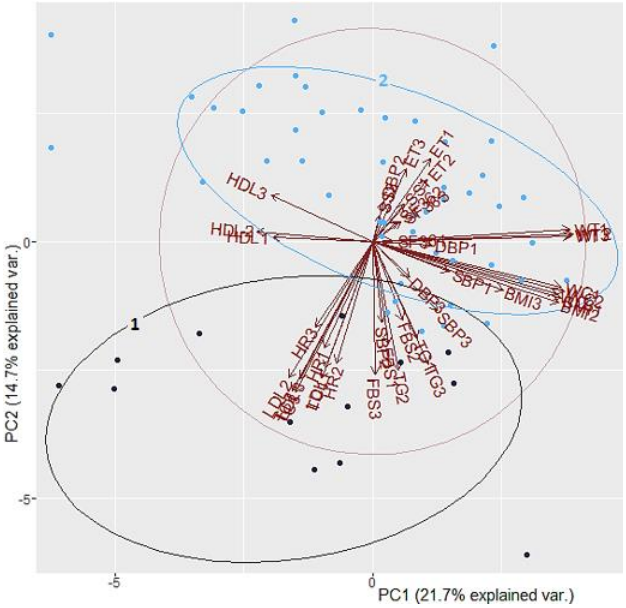

Figure 5. Two clusters found from P1, P2 and P3 data.

A Cramer's V coefficient of 0.522 was found between the clusters and total scores, suggesting relatively strong association.[3,4]

Clustering three phases with all parameters

From ***Figure 4***, the "elbow" is observed at k=4. We experimented with k=2, 3 and 4. The most stable clusters are generated at k=2.

Figure 5 shows the PCA plots for the two clusters found. Note that three points are not included to provide a clearer view of the parameters. We observed that cluster 1 is characterised by high LDL, HR, FBS and TG while cluster 2 by high ET, WT, WC, BMI and HDL. Together with higher SF36 and lower SBP, HR, FBS, TC, LDL and TG highlighted in green in ***Table 4***, it appears to suggest that patients in cluster 2 are fitter despite higher WT and BMI.

The two clusters are more well-separated than those in ***Figure 3***, where the two clusters overlap even though they are more compact, as shown in ***Table 6***. ***Table 6*** shows all the total WSS and its frequency for all 10 runs in both experiments. Clusters generated from clustering the three phases are more stable with 4 unique solutions, as

opposed to 5 unique solutions from clustering two phases.

The clusters were found to be have moderate association with a Cramer's V coefficient of 0.27 with the improvement scores. The improvement scores were calculated based on improvement found between P1 and P2, and between P2 and P3.

The clinical parameter – total improvement score pair has a nonlinear and nonmonotonic relationship. This is shown in ***Table** 7*, indicated by a low Pearson's (P) correlation with high Hoeffding's D (H) correlation whereas both low P and H values indicate random variables.[5]

This indicates that Kmeans was able to discover the hidden structures associated with improvement using a collective measure across the three phases, the improvement scores, which are not directly observable. While such structures were found, the clusters themselves (shown in ***Figure 3*** and ***Figure 5***) do not directly demonstrate improvement or otherwise.

Scatter plots were drawn to investigate in parameters with low P but medium H such as FBS in P1 (FBS1), illustrated in ***Figure 6***, as well as parameters with complete dependence such as SBP in P2 (SBP2) ***Figure 7*** using the `scatter.smooth` function in **R**.[6] This function also add a smooth curve computed by loess. Based on these two plots, there appears to be no strong correlation. Further work beyond the scope of this paper is required.

Based on the outcomes of experimental results, we consider this work to be promising as clusters with clinical association were found using a simple raw-data-based Kmeans clustering framework.

Indeed, high correlation is found between some of the parameters. Yet the removal of these parameters mean that the parameter for that phase is not represented. For now, we include all parameters in the clustering despite the low percentage variability represented in the two principal components in ***Figure 3*** and ***Figure 5***, which does not give a visual representation of high accuracy. In the future studies, we hope to explore other techniques to find relevant parameters as well as to determine the trajectories (groupings) within the longitudinal data.

Table 6. Total (T.) WSS (based on normalised values) and its (freq)uency for both clustering experiments.

	P1 &2 (k=2)		***P1,2 & 3 (k=2)***	
	T. WSS	***freq***	***T. WSS***	***freq***
1	60.95	5	91.65	1
2	62.60	1	90.12	3
3	61.58	2	90.09	5
4	61.98	1	91.32	1
5	62.47	1		

Table 7. Pearson's (P) and Hoeffding's D (H) correlation between Total Score with each parameters in the 3 phases.

	P1		***P2***		***P3***	
	P	***H***	***P***	***H***	***P***	***H***
ET	0.23	0.19	0.13	0.83	0.27	0.16
SF36	-0.09	0.95	0.08	0.52	0.09	0.68
SBP	0.08	0.58	-0.06	1	-0.23	0.01
DBP	0.17	0.47	-0.09	1	-0.13	1
HR	-0.17	0.23	-0.14	0.24	-0.22	0.06
FBS	0.09	0.49	-0.11	1	-0.18	0.49
WT	0.04	0.64	0.01	0.45	-0.07	0.46
BMI	0.05	0.8	-0.02	0.85	-0.05	0.52
WC	0.02	0.68	-0.02	0.66	-0.16	0.47
TC	0.23	0.25	-0.02	0.47	-0.13	0.03
HDL	-0.02	0.6	-0.04	0.66	0.17	0.83
LDL	0.20	0.35	-0.07	0.73	-0.12	0.1
TG	0.21	0.44	0.09	0.63	-0.15	0.13
SS	0.21	0.41	-0.31	1	-0.31	1

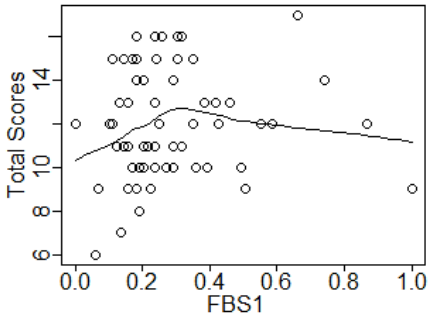

Figure 6. Scatter plot of Total Score against FBS1 (normalised).

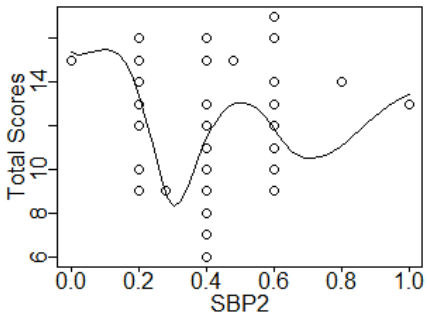

Figure 7. Scatter plot of Total Score against FBS1 (normalised).

4. Conclusion

As a preliminary study, we have experimented using a simple Kmeans clustering framework to discover clinically relevant clusters in the cardiac rehabilitation data, which contains patient data repeatedly collected from 3 different phases. Highly, clinically associated clusters were found using P1 and P2 data while moderately clinically associated clusters were found using data from all three phases. This suggests for further cluster refinement approaches to be applied, as well as exploration into other approaches such as model-based techniques, as well as application of suitable distance metric that could better model the changes across the phases, all of which, so far, has not been explored for this dataset.

Acknowledgements

This work was supported by the Universiti Brunei Darussalam under Grant UBD/PNC2/2/RG/1(311).

References

[1] T. W. Liao, *Pattern Recognition 38,* **2005**, 1857.

[2] B. Heggeseth, *Longitudinal Cluster Analysis with Applications to Growth Trajectories*, 2013.

[3] L. M. Rea and R. A. Parker, *Designing and conducting survey research*, **1992**, 203.

[4] J. W. Kotrlik, H. A. Williams and M. K. Jabor, *Journal of Agricultural Education 52.1*, **2011**, 132.

[5] D. Bhalla, http://www.listendata.com/2015/03/_detect-non-linear-and-non-monotonic.html, Last accessed: 2nd May 2016.

[6] R Core Team, *R: A language and environment for statistical computing*. https://www.R-project.org/, **2016**. Last accessed: 3rd May 2016.

Impact of intelligent biofeedback during rehabilitation of professional athletes: a model for next generation smart healthcare system

Owais A. Malik and S.M.N.A. Senanayake[*]

Faculty of Science, Universiti Brunei Darussalam, Jalan Tungku Link, Gadong, BE1410, Brunei Darussalam

**corresponding author email: arosha.senanayake@ubd.edu.bn*

Abstract

This paper presents a general framework of intelligent biofeedback for smart healthcare system and its impact on healthcare of professional athletes, especially during rehabilitation monitoring. The application of machine learning techniques along with various wireless wearable sensors facilitated in building a knowledge base system for healthcare monitoring of the subjects and providing a visual/numeric biofeedback to the clinicians, patients and healthcare professionals. The validated system can potentially be used as a decision supporting tool by the clinicians, physiotherapists, physiatrists and sports trainers for quantitative rehabilitation analysis of the subjects in conjunction with the existing recovery monitoring systems. Based on the results achieved, a conceptual design and model for next generation smart healthcare system/devices for professional athletes has been proposed.

Index Terms: biofeedback, smart healthcare, machine learning, wireless sensors

1. Introduction

Various tasks and activities are performed by the athletes during their training sessions/regimes as well as in the field. In order to improve and optimize their sports performance and prevent them from any action leading to injury, a continuous monitoring of their health conditions is crucial. Moreover, in case of an injury, observing their recovery progress becomes vital for timely return to sports and avoiding further injuries.[1] Evidence-based, informed decisions are required to be made regarding structuring training and evaluation of individuals. Thus, powerful tools are needed to be developed for performance evaluation, training enhancements, injury screening, and return-to-play assessment for a variety of athletes and sport disciplines.[2] Recording of the appropriate data/bio-signals interfaced with intelligent techniques can assist in solving this problem by designing a knowledge-based system as a decision supporting tool for clinicians, healthcare professionals, sports trainers and the athletes as well.[2,3] Such a system can provide visual and numeric biofeedback in real-time or off-line in order to improve the health conditions and/or sports performance of the athletes.[3]

This paper presents an overview of the design of an intelligent biofeedback system and its effectiveness in assessing the healthcare and sports performance of athletes having knee injury and surgery. The overall recovery evaluation performed by the developed system was found in accordance with the assessment made by the physiotherapists using standard subjective/objective scores with additional useful information. Further, the statistical results demonstrated that the use of visual biofeedback improved the rehabilitation performance of the subjects. Based on these results, a conceptual design and model for next generation smart healthcare system for professional athletes has been proposed in this paper.

2. Experimental approach

Overview of the Developed System

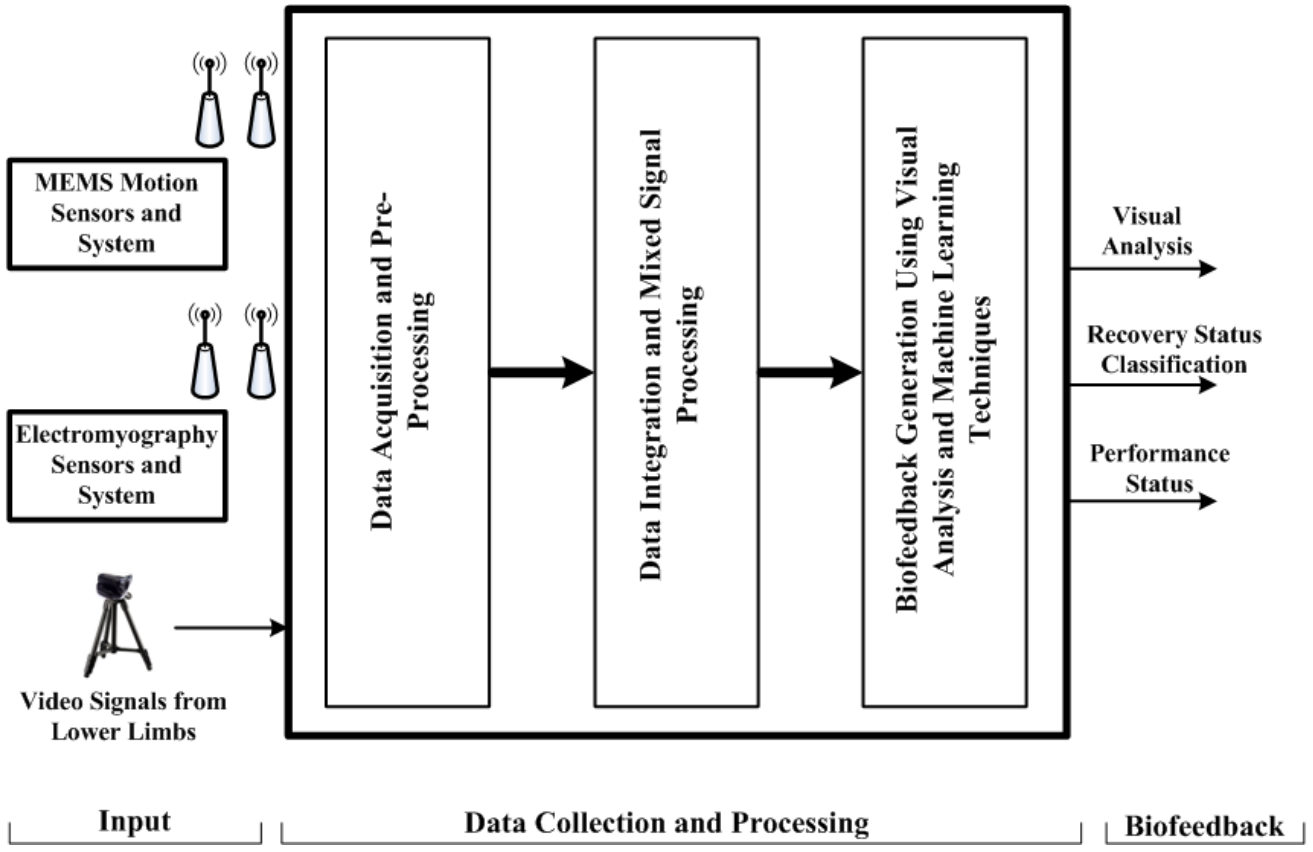

Figure 1. Components of the system

An intelligent extensible framework was designed and developed for monitoring and assessing the recovery status of athletes, and evaluating their sports performance after having knee injury or surgery. This system was developed using non-invasive body-mounted motion and electromyography (EMG) wireless sensors to capture the kinematics and neuromuscular data from human lower extremity during ambulation and single leg balance testing activities. This framework was developed in order to facilitate the clinicians, physiotherapists, physiatrists and sports trainers in determining the recovery stage of the subjects based on the data collected during different rehabilitation testing activities and identifying the subjects lacking behind the desired level of recuperation. Additionally, the feedback/solution from the previous cases was provided to assist them for taking the required therapy/training measures or accelerating their ongoing activity level.

The overall structure of the developed system is shown in ***Figure 1***. The system mainly consists of three components: 1) input (signals from wireless sensors attached to the lower extremity of subjects), 2) data collecting and processing software module and 3) output (visual analysis, recovery and performance status). Initially, the output with corresponding input pattern set is used to create a knowledge base (KB). After forming the KB, the system provides a biofeedback (recovery and performance status) to clinicians, physiatrists and physiotherapists for the test subjects and the KB is enriched/updated if the test pattern is new and/or repaired pattern.

Knowledge Base (KB)

A knowledge base (KB) is a centralized repository for information related about a particular field or domain. In this study, a KB was created in order to manage the information about the subjects' profiles and their health/rehabilitation conditions. The KB contains different types of information including raw and processed data, domain knowledge, historical data available for subjects

(pre-injury, post-injury), session data during convalescence, case library (problem-solution pair for rehabilitation monitoring), reasoning and learning models (trained intelligent methods) and other relevant data (e.g. subjects' profiles, gender, type of sports etc.). In general, the information in KB can be represented as

$$KB = [\ pre\_inj\_I_S^i,\ post\_inj\_I_S^j,\ post\_op\_I_S^k,\ \mathfrak{I}(\ pre\_inj\_I_S^i\ ),\ \mathfrak{I}(\ post\_inj\_I_S^j\ ),\ \mathfrak{I}(\ post\_op\_I_S^k\ ),\ \mathfrak{S}_p,\ \mathfrak{D},\ \mathfrak{C},\ \mathfrak{M}_t\ ]$$

where

$pre\_inj\_I_S^i$: raw input data set (kinematics, EMG and video) of a group of subjects '*S*' for different sports activities at pre-injury (i.e. healthy) stage for *i* sessions ($i \geq 1$)

$post\_inj\_I_S^j$: raw input data set (kinematics, EMG and video) of a group of subjects '*S*' for different sports activities after knee injury (i.e. before surgery) for *j* sessions ($j \geq 1$)

$post\_op\_I_S^k$: raw input data set (kinematics, EMG and video) of a group of subjects '*S*' for different sports activities after knee surgery (i.e. rehabilitation after surgery) for *k* sessions ($k \geq 1$)

$\mathfrak{I}(\ pre\_inj\_I_S^i\ )$: processed input data set (kinematics, EMG and video) of a group of subjects '*S*' for different sports activities at pre-injury (i.e. healthy) stage for *i* sessions ($i \geq 1$)

$\mathfrak{I}(\ post\_inj\_I_S^j\ )$: processed input data set (kinematics, EMG and video) of a group of subjects '*S*' for different sports activities after knee injury (i.e. before surgery) for *j* sessions ($j \geq 1$)

$\mathfrak{I}(\ post\_op\_I_S^k\ )$: processed input data set (kinematics, EMG and video) of a group of subjects '*S*' for different sports activities after knee surgery (i.e. rehabilitation after surgery) for *k* sessions ($k \geq 1$)

$\mathfrak{S}_p$: profile (e.g. gender, age, weight, height, type of injuries, sports activities etc.) of *p* subjects

$\mathfrak{D}$: domain knowledge (e.g. type of protocols followed for subjects after surgery, local/standard norms for different rehabilitation testing activities etc.)

$\mathfrak{C}$: case library consisting of problem-solution pairs (processed input, rehabilitation procedure followed, outcomes and possible suggestions) related to individuals or different group of subjects

$\mathfrak{M}_t$: trained intelligent models for each activity *t* to be monitored.

The designed KB is not a static collection of information, but it acts as a dynamic resource which has the capacity to learn and evolve with the passage of time when new problems are presented and new problem-solution pairs are added to the system. This evolution process makes it more useful for domains where subject's specific monitoring and prognosis mechanisms are required. Thus, as an integral component of rehabilitation and performance monitoring system, this KB has been used to optimize collection, organization and retrieval of relevant information for subjects.

System output - Biofeedback

In order to observe the rehabilitation progress and performance of knee injured subjects, the developed systems provides a set of outputs '$\mathfrak{O}$' consisting of visual biofeedback (*VBF*) and recovery progress indicators (*RPI*) for physiotherapists, physiatrists and clinicians.

$$\mathfrak{O} = (VBF, RPI)$$

Visual Biofeedback (VBF)

The developed visual biofeedback system provides a visual monitoring of individual and superimposed signals (kinematics and EMG) in order to identify the knee joint abnormality and muscles strength during ambulation and balance testing activities performed by the knee injured subjects. The system can present different types of individual/superimposed processed signals for inter- and intra-subject comparisons e.g.

- Knee flexion/extension with each of the processed EMG signals (envelopes) from different muscles for each rehabilitation testing/monitoring activity
- Knee abduction/adduction with each of the processed EMG signals (envelopes) from different muscles for each rehabilitation testing/monitoring activity

- Knee rotation with each of the processed EMG signals (envelopes) from different muscles for each rehabilitation testing/monitoring activity
- Comparison of activation timings, duration and normalized strength of different muscles monitored for each rehabilitation testing activity within same and/or different legs of an knee injured subject and with the average of these parameters of a group of healthy subjects
- Comparison of 3-D knee movements (flexion/extension, abduction/adduction and rotation) of non-injured (anterior cruciate ligament intact) and injured (anterior cruciate ligament reconstructed) leg of the same subject for each rehabilitation testing/monitoring activity
- Comparison of 3-D knee movements (flexion/extension, abduction/adduction and rotation) of injured leg of a subject with average 3-D movements of healthy subjects for each rehabilitation testing/monitoring activity

Recovery Progress Indicators (RPIs)

For objective assessment and recovery analysis of a knee post-operated subject during rehabilitation period, four outputs are provided by the developed system using integrated kinematics and EMG feature set.

- Current recovery stage/phase for each activity
- Percentage of the recovery progress for each activity as compared to the healthy group
- Percentage of the recovery progress within a identified stage/phase for each activity
- An overall combined recovery state for all activities monitored

Decision making

The objective biofeedback provided by the developed system is used as a supporting tool by clinicians, physiatrists, physiotherapists and sports trainers for observing the subjects with ambulation and balance impairments after knee surgery and timely intervening during the rehabilitation regimen. The current recovery progress evaluation and previously stored experiences in KB (if any) help in focusing on specific recovery problem areas and modifying the rehabilitation protocols for individuals as per the requirements.

In order to make a decision about the recovery state and performance of a subject, first the input parameters '$post\_op\_I_S^k$' are collected through sensors and video camera for each activity during a rehabilitation monitoring session and system outputs 'Θ' (as described in section 2.2) are generated using the processed data. These system outputs (indicating the objective and quantitative recovery progress of a subject) and other standard tests are then used by physiatrists, physiotherapists and trainers for suggesting and/or modifying the training and exercises during the next phase of rehabilitation. The subject is re-assessed after further rehabilitation training and the improvements or deteriorations are objectively identified. This process continues till a subject fulfils the required criteria of recovery evaluation before joining any high level sports or other demanding activities. Thus, this complementary decision support system can help in reducing duration and cost of recovery, and improving the rehabilitation process by providing accurate and timely information about the individual subjects' knee functionality after surgery.

Experimental setup

This section briefly describes the experimental setup for the study. Wireless motion and EMG sensor systems were used for data acquisition method and setup of sensors was performed using standard procedures.[2,5] Twenty six subjects (10 healthy and 16 unilateral anterior cruciate ligament reconstructed i.e. post operated knee) athletes were recruited from Performance Optimization Centre (POC) in Ministry of Defence and Sports Medicine and Research Centre (SMRC) in Ministry of Youth, Culture and Sports, Brunei Darussalam. The healthy subjects (4 females and 6 males) had no previous history of knee injury and ambulation/postural control impairments at the time of data acquisition. These subjects were having following mean and (S.D) readings: age of 29.4 (4.15) years, height 169.3 (4.30) cm, and weight 72.8 (14.17) kg. Knee post-operated subjects (6 females and 10 males) were

in range of 2 to 13 months post reconstruction with mean 7.25 (3.53) months. The mean (S.D) age, height and weight of this group were: 25.6 (4.15) years, 164.5 (5.34) cm and 68.5 (12.54) kg, respectively. All procedures were carried out according to the ethics guidelines approved by Universti Brunei Darussalam's Graduate Research Office and Ethics Committee.

Biosignal processing

In order to design and test the proposed system, 3-D kinematics and EMG parameters were recorded for healthy and post-operated subjects for five different activities: normal walking on flat surface at comfortable speed, two high speed walking activities (7 km/h and 8 km/h) on a treadmill and two single leg balance testing (eyes open - EO and eyes closed - EC) on a balance training platform (***Figure 2*** and ***Figure 3***). The selection of these activities was based on the recommendations from physiotherapists and due to presence of post-operated subjects at varying level of recovery.

The raw input data set obtained through the sensors and video recordings is processed by using a system-software developed in MATLAB 7.0. The system software has a layered architecture where each layer performs one or more tasks and the results are transferred to the next layer for further processing or output generation.

Figure 2. A test subject walking on a treadmill wearing wireless motion and EMG sensors

Figure 3. A test subject standing on single leg on a balance trainer wearing wireless motion and EMG sensors - front and back view

Relevant and key features from kinematics and EMG data were extracted during subjects' motion in order to collect data for generating data sets and then applying recovery classification and evaluation mechanisms.[2,5] A data set for each activity was formed by using the kinematics and EMG feature sets. The data set for each ambulation and balance testing activity consisted of 78 feature vectors (26 subjects × 3 trials per activity) with corresponding feature vector length. A single gait cycle (averaged gait cycle for a trial) during each ambulatory activity was represented by a feature vector of length 903 (840 EMG features + 63 kinematics features). For balance activities, the feature vector length was 159 (150 EMG features + 9 kinematics features) for each time segment per activity. Thus, a total of 9 data sets (3 for ambulation activities + 3×2 for balance testing activities) were generated for further processing. In order to remove the redundancy in feature vector/set and making the recovery evaluation system more efficient, principal component analysis was applied successfully.[2,5] The subjects were grouped into four categories based on their health condition using semi-automatic process and distribution of subjects' data points in these groups were verified by the physiotherapists. The groups were labelled as "Healthy Subjects", "Subjects at Stage 3", "Subjects at Stage 2" and "Subjects at Stage 1" representing different stages of health/recovery

condition of the subjects (stage 1 represents the initial level of recovery and stage 3 represents the advanced level of recovery). The identification of current class/status of gait/balancing patterns of a new subject provides useful complementary information in order to make adjustments in his/her rehabilitation process. Based on the patterns of 3-D kinematics and neuromuscular data, an automated identification of class/stage of gait/balance patterns of a subject for an ambulation/balancing activity is done by training and testing various intelligent classifiers.[5] Thus, for each ambulation/balancing testing activity, the class of gait/balance patterns of a subject is determined as per his/her performance during the test trials for that particular activity. An overall recovery progress output for a subject is computed by combining the results of all activities monitored during a session. Various data processing and the intelligent techniques were used for providing the recovery progress evaluation. [5]

For generating the visual biofeedback, the raw EMG data with zero mean for different muscles were full wave rectified and low pass filtered to generate linear envelopes. The linear envelopes provide useful information for assessing the strength/activation of different muscles for inter- and intra-subjects comparison. For comparing the EMG amplitude, the data were normalized for each subject using mean value of the signal of each stride/balance segment for respective muscles and data were represented as a percentage of mean.[3,5] The estimated knee orientation (flex-ion/extension, abduction/adduction and internal/external rotation) in three planes and EMG envelopes from different lower limb muscles were superimposed to observe the changes in both type of signals simultaneously.

3. Results and Discussion

This section reports the effectiveness of the design and impact of the results for healthcare monitoring of the subjects. It mainly describes the comparison of the performance of recovery stage classifiers, their validation and the impact of the overall biofeedback in order to improve the recovery of the professional athletes (details can be found here).[5]

Comparison of the recovery classifiers' performance

In order to determine the recovery stage of the subjects, three different classifiers adaptive neuro-fuzzy inference system (ANFIS), fuzzy unordered rule induction algorithm (FURIA) and support vector machines (SVM) were trained and tested for each activity based on the respective clustered data for healthy and post-operated subjects, and their performance measures were compared. The cross validations of all models were done by partitioning the data into two groups: training data (75% of the total data) and test data (25% of the total data). The training/testing phase for all classifiers was repeated 10 times and the average values of different performance measures were computed.

Both ANFIS and FURIA based classifiers generated the rules after training phase and these rules (models) were saved for further validation and re-suing for new data. However, it was found that the number of rules generated by FURIA based classifiers were, in general, less than the rules generated by ANFIS models for different activities which indicates the efficient rule learning/pruning mechanism in FURIA. The number of rules generated by ANFIS and FURIA models for four different activities is shown in T***able 1***.

Table 1. *Number of rules generated by ANFIS and FURIA classifiers for different activities using combined 3-D kinematics and EMG features*

Activity\Technique	***ANFIS***	***FURIA***
Normal walking	6	6
Walking at 7km/h	5	4
Walking at 8km/h	7	4
Single leg balance (EO)	10	4
Single leg balance (EC)	6	6

In order to evaluate the performance of different classifiers for various rehabilitation testing activities, Friedman's test (omnibus) and the Nemenyi test (post-hoc test) were used. The purpose of statistical significance testing is to help us gather evidence of the extent to which the

Table 2. Percentages of classification accuracies for all classifiers for different activities using combined 3-D kinematics and EMG features

Activity/Classifier	*FURIA*	*ANFIS*	*Linear SVM*	*Quadratic SVM*	*RBF SVM*
Normal walking	96.23	95.36	98.04	98.11	97.06
Walking at 7km/h	100.00	98.48	99.27	99.00	99.27
Walking at 8km/h	100.00	99.46	100.00	100.00	100.00
Single leg balance (EO)	97.22	84.13	99.67	93.33	84.67
Single leg balance (EC)	95.24	80.87	82.24	97.62	97.76

Table 3. Ranks of each classifier based on classification accuracies for different activities using combined 3-D kinematics and EMG features

Activity/Classifier	*FURIA*	*ANFIS*	*Linear SVM*	*Quadratic SVM*	*RBF SVM*
Normal walking	4.00	5.00	2.00	1.00	3.00
Walking at 7km/h	1.00	5.00	2.50	4.00	2.50
Walking at 8km/h	2.50	5.00	2.50	2.50	2.50
Single leg balance (EO)	2.00	5.00	1.00	3.00	4.00
Single leg balance (EC)	3.00	5.00	4.00	2.00	1.00

results returned by an evaluation metric are representative of the general behavior of our classifiers. All the classifiers were ranked based on their classification accuracies on each activity separately (***Table 2*** and ***Table 3***). For each classifier *j*, the sum of their ranks (R_j) obtained on all the activities is computed and then Friedman statistic is calculated using equation below.

$$\chi_{F^2} = \left[\frac{12}{n \times k \times (k+1)} \times \sum_{j=1}^{k} (R_j)^2 \right] - 3 \times n \times (k+1)$$

where *n* represents the number of activities and *k* is the number of classifiers.

The null hypothesis is that all the classifiers perform equally better, and the rejection of the null hypothesis means that there exists at-least one pair of classifiers with significantly different performances. By using the above equation, the value of χ_{F^2} was found 10.04. For a 2-tailed test at the 0.05 level of significance, the critical value is 7.8. Since the value of χ_{F^2} >7.8, so the null hypothesis is rejected. In case of the rejection of the null hypothesis, the omnibus test is followed by a post-hoc test whose job is to identify the significantly different pairs of classifiers. The Nemenyi test was used as a post-hoc test which computes a statistic q_{yz} between two classifiers *y* and *z* as follows:

$$q_{yz} = \frac{\overline{R}_y - \overline{R}_z}{\sqrt{\frac{k \times (k+1)}{6 \times n}}}$$

where $\overline{R}_y$ and $\overline{R}_z$ represent the mean rank of classifiers *y* and *z*, respectively.

Table 4 shows q_{yz} statistic computed using Nemenyi test for all classifiers. For level of significance 0.05 (i.e. α=0.05), q_α is 2.55. In order to reject the hypothesis that classifiers *y* and *z* perform equally well q_α must be larger than $|q_{yz}|$. Based on the results in ***Table 4***, the null hypothesis cannot be rejected for all combinations except for ANFIS-Linear SVM comparison (q_{yz}=*2.6*).

Table 4. q_{yz} statistic computed using Nemenyi test for all classifiers

Combination of Classifiers	q_{yz} *Statistic Value*
FURIA-ANFIS	-2.5
FURIA-Linear SVM	0.1
FURIA-Quadratic SVM	0
FURIA-RBF SVM	-0.1
ANFIS-Linear SVM	2.6
ANFIS-Quadratic SVM	2.5
ANFIS-RBF SVM	2.4
Linear-Quadratic SVMs	-0.1
Linear-RBF SVMs	-0.2
Quadratic-RBF SVMs	-0.1

Table 5. Area under curve (AUC) for all activities for different groups of subjects using combined 3-d kinematics and EMG features with FURIA classifiers

Activity/Subjects	*Healthy*	*Stage 3*	*Stage 2*	*Stage 1*
Normal Walking	1	1	0.9679	0.9889
Walking at 7 km/h	1	1	1	1
Walking at 8 km/h	1	1	1	1
EO Balance Testing	1	1	0.9944	0.9083
EC Balance Testing	0.9899	0.9986	0.9653	1

Table 6. Area under curve (AUC) for all activities for different groups of subjects using combined 3-d kinematics and EMG features with SVM (quadratic kernel function) classifiers

Activity/Subjects	*Healthy*	*Stage 3*	*Stage 2*	*Stage 1*
Normal Walking	0.9971	0.9858	0.9881	0.9805
Walking at 7 km/h	1	1	0.9959	0.9918
Walking at 8 km/h	1	1	1	1
EO Balance Testing	0.9915	1	0.9833	0.9167
EC Balance Testing	0.9839	1	0.9917	1

Table 7. Overall classification accuracy (percentage) of recovery stage identification for all activities based on combined 3-D kinematics and EMG features using trained classifiers (ANFIS, FURIA and SVMs) for new subjects to test the framework

Activity	*FURIA*	*ANFIS*	*Linear SVM*	*Quadratic SVM*	*RBF SVM*
Normal walking	95.83	94.34	95.23	94.71	94.24
Walking at 7km/h	100.00	97.50	100.00	99.00	99.00
Walking at 8km/h	100.00	100.00	100.00	100.00	100.00
Single leg balance (EO)	91.67	88.89	88.89	91.30	86.89
Single leg balance (EC)	94.12	76.19	80.95	90.72	92.65

Although, the statistical analysis show that almost all classifiers perform more or less similar in terms of their classification accuracies, a close analysis of other measures including sensitivity, specificity, F-measure, AUC (***Table 5*** and ***Table 6***) and number of rules generated suggest that FURIA classification models may be preferred over other models. In order to verify this, the trained models for each activity were stored and a data set for each activity consisting of data (three trials per activity) from 5 new subjects with known classes was used for evaluating the retrieval process. PCA coefficient matrices were applied on the given data, and five classification models were used to identify the classes. The classification performances of these models were compared (***Table 7***) and it was found that FURIA based classification model performed better than the other models for data from new subjects. The performance of each subject during each activity are compared with the most similar retrieved cases by using their recommendations and next stage results.

Validation of the recovery evaluation mechanism

In order to validate the proposed system, a data set of testing activities from 5 new post-operated subjects with known recovery status was used. PCA coefficient matrices were applied on the collected kinematics and EMG data (average of 10 gait cycles per trial for ambulation activities and 3 trials of 15 sec segments of balance testing activities) for new subjects, and different proposed metrics were used to determine their level of recovery condition based on transformed features. ***Table 8*** presents the mean(S.D) of percentage of recovery progress, recovery stage (using FURIA trained models) and percentage of recovery within the identified stage for three trials for five subjects during different activities monitored for testing. The percentages of different measures in ***Table 8*** are reported to the nearest whole percentile.

In order to verify the recovery evaluation of subjects, subjective assessments from two experts (the physiotherapist, and physical strength and conditioning coach) were used. An overall

Table 8. Recovery Evaluation for Five Subjects for Different Activities

Subject	***Activity***	***Recovery Progress (S.D) (%)***	***Recovery Stage***	***Recovery Progress within Identified Stage (S.D) (%)***
1	Normal Walking	80(1.85)	Stage 3	91(1.00)
	Walking at 7km/h	83(1.74)	Stage 3	91(1.10)
	Walking at 8km/h	82(1.72)	Stage 3	91(0.95)
	Balance (EO)	79(2.1)	Stage 3	88(1.24)
	Balance (EC)	68(2.54)	Stage 2	87(2.05)
2	Normal Walking	81(0.75)	Stage 3	95(0.45)
	Walking at 7km/h	83(0.78)	Stage 3	96(0.35)
	Walking at 8km/h	83(0.78)	Stage 3	96(0.38)
	Balance (EO)	81(0.98)	Stage 3	92(0.40)
	Balance (EC)	79(0.90)	Stage 3	89(0.70)
3	Normal Walking	95(1.20)	Healthy	96(0.95)
	Walking at 7km/h	93(1.05)	Healthy	96(0.87)
	Walking at 8km/h	95(0.95)	Healthy	95(0.89)
	Balance (EO)	90(1.20)	Healthy	92(0.92)
	Balance (EC)	81(1.10)	Stage 3	90(1.02)
4	Normal Walking	69(2.85)	Stage 2	91(2.10)
	Walking at 7km/h	67(2.23)	Stage 2	90(1.92)
	Walking at 8km/h	68(2.45)	Stage 2	90(1.90)
	Balance (EO)	67(1.89)	Stage 2	89(1.50)
	Balance (EC)	66(1.85)	Stage 2	88(1.45)
5	Normal Walking	70(1.97)	Stage 2	92(1.05)
	Walking at 7km/h	69(1.86)	Stage 2	91(1.01)
	Walking at 8km/h	69(1.86)	Stage 2	91(1.10)
	Balance (EO)	70(1.75)	Stage 2	89(1.01)
	Balance (EC)	69(1.86)	Stage 2	89(0.96)

assessment of current recovery status for each subject was given by these experts based on their judgments and standard physical fitness test scores (Tegner/Lysholm scores, assessment of leg press, hamstring curls, half squat and vertical/horizontal jumps etc.) for the subjects with post-operated knee. The assessment system used by the physiotherapists had four grades (Excellent, Good, Fair and Poor), each representing the health condition of a subject based on some subjective/partially objective measures. Similarly, the assessment system used by the strength and conditioning coach had five levels of grading (A, B, C, D and E), each representing the health condition of a subject based on certain subjective/partially objective tests. ***Table 9*** shows the comparison of overall subjective assessments (grade and percentages) given by the experts and an overall recovery value (stage and average percentage of recovery progress for all activities) obtained using proposed system by combining the The value of λ was found to be -0.8795. By calculating the $g(A_i)$s and $h(y_i)$s, the Choquet integral was used to compute the final recovery evaluation. The subjective assessments and the recovery stage identified by the proposed method are mostly consistent for all subjects. The percentages mentioned in the parentheses vary as these depend on the range assigned by different experts and techniques used to compute the values. The average percentage of recovery progress for all activities computed by the proposed system depends on the formation of respective clusters (groups identified for each stage of recovery). The number of clusters may vary due to the types of subjects available (after having knee surgery) for formation of the groups. However, for the given five subjects, a similarity

Table 9. Comparing subjective assessment and recovery evaluation computed by the proposed system

Subject	***Subjective Evaluation***		***Overall Evaluation by Proposed System***
	Physiotherapist	**Strength and Conditioning Coach**	
1	Good (~86.0%)	B (~80.0%)	Stage 3 (78.56%)
2	Good (~89.0%)	B (~86.0%)	Stage 3 (81.37%)
3	Excellent (~92.0%)	B (~93.0%)	Healthy (90.77%)
4	Fair (~73.0%)	C (~70.0%)	Stage 2 (67.36%)
5	Fair (~78.0%)	C (~73.0%)	Stage 2 (69.13%)

trend can be noticed between the recovery evaluation values computed by the proposed system and provided by the experts. The subjects having lower percentage of subjective assessments (subjects 4 and 5) also have low percentage of recovery value computed by the proposed system. Similarly, the subjects with higher percentage of subjective assessments (subject 1, 2 and 3) also have high percentage of recovery value computed by the proposed system.

Visualization of Biosignals' Patterns

The biofeedback system provides visual monitoring of individual and superimposed signals (kinematics and EMG) to physiotherapists, physiatrists and clinicians, as well as to the subjects. At the same time, this allows monitoring of the progress based on all processes and effectively matching with the motion patterns (previous patterns from the same subject or average patterns of healthy subjects or other knee post-operated groups/subjects) stored in the knowledge base.

This can also help in determining the time a subject might take to get back to the original performance or near original performance, or he/she might not be able to return to the previous level. This visual biofeedback has been found effective in improving the knee extension and muscle strength for the knee injured/post-operated subjects. Some examples of visualization of knee kinematics, EMG signals and their overlapping are shown in ***Figure 4*** through ***Figure 9***.

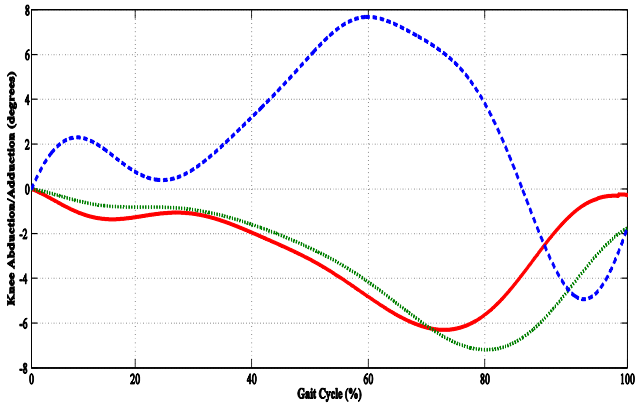

Figure 4. Knee abduction/adduction variations in the subjects during normal walking - Mean angle values in the post-operated leg (---) vs. healthy leg (....) for a subject 2 months after surgery and mean angle values for a healthy subject (____)

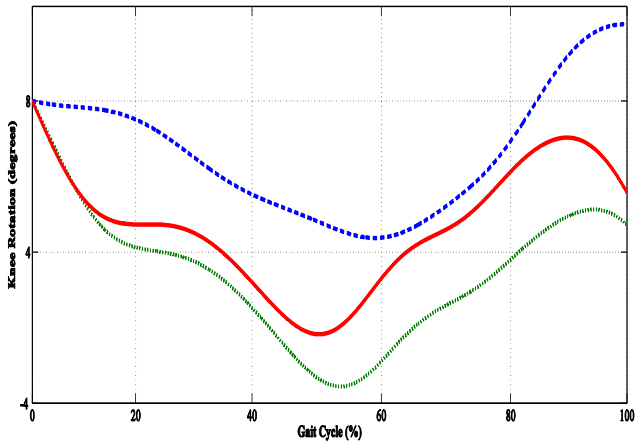

Figure 5. Knee rotation variations in the subjects during normal walking - Mean angle values in the post-operated leg (---) vs. healthy leg (....) for a subject 2 months after surgery and mean angle values for a healthy subject (____)

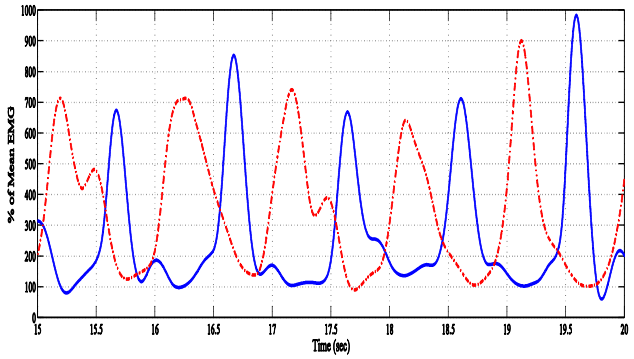

Figure 6. Comparison of percentage of mean strength and activation for biceps femoris muscles of healthy leg (– – –) and post-operated leg (___) of a subject 1 year after surgery walking at a high speed (7 km/h), representing more or less similar strength for muscles in both legs

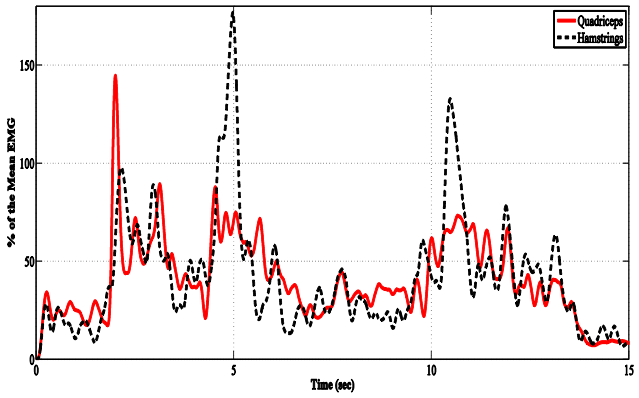

Figure 7. Comparison of the percentage of the mean EMG of quadriceps and hamstrings muscles for EO single balance testing activity for a subject after two months of surgery

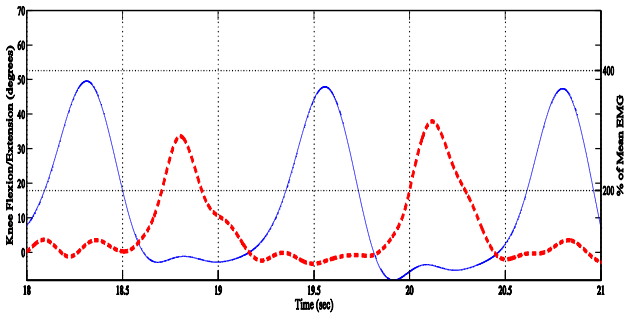

Figure 8. Activation timings and strengths of (a) biceps femoris, (b) semitendinosus and (c) vastus lateralis (---) vs. knee flexion/extension (____) of a healthy subject walking at a normal speed

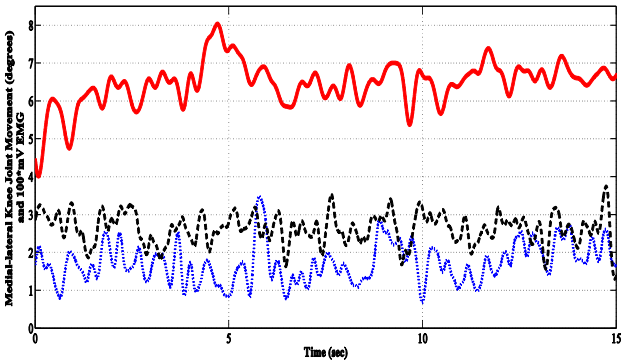

Figure 9. Superimposition of the medial-lateral knee joint movements (____), and vastus lateralis (----) and semitendinosus (-.-.-) EMG envelopes (100×mV) for a subject 2 months after knee surgery during EO single leg balance testing activity

Impact of the biofeedback

Based on the analysis of recovery stage and the visual biofeedback, vital muscle movements and kinematics signals during different gait phases and balance control for the subjects with knee surgerywere identified by the physiotherapist and the head of physical strength and conditioning, and focused training and exercises were instituted to restore the normal knee kinematics and required muscle strength for these subjects. The effectiveness of the biofeedback was evaluated by randomly assigning the subjects with knee surgery from recovery stage-2 to one of two groups: either with biofeedback (n=3) or without biofeedback (n=3). Similarly, the subjects from recovery stage-3 were also randomly allocated to one of two groups: with biofeedback (n=4) or without biofeedback (n=3). There were only 3 subjects with knee surgery found in recovery stage 1 so statistical testing of the impact of biofeedback has not been conducted. The data for these subjects were collected and monitored during the first session. In addition to following the same rehabilitation protocol as the other subjects, visual representation of the data for the subjects in the biofeedback group were used to identify the muscle movements and knee dynamics and take appropriate measures. Different parameters during ambulation at different speeds (the average knee extension angle during the terminal stance and swing phase, the peak knee flexion, the average abduction/adduction and rotation during pre-swing phase and the normalized peak values for

Table 10. p-values for different parameters using biofeedback for the subjects in recovery stage 2 during ambulation activities

Parameter Observed	***Normal Walking***	***Walking at 7km/h***	***Walking at 8km/h***
average knee extension angle during the terminal stance	0.041	0.036	0.035
average knee extension angle during the swing	0.047	0.042	0.043
peak knee flexion	0.035	0.031	0.031
average abduction/adduction during pre-swing phase	0.045	0.042	0.041
average rotation during pre-swing phase	0.205	0.195	0.191
normalized peak values for the vastus lateralis	0.042	0.040	0.040
normalized peak values for the vastus medialis	0.041	0.038	0.035
normalized peak values for the semitendinosus	0.150	0.098	0.110
normalized peak values for the biceps femoris	0.115	0.096	0.092

Table 11. p-values for different parameters using biofeedback for the subjects in recovery stage 2 during balance testing activities

Parameter Observed	***Single leg balance (EO)***	***Single leg balance (EC)***
average AP knee joint movements	0.047	0.041
average ML knee joint movements	0.043	0.040
average area of the distribution of AP-ML movements	0.025	0.038
normalized peak values for the quadriceps muscle strengths	0.039	0.038
normalized peak values for the hamstrings muscle strengths	0.189	0.176
normalized peak values for the gastrocnemius muscle strengths	0.105	0.101

the vastus lateralis, vastus medialis and hamstring muscle strengths) and single leg balance testing activities (average anterior-posterior and medial-lateral knee joint movements during the testing segment, the normalized peak values for the quadriceps, hamstrings and gastrocnemius muscle strengths) were noted for all the subjects after a period of around six weeks, to evaluate the effects of the biofeedback. An independent sample Mann-Whitney test, with $p < 0.05$ considered as the significance threshold, was used to test the differences between the groups. Significant differences ($p < 0.05$) were observed in the knee extension during the terminal stance and swing, the peak knee flexion and the average abduction/adduction during pre-swing phase, average AP and ML knee joint movements, and the average area of distribution of AP-ML movements during the testing segment for the subjects from recovery stage-2 who were treated using biofeedback as a complementary tool, in comparison with the subjected treated without biofeedback. Moreover, significant differences ($p < 0.05$) were also noted in the normalized peak values for the vastus lateralis and vastus medialis muscles for all ambulation and balance testing activities. However, no significant differences were noted between the two groups (with biofeedback and without biofeedback) in the average rotation during pre-swing phase and normalized peak values for the hamstring and gastrocnemius muscle strengths. ***Table 10*** and ***Table 11*** show the p-values for different parameters for the subjects from recovery stage 2. Significant differences ($p < 0.05$) were observed only for the average knee extension angles during the terminal stance, average abduction/adduction during pre-swing phase, average AP and ML knee joint movements, average area of distribution of AP-ML movements during the testing segments and the normalized peak values of the strength of the vastus medialis in subjects from recovery stage 3 who were treated with biofeedback compared to those treated without biofeedback.

Table 12 and ***Table 13*** show the p-values for different parameters for the subjects from recovery stage 3. Hence, these results indicate prospects of using the developed system as part of existing rehabilitation monitoring procedures to achieve a more effective and timely recovery of subjects.

Table 12. p-values for different parameters using biofeedback for the subjects in recovery stage 3 during ambulation activities

Parameter Observed	***Normal Walking***	***Walking at 7km/h***	***Walking at 8km/h***
average knee extension angle during the terminal stance	0.043	0.042	0.040
average knee extension angle during the swing	0.047	0.045	0.045
peak knee flexion	0.205	0.172	0.175
average abduction/adduction during pre-swing phase	0.189	0.175	0.171
average rotation during pre-swing phase	0.221	0.198	0.199
normalized peak values for the vastus lateralis	0.181	0.210	0.205
normalized peak values for the vastus medialis	0.039	0.032	0.033
normalized peak values for the semitendinosus	0.162	0.092	0.090
normalized peak values for the biceps femoris	0.150	0.146	0.142

Table 13. p-values for different parameters using biofeedback for the subjects in recovery stage 3 during balance testing activities

Parameter Observed	***Single leg balance (EO)***	***Single leg balance (EC)***
average AP knee joint movements	0.041	0.040
average ML knee joint movements	0.047	0.045
average area of the distribution of AP-ML movements	0.040	0.042
normalized peak values for the quadriceps muscle strengths	0.028	0.021
normalized peak values for the hamstrings muscle strengths	0.210	0.197
normalized peak values for the gastrocnemius muscle strengths	0.150	0.135

4. Next Generation Smart Healthcare System for Professional Athletes

The need for smart healthcare system is ever increasing. Hence, more efforts are being made to transform reactive care to proactive and preventive care, clinic-centric to patient-centered practice, and episodic response to continuous well-being monitoring and maintenance. Due to easy availability of low-priced and high performance sensors and computational intelligent techniques such efforts can be turned into practical system. The combination of big data analytics, intelligent knowledge-based system and health informatics can help in creating a smart healthcare system (***Figure 10***).

Layered Architecture

As a future work, we propose a general layered/modular architecture for smart healthcare system for professional athletes (***Figure 11***). Brief description about each layer is given as follows:

Layer 1: This layer consists of different types of hardware components (e.g. motion sensors, EMG sensors, EEG sensors, motion capture system, video cameras, BP/heart-rate monitor etc.) for collecting various relevant physiological, biomechanical and video signals/data for analysis. The selection of hardware components depends on the type of training/activity to be analyzed.

Layers 2 & 3: Each sensor/hardware component may have its unique data collection method. Hence, appropriate techniques need to be employed for data acquisition, storage (if required) and then filtering and pre-processing. These methods may vary based on the real-time or off-line feedback required by the user.

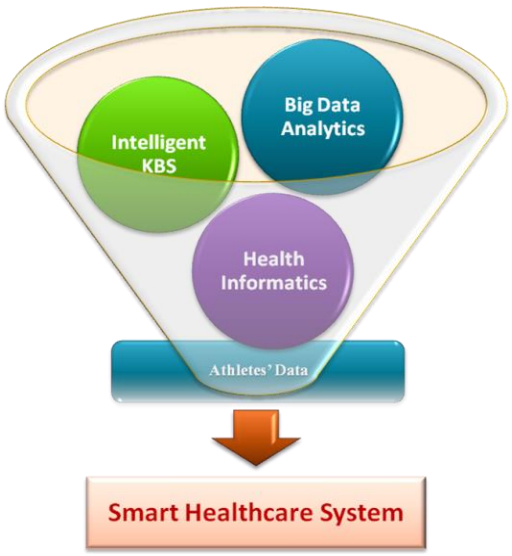

Figure 10. Smart healthcare system - major components and domains

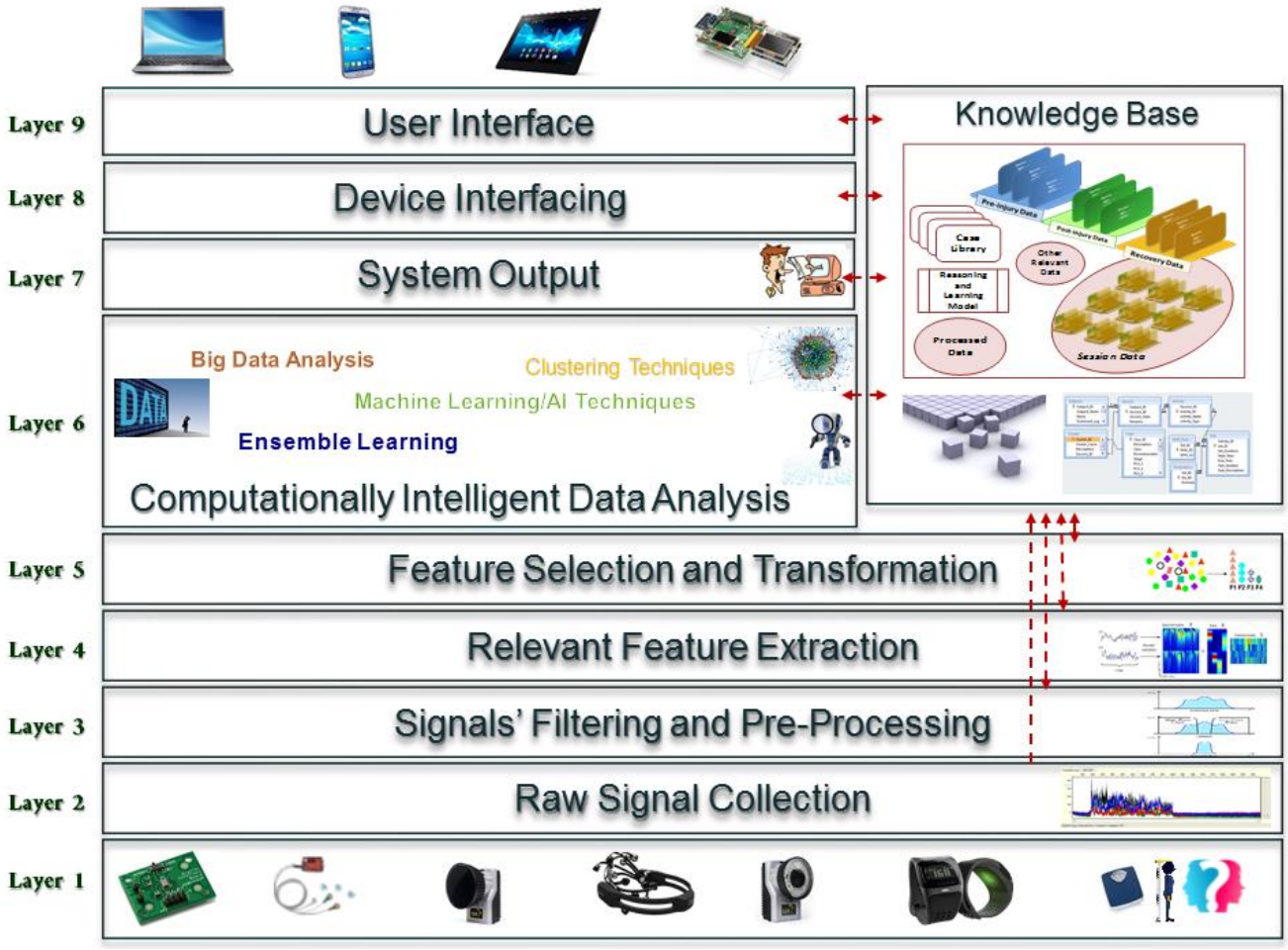

Figure 11. *Layered architecture of the proposed smart healthcare system*

Layer 4: From filtered and pre-processed data, relevant features for each type of signal will be extracted so that important information from the data can be gathered for further processing.

Layer 5: In order to efficiently apply the intelligent mechanism and retrieve the results, feature selection and transformation step may be required. This step is required for those types of signals where large number of features are available. Data fusion and integration techniques can be used for combining various types of signals.

Layer 6: Various intelligent data analysis techniques can be applied and explored in order to cluster and classification of the signals. Further, different intelligent techniques can be combined (if required) to achieve the best possible solution for classification and prediction problems. The possible usage of these techniques can be in the areas of grouping athletes based on different characteristics, recovery stage classification, classification of performance during a sports training activity, prediction of injury, prediction of time-to-return to sports, performance optimization and real-time/off-line biofeedback etc. Further, big data analytics can also be explored with the data collected from different sources (sensors, sports trainers, physiatrists and physiotherapists etc.) and stored in knowledge-base.

Layer 7: The system would be able to provide output in real-time and/or off-line. Accordingly, appropriate measures will be taken for data processing and extracting results from intelligent mechanisms.

Layer 8: The system output/biofeedback could be directed to different types of output devices

including computers/laptops and hand-held devices (mobile phones, tablets etc.) as well as to other wearable devices such as smart watches. Hence, a device interfacing mechanism would be required for directing the system output.
Layer 9: Appropriate data visualization and user-interface designing techniques will be used in order to provide easy to understand results for users of the system.

Knowledge management, design of efficient data retrieval mechanisms and data access and security issues will also be handled in the system design.

Possible benefits and contributions
Possible benefits and contributions of the Next Generation Smart Healthcare System for Professional Athletes are briefly mentioned below:

- Design of an extensible integrated framework for health/performance monitoring and intelligent diagnosis for Brunei Athletes
- Monitor and track record during various activities/sessions
- Centralize data obtained from multiple sources or devices, long-term data storage and analysis – suitable for longitudinal studies
- Predict changes in athletes' fatigue, recovery and performance readiness
- Prevent staleness and overtraining, reduce injuries
- Plan training based on the objective and scientific results, monitor and individualize training and recovery strategies more effectively
- Objective assessment → Improve motivation, build trust and involvement
- Real-time and offline feedback with accessibility (remotely) on multiple devices
- Development of healthcare data analysis expertise in Brunei – Exploring new venues
- Replication of the system for other than health informatics – Large scale data analysis

5. Conclusion

This study presented the summary of the overall results achieved and conclusions reached by developing and applying a novel approach for monitoring the recovery progress of the knee injured/post-operated subjects based on a knowledge-based framework using the hybrid intelligent techniques, visual biofeedback and multi-modal feature integration mechanism. The system has been implemented in such a way that additional tools and routines can be added based on more activities and features identified in the clinical environment. Thus, this system can be used as a complementary decision supporting tool, in conjunction with the existing rehabilitation monitoring mechanisms, to enable the clinicians, trainers and physiotherapists to objectively monitor the rehabilitation progress of athletes and their compliance to the rehabilitation protocol during different convalescence stages. This will help them accomplishing required training within specified time period and timely return to the pre-injury activities. Furthermore, based on the results achieved during the pilot study, a conceptual model for smart healthcare system for professional athletes has been proposed.

Acknowledgements
The authors acknowledge the Universiti Brunei Darussalam (UBD) for funding this research (Grant no. UBD/PNC2/2/RG/1(195) - 'Integrated Motion Analysis System') and providing academic and computing facilities to carry out this study. We would also like to acknowledge the staff at Performance Optimization Centre in the Ministry of Defence and the Sports Medicine and Research Centre in the Ministry of Culture, Youth and Sports, Brunei Darussalam for providing athletes as test subjects for this study and their continuous support and feedback during experiments. Further, this research grant led the completion of PhD of Owais A. Malik with significant outcomes as reported.

References

[1] T. E. Hewett, S. L. Di Stasi, and G. D. Myer, *Am. J. Sports Med.*, **2012**, 216-24.
[2] O. A. Malik, S. M. N. A. Senanayake and D. Zaheer, *IEEE Journal of Biomedical and Health Informatics*, **2015**, 453-463.
[3] O. A. Malik, S. M. N. Arosha Senanayake and D. Zaheer, *IEEE/ASME Transactions on Mechatronics*, **2015**, 2328-2339.

[4] S.M.N. Arosha Senanayake, O. A. Malik, M. Pg. Iskandar, D. Zaheer, *Applied Soft Computing*, **2014**, 127-141.
[5] O. A. Malik, *Ph.D. dissertation, Comp. Sc., Univ. Brunei Darussalam, Brunei Darussalam,* **2015**.

Implications of controlling factors in evolving reservoir quality of the Khatatba Formation, Western Desert, Egypt

Mohamed Ragab Shalaby[1, 2], Mohammed Hail Hakimi[3], Wan Hasiah Abdullah[4] and Md. Aminul Islam[1]

[1]Department of Geological Sciences, Faculty of Science, Universiti Brunei Darussalam, Jalan Tungku Link, Gadong, BE1410, Brunei Darussalam
[2]Geology Department, Faculty of Science, Tanta University, Tanta 31527, Egypt
[3]Geology Department, Faculty of applied Science, University of Taiz, 6803 Taiz, Yemen
[4]Geology Department, University of Malaya, 50603 Kuala Lumpur, Malaysia

**corresponding author email: ragab.shalaby@ubd.edu.bn*

Abstract

This paper sheds light on the role of petrophysical properties, framework grains and its textural properties, capillary pressure, diagenetic constitutions and events as controlling factors in evolving sandstone quality of the Khatatba Formation in the Western Desert, Egypt. Petrophysical analyses coupled with petrographic observations and diagentic studies have been carried out for many core samples in order to infer the controlling factors of reservoir quality. It has been observed that the sandstone quality of the Khatatba Formation have been adversely affected from well to well in the study area and from zone to zone in the same well and formation. Good- quality sandstones have been found with the porosity ranges from 10–17% and permeability ranges from 100 –1000 mD. The petrographic study indicates the presence of many open hydraulic fractures and dissolution phenomena which all took place in multiple phases during the late digenetic stage, leading to improvement in the reservoir quality. Dramatic reservoir quality deterioration has been recorded in many zones. The reduction of permeability and fluid pathways in addition to the mechanical compaction, solid bitumen occupying many pore spaces and fractures are observed in many zones. These cause major destroy in reservoir quality that leading to lowering the oil production compare to the initial estimation.

Index Terms: Khatatba Formation, formation damage, diagenesis, fractures, reservoir quality

1. Introduction

In the Western Desert of Egypt, the deep clastic reservoirs of the Jurassic age are an attractive petroleum exploration target. The Western Desert still has significant hydrocarbon potential, as recent oil and gas discoveries have suggested[1], with as much as 90% of oil reserves and 80% of gas in the Western Desert basins yet to be discovered[2]. The study area (***Figure 1***), lies in the northern part of the Western Desert between latitudes 30º 30"- 31º 30" N and longitudes 26º 30"- 28º 00" E.

The great oil potentiality of the Western Desert has attracted the interest of numerous researchers, authors, and oil companies. Several researchers and authors have made significant contributions related to the regional geology, petroleum prospects, source rock evaluation, sedimentology, and tectonic evolution of individual parts of the basin and adjoining areas[3-19].

The Middle Jurassic Khatatba Formation in the North Western Desert of Egypt has very good source-rock potential for hydrocarbon generation. Most of this generated hydrocarbon was expelled into coarse-grained sandstones within the Khatatba Formation, which is bounded by organic-rich shales that are source rock. The organic matter is mainly derived from the marine environment. Source-rock thickness, thermal maturity, and total organic carbon (TOC) contents

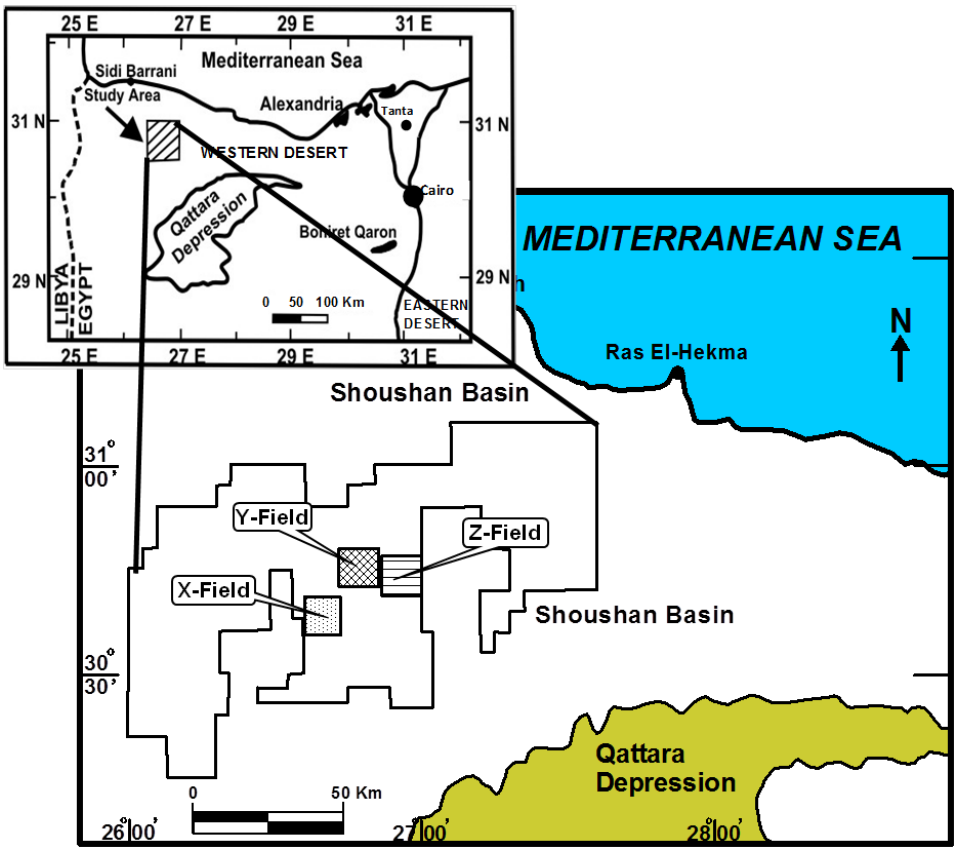

Figure 1. Location map for the study area in the North Western Desert of Egypt (modified after Shalaby et al., 2012)

controlled the amount of hydrocarbon generated and expelled from the shales. Source rock in these shales is mixed oil- and gas-prone[15-17]. The Khatatba Formation represent as the oil reservoir in the thermally mature part of the basin and have been extensively cored; thus, they offer the opportunity to examine major controls on reservoir quality. In this study, we have examined the porosity and permeability relationship of the reservoir sandstones, their close dependency on petrographic properties and diagenetic events considering the data analysed from three different producing oil fields namely X, Y and Z fields. Finally we have delineated the implications of different controlling factors in evolving the sandstone of the Khatatba Formation quality which is really critical for the area of study in terms of further exploration and production.

2. Stratigraphy and tectonic setting

The North Western Desert of Egypt consists of a number of sedimentary basins (***Figure 2***) that received a thick succession of Mesozoic sediments (***Figure 2***). The stratigraphic section of the North Western Desert (***Figure 3***) which includes the Shoushan Basin, ranges in age from Paleozoic to Tertiary. The post- Paleozoic succession in this area comprises four major cycles: Middle Jurassic, Lower Cretaceous, Upper Cretaceous, and Eocene to Miocene[4]. Each cycle begins with fluvio-deltaic siliciclastics and ends with marine carbonates[20].

The North Western Desert is characterized by a Paleozoic section overlying the crystalline basement. The Mesozoic–Tertiary sedimentary wedge is interrupted by an east–west trending structural high, which separates the Abu Gharadig Basin from a series of coastal basins. This pattern of basins and highs is masked under gently dipping, outcropping Miocene deposits[5,21]. The Shoushan Basin, which is the largest of the coastal basins, is a half-graben system affected by many tectonic faults (***Figure 2b***), with a maximum thickness of 7.5 km of Jurassic, Cretaceous, and Paleogene sediments[22-23].

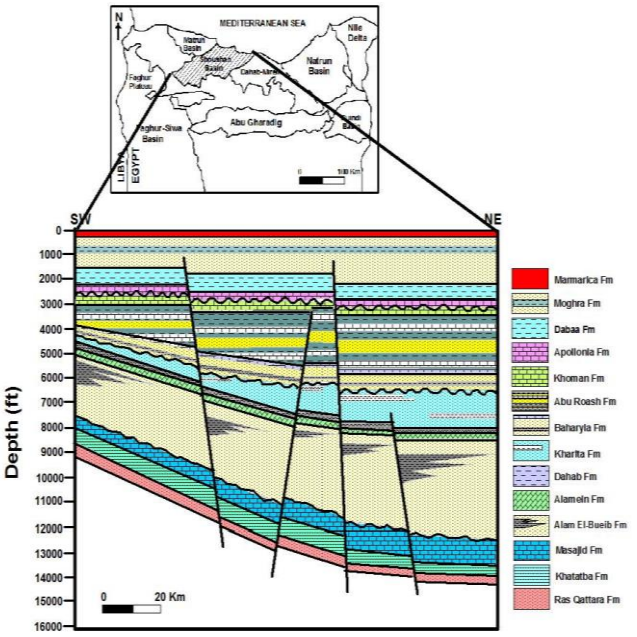

Figure 2. 2-D subsurface cross sectional view along some wells in the study area (Shalaby et al., 2013, modified after Al Sharhan and Abd El-Gawad 2008).

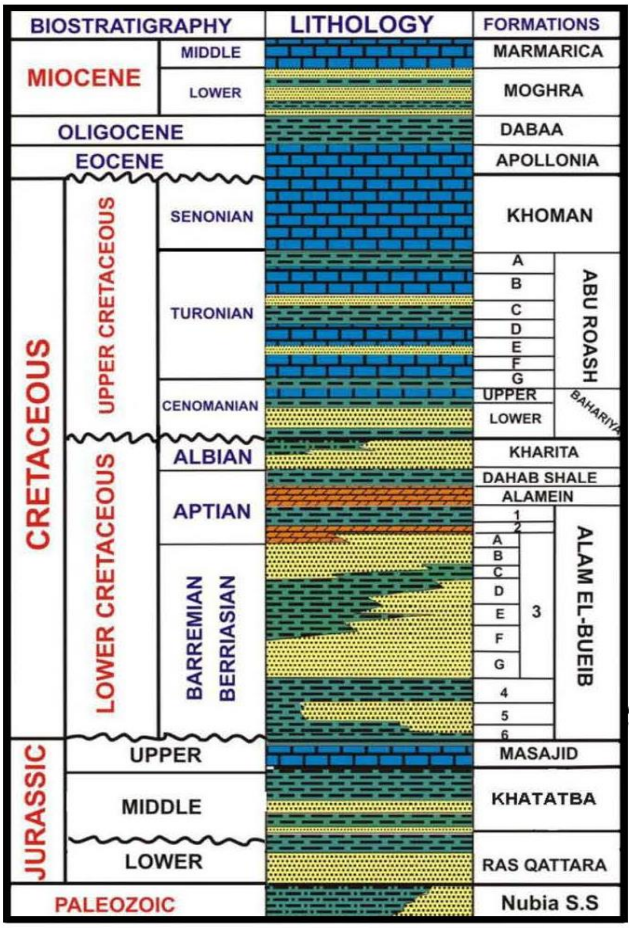

Figure 3. Simplified lithostratigraphic succession in the Western Desert of Egypt.

The earliest cycle consists of Early Jurassic non-marine siliciclastics (Ras Qattara Formation), which are underlain by the Paleozoic Nubian sandstone and are overlain by the Middle Jurassic Khatatba Formation (***Figure 3***). This Middle Jurassic Khatatba Formation is composed mainly of shales and sandstones, with a few shallow marine limestone beds. The Khatatba Formation overlies the Ras Qattara Formation and underlies the Masajid Formation and interpreted to be formed by fluvio-deltaic clastics grading upward into marine shales and limestones. The Khatatba Formation occurs in the subsurface and has been informally subdivided into lower and upper parts. The lower part of the Khatatba Formation is formed by meander-belt facies, which are overlain by an interval of braided-stream sandstones interbedded with coastal-swamp coals and carboniferous shales [24].

These sandstones are oil and gas reservoirs in some fields, whereas the coaly shale and shale facies represent the area's main hydrocarbon source rocks[26-28,18]. The coaly shales act also as seals, and thus, the Khatatba Formation represents a typical hydrocarbon source-seal-reservoir system. The upper part of the Khatatba Formation (***Figure 3***) is formed by shallow marine sandstones and shales, grading upward into a thin-bedded sequence of shale and limestone, which is a transitional unit toward the carbonates of the Masajid Formation. This formation is capped by unconformity, which records a period of uplift, tilting, partial erosion, and karstification of the Jurassic succession.[24,27]

The Upper Jurassic, shallow-marine carbonates of the Masajid Formation were deposited and represent the maximum Jurassic transgression. The Masajid Formation was either eroded from, or was not deposited on parts of the north Qattara Ridge and Umbarka Platform, although continuous marine sedimentation occurred in the Matruh sub-basin and in the SidiBirrani area. A major unconformity separates the Masajid Formation from the overlying Alam El Bueib Formation at the base of the second cycle, whose basal interval is composed of Early Cretaceous shallow-marine sandstones and carbonates. These

are followed by marine shale and a succession of massive fluvial sandstones. The sands are overlain by the alternating sands, shales, and shelf carbonates of Alam El Bueib, culminating in the Alamein dolomite associated with the Aptian transgression[25]. The Dahab shale marks the end of this cycle. The continental and shoreline sandstones of the Kharita Formation are overlain by the shallow-marine and nearshore deposits of the Bahariya Formation (Early Cenomanian). A marked deepening of depositional conditions is indicated by the deposition of the Abu Roash (G) Member (Late Cenomanian). Widespread transgression occurred during the Senonian time with deposition of the Abu Roash (F) to (A) Members (predominantly carbonates). The unconformably overlying the Khoman Chalk Formation was deposited only in the North Western Desert of Egypt. The cycle is terminated by an unconformity, above which lies the Eocene Apollonia Formation. Above this are the Dabaa and Moghra formations (marine clastics), which are capped by the Marmarica Limestone[2].

3. Experimental approach

Several core plug samples for the sandstone of the Khatatba Formation have been collected from three different oil fields in the study area in order to carry out the sedimentological studies and petrophysical analyses. Data have been obtained from the X, Y, and Z fields in the North Western Desert of Egypt. The petrophysical study has been carried out on some given samples, where the main parameters available were porosity, horizontal, and vertical permeability values. The petrographic studies have been completed using thin sections under polarizing microscope and scanning electron microscope (SEM). JEOL FESEM JSM 7600F SEM machine has been used to get better images in order to delineate the impact of different controlling factors on the evolution of reservoir quality. Standard thin sections have been prepared and were impregnated with blue epoxy to aid in the identification of pore spaces and open natural fractures, and they were stained to facilitate mineral identification. All thin sections were studied petrographically, and the diagenetic processes and products were analysed and described in detail in order to evaluate the mineral composition, cements, and pore spaces. A scanning electron microscope (SEM) study has been done, to confirm the identification of the different clay minerals, to determine the pore structure, and to determine the mode of clay occurrence within the pore spaces in the reservoir core samples.

4. Results and Discussion

Petrophysical analysis and reservoir properties: Porosity-permeability relationships

The petrophysical studies of the selected samples from the X, Y and Z fields indicate that the Khatatba sandstone is characterized by a wide variation of porosity and permeability data. We have been observed the presence of two distinctive zones or groups, each one with its own distinctive properties. Group-I or "good quality reservoir," is characterized by high porosity and permeability values. On the other hand, the Group-II or, "poor quality reservoir", is suffering big destruction of the petrophysical parameters in terms of porosity and permeability in that interval. This wide variation of results has been observed from well to well in the same field or from zone to zone in the same well, which can affect the productivity of reservoirs.

In the X-Field, the data are obtained from the X-3 and X-6 wells. It is observed from both a porosity-permeability relationship and a horizontal-to-vertical permeability relationship, (***Figure 4a*** and ***4b***), that the Khatatba sandstones show the presence of two distinctive separations between X-3 and X-6 wells. All plotted points from X-3 (***Figure 4a*** and ***4b***) are located in the upper right side of both graphs, which feature high porosity and permeability, while all plotted points from X-6 are located in the lower left side, at which low porosity and permeability are recorded (***Figure 4a*** and ***4b***).

In X-3, 56 data points have been plotted, while all available data reflect the presence of good reservoir quality, which is characterized by very good and optimistic petrophysical results. The measured core porosity is very high when accompanied by both vertical and horizontal

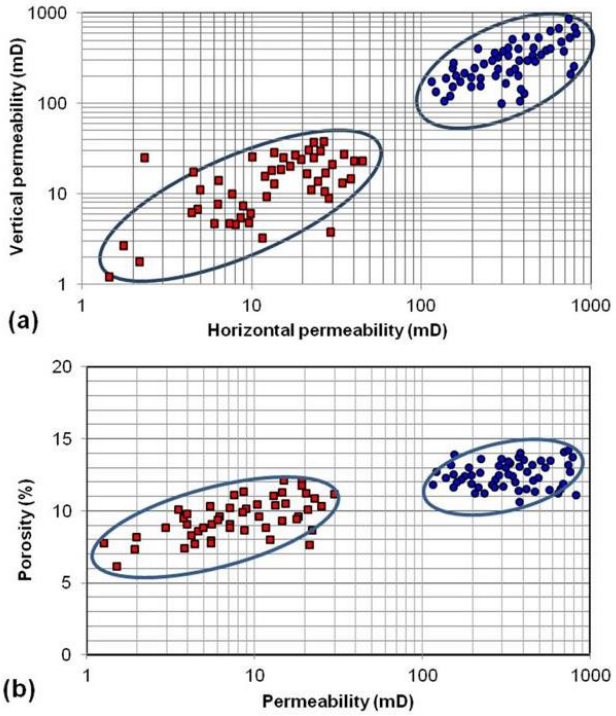

Figure 4. Cross plots showing two groups of reservoir quality in X Field: a) vertical permeability vs horizontal permeability, b) porosity vs permeability.

permeabilities, indicating good quality reservoir zones in this well. Porosity values are in the ranges of 10.6–14.2%. High permeability is recorded, while the horizontal permeability (HK) range is from 115 - 819 mD and the vertical permeability (VK) range is from 100 - 851mD (***Figure 4a*** and ***4b***).

In the X-6 well, in which 49 samples have been collected (***Figure 4a*** and ***4b***), it is found that a reduction in both porosity and permeability has been recorded. Porosity values are in the range of 6.1–12%, which is accompanied by a severe reduction in permeability in both directions. The HK recorded was 1.4– 44.7mD, while the VK was in the range of 1.2–37mD.

The results prove that the Khatatba sandstone in X-3 is characterized by very good reservoir properties in terms of porosity and permeability. They also indicate very good permeable zones, which allow the fluid to migrate and increase the productivity of the formation. In case of X-6, the data reflect that the formation has been subjected to the effect of formation damage in that well.

The petrophysical study has been carried out on data collected from the Y and Z fields. The Z-23 and Y-2X wells have been selected to study the reservoir characterization and changes in petrophysical parameters in both wells (***Figure 5*** and ***6***). A total of 62 samples have been analysed from the Z-23 well, while 44 samples have been analysed from the Y-2X well. It is observed that the Khatatba sandstone in both wells has been classified into two distinctive zones (***Figure 5*** and ***6***).

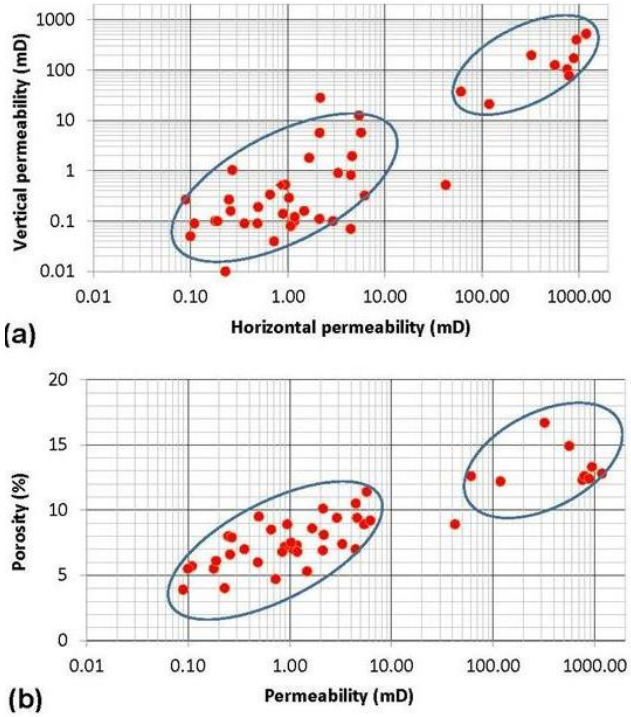

Figure 5. Cross plots showing two groups of reservoir quality in Y-2X Well: a) vertical permeability vs horizontal permeability, b) porosity vs permeability.

The same observations have been recorded in the Y-2X well (***Figure 5a*** and ***5b***). Two distinctive zones have been detected with specific petrophysical parameters. Zone-1 has good reservoir quality and is plotted in the upper right side in both graphs (***Figure 5a*** and ***5b***). Porosity is observed to be very good, in the range of 12–17%. Horizontal and vertical permeabilities are recorded as 20-600mD and 60–1300mD, respectively.

The zone affected by poor reservoir quality is presented in the lower left side in both cross-plots (***Figure 5a*** and ***5b***). Severe reduction in permeability is observed which reflects very low values in the range of 0.01–10.5mD and 0.09 - 7mD for both horizontal and vertical permeability respectively. Porosity in this zone is considered high where it records the values as being from 4–11.5%, but this zone is suffering severe destruction in permeability in both directions.

In the Z-23 Well (***Figure 6a*** and ***6b***), the first group (in the upper right portion of the graphs) indicates good reservoir quality with high porosity and permeability. Porosity values are in the range of 8 - 17%, which is accompanied by the excellent horizontal and vertical permeabilities of 11-1000 and 30 – 2000mD respectively.

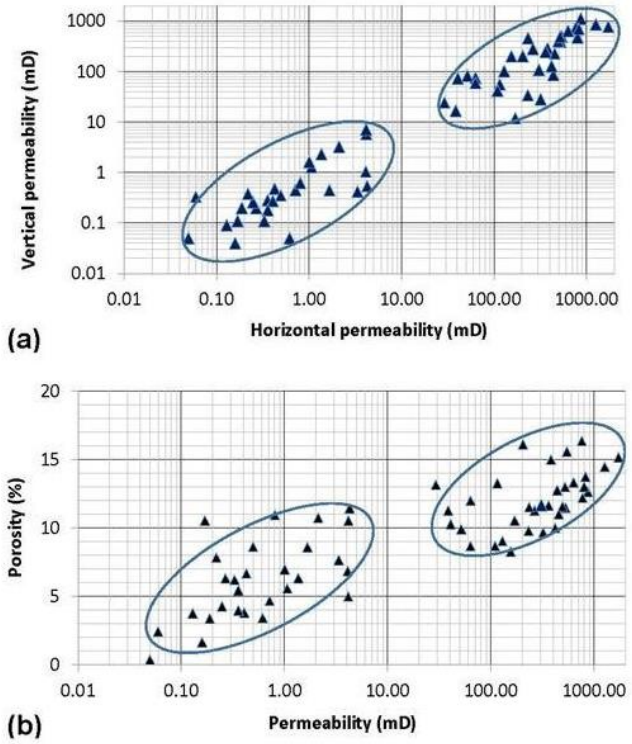

Figure 6. Cross plots showing two groups of reservoir quality in Z-23 Well: a) vertical permeability vs horizontal permeability, b) porosity vs permeability.

The second group is plotted in the lower left side of both graphs, and it reflects very low porosity and permeability. Permeability values are recorded in the range of 0.05 – 5mD and 0.02 - 9mD for vertical and horizontal permeabilities respectively (***Figure 6a*** and ***6b***). Porosity is quite low, with recorded values ranging from 0 - 11.2%.

Petrographic description and reservoir properties

The petrographic and sedimentological studies have been carried out on some samples selected from the three oil fields. It was important to study the petrography of the Khatatba sandstones using thin sections and SEM analyses. This may help to estimate the origin and evolution of porosity and permeability and the presence of any diagenetic processes that influenced the reservoir quality.

The classification of Pettijohn et al. (1987)[29] was used for the description of the studied samples. The petrographic study indicates that the Khatatba sandstones are mostly quartz arenite, composed of more than 90% quartz and about less than 3% of non-quartz content (***Figure 7***). Most framework grains are mostly subangular to subrounded with some rounded grains (***Figure 7a*** and ***7c***), and are generally moderately to well- sorted[19]. Khatatba sandstones are mainly composed of varying grain sizes ranging from fine, medium, and coarse to very coarse sand (***Figure 7b*** and ***7d***). The histograms showing the variations of grain size in some selected samples of Khatatba sandstone in the X-Field are illustrated in ***Figure 7b*** and ***7d***.

The petrographic observations are consistent with porosity-permeability relationships (***Figure 4*** and ***6***) showing the presence of both primary and secondary intergranular pore types in the studied core samples. The porosity and permeability have been affected by different factors, leading to classifying and discriminating the plotted points into two different groups of data sets. One group represents the good reservoir-quality zones with good petrophysical parameters, while the other group represents the areas that are suffering poor reservoir quality.

In X Field

The petrographic description has been carried out in order to discover the reasons for the variation in the porosity and permeability of the Khatatba sandstones between the X-3 and X-6 wells (***Figure 8*** and ***9***). The petrographic description of the X-3 well, which has high porosity and

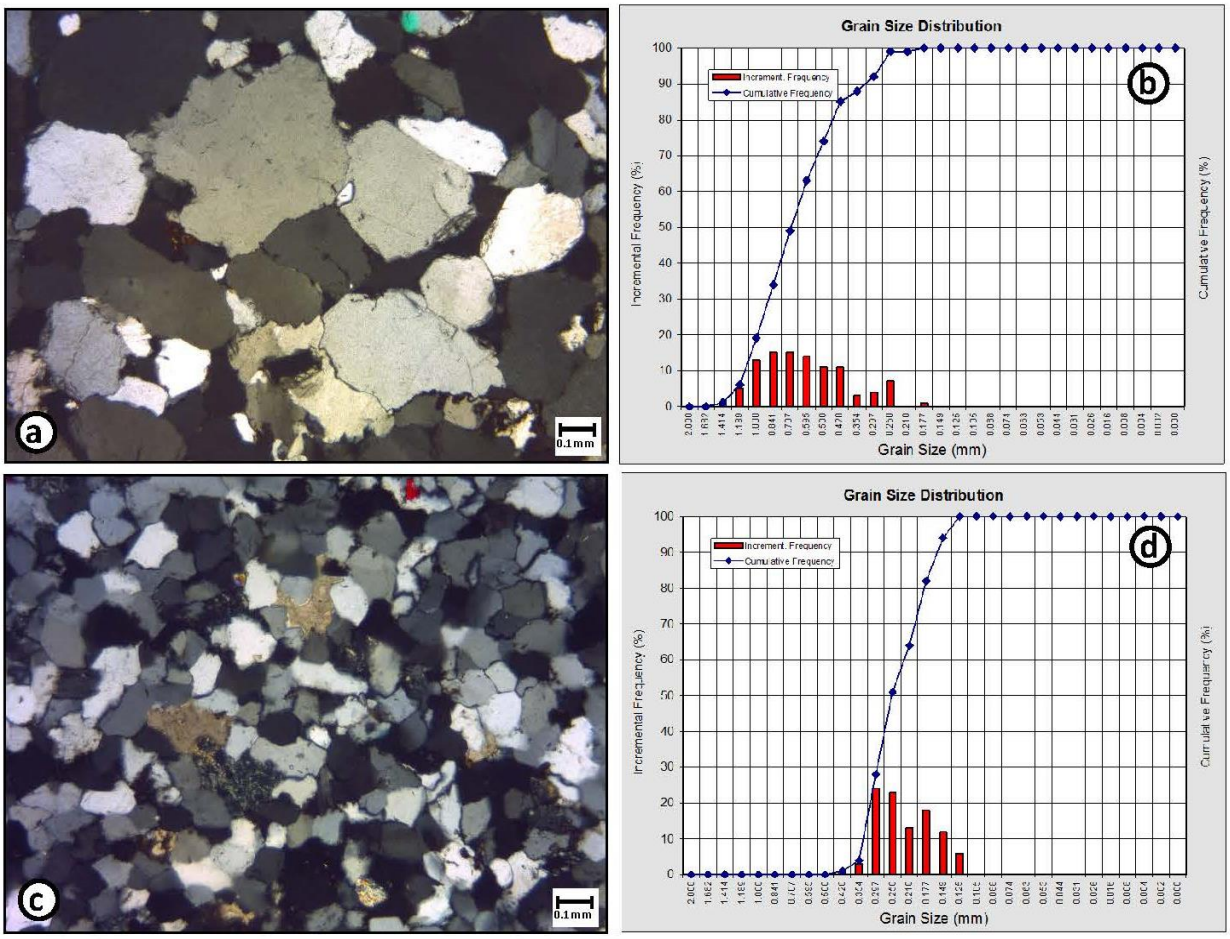

Figure 7. Grain size and grain shape in the Khatatba Sandstone in the study area. a & b) coarse grain sandstone with average grain size, c & d) fine grain sandstone with average grain size.

permeability, is illustrated in ***Figure 8***. Coarse to very coarse sandstones are observed (***Figure 8a*** and ***8c***), while primary pores are the abundant pore types (***Figure 8a*** and ***8b***). The porosity values of good-quality Khatatba sandstones in the X-3 well fall within relatively high values ranging from 10 - 14%; see ***Figure 4***. The increasing porosity and permeability of the Khatatba sandstone in the X-3 well reflect the presence of less-advanced diagenesis. This is associated with the dissolution processes (***Figure 8d***), which increase the porosity and permeability.

Petrographic observations in the X-6 well (***Figure 9***) show a reduction in porosity and permeability that is also coincident with petrophysical parameters (***Figure 4a*** and ***4b***). This may indicate that porosity in the sandstone interval of the X-6 well is severely affected by mechanical compaction and mineral cementation. Calcite cement splashes all over the quartz grains, filling all pore spaces (***Figure 9b***). According to thin-section observations, the clay minerals in the sandstones consist mainly of kaolinite (***Figure 9a*** and ***9c***). Authegenic kaolinite staining with bitumen is observed to be filling in the pore spaces between the detrital quartz grains (***Figure 9d***). The dispersed kaolinite is easily recognized as the most abundant clay mineral with variable amounts. Kaolinite has been interpreted as a by-product at the expense of K-feldspar at a temperature greater than 100^{o}C[30] and belongs to the late diagenetic history. Bitumen is found to be invading all primary and secondary pore spaces[17] and permeable zones (***Figure 9b, 9c*** and ***9d***). This also implies that porosity reduction was due to a decrease in grain size and an increase in cement. Thus, the porosity reduction appears to be pre- and post-depositional controlled. The detrital quartz grain contacts are transformed from point to long

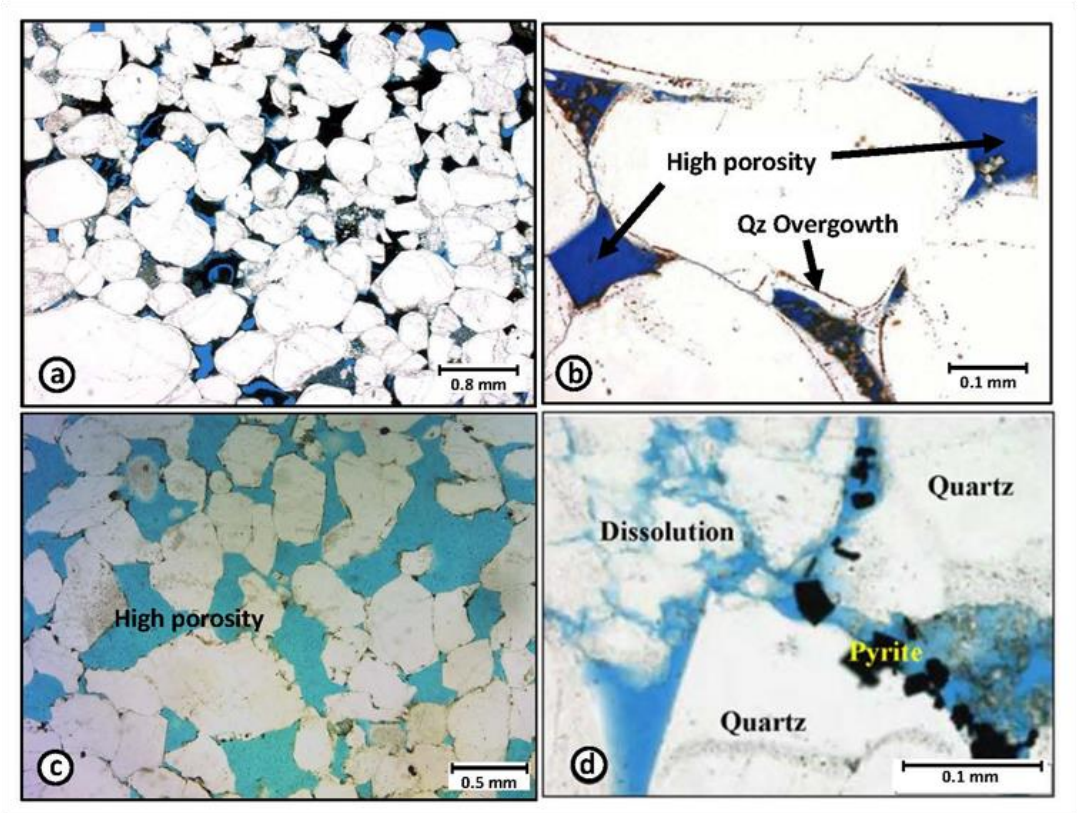

Figure 8. Good quality reservoir in sandstone of the Khatatba Formation in X-Field. a & c) primary intergranular porosity in quartz arenit sandstone with low diagenetic effect. b) Quartz overgrowth affecting some detrital grain with no effect on porosity. d) Dissolution of quartz grains increasing permeability with some pyrite cube indicating reducing environment.

and concavo-convex contacts due to sever mechanical compaction, which reduce the permeability (***Figure 9d***). SEM images have been taken (***Figure 9e*** and ***9f***) showing kaolinite filling the pore spaces between Qz grains, (***Figure 9e***). It is also observed that pyrite cubes are available, indicating a reducing environment (***Figure 9f***).

In Y Field

In the Y-2X well, the visible, intergranular porosity in the Khatatba Formation is related to the abundance of natural open hydraulic fractures that occurred during the higher mechanical compaction process (***Figure 10***). Increasing vertical permeability when compared to horizontal permeability in all examined samples can be interpreted to the presence of these open hydraulic fractures and secondary porosity (***Figure 10b***). The examined thin sections indicate that the primary porosity is abundant (***Figure 10a*** and ***10c***), and it is recorded at a high percentage (12 – 17%). The good-quality zones of the Khatatba sandstones in the Y-2X well are characterized by a very wide range of permeability more than 1000mD (***Figure 5a*** and ***5b***). It can be concluded that, the permeability values increase due to the pervasiveness of primary porosity and secondary porosity, represented by a large number of intergranular pores (***Figure 10a, 10b*** and ***10c***) and the presence of open macro and micro fractures (***Figure 10b***).

The intervals suffering low reservoir quality in the Khatatba sandstone in the Y-2X well reflect a slightly lower measured core porosity in the range of 4 - 11.5% (***Figure 11***). Petrographic observations are also coincident with petrophysical parameters showing that porosity and permeability in this sandstone interval are severely affected by mechanical compaction and mineral cementation (***Figure 11a - d***). Authegenic kaolinite is found to be filling all primary pores between the quartz grains (***Figure 11a*** and ***11c***). Quartz overgrowth (***Figure 11c***), which acts as a

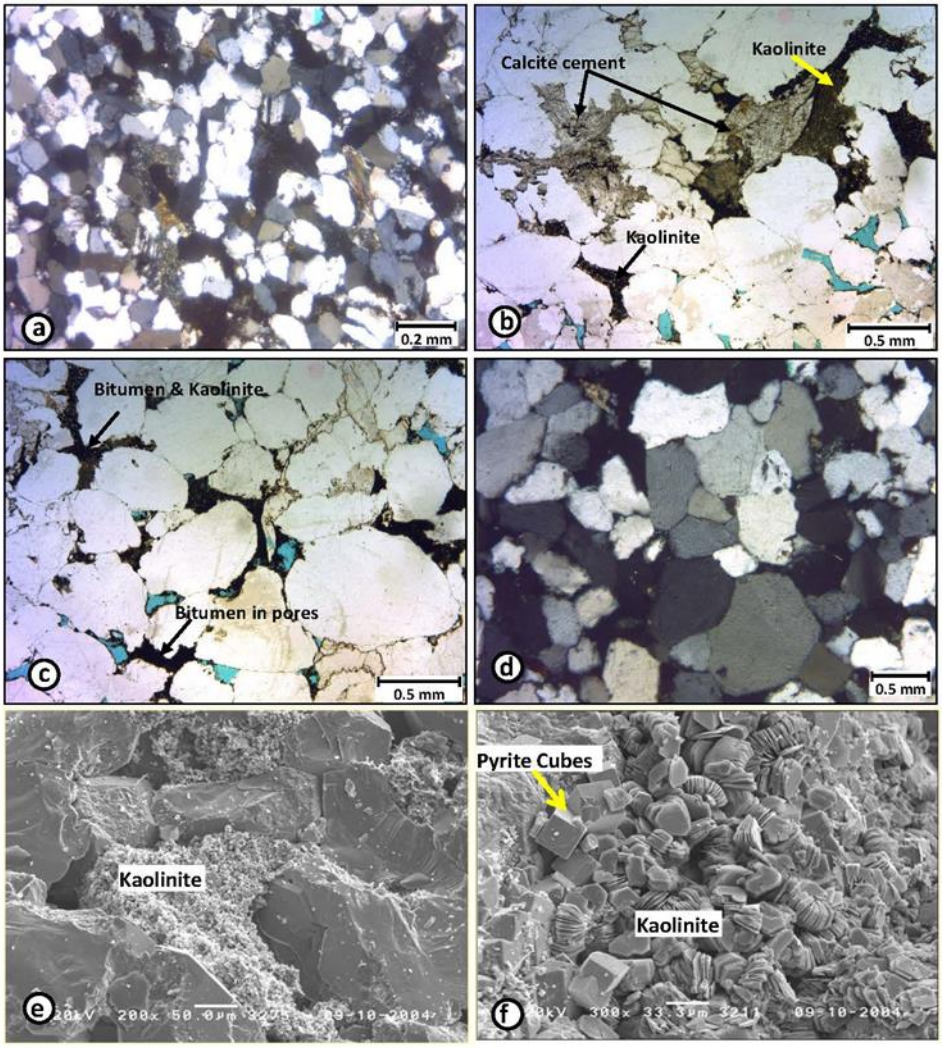

Figure 9. Low quality reservoir in the Khatatba Formation in X-Field. a & b) authigenic kaolinite and calcite cement filling the pore spaces, c) bituminous material with kaolinite filling in most of primary porosity, d) mechanical compaction, point, long, concavo-convex contacts are available, e & f) SEM image showing Kaolinite filling the pore spaces between Qz grains, f) Pyrite cubes are available for reducing environment.

pore-occluding phase, coupled with the authegenic kaolinite is destroying the porosity and permeability of the sandstone. Bitumen is also detected as blocking all available pore spaces and permeable zones (***Figure 11b*** and ***11c***). It is also filling all fractures and small fissures (***Figure 11d***) found in the sandstone of the Khatatba Formation in the Y-2X well, leading to severe loss in both porosity and permeability. Thus, the pervasive secondary porosity represented by a large amount of macro and micro fractures found in the good reservoir interval has been destroyed in the poor quality interval. These permeable zones have been sealed or blocked due to the invasion of bituminous materials in the permeable zone in addition to mechanical compaction as well as, carbonate and kaolinite cement precipitation (***Figure 11***).

In Z-Field

The petrographic descriptions of thin sections in the Z-23 well (***Figure 12*** and ***13***) indicate the presence of a higher number (8 - 17%) of primary intergranular pore types (***Figure 12***). Less diagenetic processes allow the formation to retain more permeability [VK: 30 - 2000mD, HK11 - 1000mD] (***Figure 12a, 12b*** and ***12d***). Increasing vertical permeability is also attributed to the presence of many open fractures and fissures, which are not affected much by diagenesis or any

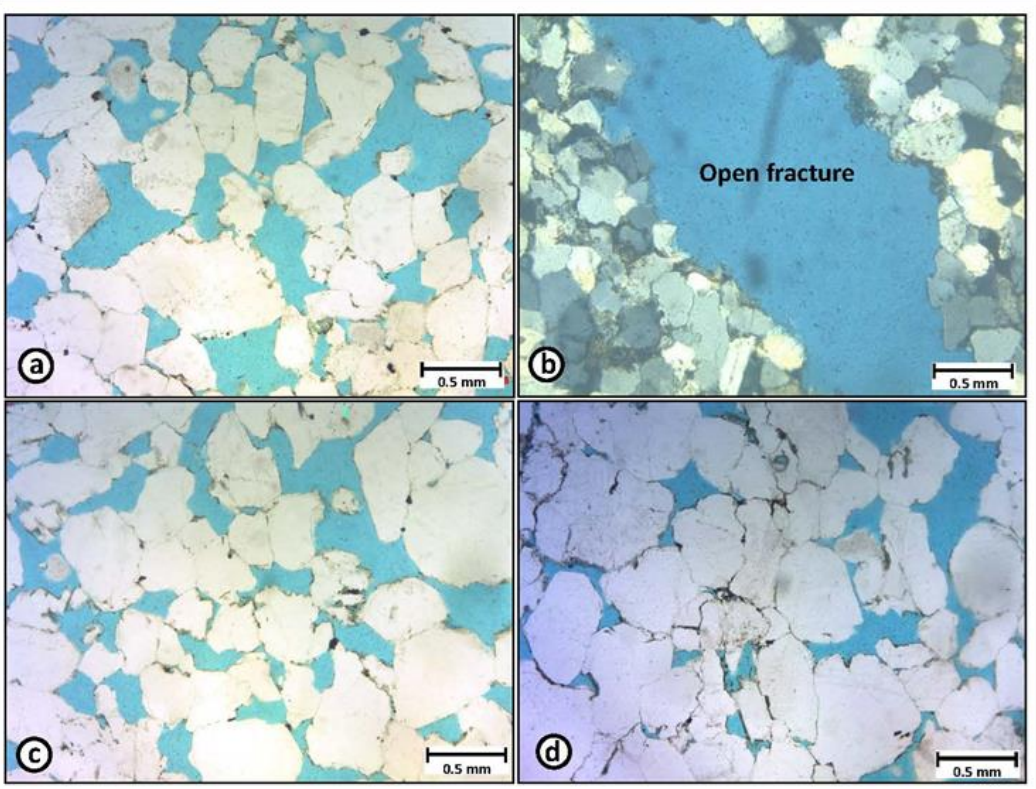

Figure 10. Good quality reservoir in sandstone of the Khatatba Formation in Y Field. a, c & d) primary intergranular porosity in quartz arenit sandstone with no diagenetic effect, and b) Open micro and macro fractures enhancing permeability.

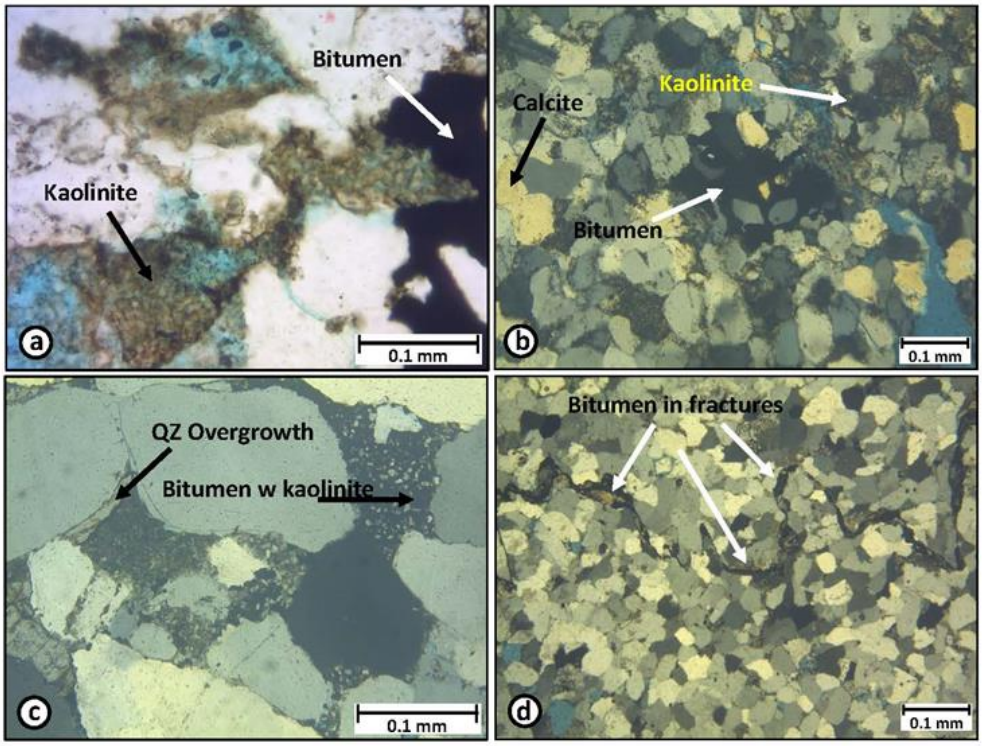

Figure 11. Low quality reservoir in sandstone of the Khatatba Formation in Y Field. a) authigenic kaolinite filling the pore spaces, b) bituminous material filling in most of primary and secondary porosity, c) quartz overgrowth together with kaolinite staining with bitumen, and d) micro fractures are fully occupied with bitumen.

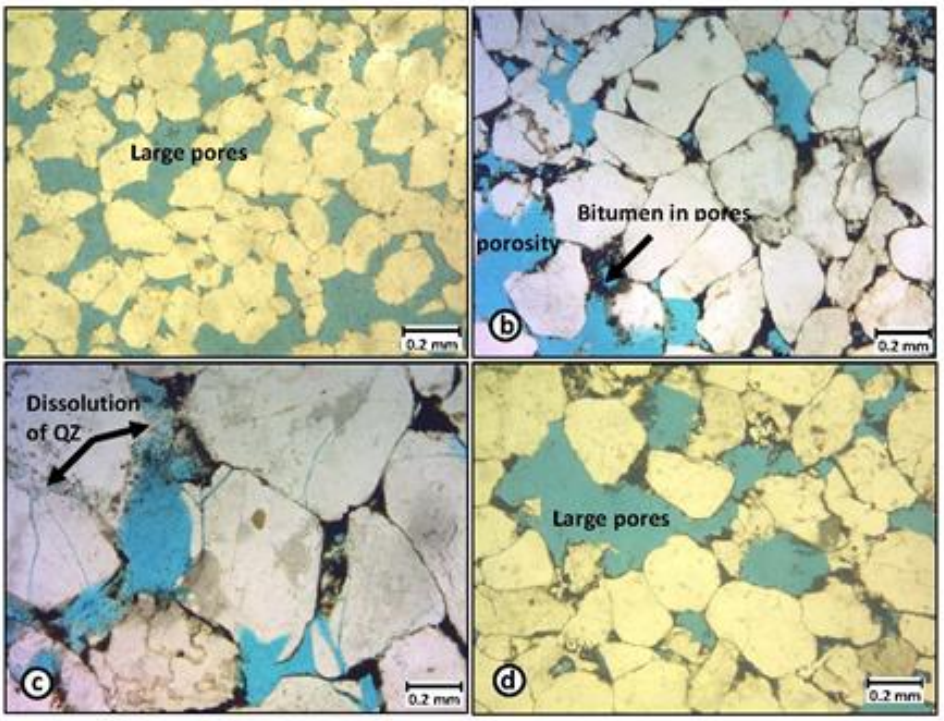

Figure 12. Good quality reservoir in sandstone of the Khatatba Formation in Z-Field. a) Primary intergranular porosity in quartz arenit sandstone with no diagenetic effect, b, c, & d) primary intergranular porosity containing few bitumen with no effect on permeability, c) dissolution of detrital quartz grain increasing porosity and permeability.

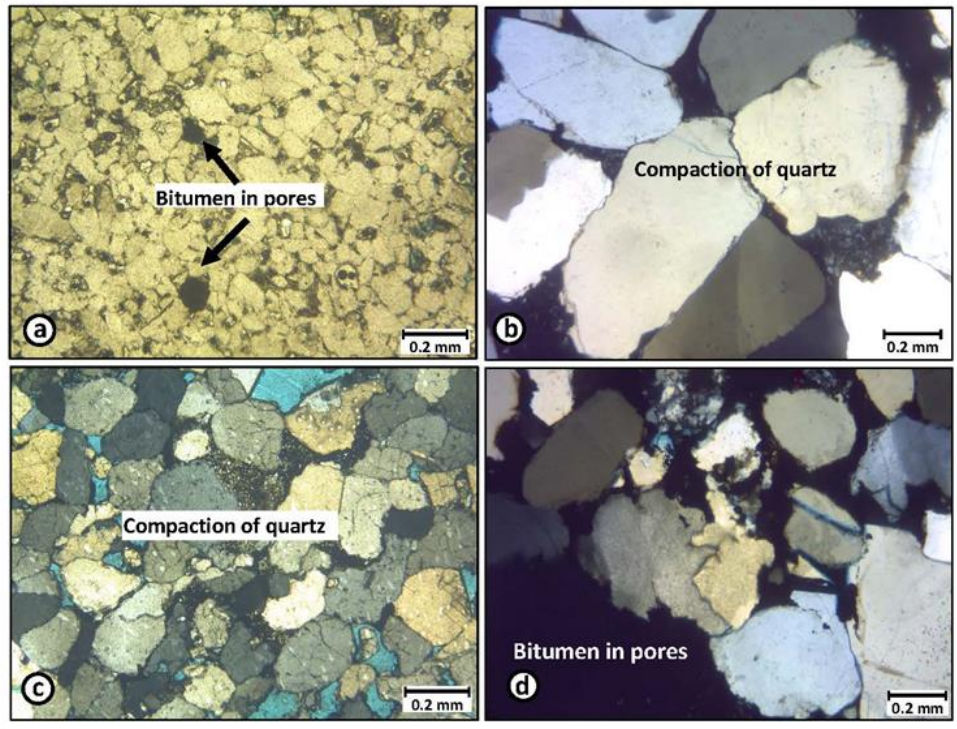

Figure 13. Low quality reservoir in sandstone of the Khatatba Formation in Z-Field. a) fine grain sandstone with bitumen blocking all pore spaces, b & d) severe compaction with kaolinite and bitumen in the remaining pores, c) crushed quartz grains by severe compaction.

formation damage. The process of dissolution is another important agent that has been recorded as enhancing the porosity and permeability of good reservoir zones in the Z-23 well. The dissolution of authigenic mineral or grains can enhance the secondary porosity type[31]. Reservoir quality of the good Khatatba sandstones in the Z-23 well is affected to some degree by dissolution, which enhanced the reservoir porosity and permeability (***Figure 12c*** and ***12d***). This resulted from the dissolution of carbonate cement and, detrital quartz grains. Evidence of dissolution has been detected, including corrosive contacts (***Figure 12c***). The presence of some bitumen trying to occupy the pore spaces has also been observed. Fortunately, a small amount of bitumen accompanied by the dissolution of quartz helps the formation to maintain good porosity and permeability when compared with the other damaged reservoir (***Figure 12b, 12c*** and ***12d***).

In the Z-23 well, poor quality reservoir zones are also observed in the sandstone of the Khatatba Formation in many samples, reflecting a sharp reduction in permeability, with a very low permeability value of less than 10mD. The maximum recorded permeability was 5mD and 9mD for both vertical and horizontal permeability respectively (***Figure 6a*** and ***6b***). Porosity is observed as being inversely correlated with digenetic processes represented by quartz overgrowth and authegenic clay mineral in the form of kaolinite (***Figure 13***). The occurrence of kaolinite as a result of the post-depositional dissolution of Khatatba sandstones indicates that k-feldspar was previously more widespread before they were getting dissolved. All digenetic features have been observed to be affecting the detrital quartz grain contacts. ***Figures 13b, 13c*** and ***13d*** show the presence of point, long, and concavo-convex contacts due to severe mechanical compaction, which results in reduction of porosity. Black-colored bituminous materials are also detected as filling in the pore spaces and blocking all pores and permeable zones (***Figure 13b*** and ***13d***).

Capillary pressure and reservoir properties

The role of diagenesis in the formation damage of the Jurassic Khatatba Formation is interpreted on the basis of pore size, pore geometry, and capillary pressure relationship. Reduction in pore throat and pore size increases the capillary pressure of the sandstone of the Khatatba Formation, leading to the destruction of permeability. In petrophysical analyses, the high pressure mercury injection has been applied to some selected samples at different depths in both the X-3 and X-6 wells. In X-3, the selected sample depths are at 13193 and 13208 ft., while in X-6, they are at 13388, 13419, and 13423 ft (***Figure 14*** and ***15***). It is found that the pressure relationship shows a typical drainage capillary pressure curve obtained by displacing the wetting phase from a porous medium with a non-wetting phase. The drainage capillary pressure curve shows that a minimum positive pressure (Pd) must be applied to the non-wetting phase in order to initiate the drainage[32]. This minimum pressure, which is known as the displacement pressure (Pd), is considered to be the threshold pressure or the entry pressure, which affects the size of the largest pores connected to the surface of the medium.

Tiab and Donaldson (2004)[32] concluded that, if the rock does not have a strong wettability preference for the initially saturating fluid, then the displacement pressure will be zero. If the rock has a strong preference for the displacing fluid, then no pressure is required in order to initiate the displacement because it will occur spontaneously. In this case, the capillary pressure will start at the initial fluid saturation of less than 1. As the pressure of the non-wetting phase is increased, smaller and smaller pores are invaded by the non-wetting fluid. Eventually, the wetting phase becomes discontinuous and can no longer be displaced from the medium by increasing the capillary pressure. Therefore, the irreducible wetting-phase saturation is achieved for the porous medium at a high capillary pressure. They also mentioned that at the irreducible wetting-phase saturation, the capillary pressure curve becomes nearly vertical. The irreducible wetting-phase saturation is a function of the grain size (pore size), the wettability of the medium, and the interfacial tension between the wetting and non-wetting fluids.

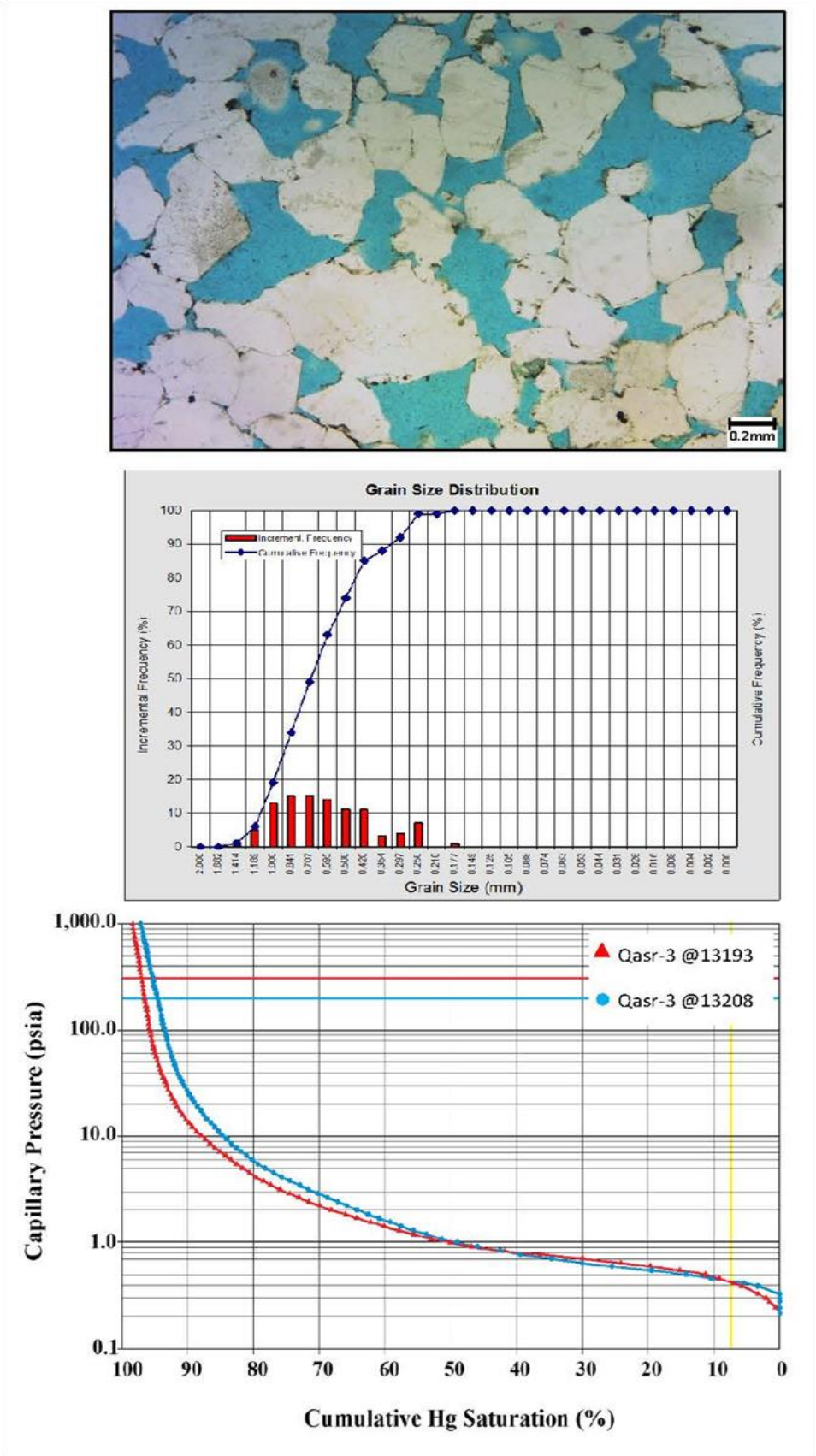

Figure 14. Shows the relationships between grain size, pore size, and capillary pressure. Low displacement pressure is recorded for high porosity, coarse grain sandstone

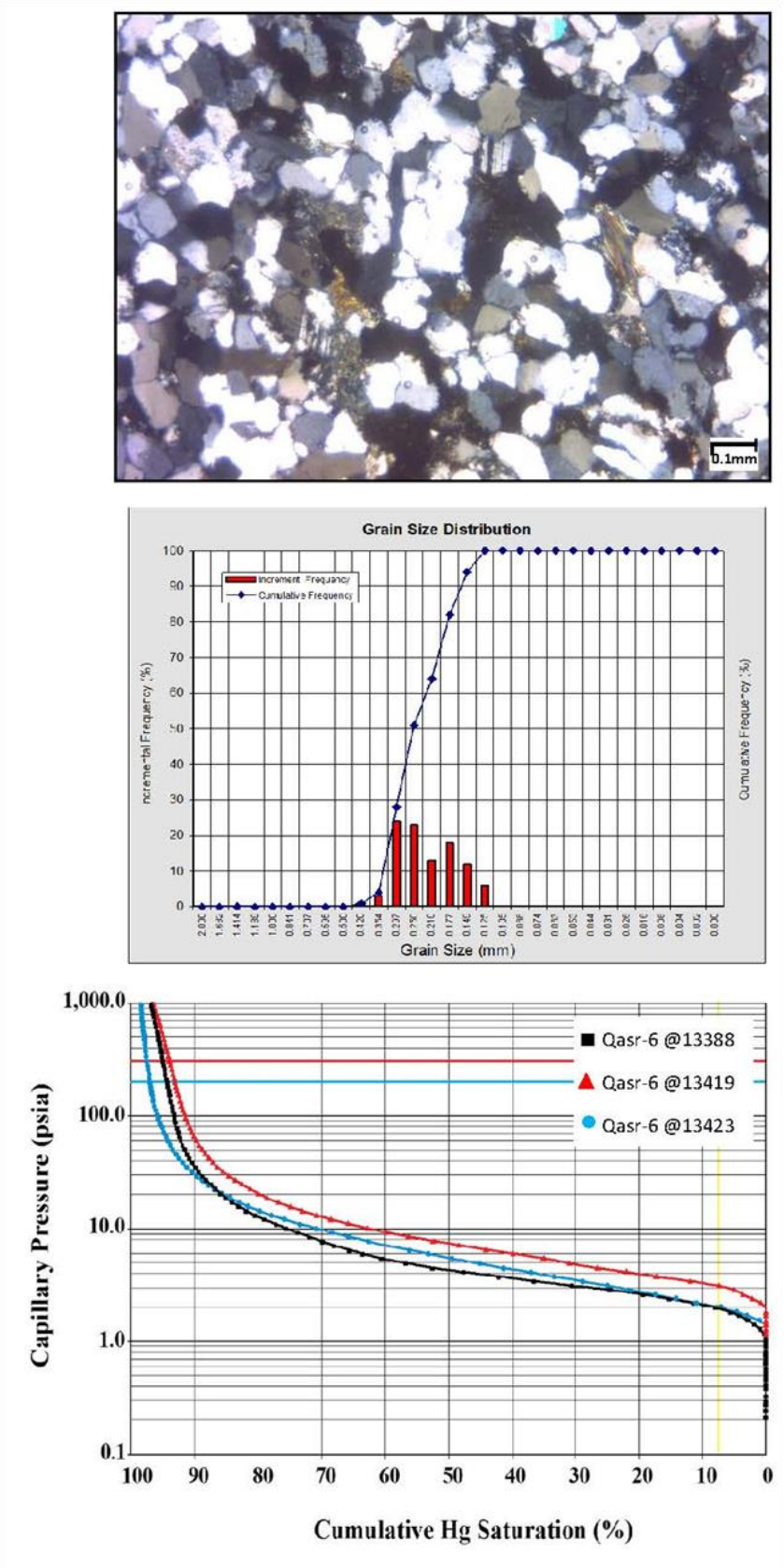

Figure 15. Shows the relationships between grain size, pore size, and capillary pressure. High displacement pressure is recorded for low porosity, fine grain sandstone.

Figures 14 and ***15*** show the relationship between grain size sorting, pore size distribution, and capillary pressure in both the X-3 and X-6 wells. ***Figure 14***, for the X-3 well, shows very good porosity in coarse-grain Khatatba sandstone (***Figure 14a***). The grain size distribution (***Figure 14b***) shows very coarse sandstone in the range of 0.250mm to 1.189mm, and all grains are homogenous and moderately well-sorted. The drainage capillary pressure curves for samples selected from X-3 (***Figure 14c***) have the least displacement pressure. Therefore, it has the largest pores connected to the surface. Its capillary pressure curve remains essentially flat as the wetting-phase saturation is decreased from 100% to 80%. This means that many of the pores are invaded by the non-wetting fluid at essentially the same capillary pressure. This indicates that the sandstone of the X-3 well has uniform pores or is well-sorted, which is consistent with data given in previous ***Figures 4*** and ***8***. It also reflects the least irreducible wetting-phase saturation (***Figure 14c***), indicating that it has relatively larger grains associated with large pores. The displacement pressure is very small, and it measured as 0.2 - 0.3 psi, which indicates that the sandstone is a coarse-grain, high- porosity reservoir.

The sandstone of the Khatatba Formation in the X-6 well, (***Figure 15***), is characterized by very fine to medium sand size (***Figure 15a***). The presence of fine- grained sand in combination with feldspar and authigenic kaolinite (***Figure 15a***) filling in the pore spaces is the result of a high reduction in porosity and permeability in that well. The grain size distribution is observed in ***Figure 15b***, which reflects fine to medium sand in the range of 0.125mm to 0.297mm. Capillary pressure curves in the X-6 well (***Figure 15c***) show higher displacement pressure when compared with those of the X-3 well. It is measured as 1–2 psi, which can be interpreted as resulting from pores that are smaller than those in the X-3 well. The capillary pressure curve at the high wetting-phase saturations is relatively flat, indicating good sorting. It has a higher irreducible wetting- phase saturation than does X-3, which is consistent with its finer grains and smaller pores.

Diagenesis and reservoir properties

It was important to study the Khatatba sandstones using thin sections petrography and SEM analyses. This may help to estimate the origin and evolution of porosity and permeability and the diagenetic processes that influenced the evolution of reservoir quality. In the Khatatba Formation, both textural frameworks and diagenetic processes have an important influence on the quality of the sandstone of the Khatatba Formation in terms of porosity and permeability. The effects of diagenetic processes on the sandstone of the Khatatba Formation include the reduction of porosity by compaction and cementation as well as, the enhancement of porosity by dissolution [33-35].

The best- quality rocks are characterized by medium to coarse grain size, good sorting with high percentages of detrital quartz, and low percentages of matrix and cement (quartz and calcite). Most quartz in sandstones occurs as rounded to subrounded monocrystalline fragments. Meanwhile, the development of the dissolution of feldspar and calcite cement contributes to the development and enhancement of secondary porosity and permeability. At the same time, open hydraulic fractures are present and are not affected by any blocking material, which provides great pathways for fluid movement (***Figure 10b***) in order, to enhance the petrophysical parameters[18].

Several secondary intergranular pores with some fractures and small fissures are also observed in the macroscopic and microscopic scale in the obtained samples from the sandstone of the Khatatba Formation (***Figure 8, 10*** and ***12***). The most important characteristics of the vast majority of fractures are that, they are typically observed as being open (non-mineralized) and, oriented sub-parallel , forming great pathways for fluid movement (***Figure 10b***). These open fractures are formed essentially due to mechanical compaction. These fractures enhance and increase the porosity and permeability. In the obtained core plug samples, the fractures have been observed in most of the samples from the top to downward of the formation. In this interval, the porosity increases

with depth due to the occurrence of micro and macro fractures, which can be identified in the thin section under a polarizing microscope or even by the eye in core plug samples.

Destruction of reservoir is affecting many of the available porous and permeable zones in the Khatatba sandstone. Several important processes such as mechanical and chemical effects, the formation of quartz and calcite cements, and the development of authigenic kaolinite are acting strongly against the reservoir's quality, leading to a reduction in porosity and permeability. The intervals those suffering damage in the Khatatba sandstone have a measured core permeability in the range of 0 to maximum 44 mD. Grain contact changes from dominantly floating to point, long contact, and concavo- convex shapes due to the progressive burial and compaction effect (***Figure 13b*** and ***13d***). Worden and Morad (2000)[36] concluded that quartz overgrowths are an important reservoir quality- deteriorating mechanism in many deep petroleum reservoirs. In the Khatatba sandstones, quartz overgrowth, and the presence of carbonate and clay cements along with other cements strongly affect the reservoir properties (***Figure 9b*** and ***11c***). The presence of quartz cementation in the form of syntaxial quartz overgrowth, is a major cause of porosity and permeability loss in many petroleum reservoirs. In the analyzed samples, quartz overgrowth is one of the most important cements, which occurred during early diagenesis due to chemical compaction[19]. The quartz overgrowth is coating the detrital quartz grains, leading to decreasing pore radii and pore throat as well as increasing the capillary pressure, which results in the reduction of porosity and permeability. Calcite is one of the most important carbonate cement splashes into the Khatatba sandstones, leading to blocking many of the pore spaces and reducing the porosity and permeability. Authigenic kaolinite has been noticed as a pore-choking cement creates a permeability barrier (***Figure 9e, 9c, 11a*** and ***11c***) and may act as an irreducible water- saturation trap[37]. It increases in abundance and affects pore geometry and pore size distribution[18-19]. Formation damage is also affecting the vast majority of these fractures where they are observed to be totally sealed (closed, blocked) and fully occupied with bituminous materials, leading to the destruction of the expected porosity and permeability.

5. Conclusions

The sandstones of the Middle Jurassic Khatatba Formation in the North Western Desert of Egypt has been studied for reservoir quality analysis. It has been observed that the Khatatba Formation has different reservoir quality degrees. It can be discriminated into two distinctive zones in terms of reservoir quality. The good and poor reservoir quality zones can be identified from well to well, from field to field, and even within the same well. In good reservoir quality zones, primary intergranular porosity is common in addition to secondary porosity. The presence of open micro and macro fractures increases the permeability. Diagenesis took place in terms of the dissolution of feldspar, quartz, and calcite cement, which increases porosity and permeability and enhances the reservoir quality as well.

In case of low or poor reservoir quality zones, the diagenetic modification, which includes mechanical and chemical compaction, as well as the precipitation of authigenic cements, has been detected through petrographic observation. These cements occurred before oil was emplaced in the sandstones and include calcite, quartz overgrowth, and kaolinite. The dominant authigeneic cemet was the kaolinite invading most of the pore spaces and forming permeability barriers. Quartz overgrowth formed during early diagenesis due to chemical compaction. Calcite is generally the abundant pore- occluding cement. It develops as small euhedral crystals or as large crystals in the primary pores, and pyrite is also detected as a minor cement.

It is recommended that precautions must be taken into consideration during formation evaluation process of the Khatatba Formation in the Western Desert of Egypt. The poor quality reservoir zones that are observed within the Khatatba Formation in the north Western Desert may lead to misinterpretation and erroneous estimation of future oil production and forecasting.

Acknowledgements
The authors are deeply grateful to the Khalda Oil Company, Egypt for providing the rock samples and other petrophysical data for this study. The authors would like to appreciate the facilities provided from the Department of Geology, University of Malaya to complete this research. Also more grateful is extended to the University of Brunei Darussalam for providing all support and assistance to finish this work.

References

[1] Dolson, J. C, Shann, M. V, Matbouly, S. I, Hammouda, H. and Rashed, R. M. GeoArabia, **2001**, 6, 211-230.
[2] Zein El-Din, M.Y., Abd El-Gawad, E. A., El-Shayb, H. M. and Haddad, I. A. Annals of the Geological survey of Egypt, **2001**, 24, 115-134.
[3] Barakat, M.G., Darwish, M. and Abdelhamid, M. L. Earth Science Journal, **1987**, 1, 120-150, Ain Shams University.
[4] Sultan, N., Abdul Halim, M. A. **1988**. EGPC 9th Exploration and Production Conference, Cairo, 1988, V. II, 1-23.
[5] El Ayouty, M.K. In The Geology of Egypt (Eds R. Said) Rotterdam, Balkema, **1990**, 567–599.
[6] Dahi, M., and Shahin, A. N. Proceedings of the 11th Petroleum Exploration and Development Conference, Cairo, The Egyptian General Petroleum Corporation, **1992**, 2, 56-78.
[7] Ghanem, M., Sharaf, L., Hussein, S. and El-Nadi, Bulletin of Egyptian Society of Sedimentology, **1999**, 7, 85-98.
[8] Khaled , K. A. Journal of Petroleum Geology, **1999**, 22, 377-395.
[9] Rossi, C., Goldstein, R. H. and Marfil, R. Journal of Geochemical Exploration, **2000**, 69–70, 91–96.
[10] Rossi, C. Marfil, R., Ramseyer, K. and Permanyer, A. Journal of Sedimentary Research, **2001**, 71, 459-472.
[11] Sharaf, L. M. Journal of Petroleum geology, **2003**, 26, 189-209.
[12] El-Nady, M., Harb, F. and Basta, J. Petroleum Science and Technology Journal, **2003**, 21, 1-28.
[13] Alsharhan, A.S., Abd El-Gawad, E.A. **2008**. Journal of Petroleum Geology, 31, 191-212.
[14] Abdou, A.A., Shehata, M.G. and Kassab, M.A.M. Australian Journal of Basic and Applied Sciences, **2009**, 3, 1206-1222.
[15] Shalaby, M.R., Hakimi, M.H., Abdullah, W.H. Marine and Petroleum Geology, **2011**, 28, 1611–1624.
[16] Shalaby, M.R., Hakimi, M.H., Abdullah, W.H. American Association of Petroleum Geologists Bulletin 96, **2012**a, 2019–2036.
[17] Shalaby, M.R., Hakimi, M.H., Abdullah, W.H. International Journal of Coal Geology, 2012b, 100 (**2012**), 26-39.
[18] Shalaby, M.R., Hakimi, M.H., Abdullah, W.H. Arab J Geosci, **2013**a, DOI 10.1007/s12517-013-1109-9.
[19] Shalaby, M.R., Hakimi, M.H., Abdullah, W.H. Geol. J., 2013b, (**2013**) DOI: 10.1002/gj.2512.
[20] May, R.M. American Association of Petroleum Geologists Bulletin, **1991**, 75, 1215–1223.
[21] Kerdany, M.T. and Cherif, O.H. **1990**. In: Said. R. (Ed.), The Geology of Egypt. Rotterdam, Balkema, pp. 407–438.
[22] El Shazly, E.M. In: Kanes, A. E. M., and Stehli, F. G. (Eds.), The Ocean Basins and Margins, Plenum, New York, **1977**, pp. 379-444.
[23] Hantar, G. North Western Desert. In: Said. R. (Ed.), The Geology of Egypt. Rotterdam, Balkema, **1990**, pp. 293–319.
[24] Keeley, M.L. and Wallis, R.J. Journal of Petroleum Geology, **1991**, 14, 49–64.
[25] Schlumberger. Well Evaluation Conference, Egypt, **1984**, 243p.
[26] Taher, M., Said, M. and El-Azhary, T. Egyptian General Petroleum Corporation, 9th Exploration and Production Seminar, Cairo, **1988**, 1–28.
[27] Keeley, M.L., Dungworth, G., Floyd, C.S., Forbes, G.A., Kin, C., Mcgarva, R.M. and Shaw, D. Journal of Petroleum Geology, **1990**, 13, 397–420.
[28] Bagge, M.A. and Keeley, M.L. (Eds.) Geological Society of London, Special Publication, **1994**, 77, 183–200.

[29] Pettijohn, F.J., Potter, E. and Siever, R. Springer Verlag, Berlin, **1987**, 553 p.
[30] Boles, J.R. In: Clays and the Resource Geologist, Longstaffe, F.J.(eds.) Mineralogical Society of Canada, Canada, **1981**, pp. 148–168.
[31] Ehrenberg, S.N. American Association of Petroleum Geologists Bulletin, 1990, 74, 1538–1558.
[32] Tiab, D., and Donaldson, E. C. Gulf Professional Publishing, Elsevier, 2nd edition, **2004**, 926pp.
[33] Selley, R.C. Elements of Petroleum geology (2nd), Academic Press limited, California, USA, **1998**, 470 p.
[34] Jin, Z. and Liu, C. Petroleum Exploration and Development, **2008**, 35, 581-587.
[35] Gier, S., Worden, R. H., William, D. J. and Hans, K. Marine and Petroleum Geology, **2008**, 25, 681-695.
[36] Worden, R.H. and Morad, S. (Eds.) International Association of Sedimentologists, Special Publication, **2000**, 29, 1–20.
[37] Islam, M.A. Journal of Asian Earth Sciences, **2009**, 35, 89-100.

Maximum boundaries for cones of continuous functions on a compact space and integral representations for linear functionals

*Foo Chui Chen and Walter Roth**

Department of Mathematical Sciences, Faculty of Science, Universiti Brunei Darussalam, Jalan Tungku Link, Gadong, BE 1410, Brunei Darussalam

**corresponding author email: walter.roth@ubd.edu.bn*

Abstract

We present a simplified and easily accessible approach to the integral representation for continuous linear functionals on a cone of continuous real-valued functions on a compact set. The measures defining these integrals are supported by the maximum boundary of the respective cones.

Index Terms: spaces and cones of continuous functions, integral representation

1. Introduction

The concept of a maximum boundary for an algebra of continuous functions on a compact space was first proposed by Georgii Šilov in 1964 [6]. It was later generalized to vector spaces of continuous functions not necessarily closed for multiplication using rather demanding and complicated techniques from Choquet theory (see [1], [4] and [2]). These also generate our results concerning integral representations for continuous linear functionals on these spaces. We offer a much simplified and more easily accessible approach in this paper while also generalizing the concepts from linear spaces to cones of continuous functions.

2. Maximum Boundaries

Let X be a compact Hausdorff space and $C(X)$ the Banach space of all continuous functions on X endowed with the maximum norm, that is

$$\|f\| = \max\{|f(x)|\ \ x \in X\}.$$

for $f \in C(X)$. A non-empty subset H of $C(X)$ is a called a *subcone* of $C(X)$ if

$$f + g \in H \quad \text{and} \quad \alpha f \in H,$$

whenever $f, g \in H$, and $\alpha \geq 0$. Linear subspaces are of course subcones in this sense. For a function $f \in C(X)$ and a closed subset Y of X we abbreviate

$$\max(f, Y) = \max\{|f(x)|\ \ x \in Y\}.$$

Given a subcone H of $C(X)$, a closed subset Y of X is called a *(maximum) boundary for* H if

$$\max(f, Y) = \max(f, X)$$

holds for all $f \in H$, that is if all functions in H attain their maximum value on Y. If H is indeed a linear subspace of $C(X)$, then the functions in H also take their minimum values on Y, since a function $f \in H$ takes its minimum value where $-f \in H$ takes its maximum value. We shall use Zorn's Lemma to prove that for every subcone of $C(X)$ there is a minimal boundary $B \subset X$ of this type. Minimality means that $B = Y$ whenever Y is a boundary for H such that $Y \subset B$.

Proposition. 2.1. *For every subcone H of $C(X)$ there exists a minimal boundary $B \subset X$.*

Proof: Let $\mathcal{B}$ denote the (non-empty) collection of all boundaries for H, ordered by set inclusion and let $\mathfrak{C}$ be a downward chain in $\mathcal{B}$. We shall verify that

$$C_0 = \bigcap\{C \in \mathfrak{C}\}$$

is a lower bound for $\mathfrak{C}$ in $\mathcal{B}$. Indeed, C_0 is closed in X and a subset of all sets in $\mathfrak{C}$. For a function $f \in H$ let

$$Y_f = \{y \in X | \, f(y) = \max(f, X)\}.$$

This is a non-empty compact subset of X, and $Y_f \cap B \neq \emptyset$ for every boundary $B \in \mathcal{B}$. If we had $Y_f \cap C_0 = \emptyset$, then we would have $Y_f \cap C = \emptyset$ for some $C \in \mathfrak{C}$ by the finite intersection property of closed sets in a compact space. Thus $Y_f \cap C \neq \emptyset$ and

$$\max(f, C_0) = \max(f, X).$$

Thus $C_0 \in \mathfrak{C}$ as claimed. Following Zorn's Lemma, $\mathcal{B}$ then contains a minimal element. □

A minimal boundary of a subcone is, however, not necessarily unique, as the following example will show.

Example 2.2. Let $X = [-1, +1]$ and let H be the subspace of all even functions in $C([-1, +1])$, that is

$$H = \{f \in C(X) | \, f(x) = f(-x) \text{ for all } x \in X\}.$$

Then $B = [0,1]$ is a minimal boundary for H. Indeed, every function $f \in H$ obviously takes its maximum (and minimum) value on B. On the other hand, if Y is a closed subset of B such that $Y \neq B$, then the open complement Y^c of Y contains a point $0 \leq x \in B$ and its negative $-x$, and there is $\varepsilon > 0$ such that both intervals $(x - \varepsilon, x + \varepsilon)$ and $(-x - \varepsilon, -x + \varepsilon)$ are contained in Y^c. There is $f \in C([-1, +1])$ such that $f(x) = 1$ and $f(y) = 0$ for all $y \notin (x - \varepsilon, x + \varepsilon)$. The function

$$y \to f(y) + f(-y)$$

is in H and attains its maximum value outside Y. Thus Y is not a boundary for H. A similar argument shows that $B' = [-1,0]$ is also a minimal boundary for H, and these boundaries are therefore not unique in this case.

This deficit can however be remedied if we impose an additional assumption on the subcone H of $C(X)$. We shall say that H *(symmetrically) separates the points of* X if for any two distinct points $x, y \in X$ there is a function $f \in H$ such that $f(x) < f(y)$. Note that for a vector subspace H this notion coincides with the usual one, that is: for any two distinct points $x, y \in X$ there is a function $f \in H$ such that $f(x) \neq f(y)$.

Lemma. 2.3. *Let H be a subcone of $C(X)$ which separates the points of X.*

(a) For any two distinct points $x, y \in X$ and $\alpha \in \mathbb{R}$ there is a function $f \in H$ such that $f(y) = f(x) + \alpha$.

(b) For a compact subset K of X and $x \in X \backslash K$ there are functions $f_1, \dots, f_n \in H$ such that the open neighborhood of x

$$U = \{y \in X | \, f_i(y) < f_i(x) + 1 \; for \; i = 1, \dots, n\}$$

is disjoint from K.

Proof: (a) Let x and y be distinct points of X and $\alpha \in \mathbb{R}$. Since H separates the points of X we can choose a function $h \in H$ such that either $h(x) < h(y)$, in the case that $\alpha \geq 0$, or $h(x) > h(y)$, in the case that $\alpha < 0$. The function

$$f = \frac{\alpha}{h(y) - h(x)} h \in H$$

has the required property.

(b) Let K be a compact subset of X and $x \in X \backslash K$. For every $y \in K$ there is by Part (a) a function $f_y(y) = f_y(x) + 2$. Set

$$U_y = \{z \in X | \, f_y(z) > f_y(x) + 1\}$$

The family $(U_y)_{y \in K}$ forms an open cover for K and therefore contains a finite subcover $U_1, \dots, U_n$ corresponding to the functions $f_1, \dots, f_n \in H$. These functions satisfy the claim of Part (b). Indeed, the open set

$$U = \{y \in X | \, f_i(y) < f_i(x) + 1 \text{ for } i = 1, \dots, n\}$$

contains the point x and is disjoint from K, since for every $y \in K$ at least one of the functions f_i has the property that $f_i(y) > f_i(x) + 1$. □

Proposition. 2.4. *For a subcone H of $C(X)$ which separates the points of X there exists a unique*

minimal boundary B, that is every other boundary for H contains B.

Proof: We have to verify only uniqueness. Let B be a minimal boundary for H and let Y be a second boundary. Let us assume to the contrary of our claim that $B \not\subset Y$. Then there is $x_0 \in B\backslash Y$. Following Lemma 3 (b) there are $f_1, \dots, f_n \in H$ such that

$$U = \{y \in X |\ f_i(y) < f_i(x_0) + 1 \text{ for } i = 1, \dots, n\}$$

contains x_0 and is disjoint from Y. The set

$$B\backslash U = B \cap (X\backslash U)$$

is closed and is a proper subset of B, since it does not contain $x_0 \in B$. Therefore due to the minimality of B it is not a boundary for H. Thus we can find a function $f \in H$ such that

$$\max(f, B\backslash U) < \max(f, X).$$

On the other hand since Y is a boundary for H we can find $y \in Y$ such that

$$f(y) = \max(f, X),$$

and since $y \notin U$ there is $k \in \{1, \dots, n\}$ such that $f_k(y) \geq f_k(x_0) + 1$. Next we choose $\alpha \geq 0$ and consider the function $g = \alpha f + f_k \in H$.

If $x \in U$ then
$$\alpha f(x) + f_k(x) < \alpha \max(f, X) + f_k(x_0) + 1.$$

If $x \in B\backslash U$, then
$$\alpha f(x) + f_k(x) \leq \alpha \max(f, B\backslash U) + \max(f_k, X).$$

Thus if we choose $\alpha \geq 0$ such that

$$\alpha(\max(f, X) - \max(f, B\backslash U)) > \max(f_k, X) - f_k(x_0) - 1$$

then we have
$$\alpha f(x) + f_k(x) < \alpha \max(f, X) + f_k(x_0) + 1$$
for all $x \in B$, and hence

$$\max(\alpha f + f_k, X) = \max(\alpha f + f_k, B) < \alpha \max(f, X) + f_k(x_0) + 1,$$

since B is a boundary for H. On the other hand we have

$$\alpha f(y) + f_k(y) = \alpha \max(f, X) + f_k(y) \geq \alpha \max(f, X) + f_k(x_0) + 1$$

Thus
$$\max(\alpha f + f_k, X) \geq \alpha \max(f, X) + f_k(x_0) + 1,$$

contradicting the above. □

The unique minimal boundary of a subcone of $C(X)$, if it exists, is also called the *Šilov boundary* of this subcone.

Integral representations for linear functionals

A *linear functional* I on a subcone H of $C(X)$ is a mapping $I : H \to \mathbb{R}$ such that

$$I(f + g) = I(f) + I(g) \quad \text{and} \quad I(\alpha f) = \alpha I(f)$$

for all $f, g \in H$ and $\alpha \geq 0$. A linear functional I on H is called *u-continuous* if there is a constant $C \geq 0$ such that

$$I(f) \leq I(g) + C \quad \text{whenever} \quad f \leq g + 1$$

for $f, g \in H$. This condition implies that I is *monotone*, that is

$$I(f) \leq I(g) \quad \text{whenever} \quad f \leq g$$

for $f, g \in H$. We observe the following:

Lemma. 3.1. If the subcone H of $C(X)$ contains a strictly positive function f_0, then every monotone linear functional on H is continuous.

Proof: Let I be a monotone linear functional on H and let $f_0 \in H$ be strictly positive. Thus

$$\alpha = \min\{f_0(x) |\ x \in X\} > 0.$$

Let $f, g \in H$ such that $f \leq g + 1$. Then

$$f \leq g + 1 \leq g + \frac{1}{\alpha} f_0,$$

and therefore

$$I(f) \leq I(g) + \frac{1}{\alpha} I(f_0)$$

using the monotonicity of I. □

We shall use the classical Riesz-Markov representation theorem (see for example Theorem

II.1.2 in [3]) for linear functionals on $C(X)$ spaces in order to derive a more general result for linear functionals on a subcone H of $C(X)$. The resulting representation measures are supported by a boundary for H.

Theorem. 3.2. *Let H be a subcone of $C(X)$ and let $B \subset X$ be a boundary for H. For every u-continuous linear functional I on H there exists a positive regular Borel measure μ on X which is supported by B and such that*

$$I(f) \leq \int_X f \, d\mu \quad for\ all \quad f \in H.$$

Proof: Let I be a u-continuous linear functional on H and let $C \geq 0$ such that

$$I(f) \leq I(g) + C \quad \text{whenever} \quad f \leq g + 1$$

for $f, g \in H$. For a function $f \in C(X)$ we denote by $f|_B$ its restriction to the subset B of X. We have

$$\max(f|_B, B) = \max(f, X)$$

for all $f \in H$, since B is a boundary for H. We define a $\mathbb{R}$-valued sublinear functional p on $C(B)$ by

$$p(f) = C \max(f, B)$$

for all $f \in C(B)$ and a $(\mathbb{R} \cup -\infty)$-valued superlinear functional q by

$$q(f) = \sup\{I(h) |\ h \in H, h|_B \leq f\}$$

for $f \in C(B)$. As usual, we set $\sup\emptyset = -\infty$. Moreover, q does not take the value $+\infty$, since $h|_B \leq f$ for $f \in C(B)$ and $h \in H$ implies that $h|_B \leq \max(f, B)$, hence $h \leq \max(f, B)$ and therefore

$$I(h) \leq C \max(f, B) = p(f),$$

using the u-continuity of I. This shows that

$$q(f) \leq p(f) \quad \text{for all } f \in C(X).$$

The sublinearity of p and the superlinearity of q are easily checked. Let us verify just one of the requirements for q: If

$$h_1|_B \leq f \quad \text{and} \quad h_2|_B \leq g$$

for $h_1, h_2 \in H$ and $f, g \in C(B)$, then

$$h_1|_B + h_2|_B \leq f + g,$$

hence

$$I(h_1) + I(h_2) \leq q(f + g)$$

and therefore

$$q(f) + q(g) \leq q(f + g).$$

Now according to the sandwich version of the Hahn-Banach theorem (see for example Corollary I.3.26 in [3]) there exists a linear functional L on $C(B)$ such that

$$q(f) \leq L(f) \leq p(f)$$

for all $f \in C(X)$. We observe the following:

(i) L is bounded, that is continuous. Indeed, if $f \leq 1$ for $f \in C(B)$, then $L(f) \leq p(f) \leq C$, hence if $\|f\| \leq 1$ then $|L(f)| \leq C$.

(ii) L is monotone. Indeed, if $f \leq 0$ for $f \in C(B)$ then $L(f) \leq p(f) \leq 0$, hence if $f \leq g$ for $f, g \in C(B)$ then $f - g \leq 0$, and therefore

$$L(f) - I(g) = L(f - g) \leq 0.$$

(iii) $L(f|_B) \geq I(f)$ for all $f \in H$. Indeed, following the definition of the superlinear functional q we have

$$L(f|_B) \geq q(f|_B) \geq I(f).$$

Next we apply the Riesz-Markov representation theorem (see Theorem II.1.2 in [3]): there is a regular Borel measure $\tilde{\mu}$ on B such that

$$L(f) = \int_B f \, d\tilde{\mu} \quad \text{for all} \quad f \in C(B).$$

The measure $\tilde{\mu}$ on B corresponds to a regular Borel measure μ on X if we set

$$\mu(A) = \tilde{\mu}(B \cap A)$$

for every Borel subset A of X. This yields

$$\int_X f \, d\mu = \int_B f \, d\mu = \int_B f|_B \, d\tilde{\mu}$$

for all $f \in C(X)$, and in particular

$$\int_X f\,d\mu = \int_B f\,d\mu = \int_B f|_B\,d\tilde{\mu} = L(f|_B) \geq I(f)$$

for all $f \in H$, our claim. □

The statement of Theorem 3.2 can be further developed in the case that H is indeed a vector subspace of $C(X)$. It has been shown (see Theorem 3.3 and Corollary 4.4 in [5]) that in this case every continuous linear functional I on the subspace H of $C(X)$ can be expressed as a difference of two u-continuous ones, that is there are u-continuous linear functionals I_1 and I_2 on H such that

$$I(f) = I_1(f) - I_2(f)$$

for all $f \in H$. Using Theorem 3.2 the functionals I_1 and I_2 can be represented by positive regular Borel measures μ_1 and μ_2, respectively. That is, we have

$$I_1(f) = \int_X f\,d\mu_1 \quad \text{and} \quad I_2(f) = \int_X f\,d\mu_2$$

for all $f \in H$. Equality in these representations follows since $-f \in H$ whenever $f \in H$. Consequently, the signed measure $\mu = \mu_1 - \mu_2$ is supported by B and represents the functional I on H, that is

$$I(f) = I_1(f) - I_2(f) = \int_X f\,d\mu_1 - \int_X f\,d\mu_2 = \int_X f\,d\mu$$

for all $f \in H$. We summarize:

Corollary. 3.3. *Let H be a linear subspace of $C(X)$ and let $B \subset X$ be a boundary for H. For every bounded linear functional $I \in H^*$ there exists a regular Borel measure μ on X which is supported by B and such that*

$$I(f) = \int_X f\,d\mu \quad for\ all \quad f \in H.$$

Examples 3.4. (a) Let X be the closed unit disc in $\mathbb{R}^2$ and let H be the subcone of $C(X)$ consisting of those functions $f \in C(X)$ that are subharmonic in the interior of X, that is

$$\frac{\partial^2 f}{\partial x^2}(x,y) + \frac{\partial^2 f}{\partial y^2}(x,y) \geq 0$$

for all (x,y) in the interior of X. The subcone H symmetrically separates the points of X and contains the constants, and it is well known that its minimal boundary (Šilov boundary) consists of the circle line in this case, that is

$$B = \{(x,y) |\, x^2 + y^2 = 1\}.$$

According to Theorem 3.2 every monotone (therefore u-continuous by Lemma 3.1) linear functional on H can be represented by a positive regular Borel measure on B. This is best dealt with in polar coordinates (r, ϕ), where the subharmonic inequality translates into

$$\frac{1}{r}\frac{\partial}{\partial r}\left(r\frac{\partial f}{\partial r}\right) + \frac{1}{r^2}\frac{\partial^2 f}{\partial \phi^2} \geq 0$$

For a point evaluation at a point in the interior of X with the polar coordinates (r, θ), that is $r < 1$, this representation is given by the Poisson Integral Formula

$$f(r,\theta) \leq \frac{1-r^2}{2\pi}\int_0^{2\pi} \frac{f(1,\phi)}{1 - 2r\cos(\theta - \phi) + r^2}\,d\phi$$

for every subharmonic function $f \in H$. The representation measure μ on B for this point evaluation is therefore the Lebesgue measure with the density function

$$(1,\phi) \to \frac{1}{2\pi}\frac{1-r^2}{1 - 2r\cos(\theta - \phi) + r^2}.$$

For the subspace L of all harmonic functions, that is $L = H \cap (-H)$, the above inequality turns into an equality, that is we have

$$f(r,\theta) = \frac{1-r^2}{2\pi}\int_0^{2\pi} \frac{f(1,\phi)}{1-2r\cos(\theta-\phi)+r^2}\, d\phi$$

for every harmonic function $f \in L$.

(b) Let X be a compact convex subset of a normed space (or a Hausdorff locally convex topological vector space). Recall that convexity means that $\lambda x + (1-\lambda)y \in X$ whenever $x, y \in X$ and $0 \leq \lambda \leq 1$. An *extreme point* of X is a point $x \in X$ such that

$$x = \lambda y + (1-\lambda)z$$

for $y, z \in X$ and $0 < \lambda < 1$ implies that $x = y = z$, that is x is not an interior point of a line segment in X. A function $f : X \to \mathbb{R}$ is said to be *convex* if

$$f(x) \leq \lambda f(y) + (1-\lambda) f(z)$$

whenever $x = \lambda y + (1-\lambda)z$ for $y, z \in X$ and $0 \leq \lambda \leq 1$. The subcone H of all convex functions in $C(X)$ symmetrically separates the points of X (this follows from the Hahn-Banach theorem) and contains the constants. According to the Krein-Milman theorem its minimal boundary B is the closure of the set of all extreme points of X.

For a concrete example let X be a closed convex polygon in $\mathbb{R}^2$ with the vertices $P_1, \dots, P_n$. Then $B = \{P_1, \dots, P_n\}$ is the Šilov boundary for H and according to Theorem 3.2 every monotone linear functional I on H can be represented by a regular Borel measure μ on B. But the measures on the finite set B are just linear combinations of point evaluations δ_{P_i}. If in particular the functional I is monotone, and therefore u-continuous, then μ is a convex combination of these point evaluations, that is

$$\mu = \lambda_1 \delta_{P_1} + \cdots + \lambda_n \delta_{P_n},$$

where $\lambda_1, \dots, \lambda_n \geq 0$ and $\lambda_1 + \cdots + \lambda_n = I(1)$. Thus

$$I(f) \leq \int_X f\, d\mu = \lambda_1 f(P_1) + \cdots + \lambda_n f(P_n)$$

for all $f \in H$. For *affine* functions, that is functions in $L = H \cap (-H)$, and a continuous (not necessarily monotone) linear functional I on L we obtain according to Corollary 3.3 a similar representation, that is

$$I(f) = \int_X f\, d\mu = \lambda_1 f(P_1) + \cdots + \lambda_n f(P_n)$$

where $P_i \in B$ and $\lambda_i \in \mathbb{R}$ for $i = 1, \dots, n$.

References

[1] E.M. Alfsen, *Compact convex sets and boundary integrals* Ergebnisse der Mathematik und ihrer Grenzgebiete, vol. 57, 1971, Springer Verlag, Heidelberg-Berlin-New York.

[2] H. Bauer, *Silovscher Rand und Dirichletsches Problem* Ann. Inst. Fourier (Grenoble) 11, 1961, 89-136.

[3] Foo Chui Chen, *Integral representations for continuous linear functionals*, MSc Thesis, 2016, Universiti Brunei Darussalam.

[4] R.R. Phelps, *Lectures on Choquet's theorem*, Lecture Notes in Mathematics, 1757 Springer Verlag, 1966, Heidelberg-Berlin-New York.

[5] W. Roth, *Real and complex linear extensions for locally convex cones*, Journal of Functional Analysis, vol. 151, no. 2, 1997, 437-454.

[6] I. Gelfand, D. Raikov and G. Šilov, *Commutative normed rings*, 1964, Chelsea (translated from Russian).

Computational study of modification of cyanidin as high efficient organic sensitizer for dye sensitized solar cells

Kalpana Galappaththi[1], Piyasiri Ekanayake[1,3], Mohammad Iskandar Petra[2]*

[1]Applied Physics Program, Faculty of Science, Universiti Brunei Darussalam, Jalan Tungku Link, Gadong, BE 1410, Brunei Darussalam
[2]Faculty of Integrated Technologies, Universiti Brunei Darussalam, Jalan Tungku Link, Gadong, BE 1410, Brunei Darussalam
[3]Physical and Geological Sciences Programme, Centre for Advanced Material and Energy Sciences, Universiti Brunei Darussalam, Jalan Tungku Link, Gadong, BE 1410, Brunei Darussalam

**corresponding author email: piyasiri.ekanayake@ubd.edu.bn*

Abstract

This study reports the results of theoretical investigation of a newly designed cyanidin based molecular structure, (*P02),* as an efficient sensitizer for dye sensitized solar cells (DSSCs). To design the structure of *P02*, chemical structure of the widely used promising natural dye sensitizer cyanidin is combined with α-cyanocinnamic acid and the resultant structure is computationally simulated by using SPARTAN'10 software package. The molecular geometries, electronic structures, absorption spectra and deprotonation energies of newly designed organic sensitizer are investigated by employing density functional theory (DFT) and time-dependent density functional theory (TDDFT) approaches using GAUSSIAN'09W software package. As a reference, DFT and TDDFT calculations are also performed on the structure of cyanadin. The solvation effect of these dyes in ethanol are included in all calculations. The computational studies on the new dye revealed that the broadening of the absorption spectra in visible region with significant shifting towards a longer wavelength region compared to the cyaniding dye, indicating that the new dye *P02* should exhibit better performances as a sensitizer in DSSCs due to its improved photon absorbtion properties.

Index Terms: density functional theory, absorption spectra, dye sensitized solar cells, cyanadin

1. Introduction

One of the current global challenge is to meet the increasing global energy consumption without effecting the environment. In this sense solar energy provides clean abundant energy and is therefore an excellent candidate for a future environmentally friendly energy source. Solar cells are devices that are able to convert solar energy into electrical energy.

The aim of solar cell research is to increase the solar energy conversion efficiency at low cost to provide a cost-effective sustainable energy source. Among the solar cells known today, dye sensitized solar cells (DSSCs), developed in 1991 by Grâtzel and coworkers in Switzerland are one class of ~~a~~ cost-effective and environmentally friendly solar cells.[1-8] These DSSCs mainly comprise with a nano structured high band gap semiconducting electrodes combined with efficient electron injection dyes. The sensitizing dye in DSSCs is mainly responsible for the capture of sunlight. To improve its efficiency, dye sensitizer should have a broad absorption spectrum as much as possible to match with large range of photons available in solar energy.[9] Therefore, the synthetic dyes used in DSSCs with higher efficiencies consist with rare earth materials and complexed structures, eventually increasing the cost of these devices. Therefore, one of the possible alternatives to replace these expensive dyes with rare earth materials is the usage of natural dyes in these

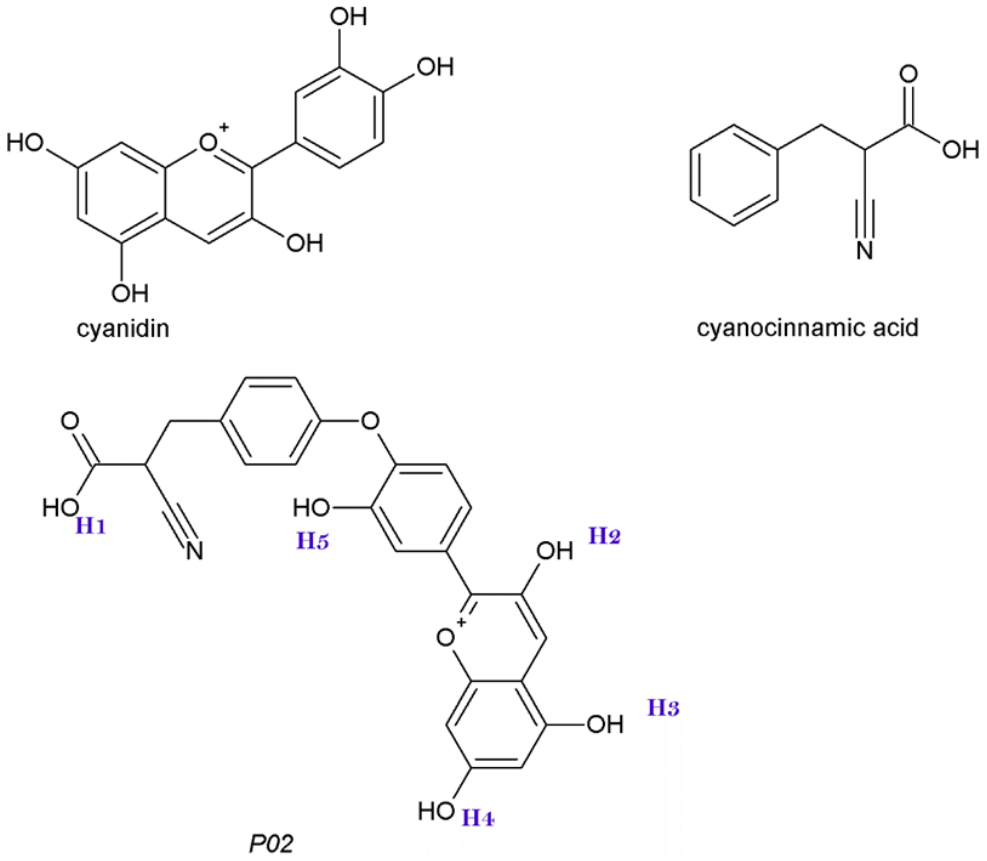

Figure 1. Fundamental molecular structure of cyanidin, cyanocinnamic acid and newly designed *P02*.

DSCSs which effectively reduce the cost and the hazardness to the environment.[10-16]

However, the reported efficiencies of DSSCs employing with natural dyes are still very poor mainly due to their poor light harvesting properties associated with them. Therefore, to improve the efficiencies of these devices with natural dyes, the dye sensitizer should have a broad absorption spectrum as much as possible to match with large range of photon energies available in the solar energy spectrum.[9] Most of the natural dyes available consist of cyanidin as the main active component of the dye and strongly absorbs around 500 nm wavelength. Therefore, synthesis of cyanidin based new dyes, having the ability to capture of more photons would be an efficient approach to solve this problem. However, before synthesizing these new dyes it is worth of finding out whether these new dyes would really show the desirable optical properties such as positions of the bands, energy gaps, etc. Hence in this study a cyanidin based organic dye is designed and computationally characterized to be used as a novel sensitizer in DSSCs, by attaching one hydroxyl group on benzene ring of cyanidin is attached–to the benzene ring of α-cyanocinnamic acid unit as shown in ***Figure 1***.

2. Computational studies

The molecular structures of *P02* and cyanidin are computed using Spartan'10 software[17] to retrieve the molecular geometric coordinates. Both density functional theory (DFT) and time-dependent density functional theory (TDDFT) calculations are performed using Gaussian'09W software.[18] The geometry of P02 and cyanidin in ground state is fully optimized using the Becke's three parameters Lee-Yang-Parr hybrid functional (B3LYP).[19] In the calculations 6-31g (d) basis set is adopted to describe metal free atoms. All the calculations are computed including solvation effect of these molecules in ethanol. The models of electron density of various energy levels of the *P02* are visualized using GaussView Version 5.0. The deprotonation energies of *P02* are calculated

Table 1: Summary of DFT computational calculation of the structures of cyanidin and *P02* in ethanol, with and without geometrical optimization

Sensitizer	Solvent Effect	Without geometric optimization			With geometric optimization		
		HOMO (eV)	LUMO (eV)	Energy gap (eV)	HOMO (eV)	LUMO (eV)	Energy gap (eV)
Cyanidin	Ethanol	-6.91	-3.82	3.10	-6.18	-3.39	2.79
P02	Ethanol	-5.31	-3.90	1.41	-6.48	-3.66	2.82

using B3LYP hybrid functional and 6-31g (d) basis set in vacuum condition.[20]

3. Results and discussion

DFT calculation

Table 1 summarizes the results obtained from repeated DFT calculations on *P02* molecule with solvent effect in ethanol for the geometrically optimized structure. The estimated electron energy values of the main two important levels i.e., highest occupied molecular orbital level (HOMO), lowest unoccupied molecular level (LUMO) and the band gap values are tabulated for both without optimized and optimized structures. It is observed that the data, especially the band gap value of *P02*, obtained after geometrical optimization in ethanol is nearly equal to band gap value of cyanidin in ethanol.

The electron injection from the excited dye molecule to the conduction band of TiO_2 is more efficient if the LUMO level is higher than conduction band edge of TiO_2. For efficient regeneration of the oxidized dye molecule to its original state by the hole conductor, the energy difference between HOMO level and energy level of redox couples must be sufficiently high. Further, the LUMO level must be above the conduction band of TiO_2 while HOMO level must be below the energy level of redox couple.[21]

The HOMO and LUMO energy levels of *P02* and cyandin, as calculated from DFT are plotted with respect to energy in vacuum level in ***Figure 2*** and the superimposed on the plots are the energy levels corresponding to the conduction band of $TiO_2$and the redox couple.[22] The results in ***Figure 2*** show that the *P02* satisfy the conditions for photo-energy conversion.

The HOMO level is a core factor of electron donor mechanism. The electron donating capability will increase when HOMO level is more negative. According to our computational results, energy levels of HOMO of cyanidin and *P02* in ethanol with geometric optimization are -6.18eV and -6.48eV, respectively, revealing that the HOMO level of *P02* is -0.3eV more negative than that of cyaniding. Hence *P02* has more electron donating ability to the HOMO level of the dye molecule with compared to that of cyanidin.

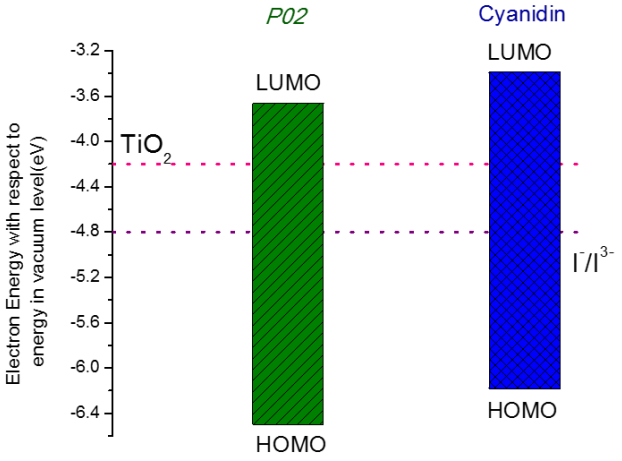

Figure 2. Energy level diagram showing HOMO, LUMO energy levels of *P02* and cyanidin, redox potential and conduction band of TiO_2. Computational results of HOMO and LUMO are obtained using B3LYP/6-31g (d) level and with geometric optimization in ethanol.

TDDFT and Optical Properties

To gain insight of the excitation energy, electronic transition, optical properties and UV/Vis absorption spectra for the singlet to singlet transition of newly designed dye *P02* and our reference dye cyanidin are simulated using TDDFT with hybrid functional B3LYP in ethanol solution. The lowest five singlet-singlet excitations are included in TDDFT calculation.

***Table 2*:** Computed excitation energies in (eV), (nm) and the oscillator strength (f) of the cyanidin and *P02* obtained by TDDFT calculations at B3LYP/6-31g (d) level with the inclusion of geometric optimization under the solvation effect of ethanol.

Sensitizer	Optimized, in ethanol			
	Calculated Energy		Oscillator strength	MO configuration
	(eV)	(nm)	(f)	(coefficient)*
Cyanidin	2.52	492.16	0.583	HOMO-> LUMO = 0.695
	2.82	439.86	0.010	HOMO-3-> LUMO = 0.318 HOMO-2 ->LUMO= 0.467 HOMO ->LUMO+1 = 0.211
	3.17	391.21	0.273	HOMO-3->LUMO = 0.322 HOMO-2->LUMO = 0.192 HOMO-1->LUMO = 0.586
	3.88	319.36	0.025	HOMO-4->LUMO = 0.687
	4.49	276	0.055	HOMO-3->LUMO = 0.516
P02	2.45	506.25	0.397	HOMO->LUMO = 0.681
	2.60	476.52	0.08	HOMO-1->LUMO = 0.653 HOMO->LUMO= 0.176
	2.86	433.73	0.068	HOMO-2->LUMO = 0.685 HOMO-1->LUMO = 0.150
	3.20	387.20	0.416	HOMO-3->LUMO= 0.676 HOMO-1->LUMO = 0.140
	3.53	351.72	0.000	HOMO-4->LUMO = 0.706

* Molecular orbital with configuration coefficient <0.1 are not shown.

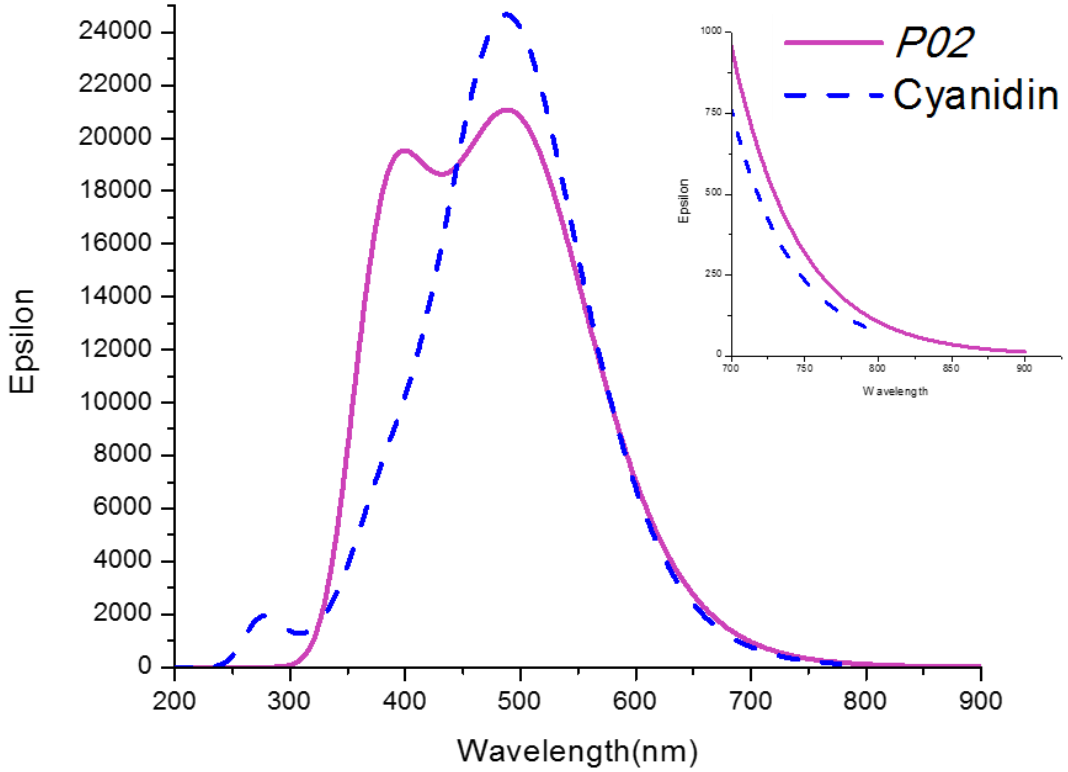

Figure 3. UV-vis absorption spectra obtained for the *P02* and Cyanidin via output of TDDFT calculations with solvation effect of ethanol solution. Inset shows an enlarged absorption spectra in 700 nm to 900 nm range.

The excitation energy, oscillator strength, configuration and molar extinction coefficient for the five states of *P02* and cyanidin dye are calculated using B3LYP on 6-31g (d) basis set are shown in ***Table 2*** and the computer simulated UV-vis absorption spectra obtained for the *P02* and cyanidin via TDDFT calculations are shown in ***Figure 3***.

Oscillator strength expresses the strength of transition to the excited states. The higher the oscillator strength, the higher the possibility of the molecule as a sensitizer.[23-25] At the first excitation state, the oscillator strength of *P02* and cyanidin are 0.397 and 0.583, respectively, and the transition is HOMO to LUMO. The maximum absorption wavelength, λ_{max}, of *P02* and cyanidin are at 506.25 nm and 492.16 nm, respectively (***Table 2***) and the corresponding energies are 2.45 eV and 2.52 eV.

At the second excitation state, the oscillator strength for the *P02* and cyanidin are 0.08 and 0.01, respectively. At this excitation state *P02* involved HOMO-1 to LUMO transition, whereas cyanidin involved HOMO – 2 to LUMO transition. The calculated energy of *P02* and cyanidin are 2.60 eV and 2.82 eV and λ_{max} are at 476.52 nm and 439.86 nm.

At the third excitation state, the *P02* and cyanidin showed 0.068 and 0.273 oscillator strength. If excitation occur at this state, the *P02* and cyanidin would displayed HOMO – 2 to LUMO and HOMO – 1 to LUMO transitions, respectively. The λ_{max} of the *P02* and cyanidin are at 433.73 nm and 391.21 nm and their corresponding energies are at 2.86 eV and 3.17 eV.

At the forth excitation state, the *P02* and cyanidin showed 0.416 and 0.025 oscillator strength. If excitation occur at this state, the *P02* and cyanidin would displayed HOMO – 3 to LUMO and HOMO – 4 to LUMO transitions, respectively. The λ_{max} of the *P02* and cyanidin are at 387.20 nm and 319.36 nm and their corresponding energies are at 3.20eV and 3.88 eV.

At the fifth excitation state, the oscillator strength for *P02* is zero and cyanidin showed 0.055 oscillator strength. If excitation occur at this state, the *P02* and cyanidin would have displayed HOMO – 4 to LUMO and HOMO – 3 to LUMO transitions, respectively. The λ_{max} of the *P02* and cyanidin are at 351.72 nm and 276 nm and corresponding energies are at 3.53eV and 4.49 eV.

P02 has produced four significant oscillator strengths up to the forth excitation states, while cyanidin only produced three significant oscillator strength at the first, third and fifth excitation states. This suggested that *P02* has more ability to sensitize the semiconductor in DSSC than the cyanidin. In addition, the λ_{max} values of the *P02* at each five excitation states shifted to longer wave lengths compared to λ_{max} of cyanidin by 14.09 nm, 36.66 nm, 42.52 nm, 67.84 nm and 75.72 nm, respectively. Also, the absorption spectra of the *P02* is broader compared to cyanidin (***Figure 3***) indicating its ability to absorb more energy. The absorption spectrum of *P02* is significantly broader at shorter wavelengths of the visible region.

Molecular Electronic Structure

Modelling of the electron density clouds behavior at the transition of various energy levels corresponding to first five excited states of *P02* is shown in ***Figure 4*** to ***Figure 8***. At different energy levels, it could be observed that electron density clouds are localized at different regions of the *P02* molecule.

P02 molecule consist of cyanidin and α-cyanocinnamic acid. One hydroxyl group on benzene ring of cyaniding is attached to benzene ring of α-cyanocinnamic acid unit. Almost all the ground state energy levels such as HOMO-4, HOMO-3, HOMO-2, HOMO-1and HOMO levels of *P02* are π-type. At the HOMO level the electron density cloud is mostly localized in the α-cyanocinnamic acid unit and the benzene ring of cyanidin. Negligible amount of electron cloud is observed on chromenylium unit, whereas the electron density cloud of the HOMO-1 are delocalized over the entire molecule of *P02*. The HOMO-2 and HOMO-3 of *P02* have similar

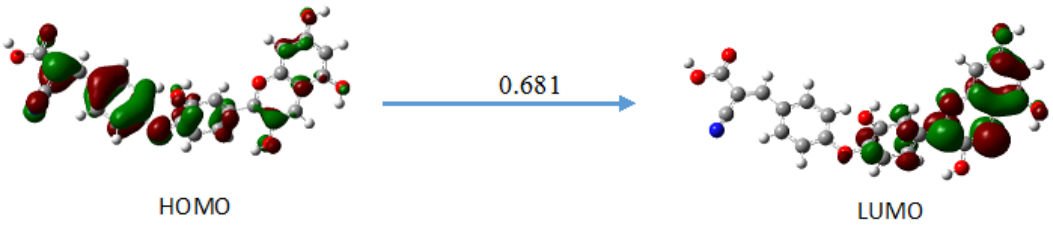

Figure 4. The electron transition for the 506.25 nm absorption of P02 in ethanol under the TDDFT calculation with isovalue of contour = 0.03.

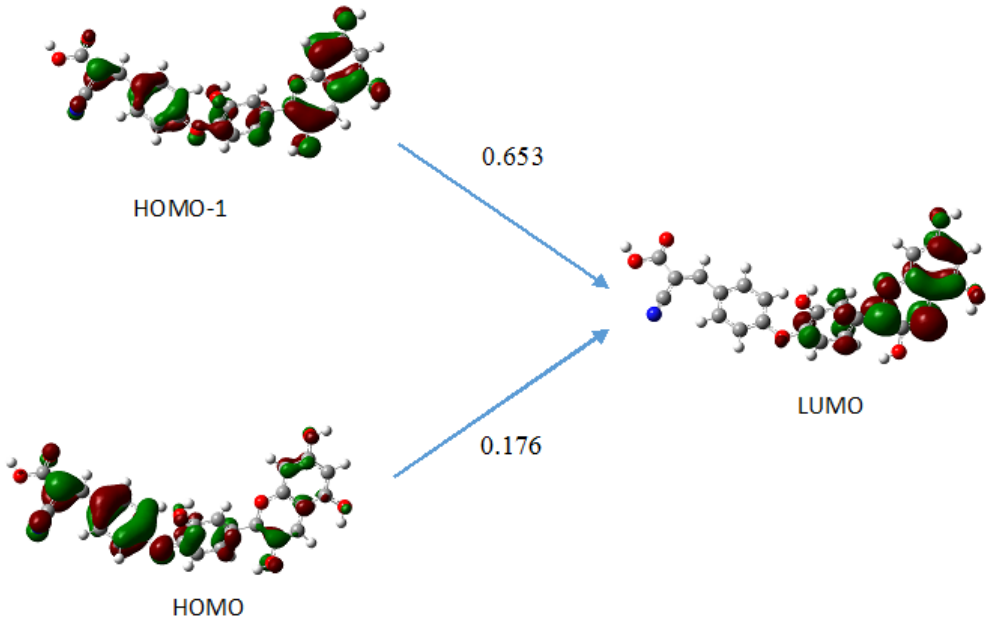

Figure 5. The electron transition for the 476.52 nm absorption of P02 in ethanol under the TDDFT calculation with isovalue of contour = 0.03.

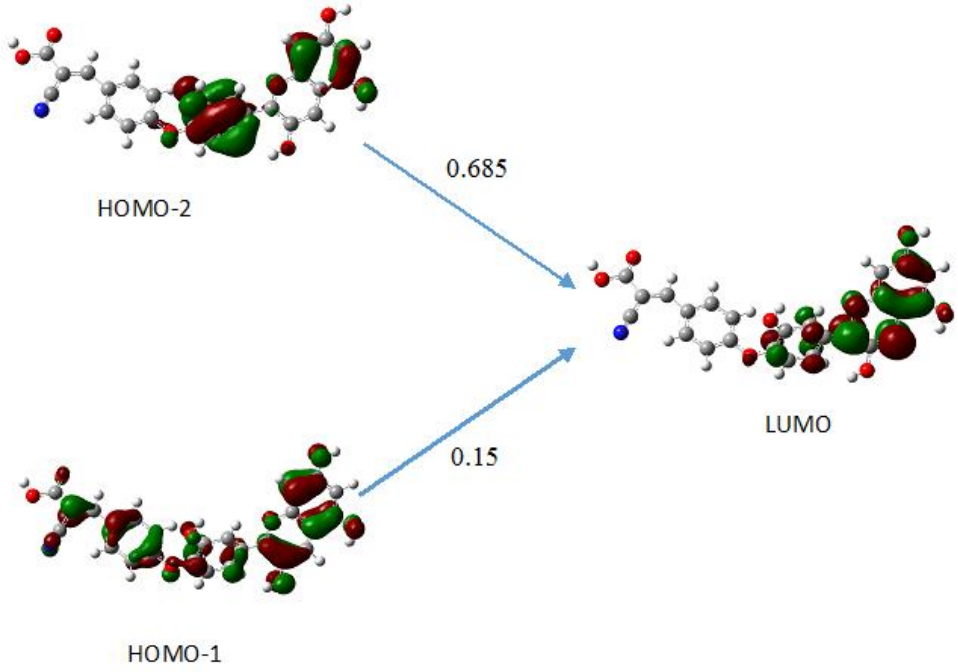

Figure 6. The electron transition for the 433.73 nm absorption of P02 in ethanol under the TDDFT calculation with isovalue of contour = 0.03.

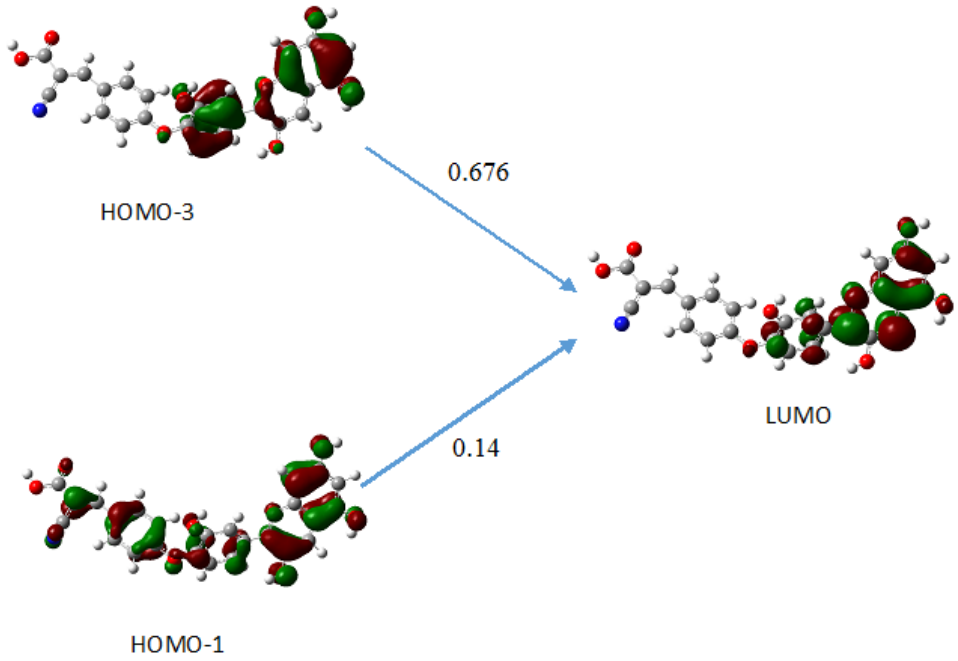

Figure 7. The electron transition for the 387.2 nm absorption of P02 in ethanol under the TDDFT calculation with isovalue of contour = 0.03.

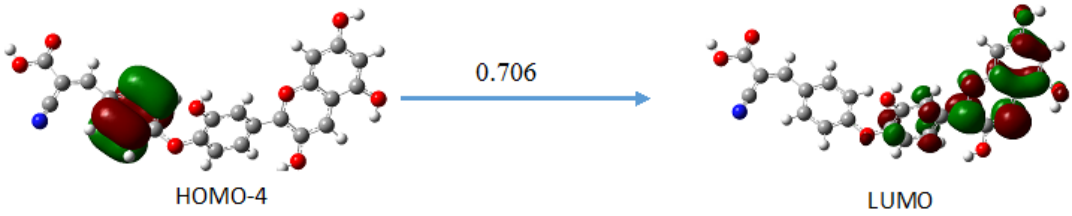

Figure 8. The electron transition for the 351.72 nm absorption of P02 in ethanol under the TDDFT calculation with isovalue of contour = 0.03.

electron density cloud patterns as electron clouds are localized over two benzene rings in cyanidin unit of *P02*. At HOMO-4, dense π type electron density cloud observed on benzene ring of α-cyanocinnamic acid unit.

In the *P02* molecule, the electron cloud of LUMO is π* type and the molecular orbital is localized at cyanidin unit. At LUMO the electron density cloud localized in cyanidin unit. Here the electron density cloud is observed to be denser in chromenylium unit than the benzenedial in cyanidin unit of *P02*. The photogenerated electrons are excited to chromenylium unit on electrode of TiO_2. Subsequently, electrons are easily injected into the conduction band of TiO_2. This electron injection is most possible from the chromenylium unit as it has denser electron density cloud in the LUMO π* state. Therefore, the anchoring groups of *P02* molecule that may efficiently inject electrons into the TiO_2 are deduced to be the hydroxyl groups H2, H3, H4 and H5 (***Figure 1***).

Proton affinity

Deprotonation energy is calculated by the energy difference between the optimized protonated and deprotonated *P02* dye molecule in B3LYP/6-31g (d) level of theory under vacuum condition[19, 20], as shown in ***Table 3***. The common anchoring group of natural dyes are the hydroxyl (–OH) group and the carboxyl group (–COOH).[20] The *P02* molecular structure contains four hydroxyl groups and one carboxyl group. H1 (see ***Figure 1***) has shown the highest deprotonation energy while H4 has shown the smallest deprotonation energy. The descending order of the deprotonation energies are H1 > H2 > H3 > H5 > H4. The difference in

Table 3. Single deprotonation energies (kJ mol^{-1}) of the *P02* sensitizer.

	Deprotonation energies (kJ mol^{-1})				
Sensitizer	**-H1$^+$**	**-H2$^+$**	**-H3$^+$**	**-H4$^+$**	**-H5$^+$**
P02	283.4	250.5	236.5	232.2	233.0

deprotonation energy between H1 and H4 is 51.2 kJ mol^{-1}. The lowest value of the deprotonation energy indicates the most probable group that could anchor onto TiO_2. [26, 27] Therefore, from the results of these calculations, we can deduce that the most possible anchoring group of *P02* is H4. When the three most probable anchoring groups H3, H4 and H5 are compared, electron density cloud localization, calculated from TDDFT, only occurs on H3 and H4, but not on H5, deducing H3 and H4 as the most beneficial anchoring groups of *P02*.

4. Conclusions

The molecular geometries, electronic structures, absorption spectra and deprotonation energies of newly designed molecule of *P02* sensitizer are investigated by using DFT and TDDFT computational calculations. By evaluating HOMO and LUMO energy levels, obtained from DFT calculations of geometrically optimized structure of *P02* molecule with solvent effect in ethanol, it was revealed that *P02* satisfies main requirement for an efficient electron injection with the LUMO level of P02 higher than the conduction band of the TiO_2 and the HOMO level of *P02* sufficiently lower than the redox couple. Furthermore, the *P02's* HOMO energy level is -0.3eV more negative than cyanidin's HOMO energy level. Hence *P02* has more electron donating ability with compared to that of cyanidin. The UV-vis absorption spectra revealed that the *P02* complex exhibits broader absorption indicating its ability to absorb wider energy range in the visible region.

Though there is a carboxyl group in *P02*, the electron affinity calculations reveal that it has the highest deprotonation energy compared to the hydroxyl groups indicating its lowest possibility to anchor onto TiO_2. The most probable anchoring groups are H4 and H5 and H3, in the descending order. In addition, at the excited states the electron clouds are localized towards the hydroxyl groups, especially H4 and H3, in the cyanidin unit of *P02*. All these results suggest the more promising sensitization ability of *P02* which is designed by modifying the sensitizer cyanidin.

Acknowledgements

Brunei Research Council (BRC) Science and Technology Research Grant S&T 17 is acknowledged for financial support.

References

[1] P. Ekanayake, M.R.R. Kooh, N.T.R.N. Kumara, A. Lim, M.I. Petra, N.Y. Voo, C.M. Lim, *Chemical Physics Letters*, **2013**, 585, 121-127.

[2] B. O'Regan, M. Grätzel, *Nature*, **1991**, 353,737–740.

[3] Tennakone, K., et al., *Journal of Photochemistry and Photobiology A: Chemistry*, **1996**, 94(2-3), 217-220.

[4] Calogero, G., et al., *International Journal of Molecular Sciences*, **2010**, 11(1), 254-267.

[5] Polo, A.S. and N.Y. Murakami Iha, *Solar Energy Materials and Solar Cells*, **2006**, 90(13), 1936-1944.

[6] Hagfeldt, A., et al., *Chemical Review*, **2010**, 110, 6595-6663.

[7] Polo, A.S., M.K. Itokazu, and N.Y. Murakami Iha,. *Coordination Chemistry Reviews*, **2004**, 248(13-14), 1343-1361.

[8] Smestad, G.P. and M. Gratzel, *Journal of Chemical Education*, **1998**, 75(6), 752.

[9] Siriporn Jungsuttiwong , Ruangchai Tarsang, Taweesak Sudyoadsuk, Vinich Promarak, Pipat Khongpracha, Supawadee Namuangruk, *Organic Electronics*,**2013**, 14,711–722

[10] Narayan, M.R., *Renewable and Sustainable Energy Reviews*, **2012**, 16(1), 208-215.

[11] Fernando, J.M.R.C. and G.K.R. Sendeera, *Current Science*, **2008**, 95(5), 4.

[12] Calogero, G., et al., *Solar Energy*, **2012**, 86(5), 1563-1575.

[13] A. Lim, N. Haji Manaf, K. Tennakoon, R.L.N. Chandrakanthi, L.B.L. Lim, J.M.R.S.

Bandara, P. Ekanayake, *Journal of Biophysics*, **2015** ,8.
[14] A. Lim, N.T.R.N. Kumara, A.L. Tan, A.H. Mirza, R.L.N. Chandrakanthi, M.I. Petra, L.C. Ming, G.K.R. Senadeera, P. Ekanayake, *Spectrochimica Acta Part A: Molecular and Biomolecular Spectroscopy*, **2015**, 138, 596-602.
[15] N.T.R.N. Kumara, P. Ekanayake, A. Lim, M. Iskandar, C.M. Lim, *Journal of Solar Energy Engineering*, **2013**, 135, 031014-031014.
[16] A. Lim, D.N.F.B. Pg Damit, P. Ekanayake, *Ionics*, **2015**, 21, 2897-2904.
[17] B. Deppmeier, A. Driessen, T. Hehre et al., "*Spartan'10*," Wavefunction, **2011**.
[18] M. J. Frisch, G. W. Trucks, H. B. Schlegel et al., "*Gaussian 09*," Revision C.01, Gaussian,Wallingford, Conn, USA, **2010**.
[19] C. Lee, W. Yang, R.G. Parr, *Physical Review*, **1988**, B 37,785.
[20] C. Qin, A.E. Clark, *Chemical physics letters*, **2007,** 438, 26-30.
[21] G. Calogero et al., *Photochem. Photobiol. Sci*., **2013**, 12, 883.
[22] H.C. Chu et al., *Dyes Pigments*. **2012**, 93, 1488-1497.
[23] F. De Angelis, S. Fantacci, A. Selloni, M.K. Nazeeruddin, M. Gratzel, *J.Phys. Chem. C*, **2010**, 114, 6054-6061.
[24] F. De Angelis, S. Fantacci, A. Selloni, M.K. Nazeeruddin, M. Gratzel, *J. Am, Chem. Soc*. **2007**, 129, 14156-14157.
[25] N. T. R. N. Kumara, Muhammad Raziq Rahimi Kooh, Andery Lim, et al., *International Journal of Photoenergy*, **2013**, Article ID 109843.
[26] T.R. Heera, L. Cindrella, *J. Mol. Model*. **2010**, 16, 523.
[27] Ming-Jing Zhang, Yuan-Ru Guo, Gui-Zhen Fang, Qing-Jiang Pan, *Computational and Theoretical Chemistry*, 2013**,** 1019, 94-100.

SCIENTIA BRUNEIANA

NOTES TO CONTRIBUTORS

Manuscript Submission and Specifications

Scientia Bruneiana is published twice a year. The deadline for submission of manuscripts is **30th June for the end of year edition** and the **31st December for the May edition**.

Manuscripts should be submitted to the Chief Editor, Dr. Abby Tan Chee Hong, Faculty of Science, UBD (abby.tan@ubd.edu.bn), in Microsoft Office Word (.DOCX) format.

Papers will be refereed prior to acceptance. Authors are welcome to suggest potential international referees.

Articles outlining original research findings as well as mini-review articles are welcomed. There are two special categories: "Brief Communications" and "Research Notes". Contributions to either category should be 300 to 1000 words long (no more than 3 pages in length). The "Research Notes" section is earmarked for summaries of the results and outcomes of projects receiving UBD Science Faculty research grants.

Manuscripts should be written in English (British or American). All manuscripts should be in 12pt Times New Roman, **single-spaced**, **single column** and A4 formatted (2cm margins from the edge).

Title page

The first page should include the title of the article, author's names and addresses of the institutions involved in the work. The paper title is only capitalized on proper nouns and the first letter. Latin, scientific genus and species should be italicized. The authors' affiliations are denoted with a superscripted number and the corresponding author denoted with a * at the end of the author's name. Only the corresponding author's email need to be listed.

Example format of the title page:

First record and conservation value of *Periophthalmus malaccensis* Eggert from Borneo

First Author[1], John H. Smith[2,3], Muhamad Ali Abdullah[2] and Siti Nurul Halimah Hj. Ahmad[1]*

[1]Environmental and Life Sciences, Faculty of Science, Universiti Brunei Darussalam, Jalan Tungku Link, Gadong, BE1410, Brunei Darussalam
[2]Department of Chemical Sciences, Faculty of Science, Universiti Brunei Darussalam, Jalan Tungku Link, Gadong, BE1410, Brunei Darussalam
[3]Department, University, Street Address, Postcode, Country

**corresponding author email: first.author@ubd.edu.bn*

Abstract Page and Index Terms

The second page of the manuscript should include the abstract (up to 300 words) and index terms (subject heading, or descriptor, in information retrieval, that captures the essence of the topic of a document).

Example format of the abstract and index terms page:

Abstract

The abstract is a self contained description of the work in one paragraph of up to 300 words. It must include no references or foot notes, but it must describe the key points of the work. This should include

a description of the work that was done and why it was it done. It should include brief conclusions and any significant numerical findings such as derived constants or important parameters.

Index Terms: resolution, spectroscopy, microscopy

Main body of text

For original research articles, the main body of text of the manuscript should include the following appropriately numbered sections: **1. Introduction**, **2. Experimental approach**, **3. Results and Discussions** and **4. Conclusion** followed by **Acknowledgements**, **References** and **Appendices** (if necessary).

Each different numbered section may contain italicised subheadings which are numbered appropriately, e.g. *2.1*, *3.1*, etc.

Review articles will obviously not conform to this format. In the case of other submissions where the above format may be unsuitable, you are advised to contact the editor prior to submitting the article.

Reference to figures, tables and equations

The main body of text should not include figures and/or tables, but should refer to figures and tables. If a certain figure or table was not referred to in the main body of text then it will be considered irrelevant and therefore will not be included in the publication. When referring to the figure or table in the text, the words figure and/or table should be bold and italicized e.g. ***Figure 1*** and ***Table 1***. The words "figure" and "table" should be spelled out in full and not abbreviated. For further instructions on figures and tables (including dimensions, colour schemes and formats), please refer to the figures and tables section.

Equations could be displayed in-line or centred by itself, but must be accompanied by a number and individual terms/symbols explained. When When referring to the equation in the text, the word "Equation" should be bold and italicized e.g. ***Equation 1***. The words "Equation" should be spelled out in full and not abbreviated.

Example format of equation:

An example of an equation is shown for ***Equation 1***, Weber Morris intraparticle diffusion:

$$q_t = k_{id} t^{1/2} + C \qquad (1)$$

and Boyd model (***Equation 2***):

$$F = 1 - \frac{6}{\pi^2} exp(-B_t) \qquad (2)$$

where F = q_t / q_e, F is the fraction of solute adsorbed at any time, t and B_t is mathematical function of F.

In-line citation style

The in-line citation should be in the following format (superscripted numbers):

Various studies have been found to link parameter A to parameter B.[1]

Please note that superscripted numbers should go after punctuation. e.g. "Studies show that A is linked to B.[1-5]" and "Even though studies show this,[3,4] there are others that contradicts this.[6-8]"

References

The reference list should only include references cited in the text and should be listed in the references section in the following format:

Journal article

[1] J. H. Surname and J. E. Doe, *Journal*, **Year**, Vol., Pages.

Textbook/Chapter of a book
[2] J. H. Surname and J.E. Doe, Title of Textbook (and Chapter), **Publication Year**, Pages

Dissertation/Thesis
[3] J.H. Surname, Title of Thesis, *PhD/Master's Thesis*, **Year**, University

Webpages/Online Databases
[4] Website/Database name/body: URL (date accessed 01/01/2016)

Figures and Tables

A list of tables, figures and captions should be given at the end of the manuscript after the reference list. These must be appropriately numbered in the order that they appear in the paper. Each table and figure must be adequately discussed and referenced in the text. It is important that you do not include tables and figures in the main body of text of your submitted manuscript.

Sizing

Please keep tables/figures/images/illustrations to have a **maximum width of either 8.4 cm (single column) or 17.5 cm (double column)**, with enough clarity that the images does not appear blurred, skewed or pixelated (unless the pixelation is unavoidable from the raw data collection).

Text

Texts in figures and tables should be 10pt, using either Times New Roman, Arial or Calibri font, with consistent font size and style throughout the manuscript's figures/tables/artwork/images/illustrations. Please ensure that texts do not fall below 8pt size as this will greatly affect readability of said text.

Colour

Colour images are highly encouraged for the on-line issue, however they should be designed such that the information is still obvious in grey-scale too for the print version.

Graphs

Graphs could either be saved as an embedded graph format in DOCX or as an image (JPEG or TIFF). Graphs should have clearly-labelled axes and lines that can be distinguished in both color for on-line and grey-scale for print version. You can use dotted and dashed lines etc, or you can use different data point types when appropriate to discriminate between data sets.

Tables

Tables could either be saved as an embedded table format in DOCX or as an image (JPEG or TIFF), with appropriate captions/titles.

Captions

All figures and tables should be appropriately captioned. The caption should be sufficiently able to explain the figure/table without the reader having to refer to the main text. The words "figure" and/or "table" should be bold. italicized and spelled out fully (not abbreviated), followed by a full stop (also bold and italicized). The rest of the caption should not be bold and italicized (unless it is a scientific genus or species).

Example format for figure/table caption:

> ***Figure 1.*** *Periophthalmus malaccensis* collected in Sungai Bunga, Brunei (UBDM MBu081013mal); a. freshly dead specimen, lateral view; b. live specimen; c. freshly dead specimen, ventral view, detail (scale bars are 10 mm long).

Manuscripts that do not conform to the above instructions will be returned without review.

CALL FOR PAPERS

Scientia Bruneiana
A Journal of Natural and Applied Sciences

The *Scientia Bruneiana (SciBru)*, a new online and print publication by the Faculty of Science at Universiti Brunei Darussalam, is seeking submissions of original research and review articles in the field of natural and applied sciences. *SciBru* is dedicated to publishing high quality research and reviews. We would appreciate if you, your colleagues and research students can submit papers in forthcoming edition of *SciBru* in all areas of **Natural and Applied Science**.

Submission Guidelines

Authors please refer to submission rules specified in the "/information/authors" section of the *SciBru* website http://scibru.fos.ubd.edu.bn/ for preparation and submission of their papers.

About Universiti Brunei Darussalam (UBD)

UBD was founded in 1985 and is the premier university of Brunei Darussalam.

Since 2009, UBD has transformed from a traditional teaching university into a university that incorporates both teaching and research. Over the past 7 years, the Sciences has played a significant contribution towards drastic outcomes in research and innovation. Among them, researchers have managed to secure substantive internal and external research grants. This has allowed the advancement of the sciences which in turn has led to the establishment of a global connectivity while maintaining regional identity and the nation's needs.

Contact Details

Chief Editor: **Abby Tan Chee Hong**

Dean, Faculty of Science,
Universiti Brunei Darussalam,
Jalan Tungku Link, BE 1410,
Brunei Darussalam
Email: abby.tan@ubd.edu.bn